

Historical Survey of Free Electron Lasers

M. E. Couprie

Synchrotron SOLEIL, Saint-Aubin, France

Abstract

Free electron lasers are presently unique tuneable powerful lasers ranging from the infrared to the X-ray, serving for the exploration of light–matter interaction. They make use of a simple and elegant gain medium. The coherent radiation is generated using free electrons in a periodic permanent magnetic field generated by a so-called undulator as an amplification medium. The light–electron interaction in the undulator leads to a bunching process, setting in phase the electron emitters and establishing a longitudinal coherence. The amplification of the light wave takes place to the detriment of the kinetic energy of the electrons. First, the origins of the free electron laser, starting from the photon–matter interaction, the early times of synchrotron radiation and the undulator, the development of vacuum tubes, masers, and lasers are introduced. Then, motivated by the search of an exotic laser, the invention of the free electron conceptual idea laser is discussed, with a quantum approach followed by a classical one. The first low gain free electron laser experiments are then presented. Finally, some insight is given in the case of the high gain free electron lasers.

Keywords

Free electron laser; laser; undulator.

1 Introduction

In the early times, free electron lasers (FELs) appeared as exotic lasers. In 1990, C. Brau (ninth FEL Prize in 1996) introduced them as such: They “represent an altogether new and exciting class of coherent optical sources. Making use of a simple and elegant gain medium—an electron beam in a magnetic field—they have already demonstrated broad wavelength tuneability and excellent optical-beam quality. For the future they offer the possibility of generating the greatest focused power ever achieved by a laser. But even before this is achieved, the unique advantages of free electron lasers, especially their tuneability, will make them useful for a variety of important applications in science and medicine” [1]. Indeed, nowadays, they provide the most powerful lasers in the X-ray range, with ultra-short pulse duration. The present advent of tuneable X FELs with unprecedented intensities enables new investigation of matter with ultra-high intensities, ultra-short pulses, etc. It could be considered as a second revolution, following the invention of the laser, which led to the development of optical lasers which has changed our current life.

The FEL spontaneous emission corresponds to the undulator radiation emitted by the relativistic electrons. The electrons are not bound to nuclei in atoms and molecules, and vibrate at specific frequencies. In contrast, the FEL vibration frequency can be adjusted by changing the magnetic field or the energy of the electrons, resulting in a broad wavelength tuneability. Indeed, “The electrons in a free electron laser have the form of an electron beam in a vacuum, much like the beam in the picture tube of a television set except that the electrons have much higher energy and intensity. Electrons bound in atoms and molecules vibrate only at specific frequencies. Thus the laser light from conventional lasers, which make use of bound electrons, appears only at these specific frequencies. On the other hand, the electrons in a free electron laser are forced to vibrate by their passage through alternating magnetic field. Thus, the vibration frequency can be adjusted by altering the construction of the magnetic field or by

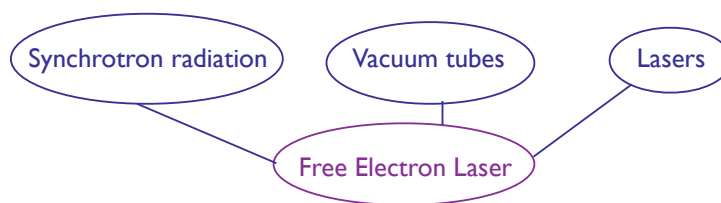


Fig. 1: Schematic presentation of the origins of the free electron laser

changing the speed of the electrons passing through the magnetic field. This changes the laser frequency or, equivalently, the wavelength”. The gain process results from the energy exchange between the light and the electrons. The optical beam presents an excellent optical beam quality and can achieve high power.

This historical survey on the free electron laser aims at describing how the new ideas have emerged and how the field progressed. Some citations are taken from the original papers, to show how the understanding at a given time was. This report gathers also the main results which define major steps to my own understanding and personal experience. The work of the FEL Prize winners, listed in the Appendix, is mentioned. The progress of the FEL field is also closely related to technological advances, which cannot be discussed in detail but which are underlined when crucial. Drawing a history survey [2, 3] on FEL implies some choices in the discussed items, which are necessarily subjective. I apologize in advance for all the important works which have not been cited.

First, the scientific context enabling the emergence of the FEL concept is explained: the development of vacuum tubes in the twentieth century, together with the invention of the laser in 1958 [4] and the first laser operation in 1960 [5]. Then, the discovery of the FEL [6] by J. M. J. Madey (1943–2016, first FEL Prize, 1988) which took place in such a context is reported. FELs combine specificities of synchrotron radiation, vacuum tubes, and lasers, as indicated in Fig. 1. The FEL was treated with a quantum approach, as stimulated Compton Back Scattering.

Then the first applied classical treatments to FELs are reported. A section describing the first experimental results follows, with some newly proposed concepts. The last section deals with high gain developments, including high gain FEL theory and the proposed concept of Self-Amplified Spontaneous Emission (SASE), the major experimental steps for SASE operation and some hints on further developments (seeding, echo).

2 The origins of the free electron laser

The scientific context favourable for the emergence of the free electron laser concept is hereafter described. The understanding of the interaction between light and matter was established at the beginning of the twentieth century. Then, the century knew an intense development of vacuum tubes accompanied by the discovery of the laser in the sixties. The emergence of the free electron laser concept benefited from the interplay between these two domains.

2.1 The photon–matter interaction processes

The laser concept relies on the prediction of energy enhancement by atom de-excitation by Albert Einstein (1879–1955, Nobel Prize in 1921) in 1917 [7] in the analysis of the black-body radiation, while absorption and spontaneous emission were the known light matter interactions at that time. The process was called later stimulated emission by J. Van Vleck in 1924 [8, 9]. In the absorption case, a photon is absorbed and drives an atom to an excited state. The excited atom being unstable, it emits a spontaneous photon after a duration depending on the lifetime of the excited level. In the stimulated emission case, a photon is absorbed by an excited atom, which results in the emission of two photons with identical

wavelength, direction, phase, polarization, while the atom returns to its fundamental state. Einstein was mainly interested by thermal radiation and exchanges of momentum in different process, but not specifically by the production of light by matter. Stimulated emission was seen as addition of photons to already existing photons, and not as the amplification of a monochromatic wave with conservation of its phase. The notion of light coherence, related to its undulatory properties, was not considered at that time.

2.2 The early times of synchrotron radiation

Synchrotron radiation, the electromagnetic radiation emitted by accelerated charged particles, is generally produced artificially in particle accelerators, but it can be also observed in astrophysics [10, 11], such as in the Sun where hydrogen submitted to loops of magnetic fields emits visible light in the centre and on the edges in the X-ray domain.

Let's introduce some notations. Let's consider a laboratory region, without current, with a laboratory referential $(0, x, z, s)$ with the frame (x, z, s) [12], as shown in Fig. 2 where s is the longitudinal, x the horizontal, and z the vertical direction.

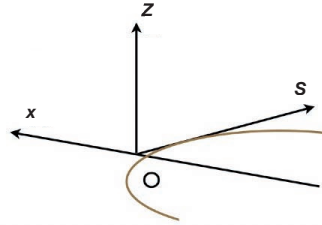


Fig. 2: Axis coordinates

Consider then a relativistic electron of energy E and velocity v with respect to the laboratory frame. Its relativistic factor γ is given by $\gamma = \frac{E}{m_0 c^2}$ (with m_0 the electron mass, e the particle charge, and c the speed of light). It can be expressed as :

$$\gamma = \frac{1}{\sqrt{1 - \beta^2}} \quad (1)$$

with $\vec{\beta}$ the normalized velocity of the electron, expressed as :

$$\vec{\beta} = \frac{\vec{v}}{c}. \quad (2)$$

Theoretical foundations of synchrotron radiation were established at the end of the 19th century by J. Larmor [13], who first proposed a specific prediction of time dilation: "... individual electrons describe corresponding parts of their orbits in times shorter for the [rest] system in the ratio, as given by $\sqrt{1 - v^2/c^2}$ ".

Then, A. M. Liénard [14] provided the first correct calculation of the power emitted by an accelerated charged particle, as proportional to $(E/mc^2)^4/R^2$ with m the particle mass, R the orbit radius. The angular and spectral distribution and polarization properties were then described by G. A. Schott [15, 16]. Radiation is emitted in a narrow cone of aperture $1/\gamma$.

In 1944, D. D. Ivanenko and I. Y. Pomeranchuk estimated a calculated limit on the energy obtainable in a betatron (of the order of 0.5 GeV) due to energy losses from radiating electrons [17]. Particles slow down and lose synchronism. Because of the spread in revolution frequency with energy, the frequency cannot simply be reduced to maintain synchronism [18] but the particle bunch should be injected in the radiofrequency (RF) at a proper phase (phase stability), as proposed by E. M. McMillan [19] and V. I. Veksler [20] in a 'synchrotron'-type accelerator, which was then built [21]. Julian Seymour

Schwinger (1918–1994, Nobel Prize in 1965) described the peaked spectrum and predicted that higher photon energies should be observed [22, 23].

After the construction of first accelerators, J.-P. Blewett measured the particle energy loss on the 100 MeV betatron and he found it to be in good agreement with the theoretical expectation, but failed to observe synchrotron radiation in the microwaves [24, 25]. The first synchrotron radiation was then observed in the visible tangent to the electron orbit one year later on the 70 MeV General Electric synchrotron, of 29.3 m radius and 0.8 T peak magnetic field [26]. The rapid increase of the intensity with the electron beam energy was measured (fourth power of the energy). The emitted light was found to be polarized with an electron vector parallel to the plane of the electron orbit.

2.3 The undulator

2.3.1 Invention of the undulator

After considering the synchrotron radiation emitted in bending magnets, it is of interest to analyse what happens with a succession of alternated dipoles, as mentioned by V. L. Ginzburg (1916–2009, Nobel Prize in 2003) who first pointed out the radiation emitted by relativistic electrons performing transverse oscillations [27].

H. Motz calculated the field created by a relativistic particle in a magnetic sinusoidal field (i.e. such as produced by undulators) [28, 29], as shown in Fig. 3. He also examined the influence of the bunching of the electrons on the coherence of the radiation. He then observed the polarized visible radiation from an undulator installed on the 100 MeV Stanford accelerator [30]. A buncher set-up after a 3.5 MeV accelerator achieved 1 W peak power at 1.9 mm thanks to the bunching of the electrons. In parallel, the emission of the radiation spectrum produced from an undulator installed on a 2.3 MeV accelerator was investigated by R. Combe and T. Frelot [31]. For the following, it is useful to recall the electron trajectory when it is submitted to the undulator magnetic field and the basics of undulator radiation.

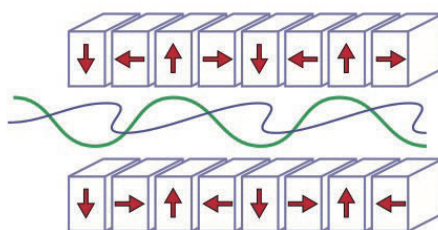


Fig. 3: Planar undulator scheme, creating a periodic magnetic field created by two arrays of permanent magnets arranged in the Halbach configuration [32]. Vertical magnetic field in green, electron trajectory in blue.

2.3.2 Electron movement in an undulator

Let's consider a relativistic electron travelling in an undulator of total length L_u and spatial period λ_u . Let's suppose that the relativistic electron of energy E and velocity v with respect to the laboratory frame is introduced along the s direction. For a relativistic factor $\gamma \gg 1$, $\frac{1}{\gamma} \ll 1$ and the reduced velocity $\beta^2 = 1 - \frac{1}{\gamma^2}$ can be approximated as $\beta \approx 1 - \frac{1}{2\gamma^2}$.

2.3.2.1 Electron movement in a planar undulator

In the case of a planar undulator, creating a field along the vertical direction expressed in the $[0, L_u]$ interval as

$$\vec{B}_u = B_u \cos\left(\frac{2\pi}{\lambda_u} s\right) \vec{z} = B_u \cos(k_u s) \vec{z} \quad (3)$$

with the undulator wavenumber k_u given by $k_u = \frac{2\pi}{\lambda_u}$. The undulator deflection parameter K_u expressed as $K_u = \frac{eB_u\lambda_u}{2\pi m_0 c}$ is given in practical units as $K_u = 0.934B_u(T)\lambda_u$ (cm).

The integration of the fundamental equation of the dynamics applying the Lorentz force leads to

$$\vec{\beta} \begin{pmatrix} \frac{K_u}{\gamma} \sin(k_u s) \\ 0 \\ 1 - \frac{1}{2\gamma^2} - \frac{K_u^2}{2\gamma^2} \sin^2(k_u s) \end{pmatrix} \quad (4)$$

and on average over one undulator period:

$$\langle \vec{\beta} \rangle \begin{pmatrix} 0 \\ 0 \\ 1 - \frac{1}{2\gamma^2} \left(1 + \frac{K_u^2}{2}\right) \end{pmatrix}. \quad (5)$$

Since the velocity in the vertical direction is zero, the movement takes place in the horizontal plane (x, s). Introducing $k_u s = \omega_u t$ with $\omega_u = k_u c$, a further integration without taking into account the integration constants (there are indeed termination magnets enabling the electron to enter at the origin position) leads to

$$\begin{cases} x = \frac{K_u c}{\gamma} \int \sin(\omega_u t) dt = \frac{K_u c}{\gamma \omega_u} \cos(\omega_u t), \\ z = 0, \\ s = c \left(1 - \frac{1}{2\gamma^2} - \frac{K_u^2}{4\gamma^2}\right) t + \frac{K_u^2 \lambda_u}{16 \pi \gamma^2} \sin(2\omega_u t) = \langle v_s \rangle ct + \frac{K_u^2 \lambda_u}{16 \pi \gamma^2} \sin(2\omega_u t). \end{cases} \quad (6)$$

The maximum amplitude of the transverse motion is $\frac{K_u \lambda_u}{\gamma 2\pi}$. In the longitudinal direction, oscillations occur at twice the frequency, with a maximum amplitude of $\frac{K_u^2 \lambda_u}{16 \pi \gamma^2}$ generally of much smaller amplitude than in the transverse direction.

2.3.2.2 Electron movement in a helical undulator

In the case of a helical undulator creating a magnetic field in both horizontal and vertical directions given by

$$\begin{cases} \vec{B}_{ux} = B_{ux} \sin\left(\frac{2\pi}{\lambda_u} s\right) \vec{x} = B_u \sin(k_u s) \vec{x}, \\ \vec{B}_{uz} = B_{uz} \cos\left(\frac{2\pi}{\lambda_u} s\right) \vec{z} = B_u \cos(k_u s) \vec{z}, \\ \vec{B}_{us} = 0, \end{cases} \quad (7)$$

a first integration of the Lorentz equation leads to

$$\vec{\beta} \begin{pmatrix} -\frac{K_u}{\gamma} \sin(k_u s) \\ -\frac{K_u}{\gamma} \cos(k_u s) \\ 1 - \frac{1}{2\gamma^2} - \frac{K_u^2}{2\gamma^2} \end{pmatrix}. \quad (8)$$

Taking integration constants equal to zero, a further integration leads to

$$\begin{cases} x = -\frac{K_u c}{\gamma} \int \sin(\omega_u t) dt = \frac{K_u c}{\gamma \omega_u} \cos(\omega_u t), \\ z = \frac{K_u c}{\gamma} \int \cos(\omega_u t) dt = -\frac{K_u c}{\gamma \omega_u} \sin(\omega_u t), \\ s = c \left(1 - \frac{1}{2\gamma^2} - \frac{K_u^2}{4\gamma^2}\right) t = \langle v_s \rangle ct. \end{cases} \quad (9)$$

The electron trajectory on axis is helical. There is no oscillatory movement in the longitudinal direction at twice the frequency.

2.3.3 Undulator radiation

Let's now consider the specific features of the undulator radiation.

2.3.3.1 Resonance

Electrons wiggling inside the undulator emit synchrotron radiation, as in a succession of bending magnets. They emit synchrotron radiation due to their acceleration in the transverse plane. For each period, the radiation is emitted in a narrow cone of aperture $1/\gamma$ in the forward direction.

The radiation emitted along the undulator interferes constructively depending on the phase lag between the electron and the front of the emitted wave train. One can then introduce the resonance condition: when the electron progresses by λ_u , the wave has travelled by $(\lambda_u + \lambda)$ or more generally by $(\lambda_u + n\lambda)$ with n an integer, the radiation of one electron from the different periods interfere and can add constructively for these wavelengths λ_n , as shown in Fig. 4.

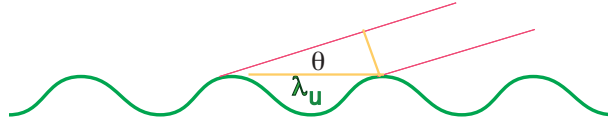


Fig. 4: Undulator resonance condition: when the electron progresses by λ_u , the wave has travelled by $\lambda_u + \lambda$, t_o being the time origin, v_s being longitudinal velocity of the electrons.

In introducing the path difference between the two rays: $n\lambda_n$, one has $c\lambda_u/v_s - \lambda_u \cos \theta/c = n\lambda_n$ leading to

$$n\lambda_n = \lambda_u(1 - \beta_s \cos \theta)/\beta_s. \quad (10)$$

Synchrotron radiation being emitted ahead for small angles, one can approximate $\cos \theta$ by $(1 - \theta^2/2)$, and using $\beta_s = \langle \beta_s \rangle = 1 - 1/2\gamma^2 - K_u^2/4\gamma^2$ for a planar undulator, the resonant wavelength becomes

$$\lambda_n = \frac{\lambda_u}{2n\gamma^2} \left(1 + \frac{K_u^2}{2} + \gamma^2\theta^2\right). \quad (11)$$

In the case of a helical undulator (with $\beta_s = \langle \beta_s \rangle = 1 - 1/2\gamma^2 - K_u^2/2\gamma^2$), the resonant wavelength is given by

$$\lambda_n = \frac{\lambda_u}{2n\gamma^2} (1 + K_u^2 + \gamma^2\theta^2). \quad (12)$$

This is the so-called ‘undulator resonance’ wavelength, setting the undulator radiation as a series of harmonics, of order n . The wavelength λ_n of the emitted radiation can be varied by changing the

electron beam energy or by a modification of the undulator magnetic field (by changing the gap for permanent magnet insertion devices or the power supply current for electromagnetic insertion devices). The infrared spectral range can be reached with reasonable beam energies. The X-ray regime requires the use of high electron beam energies. Larger wavelengths are obtained for off-axis radiation.

2.3.3.2 Radiated spectrum

The wave packet emitted by each electron contains only a finite number N_u of oscillations as shown in Fig. 5. Thus, in the time domain, the observer receives a train of N_u magnetic periods. The frequency is imperfectly defined. The radiation spectrum corresponds to the Fourier transform of the wave packet emitted by the electron.

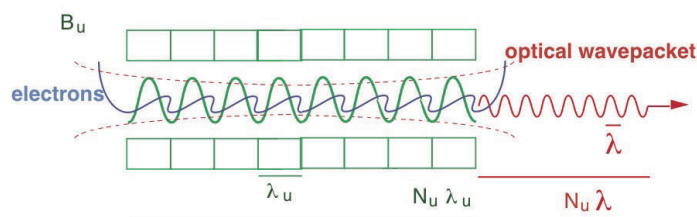


Fig. 5: Radiation train emitted from the undulator of period N_u periods λ_u . The electron moves along the undulator length with a speed v ($vt = N_u \lambda_u$) and emits a wave packet whose length is $(c - v)t = N_u \lambda$. The wave packet contains the same number of periods as the undulator, i.e. N_u .

The electron radiates uniformly from the undulator entrance to its end, so the wave packet has a square envelope. For the optical wave central wavelength $\lambda_l = \frac{2\pi c}{\omega_1}$, the intensity is given by

$$I(\omega) \propto \left| \int_0^{N_u \lambda_u / c} \exp[-i(\omega - \omega_1)t] dt \right|^2 \propto \left\{ \text{sinc} \frac{2\pi N_u (\omega - \omega_1)}{2\omega_1} \right\}^2 \quad (13)$$

with n the harmonic number. The on axis radiation spectrum, square of the Fourier transform of this train, is then composed of a series of square sinus cardinals, centred on odd harmonics. The radiation spectrum in the forward direction is thus nearly monochromatic, i.e. it is composed of narrow spectral lines at a well-defined wavelength λ_n . The linewidth of the radiation, called per analogy to conventional lasers the ‘homogeneous linewidth’ is of the order of

$$\left(\frac{\Delta \lambda}{\lambda_n} \right)_{\text{hom}} \approx \frac{1}{n N_u}. \quad (14)$$

This so-called ‘homogeneous linewidth’ refers to the case of a single electron. The emission presents then a narrowband in the frequency domain. In other words, the emitted field interferes between different points of the trajectory, leading to sharp spectral peak emission. The higher the number of undulator periods, the smaller the radiated bandwidth. In the case of a single electron, the undulator intensity then scales as N_u^2 .

An example of spectrum is given in Fig. 6 with an ideal and real electron beam. For the one electron emission (or ideal electron beam, i.e. filament mono-energetic electron beam) shown in Fig. 6 (a), the radiated line width is ruled by the homogeneous width. However, a real electron beam is not mono-energetic (it has intrinsic energy spread) and presents a transverse size and divergence (emittance contribution).

When adding the emittance term in Fig. 6(b), a satellite peak appears on the red side of the line, and the even harmonics are growing. The linewidth broadening can be interpreted with the contributions

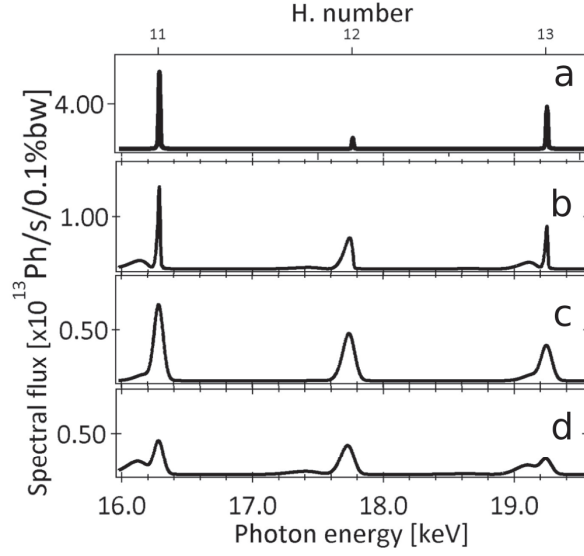


Fig. 6: Spectral flux in the case of a U20 undulator (0.97 T peak field) with 2.75 GeV electrons on the 11th and 13th harmonics: (a) case of a filament monoenergetic electron beam, (b) emittance of 3.9 nm mrad in horizontal and 39 pm mrad in vertical direction, (c) energy spread of 0.1% energy spread, (d) with the contribution of the emittance of (b) and energy spread of (c).

given by the electron beam emittance (with the beam size σ and divergence θ) through the electron beam divergence and size as

$$\left(\frac{\Delta\lambda}{\lambda_n}\right)_{\text{div}} \approx \frac{\gamma^2\theta^2}{1 + \frac{K_u^2}{2}}, \quad (15)$$

$$\left(\frac{\Delta\lambda}{\lambda_n}\right)_{\sigma} \approx \frac{2\pi^2 K_u^2}{(1 + K_u^2/2)} \frac{\sigma_z^2}{\lambda_u^2}. \quad (16)$$

When adding the energy spread Fig. 6 (c), the line widens symmetrically. This energy spread ($\frac{\sigma_\gamma}{\gamma}$) induced spectral broadening contribution is modelled as

$$\left(\frac{\Delta\lambda}{\lambda_n}\right)_{\sigma_\gamma} \approx \frac{2\sigma_\gamma}{\gamma} \quad (17)$$

The two contributions are added in (Fig. 6d): the lines are damped and widened. The modification of the undulator line can be interpreted as ‘inhomogeneous’ broadening, which results from different contributions: the electron beam energy spread, size, and divergence. Analytically, one can make the quadratic sum of the different contributions as a first approximation.

When inhomogeneous bandwidth becomes dominant, the intensity is proportional to N_u , i.e. $I \propto N_u$. Such a linewidth provides a certain longitudinal coherence length, but is far from the Fourier limit.

2.3.3.3 Undulator emission angle

Because of the wiggling trajectory in the transverse plane (i.e. horizontal for a vertical field), the opening angle is given by the excursion of the reduced velocity, i.e. K_u/γ . For the planar undulator (vertical field case), the vertical opening angle is given by $1/\gamma$ as for the usual synchrotron radiation case. For a helical undulator, the angles are given by the velocity excursions in both planes. The radiation is well collimated and presents some transverse coherence, depending on the considered wavelength and on the electron beam contribution.

2.3.4 Temporally coherent emission

Let's discuss further the temporal properties of the radiation. In general, the radiation from the different electrons adds incoherently, and the radiated intensity is proportional to the number of electrons N_e . Longitudinal coherence occurs if the different electrons emit in phase, leading to a radiated intensity scaling as N_e^2 . Electrons being in phase can occur either if the electron bunch length is small with respect to the considered wavelength of emission, or if a modulation is imprinted on the electron bunch [33], such as in the free electron laser process. Figure 7 illustrates the three cases of incoherent beam in (a), a bunch short than the wavelength in (b), and of a bunched beam in (c). The bunched case was already considered by Motz [28]. Intermediate case can occur also with abrupt changes in the electronic density, such as with edge radiation from bending magnets.

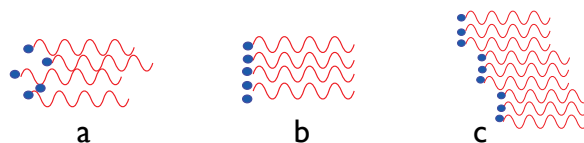


Fig. 7: Distribution of electrons: (a) random distribution leading to incoherent emission, (b) short electron bunch with respect to the radiated wavelength, (c) case of the bunched electron beam.

The normalized longitudinal distribution $n(s)$ can be expressed as $n(s) = N_e S(s)$ with $S(s)$ being the form factor. The corresponding electric field is then expressed by $E(\omega) = E_o(\omega) N_e f(\omega)$ with $E_o(\omega)$ the electric field of one electron and $f(\omega)$ the form factor in the frequency domain, given by

$$f(\omega) = \int_{-\infty}^{\infty} S(s) \exp\left(i \frac{\omega s}{c}\right) ds. \quad (18)$$

The electric field results from the sum of the fields emitted by each electron, according to

$$I(\omega) = I_o(\omega) [N_e(N_e - 1)f(\omega)^2 + N_e]. \quad (19)$$

The intensity expression comports two terms, one scaling as the square of the number of electrons (for the coherent emission) and another scaling (for the incoherent synchrotron radiation). The coherent term involves the form factor. In case of short Gaussian electron bunches, one gains typically several orders of magnitude on the radiated intensity.

In the case of a bunched beam, one has

$$S(s) = \sum_{m=1}^M S(s - m\lambda_n). \quad (20)$$

When a form factor is introduced, the undulator emission can become longitudinally coherent emission for λ_n . The form factor resulting from the bunching efficiency is similar to the form factor in Bragg diffraction. The first observation was achieved in 1989 [34].

2.4 The development of vacuum tubes

Let's consider now the domain of vacuum tubes, when bunched electrons are currently generated. The electron beam in vacuum tubes witnessed a rapid and spectacular development at the beginning of the twentieth century for the current amplifier applications such as radiodiffusion and radar detection for icebergs or military use, where high frequency oscillations are needed. Electron beams in vacuum tubes rely on the interaction of a free electron of relativistic factor γ given by $\gamma = \frac{E}{m_0 c^2}$ (with E its energy,

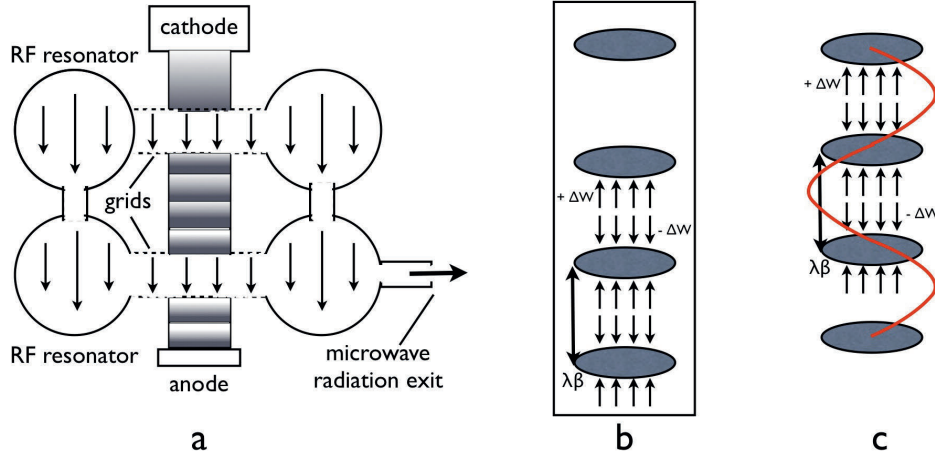


Fig. 8: Klystron principle: (a) klystron scheme, (b) electron bunching by energy modulation in the klystron drift space, electrons accumulate in bunches, (c) phased electron in the second klystron cavity, electric field in red.

m_0 the electron mass, e the particle charge, and c the speed of light), $\vec{\beta}$ the normalised electron velocity and an electromagnetic wave of electric field \vec{E} with $\vec{E} = \vec{E} \sin(kz - \omega t)$ with k the wavenumber and ω the pulsation according to :

$$\frac{d\gamma}{dt} = \frac{e\vec{\beta} \cdot \vec{E}}{mc}. \quad (21)$$

A first example of the high-power electron vacuum tube is given by the magnetron, now used for microwave ovens. Electron bunches passing through open cavities excite RF wave oscillations by interaction with the magnetic field, the frequency being determined by the geometry of the cavity. The magnetron can act only as an oscillator for the generation of the microwave signal from the direct current supplied to the tube.

The second example is given by the klystron, invented by the Russel and Sigurd Varian brothers [35]. It consists of two cavities (metal boxes along the tube), as shown in Fig. 8(a) [36].

In the first cavity, an electric field oscillates on a length Δs at a frequency $\nu = 2\pi f$ ranging between 1 and 10 GHz (i.e. with corresponding wavelengths of 30–33 cm). The electrons, generated at the cathode, enter in the first cavity where the input RF signal is applied. They can gain energy according to

$$\Delta W_1 = \int_0^{\Delta s} ec\vec{\beta} \cdot \vec{E} dt \simeq ecE \cdot \beta \cos(\omega t) \cdot \frac{\Delta s}{\beta} = ecE \cdot \Delta s \cdot \cos(\omega t). \quad (22)$$

The sign of ΔW_1 depends on the moment t when the electron arrives inside the cavity. ΔW_1 is modulated in time at a temporal period $T = \frac{2\pi}{\omega}$ or spatial period $\lambda\beta$. On average for the electrons, $\Delta W_1 = 0$ since the electrons have different phases.

Then, the electrons enter into the drift space (see Fig. 8(b)), and they accumulate in bunches. The drift space length is adjusted to enable an optimal electron bunching.

In the second cavity, the electrons have the same phase with respect to the electromagnetic wave, since they have been bunched (see in Fig. 8c). The second energy exchange is given by

$$\Delta W_2 = \sum_{\text{electrons}} \int_0^{l_2} ec\vec{\beta} \cdot \vec{E}_{\text{RF}} dt = N_e ecEL_2 \cos(\omega t) \quad (23)$$

with L_2 the interaction region in the second cavity, E_{RF} the electric field. The phase of the electrons in the second cavity is ruled by the electrons themselves. The gain in electric field can be very high (practically, 10^3-10^6).

Schematically, the klystron can be understood as a block for the bunching, with another one for the phased interaction with the field. In such a case, a high intensity electron beam excites the RF wave in the second cavity (see Fig. 9). The klystron can be operated in the oscillator mode with a feedback loop on the radiation, where the cavity and the waveguides should be of the order of the wavelength. While looking for larger values of the frequency, i.e. for short wavelengths, the manufacturing of the cavities and waveguides thus limits the operation of the klystron to the microwave region. Another system should be realized for the micrometre and submicrometre spectral ranges.

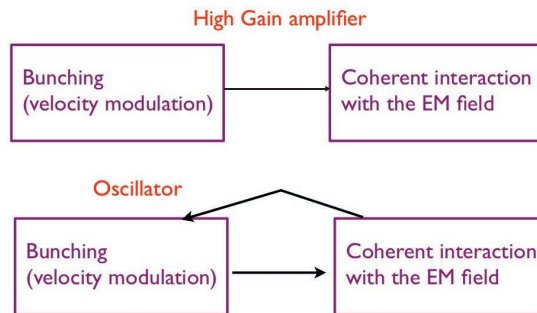


Fig. 9: Bloc diagram of the klystron: amplifier and oscillator cases

More generally, an electron bunch can be accelerated or decelerated by a wave for which the period is longer than the electron bunch one. The linear accelerator relies on such a principle, as seen in Fig. 10. The electrons are produced in an electron gun: a thermo-ionic gun or a photoinjector where the electrons are then generated in trains. With the conventional thermo-ionic gun, the electrons travel into the so-called buncher (a sub-harmonic or harmonic cavity) on the edge of the RF wave, for acquiring energy spread and being bunched by the velocity modulation, as in the klystron case. Then, the electron beam is accelerated by an intense RF wave produced by a klystron and sent in the cavities of the accelerating sections, which can be considered as a series of coupled cavities or as a waveguide where irises slow down the phase of the RF wave to become equal to that of the electrons. In the accelerating sections, the electrons should have the same phase with respect to the RF wave. To be so, they are arranged in small bunches ('bunching'). For example, for a RF frequency of 1.3 GHz, the period is of 0.77 ns, 1° phase corresponds to 2.1 ps.

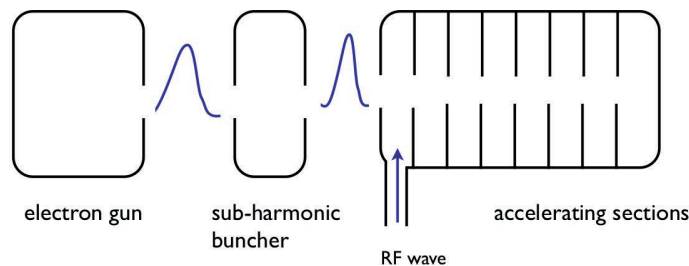


Fig. 10: Scheme of the linear accelerator: electron gun, buncher, accelerating sections

Vacuum tubes such as klystrons, magnetrons, and more generally electronics, discovered at the end of the thirties, underwent a wide development during the second World War with applications such as radiodiffusion and radar detection, where oscillators with high frequencies are needed. The sources generally use electron beams submitted to electric or magnetic fields, where the ‘bunching’ is the key concept for the wave amplification. The use of resonant cavities at the frequency of the emitted wavelength can efficiently insure the retroaction needed for the production of a coherent wavelength.

This field of electronics enabled us to understand that in setting a loop on a wide band amplifier (in connecting one part of its output to its entry), one can transform it into a very monochromatic oscillator. This concept will be used later for the maser and laser inventions.

2.5 The ubitron: undulating beam interaction

FEL precursor works considered whether wave amplification [37] was possible. Then, the ubitron, for ‘undulating beam interaction’ was invented by R. M. Phillips (FEL Prize in 1992 at General Electric Microwave Laboratory), who reports on its discovery [38] in the following terms: “The ubitron (acronym for undulating beam interaction) is a FEL which was setting records for RF power generation 15 years before the term ‘free electron laser’ was coined. As is often the case, the invention of the ubitron was accidental. The year was 1957 and I was searching, at the GE Microwave Lab, for an interaction which would explain why an X-band periodically focussed coupled cavity TWT oscillated when a solenoid focused version did not. The most apparent difference between the two was the behaviour of the electron beam; one wiggled while the other simply spiralled. Out of a paper study of ways of coupling an RF wave to an undulating axially symmetric electron beam came the idea of coupling to the TE_{01} mode by allowing the wave to slip through the beam such that the electric field would reverse direction at the same instant the electron velocity is reversed.”

The ubitron is a high-power travelling wave tube which makes use of the interaction between a magnetically undulated periodic electron beam and the TE_{01} mode in an unloaded waveguide [39]. The scheme is illustrated in Fig. 11. The basic idea is to couple the TE_{01} mode by allowing the wave to slip through the beam such that the electric field reverses direction at the same instant the electron velocity is reversed. Several beam guide ubitron configurations (planar, coaxial, circular) can be considered, and they can provide 100 times the interaction area of a TWT (Travelling Wave Tube). The electron–wave interaction exhibits the same type of first-order axial beam bunching characteristic of the conventional slow wave travelling wave tube. In consequence, the ubitron can be used in extended interaction klystrons and electron accelerators, as well as travelling wave tubes.

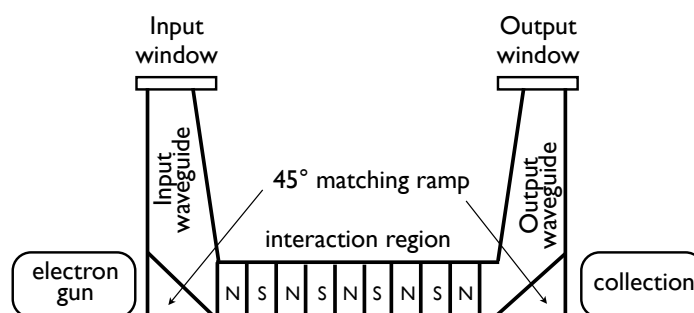


Fig. 11: Scheme of the ubitron: an electron beam from an electron gun, wiggling with axial symmetry, can couple to an RF wave. Alternated magnetic poles provide the axial symmetry.

First experiments used an undulated pencil beam in a rectangular waveguide [40]. They presented unique features such as a very broad interaction bandwidth which results from the absence of a dispersive slow wave circuit, a variable interaction phase velocity, and hence, variable saturation power level.

Among the physical embodiments of the ubitron are a number of higher-order mode waveguides and beam configurations. They opened at that time interesting prospects for high-power millimetre wave amplification. As reports C. Brau [1], “the ubitron uses the same configuration of electron beam and magnetic field as proposed by Motz, but at a high enough electron density that space-charge waves are excited by the electron beam”. High power (>1 MW) and high efficiency ($>10\%$) were obtained at wavelengths from 10 cm to 5 mm. However, other devices developed at about the same time, such as the travelling-wave tube, offered higher gain and other advantages, and the ubitron was not actively pursued.

Studies were extended to the interaction of relativistic particles and waves in the presence of a static alternated magnetic field [41]. The possibility of achieving stimulated emission [42] was also considered.

2.6 The maser discovery

After the second World War, RF sources and detectors developed for radar and transmission were also used for fundamental research, in particular Hertzian spectroscopy of atoms and molecules, radio-astronomy, and magnetic nuclear resonance. In the early fifties (1953), Charles Townes (1905–2015, Nobel Prize in 1964) [43] in the USA (Columbia University, New York), Nicolay Gennadiyevich Basov (1922–2001, Nobel Prize in 1964) in 1952), and Aleksandr Mikhailovich Prokhorov (1916–2002, Nobel Prize in 1964) in the Soviet Union (Lebedev Institute, Moscow) independently aimed at creating new microwave sources in replacing the amplification by an electron beam amplification with the help of the stimulated emission process in molecules. In order to make a ‘quantum’ microwave oscillator, they introduced excited molecules into a microwave cavity which was resonant to the frequency of the molecule transition. They met for the first time in 1959 in the USA at the first Quantum Electronics Conference. Some physicists were sceptical, including N. Bohr (1885–1962, Nobel Prize in 1922), who was not very familiar with recent advances in electronics and could hardly admit that the phase coherence of the oscillator could last longer than the excited state lifetime. To perform the population inversion required for the stimulated emission, Townes, Basov, and Prokhorov had the idea to use the spatial separation of excited molecules (Stern–Gerlach type), which is efficient but not very practical. The population inversion can also be performed in an easier manner by a proper excitation of the radiation of the atoms and molecules. In 1949, Alfred Kastler (1902–1984, Nobel Prize in 1966) and Jean Brossel proposed and developed ‘optical pumping’, based on the use of circularly polarized light for selectively filling some Zeeman sub-levels of atoms. In 1951, E. Purcell and R. Pound, working on nuclear magnetic resonance, showed that RF radiation enables us to create samples of ‘negative temperature’, i.e. a population inversion. Inspired by the resonators of vacuum tubes, the light feedback is ensured by a cavity resonant on its fundamental mode.

In 1954, the first maser (microwave amplification by stimulated emission of radiation) was operated in the microwave region by Charles Townes [43] at Columbia University with the NH_3 molecule. In 1954, N. Bloembergen (Nobel Prize 1981 on laser spectroscopy and non-linear optics), Basov, and Prokhorov proposed the 3-level maser concept: with a proper illumination of a solid such as a ruby crystal, population inversion takes place. It is easier to operate than the equivalent gas-based maser. It has been used in particular as a very low noise amplifier.

Masers also exist naturally in stars.

The new domain of ‘quantum electronics’ has emerged from the interplay between the scientific fields of electronic vacuum tubes and quantum properties of matter and it has seen an extraordinary spread and has raised a lot of interest. The question was then of the extension of the maser to the optical wavelengths.

2.7 The laser discovery

In order to achieve an optical maser, the maser cavity resonant on its fundamental mode must become extremely small (of the order of 1 micrometre) and this was not possible at that time. Nowadays, these cavities are manufactured using nanotechnologies (for VCSEL (vertical cavity surface emitting laser) semi-conductor lasers). Charles Townes and Arthur L. Schawlow (1921–1999, Nobel Prize in 1981 on laser spectroscopy and non-linear optics) at Bell Labs, G. Gould (1920–2005) at Columbia [44], and A. Prokhorov at the Lebedev Institute proposed feedback with an open resonant cavity (Fabry–Perot-type used in spectroscopy). These ‘optical lasers’ were named lasers for light amplification by stimulated emission of radiation.

In a Fabry–Perot cavity of length L_c , the light makes round trips between the two mirrors on which it is reflected. C. Townes and A. Schawlow said, in their reference paper [4]:

“The extension of maser techniques to the infrared and optical region is considered. It is shown that by using a resonant cavity of centimetre dimensions, having many resonant modes, maser oscillation at these wavelengths can be achieved by pumping with reasonable amounts of incoherent light. For wavelengths much shorter than those of the ultraviolet region, maser-type amplification appears to be quite impractical. Although using of a multimode cavity is suggested, a single mode may be selected by making only the end walls highly reflecting, and defining a suitably small angular aperture. Then extremely monochromatic and coherent light is produced. The design principles are illustrated by reference to a system using potassium vapor”.

A scheme of such an optical cavity is shown in Fig. 12.

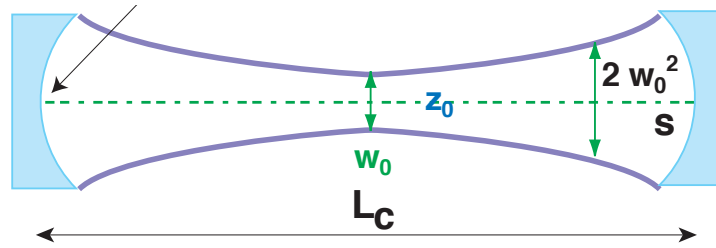


Fig. 12: Scheme of an optical resonator

For the light to interact at each pass with the amplifier medium, and to get larger, it should be in phase with the one from the previous pass. In other words, the optical path for one round trip should be equal to an integer number p of wavelengths λ , i.e. $2L_c = p\lambda$. For a fixed cavity length L_c , only the wavelengths verifying $\lambda = \frac{2L_c}{p}$ can be present in the ‘optical maser’ light, defining the longitudinal modes of the cavity associated with different values of p . The shift in frequency between two modes is given by $\nu = \frac{c}{\lambda} = \frac{c}{2L_c}$.

In practice, in order to focus the light transversally and to avoid diffraction losses, one of the mirrors should be concave. The light circulating in the optical resonator is not a plane wave, and the radius of the light changes along its propagation direction [45,46]. In case of a cavity with two concentric mirrors, the light radius is minimum at the waist w_0 and diverges according to $w(s) = w_0 \sqrt{1 + \frac{s^2}{Z_R^2}}$ with Z_R the Rayleigh length, i.e. the distance from the waist for which the radius of the light beam is increased by a factor $\sqrt{2}$, given by $Z_R = \frac{\pi w_0^2}{\lambda}$. This corresponds to the diffraction of light by an aperture of diameter $2w_0$. The radiation at the entry and at the exit of the cavity have the same characteristics. The divergence of the light beam θ_r can be expressed as $\theta_r = \frac{\lambda}{\pi w_0}$. The higher the focus, the smaller the waist and the higher the beam divergence. The beam is very directional, it can be adapted (focused or expanded) to the users need with the help of mirrors and lenses. In the case of a He–Ne laser at 633 nm with a waist of 600 μm , the Rayleigh length is of the order of 2 m. Over 2 m propagation length, the light beam diameter remains practically constant.

Following the publication of the theoretical paper by Arthur L. Schawlow and C. Townes on ‘Infrared and Optical masers’ in 1958 [4], different laboratories entered the race to demonstrate experimentally the ‘optical maser’. It was won by an outsider in 1960, Theodore Maiman (1927–2007), who had the idea to realize a pulsed and not a CW (continuous) source, for which the oscillation conditions take place transiently. On May 6 1960, Maiman achieved the first working laser by generating pulses of coherent light from a fingertip-sized lump of ruby (chromium in corundum) illuminated by a flash lamp [5,47] in Malibu (USA). The device was extremely simple. Several ‘optical masers’ followed [48]. The calcium fluoride laser was achieved by Mirek Stevenson and Peter Sorokin at General Electric in 1960. The He–Ne laser was operated by Ali Javan (1926–2016), Bill Bennett, and Don Herriott in 1961 [49], with the population inversion achieved with a discharge on the Ne atoms bringing a fraction of the He atoms to metastable states, the He atoms being relaxed by collision with Ne atoms in transmitting to them their energy excess. Then, in 1962 followed the semi-conductor AsGa laser (diode laser) where a p–n junction of the gallium arsenide semiconductor through which a current was passed and it emitted near-infrared light from recombination processes with very high efficiency, first operated by R. Hall (1919–) [50] and others [51].

3 The invention of the free electron laser concept

3.1 The FEL concept emergence: motivations for an exotic laser

Early work on stimulated bremsstrahlung was conducted at the beginning of the twentieth century [52,53] and later [54].

Following the discovery of the laser, much less interest was devoted to the electron tube based systems. The Gaussian eigenmodes of free space provided an alternative to the coupled slow wave structures of the prior electron devices. In addition, the laser radiation is independent of phase.

In the original paper from A. Schawlow and C. Townes [4], it was written that “As one attempts to extend maser operation towards very short wavelengths, a number of new aspects and problems arise, which require a quantitative reorientation of theoretical discussions and considerable modification of the experimental techniques used” and “These figures show that maser systems can be expected to operate successfully in the infrared, optical, and perhaps in the ultraviolet regions, but that, unless some radically new approach is found, they cannot be pushed to wavelengths much shorter than those in the ultraviolet region”.

J. M. J. Madey (1943–2016, first FEL Prize in 1988) [55], from Stanford University, thought that “A. Schawlow and C. Townes descriptions of masers and lasers coupled with the new understanding of the Gaussian eigenmodes of free space offered a new approach to high frequency operation that was not constrained by the established limits to the capabilities of electron tubes” [56] and he wondered whether there was “a Free Electron Radiation Mechanism that Could Fulfill these Conditions” and considered the different possible radiation processes. He first examined Compton scattering, as shown in Fig. 13, which appeared as the most promising candidate. Indeed, stimulated Compton backscattering has been analysed by Dreicer in the cosmic blackbody radiation [57].

First analysis of the stimulated Compton backscattering was carried out by Pantell (eighth FEL Prize in 1995, shared with G. Befeki (1925–1995)) [42]. Precursor works include the study of stimulated emission of bremsstrahlung [58], and of the possibility of frequency multiplication, and wave amplification by means of some relativistic effects [37], radiation transfer and investigations into whether negative absorption (i.e. amplification) could be possible in radio astronomy [59].

The Compton backscattering (CBS) process between a laser pulse and a bunch of relativistic particles (electrons, positrons, etc.) leads to the production of high-energy radiation coming from the head-on collision between the photons and the particles. In order to reduce the divergence of the scattered radiation, it is better to use a relativistic electron beam, which radiation cone is reduced to $1/\gamma$. For relativistic particles (i.e. $\gamma \gg 1$), the energy of the produced photons E_{CBS} is given by

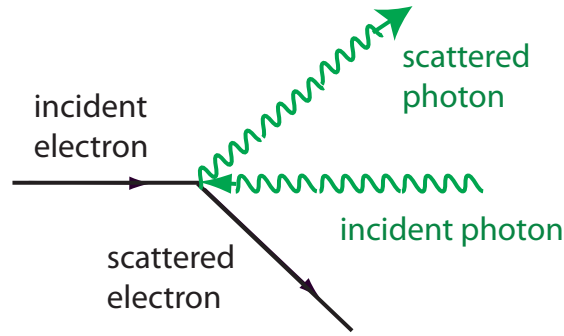


Fig. 13: Compton backscattering scheme

$$E_{\text{CBS}} = \frac{4\gamma^2 E_{\text{ph}}}{1 + (\gamma\theta)^2} \quad (24)$$

with E_{ph} the energy of the initial photon beam, θ the angle between the CBS photons and the electron beam trajectory. The energy of the relativistic electrons can easily be changed, so the CBS radiation could be tuneable.

J. M. J. Madey had the idea to make the phenomenon more efficient by using the magnetic field of an undulator [6]. He was aware of the theoretical [28] and experimental [30] work of Motz, where radiation from bunched beams has been observed. He considered that “Relativistic electrons can also not tell the difference between real and virtual incident photons, permitting the substitution of a strong, periodic transverse magnetic field for the usual counter-propagating real photon beam” [56]. The proposed FEL scheme is shown in Fig. 14.

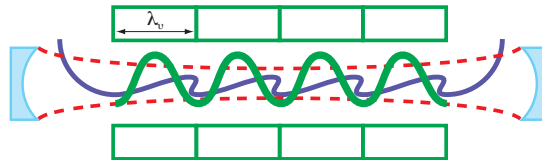


Fig. 14: Scheme of the FEL oscillator with the gain medium consisting of relativistic electrons in the undulator

3.2 The FEL quantum approach

J. M. J. Madey then calculated in the frame of quantum mechanics the gain due to the induced emission of radiation into a single electromagnetic mode parallel to the motion of a relativistic electron through a periodic transverse dc magnetic field [6]. He found that finite gain is available from the far-infrared through the visible region, raising the possibility of continuously tuneable amplifiers and oscillators in such a spectral range, and he envisioned further the possibility of partially coherent radiation sources in the ultraviolet and X-ray regions to beyond 10 keV. He introduced the notion of the ‘free electron laser’ [6].

According to the Weisächer–Williams approximation, the undulator field of period λ_u can be assumed to be a planar wave of virtual photons. It enables an easier way to relate the transition rates to more easily calculable Compton scattering rates. By Lorentz transformation, the wavelength λ' of a planar wave in the moving frame of the electrons in the undulator is given by

$$\lambda' = \frac{\lambda_u}{\gamma_s} \quad (25)$$

with γ_s the Lorentz factor of the scattered electron. Photon emission and absorption are forbidden by conservation of energy and momentum. For free electrons, one can then consider a two photon process, such as Compton scattering, as shown in Fig. 15.

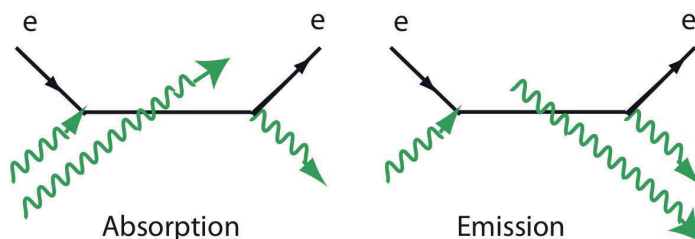


Fig. 15: Feynman diagrams of Compton scattering

The emission is then again given by the Doppler effect, according to

$$\lambda = \frac{\lambda'}{(1 + \beta_s)\gamma_s} = \frac{\lambda_u^2}{2\gamma_s^2} \approx \frac{\lambda_u^2}{2\gamma^2}. \quad (26)$$

For stimulated Compton scattering, the diffusion transition rate τ_d should be larger than the absorption one τ_a . One can define the gain g as

$$g = \tau_d - \tau_a. \quad (27)$$

The original calculation, performed in [6, 60], is not reproduced here. It was also found that the gain expression does not depend on Planck's constant h . Further developments followed [61].

The ubitron can also be considered as another precursor of the FEL [39].

3.3 The FEL regimes

Different regimes can be considered [62]. The FEL can thus be described as a stimulated Compton scattering device, as shown in Fig. 16. If the electronic density is large enough, a plasma wave can develop.

3.3.1 The Compton FEL regime

In the Compton regime, the scattered wavenumber k'_s equals the incident wavenumber k'_i :

$$k'_s = k'_i. \quad (28)$$

3.3.2 The Raman FEL regime

In the Raman regime, the scattered wavenumber k'_s is the sum/difference of the incident wavenumber k'_i and of the plasma wavenumber k'_p , leading to the Stokes and anti-Stokes lines.

$$k'_s = k'_i \pm k'_p. \quad (29)$$

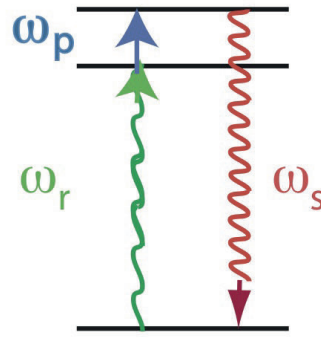


Fig. 16: Stimulated Compton scattering scheme in the electron frame, with ω_p the plasma pulsation, ω_r the resonant pulsation, and ω_s the scattered pulsation.

In the laboratory frame, it comes to $\omega_s = \omega_i \pm \omega_p$ where the plasma pulsation ω_p is given by $\omega_p = \sqrt{\frac{n_e e^2}{\epsilon_0 m_0 \gamma^3}} = \sqrt{\frac{J_e e}{\epsilon_0 m_0 c \gamma^3}}$ with n_e the electronic density, ϵ_0 the vacuum permeability, and J_e the current density $J_e = n_e e c$.

Practically, one considers that the FEL is in the plasma regime if the number of plasma oscillations N_p done by the electron while it travels into the undulator is at least one:

$$N_p = \frac{N_u \lambda_u}{\lambda_p} = \frac{N_u \lambda_u \omega_p}{2\pi c} = \frac{N_u \lambda_u}{2\pi c} \sqrt{\frac{J_e e}{\epsilon_0 m_0 c \gamma^3}}$$

Thus $N_p > 1$ if $J_e < \frac{4\pi^2 \epsilon_0 m_0 c^3 \gamma^3}{e N_u^2 \lambda_u^2}$.

The regimes of FEL are recapitulated in Fig. 17.

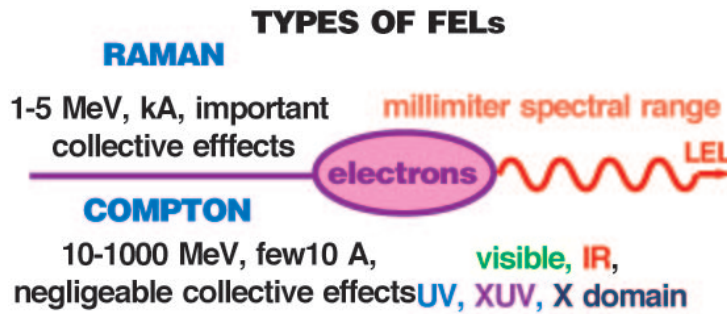


Fig. 17: Comparison between Compton and Raman FELs

4 The FEL classical approach (low gain regime)

4.1 Stimulated scattering in a plasma fluid type approach

P. Sprangle (fourth FEL Prize, in 1991) continued the exploration of stimulated Compton scattering of an electromagnetic wave from relativistic electrons [42, 61] using a plasma approach. Sprangle and Granatstein examined the stimulated cyclotron resonance scattering and production of powerful submillimetre radiation [63] and stimulated collective scattering from a magnetized relativistic electron beam [64]

where the pump satisfies the dispersion relation associated with the beam in the magnetic field and the scattered waves consist of collective plasma oscillations as well as right- and left-polarized electromagnetic waves, travelling parallel and antiparallel to the beam. The frequency of the forward-scattered electromagnetic wave is Doppler shifted. Conditions for enhanced stimulated scattering and growth rates were found [64]. An original following work on noise excitation analysis [65] can be mentioned. Variants of FEL were considered, such as the gyrotron with a uniform magnetic field [66]. Saturation and phase (wave refractive index) were analysed [67]. The Raman-type theoretical developments are not detailed here [68, 69].

4.2 The FEL classical approach using the Weizsäcker–Williams approximation and electronic distribution function

F. A. Hopf *et al.* [70] continued the investigation of stimulated emission of radiation in a transverse magnetic field. He pointed out that the theories explored so far [6, 42, 57, 60, 61] were all “quantum mechanical in nature. They give impression that they have to be so, since it is argued that it is the electron recoil $\Delta p = h/\lambda_c$ where λ_c is the Compton wavelength, which is the source of the finite gain. Furthermore, quantum approaches, while agreeing on the structure of the gain formula, differ from one another by orders of magnitude in numerical coefficients” [70]. He then shows that “this problem is completely classical, and that the gain is produced by a bunching of the electron density in the presence of a field”.

He works directly in the laboratory frame. Considering the Weizsäcker–Williams approximation and in the case of the extreme relativistic limit, the static undulator field of period λ_u can be replaced by a pure electromagnetic field of wavelength $\lambda_i = (1 + \beta_s)\lambda_u \approx 2\lambda_u$. The electron motion is treated via the collisionless relativistic Boltzmann equation, according to

$$\frac{df}{dt} = \frac{\partial f}{\partial t} + \dot{x}_i \frac{\partial f}{\partial x_i} + \dot{P}_i \frac{\partial f}{\partial P_i} = 0, \tag{30}$$

with \mathbf{P} the canonical momentum, \mathbf{x} the position and dot the total derivative with respect to time.

The total number of electrons $N(t)$ is given by $N(t) = \int d^3x \int f(\mathbf{x}, \mathbf{P}, t) d^3P$.

The Boltzmann equation is coupled to the transverse current \mathbf{J}_t via the Maxwell equation, and is given by

$$\mathbf{J}_t = e \int \mathbf{v}_T f(\mathbf{x}, \mathbf{P}, t) d^3P, \tag{31}$$

with \mathbf{v}_T the transverse velocity. The scheme is sketched in Fig. 18.

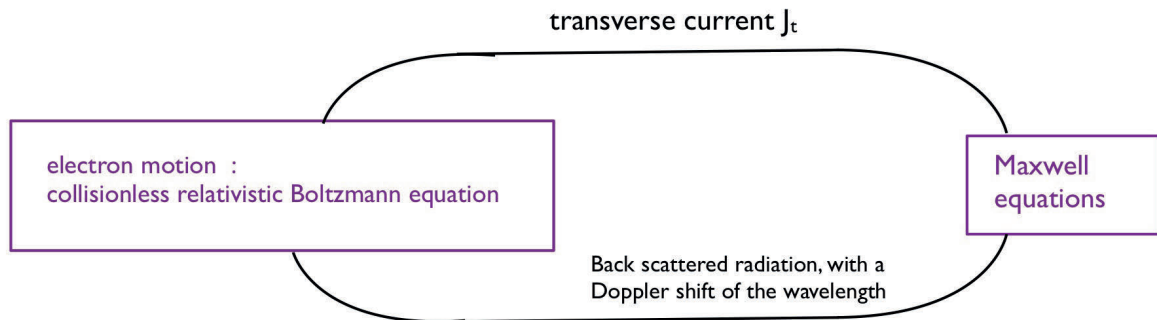


Fig. 18: Diagram of the low gain FEL classical theory using the Boltzmann equation for the movement of the electrons in the undulator and the scattering process.

By assuming that:

- the electromagnetic field is transverse and depends on s and t ;
- the transverse velocity spread of the electronic distribution is neglected since the electrons propagate with a relativistic velocity along the direction s ;
- the mass shift for electric fields smaller than 10^{12} V/m,

the problem is reduced to a one-dimensional one. The interaction term of the reduced Boltzmann equation is similar to the one in the Klein–Gordon Hamiltonian, and the source term of the reduced Maxwell equation is “proportional to a density times an electric field. This is exactly the same as in usual scattering problems, where the d’Alembertian of the electric field is proportional to the second derivative of the polarization, which is in turn proportional to a density times the electric field. Hence, we see at this point that the problem at hand is nothing else than a usual classical scattering problem, complicated only by the fact that we deal here with relativistic particles” [70]. Then, the reduced distribution is developed in perturbation series, the first order giving the small-signal theory. In this case, only two modes of the field are kept, the incident one (i.e. the static periodic magnetic field in the Weizsäcker–Williams approximation), and the scattered one. The relevant scattered mode in the up-conversion scheme is the backscattered radiation, which propagates in the direction of the electron beam. Its wavelength is Doppler shifted, as seen previously. New assumptions are made:

- the amplitude and phase are slowly varying;
- the depletion of the incident field is neglected since it is assumed to be very intense;

enabling us to find the first-order term of the reduced electron distribution function $h^{(1)}(s, P_s, t)$, expressed as

$$h^{(1)}(s, P_s, t) = -\frac{e^2(k_s + k_i)n_e A_i^* A_s}{P_s} \frac{dF}{dP_s} \frac{\exp(-i\mu s) - 1}{\mu} \exp(-i\Delta\omega(t - s/v_s)) + c.c. \quad (32)$$

where k_i (respectively k_s) is the wavenumber of the incident (scattered) field, A_i (respectively A_s) is the vector potential of the incident (scattered) field, $F(P_s)$ the initial electron momentum distribution, $\Delta\omega = \omega_s - \omega_i$ with ω_i (respectively ω_s) the pulsation of the incident (scattered) field, and $\mu = \Delta\omega - (k_s + k_i)$. “ $h^{(1)}(s, P_s, t)$ describes electron density fluctuations [70] (bunching) which are responsible for the scattering”. Here, Hopf is pointing out that the bunching is a key process for the FEL interaction. Introducing the reduced electron distribution into the Maxwell equations, one finds the small-signal low gain expression. In the case of the small cavity limit (where the initial electron momentum distribution function $F(P_s)$ can be taken as a δ function, i.e. to the limit of a homogeneously broadened medium), the total small-signal gain is given by

$$g \cong 64\pi^2 r_o^2 F_f \frac{n_e}{mc^2} \frac{k_i^{1/2}}{k_s^{3/2}} L_c^2 I_i \frac{d(\sin \eta_c / \eta_c)^2}{d\eta_c} \quad (33)$$

with $\eta_c = \mu L_c / 2$, r_o the classical radius of the electron, F_f the filling factor term representing the transverse overlap (ratio of the electron beam transverse to the section of the optical beam in the cavity), I_i the incident flux. Different cases occur.

- If $\eta_c = 0$ there is exact conservation of momentum, and no net gain.
- If $\eta_c < 0$ (i.e. for electrons with a velocity $v > v_o$), the net result is a gain. It is the equivalent of the Stokes line in Raman scattering.
- If $\eta_c > 0$ (i.e. for electrons with a velocity $v < v_o$), the net result is an absorption. It is the equivalent of the anti-Stokes line in Raman scattering.

The maximum gain is found for $\eta_c = -\pi/2$ in agreement with the Madey result derived in the quantum mechanics frame within a factor 0.8. It is worth citing part of the conclusion “that the free-electron laser is a completely classical device. The stimulated scattering producing amplification is due to electron bunching, rather than to the Compton recoil, as argued previously. This result not only is important from an academic viewpoint, but also greatly simplifies the analysis of the strong-signal regime and of the saturation of this new laser” [70]. The major step here is the understanding that the gain results from a bunching of the electronic density in the presence of a field.

Two months later, Hopf continued with the strong-signal case “In order to assess the potential of any practical laser device, it is necessary to *complement* the small-signal theory by an analysis of the mechanism of saturation” [71]. In the strong signal case (i.e. for ‘long’ undulator, ‘high’ current), the change of electric field in one pass cannot be neglected anymore. The undulator is still treated in the frame of the Weizsäcker–Williams approximation. The coupled Maxwell–Boltzmann equations are reduced differently from the small-signal case where the longitudinal part of the Boltzmann distribution function h was expanded in powers of $|A_i A_s|$ limited to the first order. Here, h is then expressed as a harmonic expansion (previous expansion to higher orders would diverge), leading to a set of generalized Bloch equations in keeping the first term of the expansion. These generalized Bloch equations have “a striking resemblance to the optical Bloch equations” involving an equivalent “population inversion” and “polarization” term. “However, it differs from them in two respects”. “This difference in structure lies in the fact that in a free electron laser, the gain is not proportional to the electron distribution function. It is its derivative with respect to p_s , (rather than the gain itself) which plays the role of an inversion.” By supposing that the saturation mechanism corresponds to “deceleration of the electrons through the gain line to the point of zero gain”, one can express a saturation flux and find the “maximum field extractable from a free-electron laser (i.e. the output field when the laser is in the saturation regime)” [71] as

$$A_{\text{sat,max}} \cong \left[\frac{\lambda_s}{L_c} \right]^2 \frac{M^2 c^2 \gamma^4}{e^2} A_i. \quad (34)$$

He then computed the efficiency in the case of the Stanford experiment, and found it to be of the order of 5×10^{-3} . He deduces that “This implies that free electron lasers have the potential to work at high power, but they must be operated in a pulsed mode, with small per shot efficiency.” He just pointed out that the previously described analysis is very simplified: “In reality, a more detailed analysis shows that a major contribution to the saturation is a strong alteration of the electron distribution such that the laser eventually reaches the large- cavity limit”. Hopf *et al.* had shown here that FELs “have the potential to work at high power”.

The expansion of the Boltzmann distribution function was then not limited to the first term, and the problem reduces to the Klein–Gordon equation [72]. A theory including Raman scattering has also been developed [62, 73, 74].

In Madey’s and Hopf’s approaches, the FEL has been explained in terms of collective phenomena. Single particle theory can also be applied, as described below.

4.3 The classical approach considering the relativistic motion of the electrons in the undulator

W. B. Colson (Second FEL prize, 1989) aimed at a broader theoretical framework. He analysed the radiation from electrons travelling through a static transverse periodic magnetic field with classical, semi-classical, and quantum field theories. He considered the radiation characteristics of the electrons in the undulator and developed stimulated emission rates and laser evolution equations describing exponential gain and saturation [75]. His paper was published the same month as the second publication by F. A. Hopf [71]. He insisted on the importance of including the filling factor term, representing the overlap between the electron beam and the optical wave. W. B. Colson received the Second FEL Prize after

J. M. J. Madey, in 1989 “Bill laid the foundation for the classical theory of Free Electron Laser, enabling a wide audience to understand the operating principles of FEL”. He gave “an outstanding contribution to the understanding of free electron laser mechanisms”.

4.3.1 Resolution of the one-body classical Lorentz equation in the presence of a periodic magnetic field and a plane electromagnetic wave

W. B. Colson looked for a more appropriate magnetic field description and by “solving the one-body classical Lorentz force equation in presence of periodic magnetic field and a plane electromagnetic wave” [76,77]. He found that “the non-linear electron dynamics to the phase space paths of a simple pendulum in the limit of small gain. The position and energy of a single electron are simply expressed as a function of time”. He was able to determine the gain and to link it to the derivative of the sinc-like function describing the spontaneous emission [75], the electron modulation, and the saturation for strong laser fields corresponding to closed phase space paths, where the electron beams becomes resonant and the gain drops. He insisted on the “importance of the electron beam produced by the FEL device. The combined magnet and radiation fields conspire in a controlled way to yield a *coherently modulated relativistic electron beam*”. It is found that the evolution of the system follows the pendulum equation which has been widely adopted and will be presented below. The FEL Prize recipient receives a clock, symbolizing the FEL pendulum equations! Phase space paths are illustrated in Fig. 19. The electrons that are initially resonant and on a phase equal to an integer p times π , corresponding to points in phase space located at $(p\pi, 0)$, do not contribute to work. Electrons near these points evolve very slowly in time, with motion at ‘even- p ’ points being stable and ‘odd- p ’ unstable. In analogy, a simple pendulum would be at the bottom (p -even) or top (p -odd) of its arc. If an electron is not at a critical point, the radiation field alters its energy and position. A shift in relative position, proportional to the square of the pendulum frequency, occurs and redistributes electrons along the beam axis. For an initially uniform, mono-energetic beam, half the electrons within a given λ_r are positioned such that work is done on them; they gain energy and move ahead of the average flow. The rest of the electrons loose energy to the radiation field and move back. This causes the ‘bunching’ of the beam. Electrons can undergo closed and open orbits.

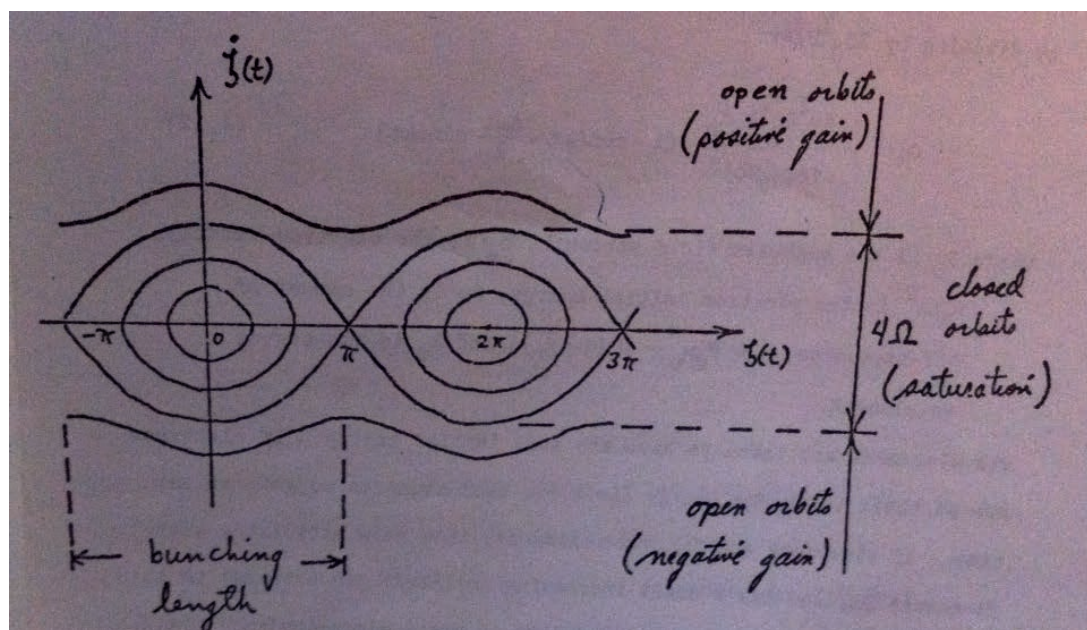


Fig. 19: Electron phase space paths in the case of the pendulum for a helical undulator (low gain regime), from [78]

Then, the electron motion is depicted with a Hamiltonian approach, while the phase space repre-

sensation of the pendulum is deepened and the influence of the detuning (delay between the electrons in the undulator and optical pulses in the optical cavity) is studied [79]. The importance of the ‘bunched’ beam is emphasized and the use of an external laser with a static periodic field to create the modulation at optical wavelengths is considered.

The model is then described self-consistently, using single particle dynamics and Maxwell’s equations. The optical wave evolution is governed by Maxwell’s equation in the presence of an electron current. Assuming that the amplitude and phase are slowly varying, two differential equations describing the amplitude and the phase of the wave are found. The dynamics of the electrons is ruled by the Lorentz equations in the presence of the combined static and radiated fields. The total current results from the sum of all individual particle currents. The two sets of equations are then combined. It is found that the microscopic electron bunching drives the amplitude and phase of the optical wave [80] as shown in Fig. 20. The saturation is well described within the frame of the self-consistent pendulum equation: “When the radiation field becomes large, the electron becomes trapped in closed orbits of the pendulum phase space. In the beam frame, the bunching electrons will have moved on the order of an optical wavelength: at this point, the gains tops and the laser saturates” [80].

The model is then applied to study the operation on higher harmonics [81–83], as developed later.

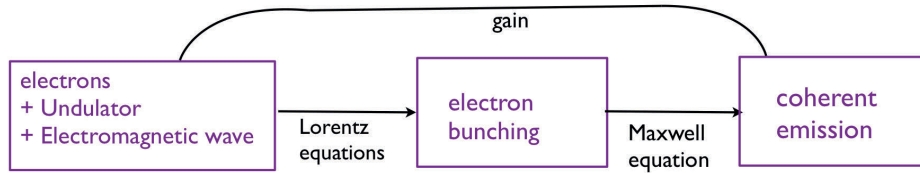


Fig. 20: Diagram of the low gain FEL classical theory using the movement of the electrons in the undulator and the interaction with the electromagnetic wave.

This approach using the description of the electron motion in the undulator, energy exchange, properly described with the pendulum equation enables us to explain the laser gain, saturation, and coherent electron beam modulation. It is described, complete with informative phase space plots, in the textbook [84]. A tutorial is also available [85].

4.3.2 Ponderomotive phase

Let’s consider a plane wave travelling in the same direction as the electron, with its electric field in the trajectory plane. This wave can be the stored spontaneous emission in the optical cavity. The electrons in a vertical magnetic field of a planar undulator are submitted to the electric field \vec{E}_1 given by $\vec{E}_1 = E_1 \cos(k_s - \omega t + \phi) \vec{e}_s$ propagating along the direction s , with ϕ the phase of the monochromatic plane wave with respect to each single electron. The work ΔW between the times t_1 and t_2 is given by

$$\Delta W = e \int_{t_1}^{t_2} c \vec{\beta} \cdot \vec{E}_1 dt. \quad (35)$$

The energy exchange only takes place via the transverse component of the velocity, so the vertical magnetic field efficiently couples the electrons and the radiation. Using $\beta_x = \frac{K_u}{\gamma} \sin(k_u s)$:

$$\Delta W = \int_{t_1}^{t_2} \frac{e K_u E_1}{\gamma} \sin(k_u s) \cos(k_s - \omega t + \phi) dt. \quad (36)$$

Using $s = c\beta_s t$, $k_u s = \omega_u \beta_s t$, $k_s = \omega \beta_s t$, and defining $\Delta\Omega_1 = (\omega_u \beta_s + \omega(1 - \beta_s))$ and $\Delta\Omega_2 = (\omega_u \beta_s - \omega(1 - \beta_s))$, after some trigonometry we have: $\Delta W = \int_{t_1}^{t_2} \frac{e K_u E_1}{2\gamma} (\sin(\Delta\Omega_1 t + \phi) + \sin(\Delta\Omega_2 t - \phi)) dt$. A wave beating with two frequencies $\omega_u \beta_s \pm \omega(1 - \beta_s)$ takes place.

The so-called ponderomotive phase ψ , i.e. the phase of the n th harmonic of the electron wiggles with respect to the wave, is introduced as

$$\psi = (nk_u + k)s - \omega t. \quad (37)$$

The energy exchange due to the ponderomotive phase ψ is developed at first order, resulting in $\Delta W = - \int_{t_1}^{t_2} \frac{eK_u E_1}{2\gamma} (\sin(\psi + \phi - (n-1)k_u s) - \sin(\psi + \phi - (n+1)k_u s)) dt$.

Provided that the energy changes slowly compared with the period of an undulator, the longitudinal motion can be expressed as the sum of the fast term along the s direction at twice the pulsation and the slow evolution \tilde{s} caused by the FEL interaction, according to $s = \tilde{s} + s_w$ where the mean motion satisfies $\langle \beta_s \rangle = 1 - \frac{1}{2\gamma^2} (1 + \frac{K_u^2}{2})$ in which the energy γ varies along the length of the undulator. To first order in $\frac{1}{\gamma^2}$, the longitudinal oscillation can be written as $s_w = \frac{K_u^2 \lambda_u}{16\pi\gamma^2} \sin(2\omega_u t) = \frac{K_u^2}{8\gamma^2 k_u} \sin(2k_u \tilde{s})$. The phase can be expressed as

$$\psi = \zeta + \psi_w, \quad (38)$$

with $\psi_w = \frac{K_u^2 k}{8\gamma^2 k_u} \sin(2k_u \tilde{s})$ and $\zeta = (nk_u + k)\tilde{s} - \omega t$. The ponderomotive phase evolves as

$$\frac{d\zeta}{dt} = (nk_u + k) \frac{d\tilde{s}}{dt} - \omega = (nk_u + k) \left(1 - \frac{1 + \frac{K_u^2}{2}}{2\gamma^2} \right) c - kc = nk_u - nk_u \left(\frac{1 + \frac{K_u^2}{2}}{2\gamma^2} \right) c - k \frac{1 + \frac{K_u^2}{2}}{2\gamma^2} c.$$

Since $nk_u \ll k$, it becomes

$$\frac{d\zeta}{dt} = nk_u c - k \frac{1 + \frac{K_u^2}{2}}{2\gamma^2} c.$$

Then ψ given by $\psi = \zeta + \psi_w$ is inserted into the energy exchange expression, leading to

$$\Delta W = - \int_{t_1}^{t_2} \frac{eK_u E_1}{2\gamma} (\sin(\zeta + \psi_w + \phi - (n-1)k_u \tilde{s}) - \sin(\zeta + \psi_w + \phi - (n+1)k_u \tilde{s})) dt. \quad (39)$$

4.3.3 FEL resonance

The plane wave travelling in the same direction as the electron is shown in Fig. 21. The electron is resonant with the light wave of wavelength λ_r if, when the electron progresses by λ_u , the wave has travelled $\lambda_u + \lambda_r$ or more generally, with n being an integer, by $\lambda_u + n\lambda_r$.

The travel times of the electron and the photon can be written as $\frac{\lambda_u}{v_s} = \frac{\lambda_u + n\lambda_r}{c}$, so

$$\lambda_r = \frac{\lambda_u}{n} \left(\frac{1}{\beta_s} - 1 \right) = \frac{\lambda_u}{n} \left(\frac{1 - \beta_s}{\beta_s} \right) = \lambda_u \frac{1 - \beta_s^2}{\beta_s (1 + \beta_s)}.$$

In the planar undulator case, with $\beta_s \approx 1$ and $1 - \beta_s^2 = \frac{1}{\gamma^2} + \frac{K_u^2}{\gamma^2}$, the resonant wavelength becomes

$$\lambda_r = \frac{\lambda_u}{2n\gamma^2} \left(1 + \frac{K_u^2}{2} \right) \quad (40)$$

and in the helical undulator case

$$\lambda_r = \frac{\lambda_u}{2n\gamma^2} (1 + K_u^2). \quad (41)$$

The infrared spectral range can be reached with reasonable beam energies. The resonance can also be scanned either by changing the electron beam energy or by modifying the magnetic field of the undulator.

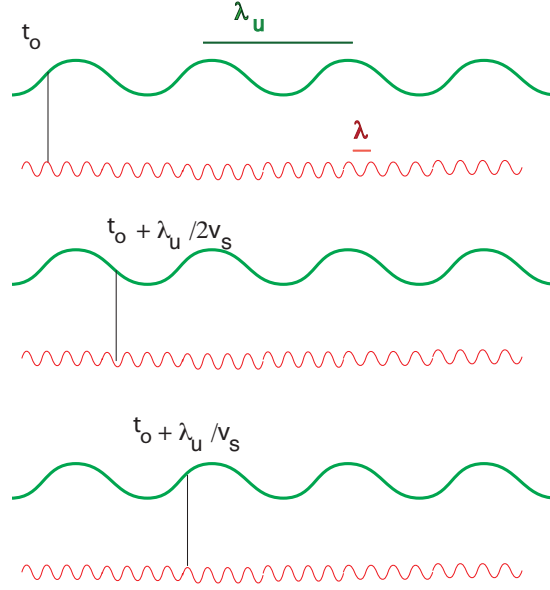


Fig. 21: Undulator resonance condition: when the electron progresses by λ_u , the wave has travelled by $\lambda_u + \lambda$, t_0 is the time origin, v_s is the longitudinal velocity of the electrons.

The resonance is generalized for the electron phase to be stationary $\frac{d\zeta}{dt} = 0$, it leads to the expression of the resonant energy given by the undulator γ_r ,

$$\gamma_r^2 = \frac{1}{2n} \left(1 + \frac{K_u^2}{2}\right) \frac{\lambda_u}{\lambda} = \frac{1}{2n} \left(1 + \frac{K_u^2}{2}\right) \frac{k}{k_u}. \quad (42)$$

One considers electrons with a relative energy difference with respect to the resonance given by

$$\eta = \frac{\gamma - \gamma_r}{\gamma}. \quad (43)$$

4.3.4 Pendulum equations

Let us consider now the phase given by

$$\zeta = (nk_u + k)\tilde{s} - \omega t. \quad (44)$$

It evolves as

$$\frac{d\zeta}{dt} = (nk_u + k) \frac{d\tilde{s}}{dt} - \omega = (nk_u + k) \left(1 - \frac{1 + \frac{K_u^2}{2}}{2\gamma^2}\right) c - kc = nk_u - nk_u \left(\frac{1 + \frac{K_u^2}{2}}{2\gamma^2}\right) c - k \frac{1 + \frac{K_u^2}{2}}{2\gamma^2} c.$$

Since $nk_u \ll k$, it becomes $\frac{d\zeta}{dt} = nk_u c - k \frac{1 + \frac{K_u^2}{2}}{2\gamma^2} c$. Then, using $1 + \frac{K_u^2}{2} = \gamma_r^2 2n \frac{k_u}{k_r}$, one finds

$$\frac{d\zeta}{dt} = nk_u c - nk_u c \frac{\gamma_r^2}{\gamma^2} = nk_u c \left(1 - \frac{\gamma_r^2}{\gamma^2}\right) = nk_u c \frac{(\gamma - \gamma_r)(\gamma + \gamma_r)}{\gamma^2} = 2nk_u c \frac{(\gamma - \gamma_r)}{\gamma}.$$

It then becomes

$$\frac{d\zeta}{dt} = 2nk_u c \eta. \quad (45)$$

With the Lorentz equation $\frac{d\gamma}{dt} = \frac{e\vec{E}\cdot\vec{v}}{m_0c^2}$, one gets

$$\frac{d\gamma}{dt} = -\frac{eE_1K_u}{2\gamma m_0c} \left[J_{\frac{n-1}{2}}(\xi) - J_{\frac{n+1}{2}}(\xi) \right] \sin(\zeta + \phi).$$

So

$$\frac{d\eta}{dt} = -\frac{eE_1K_u}{2\gamma^2 m_0c} [JJ] \sin(\zeta + \phi). \quad (46)$$

Combining the two equations:

$$\frac{d^2\zeta}{dt^2} = 2nk_u c \frac{d\eta}{dt} = -\frac{2nk_u c e E_1 K_u}{2\gamma^2 m_0 c} [JJ] \sin(\zeta + \phi) = \frac{ne^2 E_1 B_u}{\gamma^2 m_0^2 c} [JJ] \sin(\zeta + \phi).$$

Noting that

$$\Omega = \frac{e}{\gamma m_0} \sqrt{\frac{nE_1 B_u \left[J_{\frac{n-1}{2}}(\xi) - J_{\frac{n+1}{2}}(\xi) \right]}{c}} \quad (47)$$

we find that

$$\frac{d^2\zeta}{dt^2} = -\Omega^2 \sin(\zeta + \phi). \quad (48)$$

There is a close analogy with the pendulum equation $\frac{d^2\theta}{dt^2} + \frac{g}{\ell} \sin\theta = 0$, where g is acceleration due to gravity, ℓ is the length of the pendulum, and θ is the displacement angle. The analogy of θ is ψ , the phase of an electron with respect to the superposition of the optical and undulator fields. The pendulum equation is a non-linear differential equation, with an analytic solution using time-dependent elliptical Jacobi functions.

The electrons are submitted to the free electron laser sinusoidal ponderomotive potential given by $-\Omega \cos\psi$. It has the form of the potential of a pendulum, in which ψ is the angle of the pendulum at its equilibrium position. One usually represents the energy evolution in the energy phase space, as illustrated in Fig. 22.

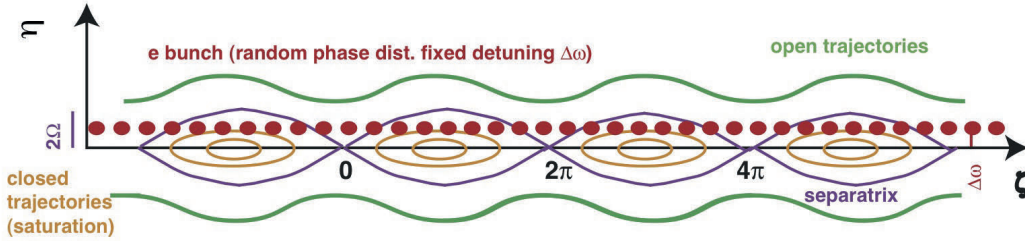


Fig. 22: Electron trajectories in energy phase space representation. The vertical axis represents the deviation with respect to resonance, the horizontal axis the electron phase with respect to the ponderomotive potential. Green: open trajectories with energy oscillations. Orange: closed trajectories of particles by the ponderomotive potential. Maximum kinetic energy is given to/taken from the optical wave for half a rotation, i.e. for highest and lowest positions.

The initial phase of the electron is simply given by its position along the electron bunch, this determines its energy variation and thus its bunching. The electrons enter the undulator with a specific phase. On resonance $\gamma = \gamma_r$, i.e. $\eta = 0$, there is no energy transfer. Near resonance, the optical wave and the electrons exchange energy, the electrons gather around positions for which the energy variation $\delta\gamma m_0 c^2$ keeps a constant sign. The modulation depends on the electric field of the wave. Above resonance ($\gamma > \gamma_r$), there is a net positive energy transfer from the electron beam to the optical

wave. Positive energy exchange (gain) or negative one (absorption) occurs $\eta \neq 0$ depending on the sign of η .

At small amplitudes, with the approximation $\sin \psi = \psi$, one gets the harmonic oscillator case. The equation can be analytically solved only assuming Ω small, i.e. for low amplification since $\Omega \propto \sqrt{E_1}$. With increasing angular momentum, the motion becomes unharmonic. The trajectories are closed, inside the ‘bucket’. The closed motions correspond to oscillations of the pendulum. When trapped in the ponderomotive field $-\Omega^2 \cos \phi$, the particles bounce back and forth on the borders of the potential, and rotate in phase space. Trapped particles undergo oscillations in the buckets of the potential. The closed trajectories in phase space correspond to those of an oscillating pendulum around its equilibrium position.

Above the peaks of the potential, at very large angular momentum, the motion becomes unbounded, the trajectories are open (green), and the movement corresponds to a complete rotation of the pendulum around its pivot. The particles can follow open trajectories from one potential well to another: they present oscillations in energy and an evolving phase. They can also be trapped in the ponderomotive field $-\Omega^2 \cos \phi$, and rotate in phase space.

4.3.5 First-order energy exchange and bunching

4.3.5.1 First-order energy exchange

In the case of the optical wave resonant to the undulator wavelength, i.e. if the pulsation of the incident wave is equal to the resonant wavelength, which means for $\omega = \frac{\beta_s \omega_u}{1 - \beta_s}$, $\Delta\Omega_2 = 2\omega_u \beta_s$ and $\Delta\Omega_1 = 0$. The work integrated over one undulator period, i.e. between $t_1 = 0$ and $t_2 = \frac{\lambda_u}{\beta_s c}$ is

$$\Delta W = - \int_{t_1=0}^{t_2=\frac{\lambda_u}{\beta_s c}} \frac{eK_u E_o}{2\gamma} (\sin(\phi) + \sin(2\beta_s \omega_u t - \phi)) dt = 0.$$

The work due to the force applied by the electric field averaged over one undulator period is zero. For $\lambda = \lambda_r$, there is no average energy exchange at first order: half of the electrons gain energy, half of them loose energy.

In the case of an optical wave slightly detuned with respect to the undulator wavelength, using $\frac{k}{k_r} = 4n\gamma_r^2 \frac{1}{2 + K_u^2}$, the oscillatory term of the phase becomes

$$\psi_w = \frac{K_u^2}{8\gamma^2} 4n\gamma_r^2 \frac{1}{2 + K_u^2} \sin(2k_u \tilde{s}) = n \left(\frac{\gamma_r}{\gamma} \right)^2 \frac{K_u^2}{4 + 2K_u^2} \sin(2k_u \tilde{s}) = n\xi \sin(2k_u \tilde{s}),$$

where ξ is defined by

$$\xi = \frac{K_u^2}{2(2 + K_u^2)} \left(\frac{\gamma_r}{\gamma} \right)^2. \quad (49)$$

The phase then becomes

$$\psi = \zeta + n\xi \sin(2k_u \tilde{s}). \quad (50)$$

The electron phase ζ contains only the slowly varying part of the s motion \tilde{s} , the second term corresponds to the rapidly oscillatory term. In replacing this new expression of the phase in the energy exchange expression, the corresponding energy exchange term can be written as

$$\Delta W = - \int_{s_1}^{s_2} \frac{eK_u E_1}{2\gamma} \sin(\zeta + \phi - (n-1)k_u \tilde{s} + n\xi \sin(2k_u \tilde{s})) \\ - \sin(\zeta + \phi - (n+1)k_u \tilde{s} + n\xi \sin(2k_u \tilde{s})) dt.$$

On expanding the sines, it becomes

$$\begin{cases} \sin(\zeta + \phi - (n-1)k_u s + n\xi \sin(2k_u \tilde{s})) \\ = \sin(\zeta + \phi) \cos(n\xi \sin(2k_u \tilde{s}) - (n-1)k_u \tilde{s}) + \cos(\zeta + \phi) \sin(n\xi \sin(2k_u \tilde{s}) - (n-1)k_u \tilde{s}) \\ - \sin(\zeta + \phi - (n+1)k_u s + n\xi \sin(2k_u \tilde{s})) \\ = -\sin(\zeta + \phi) \cos(n\xi \sin(2k_u \tilde{s}) - (n+1)k_u \tilde{s}) - \cos(\zeta + \phi) \sin(n\xi \sin(2k_u \tilde{s}) - (n+1)k_u \tilde{s}). \end{cases}$$

Assuming that the energy γ and the light wave electric field E_1 change slowly, one can average the oscillating terms over one undulator period. The second and fourth terms then vanish by symmetry. The average of the first and third terms is performed using the integral representation of the Bessel functions of order m and of variable z [86] given by

$$J_k(z) = \frac{1}{2\pi} \int_0^{2\pi} \cos(z \sin \theta - k\theta) d\theta. \quad (51)$$

For k equal to half an integer, the integral vanishes by symmetry. Using $\theta = 2k_u \tilde{s}$, $z = n\xi$, and $m = \frac{n-1}{2}$ or $m = \frac{n+1}{2}$, it becomes

$$\Delta\gamma = -\frac{eE_1 K_u N_u \lambda_u}{2\gamma m_o c^2} \left[J_{\frac{n-1}{2}}(\xi) - J_{\frac{n+1}{2}}(\xi) \right] \sin(\zeta + \phi). \quad (52)$$

This expression gives zero for even m values. This recalls the vanishing of the even harmonics of the spontaneous emission on the axis, while considering that the electron beam average over one period is parallel to the undulator axis. In the slow varying phase ϕ and electric field E_1 approximation, these functions can be estimated in using their values for \tilde{s} .

Besides, the homogeneous width of the spontaneous emission is given by $\frac{1}{nN_u}$. This spontaneous emission width provides also the non-linear interaction region in the frequency space. By differentiating the resonance equation, one gets

$$\frac{\delta\gamma}{\gamma} = \frac{1}{2} \frac{\delta\lambda}{\lambda} = 0 \left(\frac{1}{2nN_u} \right). \quad (53)$$

Only energies within a relative difference $\frac{1}{2nN_u}$ can play a role. At a low-order derivation, the energy exchange can be written as

$$\Delta\gamma = -\frac{eE_1 K_u N_u \lambda_u}{2\gamma_r m_o c^2} \left[J_{\frac{n-1}{2}}(\xi) - J_{\frac{n+1}{2}}(\xi) \right] \text{sinc}(\pi N_u \eta) \sin(\zeta + \phi), \quad (54)$$

with η the relative energy difference and ξ given by $\xi = \frac{K_u^2}{2(2+K_u^2)}$.

The sign of the $\Delta\gamma$ depends on the phase $\zeta + \phi$ between the electron and the optical wave. If one electron is accelerated, i.e. for $\Delta\gamma > 0$, another electron located longitudinally one-half wavelength ahead or behind is decelerated by the same amount $\Delta\gamma < 0$. The longitudinal distribution of the electrons being much wider than the wavelength, the phase ϕ is uniformly distributed between 0 and 2π . In consequence, the first-order net energy exchange $\langle \Delta\gamma_1 \rangle_{\text{electrons}}$ between the electron bunch and the optical wave is zero over the electron bunch:

$$\langle \Delta\gamma_1 \rangle_{\text{electrons}} = 0. \quad (55)$$

For the interaction to occur, λ should be slightly different from λ_r : for $\lambda > \lambda_r$ amplification occurs (gain and beam deceleration) whereas for $\lambda < \lambda_r$ the optical wave is absorbed (the beam is accelerated).

4.3.5.2 Root-mean-square energy variation

The root-mean-square (RMS) energy variation, averaged over the electrons, can be expressed as

$$\langle \Delta\gamma^2 \rangle = \frac{1}{2} \left(\frac{eK_u N_u \lambda_u}{2\gamma_T m_o c^2} \right)^2 \langle E_1 \rangle^2 \left[J_{\frac{n-1}{2}}(\xi) - J_{\frac{n+1}{2}}(\xi) \right]^2 \text{sinc}^2(\pi N_u \eta) \quad (56)$$

where $\langle E_1 \rangle^2$ is the average of the square of the electric field over the electron beam. The electrons, after propagation, are then accelerated or decelerated by energy enhancement or loss. This leads to a longitudinal spatial modulation, known as ‘electron bunching’ or ‘electron microbunching’. Electrons are bunched around a phase $\psi + \phi$, multiple of 2π . The electronic density is then modulated with a period equal to the resonant wavelength. The electrons are put in phase, the elementary oscillators are set in coherence. This bunching is similar to the one taking place in the klystron, as introduced earlier. On a planar undulator, the bunching also occurs at the odd harmonics of the resonant wavelength. This is the basic concept for ‘coherent harmonic generation’ [81–83].

4.3.5.3 Ponderomotive field

Considering the energy exchange given by $\frac{d\gamma}{dt} = -\frac{eE_1 K_u}{2\gamma m_o c} \left[J_{\frac{n-1}{2}}(\xi) - J_{\frac{n+1}{2}}(\xi) \right] \sin(\zeta + \phi)$ and in considering the analogy with the interaction of an electron with an axial electric field according to $\frac{d\gamma}{dt} = -\frac{e}{m_o c} \beta_s E_p$ with E_p the so-called ponderomotive field, one gets

$$\langle E_p \rangle = -\frac{E_1 K_u [JJ]}{2\gamma} \sin(\zeta + \phi) \quad \text{with} \quad [JJ] = \left[J_{\frac{n-1}{2}}(\xi) - J_{\frac{n+1}{2}}(\xi) \right]. \quad (57)$$

The corresponding electron potential is $V_p = e \int_0^t \langle E_p \rangle ds'$. The electrons behave as though they were particles in a sinusoidal potential given by $-\Omega \cos \psi$, or the so-called ponderomotive potential of the free electron laser. When in the potential the particles bounce back and forth on the borders of the potential. Particles undergo trapped oscillations in the buckets of the potential, as shown in Fig. 23.

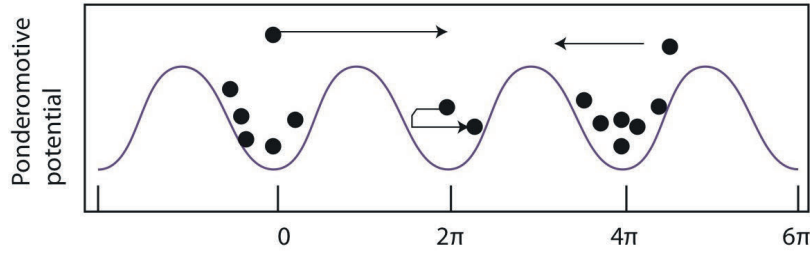


Fig. 23: Ponderomotive potential

4.3.5.4 Bunching process

Some electrons gain energy, others lose energy. The average longitudinal velocity is changing along the propagation in the undulator. From $\tilde{\beta}_s^2 = 1 - \frac{1 + \frac{K_u^2}{2}}{\gamma^2}$, one gets $\Delta\beta_s \approx \left(1 + \frac{K_u^2}{2} \right) \frac{\Delta\gamma}{\gamma^3}$.

The energy variation averaged over the phases is zero at first order in E_1 . An individual electron with a phase ϕ gains or loses energy, so its position relative to the unperturbed $s = \tilde{v}t$ position is advanced or retarded. Because the amplitude of the interaction only depends on the longitudinal position of the electron in the electron bunch with periodicity λ_r , the electrons tend to bunch along given positions, separated by λ_r . This bunching (λ_r separation) takes place by velocity modulation (electrons set in

phase). As for the klystron, the electrons tend to gather around preferred positions separated by the resonant wavelength λ_r .

One first replaces the energy exchange in the longitudinal velocity variation for $n = 1$, and we get

$$\Delta\beta_s = -D(\cos(\Delta\Omega_2 s/\tilde{v}_s + \phi) - \cos\phi) \quad \text{with} \quad D = \frac{(1 + \frac{K_u^2}{2}) e E_1 K_u [JJ]}{\gamma^4 2 m_0 c \Delta\Omega_2} \quad (58)$$

with $\Delta\Omega_2 = \omega_u \beta_s - \omega(1 - \beta_s)$. Then one evaluates the longitudinal position as

$$s(t) = \int_0^t v_s(t') dt' = \int_0^t (\tilde{v}_s + c\Delta\beta_s) dt' = \tilde{v}_s t - cD \int_0^t (\cos(\Delta\Omega_2 t' + \phi) - \cos\phi) dt'$$

$$s(t) = \int_0^t v_s(t') dt' = \tilde{v}_s t - cD \left[\frac{(\sin(\Delta\Omega_2 t + \phi) - \sin\phi)}{\Delta\Omega_2} - t \cos\phi \right]. \quad (59)$$

One finds here the longitudinal bunching, as seen in the klystron case. It is illustrated in Fig. 24.

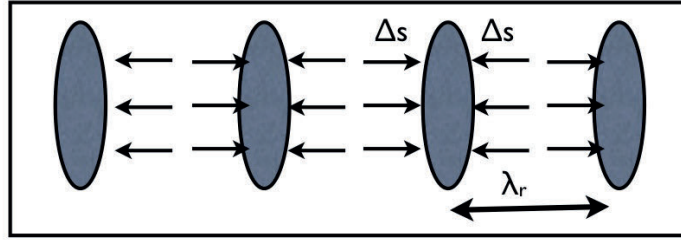


Fig. 24: Electron bunching due to the electron/optical wave interaction

One uses now the expression of the longitudinal position of the electron in the electric field expression. It becomes

$$E_1(t) = E_1 \cos(ks - \omega t + \phi) = E_1 \cos\left(k\tilde{v}_s t - \frac{kcD}{\Delta\Omega_2} [\sin(\Delta\Omega_2 t + \phi) - \sin\phi - \Delta\Omega_2 t \cos\phi] - \omega t + \phi\right). \quad (60)$$

One defines the phase slippage $\Delta\phi$ as

$$\Delta\phi = -\frac{\omega D}{\Delta\Omega_2} [\sin(\Delta\Omega_2 t + \phi) - \sin\phi - \Delta\Omega_2 t \cos\phi] \quad (61)$$

$\Delta\Omega_2$ is given by $\Delta\Omega_2 = \omega_u \beta_s - \omega(1 - \beta_s)$. Using $1 - \langle\beta_s\rangle = \frac{1}{2\gamma^2} (1 + \frac{K_u^2}{2}) = \frac{\lambda_r}{\lambda_u} = \frac{\omega_u}{\omega_r}$, i.e. $\omega_u = \omega_r(1 - \beta_s)$, it becomes $\Delta\Omega_2 = \omega_u \beta_s - \omega \frac{\omega_u}{\omega_r}$. With $\beta_s \approx 1$

$$\Delta\Omega_2 = \omega_u \left(1 - \frac{\omega}{\omega_r}\right). \quad (62)$$

Considering this electron bunching will enable us to evaluate the second-order energy exchange.

4.3.6 Second-order energy exchange

The second-order energy exchange is calculated using in the energy exchange expression the electric field expression taking into account the density modulation of the electron beam.

For a low electric field E_1 and low gain, $\Delta\phi$ is close to 0, and one develops $\sin(\Delta\Omega_2 t - \phi - \Delta\phi) = \sin(\Delta\Omega_2 t - \phi) - \Delta\phi \cos(\Delta\Omega_2 t - \phi)$. One then averages over all phases ϕ and it remains as

$$\left\langle \frac{d\gamma}{dt} \right\rangle_{\phi} = \frac{b}{2} (-\sin(\Delta\Omega_2 t) + \Delta\Omega_2 t \cos(\Delta\Omega_2 t)) \quad \text{with} \quad b = -\frac{eE_1 K_u [JJ] \omega D}{2\gamma m_0 c \Delta\Omega_2}. \quad (63)$$

In integrating over the electron transit time through the undulator $\tau = L_u/\tilde{v}_s$, one obtains the second-order energy change per electron:

$$\langle \Delta\gamma_2 \rangle_{\phi} = \int_0^{\tau=L_u/\tilde{v}_s} \left\langle \frac{d\gamma}{dt} \right\rangle_{\phi} dt = \frac{b}{2\Delta\Omega_2} (2 - 2\cos\Delta\Omega_2\tau - \Delta\Omega_2\tau \sin(\Delta\Omega_2\tau)).$$

By multiplying by τ^3 , replacing $(1 + K_u^2/2) = 2\gamma^2\lambda/\lambda_u$, b , and D , one gets

$$\langle \Delta\gamma_2 \rangle_{\phi} = \frac{e^2\pi}{2m_0^2c^4} \frac{K_u^2}{\lambda_u} [JJ]^2 E_1^2 \frac{L_u^3}{\gamma^3} \frac{(2 - 2\cos\Delta\Omega_2\tau - \Delta\Omega_2\tau \sin(\Delta\Omega_2\tau))}{(\Delta\Omega_2\tau)^3}. \quad (64)$$

Let us define the function $g(x)$ by $g(x) = \frac{2-2\cos x - x \sin x}{x^3}$. The function $g(x)$ is antisymmetric in x and has a maximum of 0.135 at $x = 2.6$.

Multiplying by τ^3 , replacing $(1 + K_u^2/2) = 2\gamma^2\lambda/\lambda_u$, b , and D , one gets

$$\langle \Delta\gamma_2 \rangle_{\phi} = \frac{e^2\pi}{2m_0^2c^4} \frac{K_u^2}{\lambda_u} [JJ]^2 E_1^2 \frac{L_u^3}{\gamma^3} \frac{(2 - 2\cos\Delta\Omega_2\tau - \Delta\Omega_2\tau \sin(\Delta\Omega_2\tau))}{(\Delta\Omega_2\tau)^3}. \quad (65)$$

4.3.7 Gain

4.3.7.1 Gain expression in the low gain regime

The optical wave is the FEL spontaneous emission given by the synchrotron radiation emitted by the electrons passing through N_u periods of the undulator and stored in an optical cavity, as shown in Fig. 25, where the electron bunching is indicated. The mirrors of the optical resonator perform the optical feedback, such that the light pulse performs multiple passes in the cavity. The gain is evaluated for small variations of the optical field.

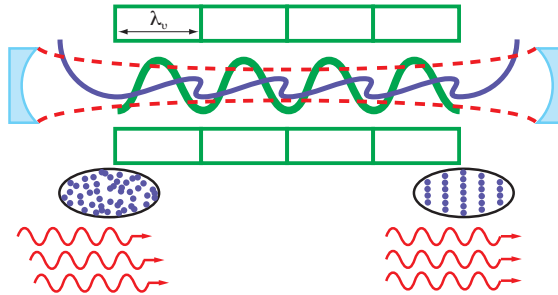


Fig. 25: FEL configuration with an optical cavity: the energy exchange between the optical light (initially the spontaneous emission stored in the optical cavity) and the electrons is then transformed into density modulation while the electron progress is due to velocity bunching. This results in a microbunching of the electrons which can then emit coherently in phase with the optical wave that gets amplified.

The first-order energy exchange averaged over the electrons is zero. The second-order energy exchange $\langle \Delta\gamma_2 \rangle$ averaged over phases with the bunched electron distribution has been calculated. The change in electromagnetic power ΔP is given by

$$\Delta P = -\frac{I}{e} m_o c^2 \langle \Delta \gamma_2 \rangle. \quad (66)$$

For a small variation of the optical field, the gain G per pass can be expressed as the second-order energy exchange divided by the incident field energy, according to

$$G = \frac{m_o c I \langle \Delta \gamma_2 \rangle}{e \epsilon_o \int E_1^2 dS} = \frac{m_o c^2 \rho_e \langle \Delta \gamma_2 \rangle}{\frac{1}{2} \epsilon_o E_1^2} \quad (67)$$

where ϵ_o is the vacuum permeability, ρ_e the electronic density in the volume, the radiation field being integrated over the longitudinal coordinates. The small signal gain is given by

$$G = \frac{2\pi e^2}{\epsilon_o m_o c^2} \rho_e \frac{K_u^2}{\lambda_u} \left(\frac{L_u}{\gamma} \right)^3 \left[J_{\frac{n-1}{2}}(\xi) - J_{\frac{n+1}{2}}(\xi) \right]^2 \frac{\partial}{\partial \gamma} \left(\frac{\sin(\pi N_u \eta)}{(\pi N_u \eta)} \right)^2. \quad (68)$$

For the interaction to occur, λ should be slightly different from λ_r . For $\lambda > \lambda_r$ amplification occurs (gain and beam deceleration) whereas for $\lambda < \lambda_r$ the optical wave is absorbed and the beam is accelerated. Depending on the sign of $(\lambda - \lambda_r)$, the optical wave is either absorbed to the benefit of a gain of kinetic energy of the electrons, or is amplified to the detriment of the kinetic energy of the electrons. The electrons are bunched and are in phase with the incident electric field. The emission from the bunched beam then adds coherently to the incident wave that gets amplified.

The small signal gain varies as $1/\gamma^3$. The higher the energy, the lower the gain. Since short wavelength operation requires the use of high electron beam energies (because of the resonance condition), for the same undulator length, the gain is smaller at short wavelengths than at longer ones. The gain is proportional to the electronic density (thus to the beam current I). The more electrons interact, the larger the gain. For short wavelength FELs where the gain is naturally small, one should employ beams with high electronic densities.

The gain is also proportional to the third power of the undulator length. The longer the undulator, the higher the gain up to certain limits that are given by the gain bandwidth ($1/nN_u$, because of the interference nature of the interaction), and by the slippage (temporally, the light pulse should remain in the longitudinal bunch distribution for the interaction to occur). So the number of undulator periods cannot be excessively large. Similarly, both the optical light and electron bunch should overlap properly all long the undulator propagation.

4.3.7.2 *Madey's theorems*

Remarkably, the gain is the derivative of the spontaneous emission, as understood thanks to the Madey theorems [60, 87]. They are given by

$$\frac{d\Phi}{d\Omega}(\theta = 0) = \frac{2\alpha m_o^2 c^4 I \langle \Delta \gamma^2 \rangle}{e^2 \lambda^2 \langle E_1^2 \rangle}, \quad (69)$$

$$\langle \Delta \gamma_2 \rangle = \frac{1}{2} \frac{\partial \langle \Delta \gamma^2 \rangle}{\partial \gamma}, \quad (70)$$

with α the fine structure constant, I the beam current, $\frac{d\Phi}{d\Omega}(\theta = 0)$ the angular spectral flux on axis of the undulator spontaneous emission. The first theorem relates the energy spread $\langle E_1^2 \rangle$ introduced by the optical wave to the spontaneous emission of the undulator. According to the second theorem, the second-order energy exchange $\langle \Delta \gamma_2 \rangle$ is proportional to the derivative of the spontaneous emission of the undulator. Due to the resonance relationship linking the particles energy to the emission wavelength, the spectral 'gain' distribution is close to the wavelength derivative of the spontaneous emission spectrum

versus λ . The Madey theorem is valid for a gain smaller than 0.2. The gain can be expressed as the derivative of the undulator spontaneous emission.

4.3.7.3 Gain correction terms

Gain corrections terms should be introduced.

The transverse filling factor F_f accounts for a non-perfect transverse overlap between the laser transverse modes and the transverse dimensions of the electron beam σ_x and σ_z . For a laser of TEM_{00} mode of waist w_o , it is given by $F_f = \frac{1}{\sqrt{1+(\frac{w_o}{2\sigma_x})^2}\sqrt{1+(\frac{w_o}{2\sigma_z})^2}}$. The filling factor has been calculated using Gaussian spherical wavefronts of the optical wave, leading to a deviation from the Madey's theorems, and a new optimization of the energy extraction [88], as shown in Fig. 26.

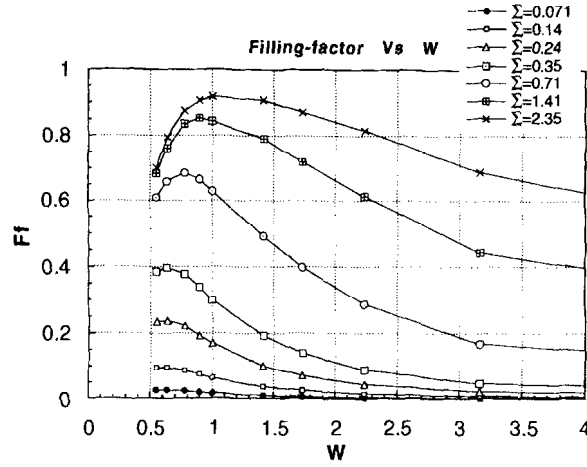


Fig. 26: Filling factor in the case for Gaussian optical beams for different values of the normalized waist $W_i = w_i \sqrt{\frac{\pi}{\lambda L_u}}$ and electron beam transverse sizes $\Sigma_i = \sigma_i \sqrt{\frac{\pi}{\lambda L_u}}$. from [89].

Besides, according to the Madey's theorem, spontaneous emission inhomogeneous broadening (presented in 2.3.3.2) due to energy spread and emittance affect directly the gain. The inhomogeneous reduction factor F_{inh} is

$$F_{inh} = \left[1 + \frac{(\frac{\Delta\lambda}{\lambda_n})^2_{\sigma_\gamma}}{(\frac{\Delta\lambda}{\lambda_n})^2_{hom}}\right]^{-1} \cdot \left[1 + \frac{(\frac{\Delta\lambda}{\lambda_n})^2_{div}}{(\frac{\Delta\lambda}{\lambda_n})^2_{hom}}\right]^{-1} \cdot \left[1 + \frac{(\frac{\Delta\lambda}{\lambda_n})^2_{\sigma}}{(\frac{\Delta\lambda}{\lambda_n})^2_{hom}}\right]^{-1}.$$

The longitudinal overlap between the electron bunch of RMS length σ_1 and the optical wave should be maintained. The light wave is in advance by $N_u \lambda$ with respect to the electrons, and for short electron bunch distributions, it could escape. The corresponding correction factor F_g is $F_g = \left[1 + \frac{N_u \lambda}{\sigma_1}\right]^{-1}$.

The small signal gain can be expressed as

$$G = \frac{2\pi e^2}{\epsilon_0 m_o c^2} \rho_e F_f F_{inh} F_g \frac{K_u^2}{\lambda_u} \left(\frac{L_u}{\gamma}\right)^3 \left[J_{\frac{n-1}{2}}(\xi) - J_{\frac{n+1}{2}}(\xi)\right]^2 \frac{\partial}{\partial \gamma} \text{sinc}^2(\pi N_u \eta), \quad (71)$$

$$G = n \frac{\pi^2 r_o \lambda_u^2 N_u^3 K_u^2}{\gamma^3} F_f F_{inh} F_g \rho_e \left[J_{\frac{n-1}{2}}(\xi) - J_{\frac{n+1}{2}}(\xi)\right]^2 \frac{\partial}{\partial \gamma} \text{sinc}^2(\pi N_u \eta), \quad (72)$$

with $r_o = \frac{1}{4\pi\epsilon_0} \frac{e^2}{m_o c^2}$ the classical radius of the electron (2.82×10^{-15}).

4.4 The classical approach in the moving frame

In such an approach, developed in Italy [90, 91] in particular by Alberto Renieri (seventh FEL Prize in 1994) and Guisepe Dattoli (seventh FEL Prize in 1994), the Weizsäcker–Williams approximation, still valid for ultra-relativistic electrons, is used. The FEL corresponds to a stimulated scattering process from the so-called ‘pseudo-radiation field’ into a true radiation field travelling in the same direction as the electron beam. The FEL modelled by a stimulated Thomson scattering process is described using the Hamiltonian formalism [90].

The selected frame is a moving one [91], “chosen in such a way that the periodic structure transforms into a (pseudo) radiation field whose frequency coincides with the frequency of the stimulating field”. This frame choice presents different advantages.

- “The physical processes of scattering from one field to the other and vice versa become apparent. Indeed, in that frame, the two fields are treated on the same step, although they are quite different in the laboratory frame.”
- “Relativistic calculations can be avoided. In fact, in that frame, the electrons have non relativistic velocity, and the momentum exchanged with the fields is not sufficient to give the electrons a relativistic velocity.”
- “In the limit in which the laser operation can be described in terms of ensemble averages over independent single particles, it becomes possible to follow the history for each electron in the field with simple equations of motion.” [91]

This FEL description in the moving frame reduces to the pendulum equations, which are not Lorentz invariant and are valid in that frame only. A quantum mechanical density matrix description of the system is able to conciliate this approach with the one proposed by Hopf. A Hamiltonian completes the overall description of the process.

Under the approximation that the electrons do not contribute much to the laser intensity and follow adiabatically the field, the FEL evolution can be described by the pendulum equations. Figure 27 shows the phase space plots, with W scale momentum, Ω interaction frequency, ψ interaction phase, “essentially the position coordinate canonical to W ” [91].

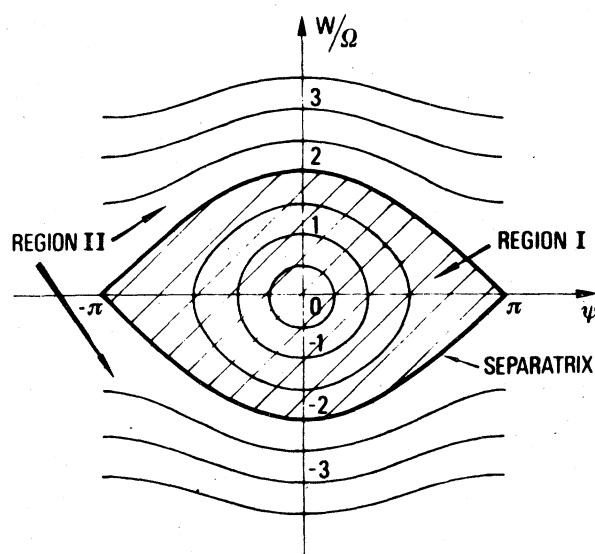


Fig. 27: Phase space plot of the FEL modelled using the pendulum equation, from [91]: W scale momentum, Ω interaction frequency, ψ interaction phase, “essentially the position coordinate canonical to W ”.

It shows two zones.

- Zone I with closed paths for W and ψ .
- Zone II with W with periodic trajectories while ψ increases steadily with time.
- Separatrix with both aperiodic motions of W and ψ , depending on the value of laser intensity through Ω and its evolution.

The electron motion can then be solved using the Jacobi elliptical functions.

The dimensionless laser intensity is introduced “it measures the ratio of the small-signal oscillation frequency (Rabi flipping) against the Doppler shift determined by the initial electron momentum” [91] and enables us to follow the evolution of the gain towards saturation. After this single particle classical theory, where amplification is due to the single electron stimulated Thomson scattering, the Hamiltonian description has been further examined [92] in considering the multiple electron effects [93, 94], gain-spread expressions [95], and in accounting for self-consistency. FEL pulse propagation and synchronization of the pulses in the optical resonator and the electron bunches in the resonator are examined: it is found that the ‘lethargy’, i.e. “the slowing down of the laser oscillation in the cavity owing to the interaction with the electrons” leads to the presence of “supermodes” [96, 97]. An equivalent refractive index can be defined. The FEL evolution has been described with the logistic function [98].

Different lectures are gathered in textbooks [99, 100].

4.5 Early FEL developments in the former Soviet Union

In Russia, which was quite isolated at that time, development took also place on the FEL. FEL progress was made independently in Russia and outside.

A meeting was held in December 1980 in the frame of the Academy of Science to discuss the development of free electron lasers [101]. Different work progress was reported: M. V. Fedorov (Lebedev Institute) on the different types of FELs, M. I. Petelin, A. A. Kolomenskii, A. A. Ruxadz (Institute of Applied Physics, Nijni-Novgorod) on the possibility of a mm range FEL on Sinus-4, A. N. Didenko (Institute of Nuclear Physics in Tomsk) on an undulator experiment on an induction linac and on the use of ‘Sirius’ synchrotron (500–900 MeV), N. A. Vinokurov (Institute of Nuclear Physics in Novosibirsk) on the use of the optical klystron on the VEPP3 storage ring, A. A. Varfolomeev and D. F. Zaretskii, S. P. Kapitsa (Institute of problems of Physics) on a proposition of FEL on a microtron, N. V. Karkov (Lebedev Institute in Karkhov) on the use of FEL for isotope separation at 16 μm . Prospects for short wavelength operation and high efficiency FEL were given.

In Novosibirsk, at the Institute of Nuclear Physics (presently called the Budker Institute), the team was working both on the theory and was also thinking of a test experiment for a storage ring FEL. In order to enhance the gain, N. A. Vinokurov (fourth FEL Prize in 1991) and A. N. Skrinsky proposed the optical klystron, a device to artificially enhance the gain. They investigated the maximum power that could be extracted.

4.5.1 The optical klystron

The optical klystron proposed by N. A. Vinokurov [102–105], represented in Fig. 28, is made of a first undulator creating the electron energy modulation, a dispersive section of length L_d and peak field B_d creating a wide wiggler of magnetic field enabling the energy modulation to be transformed into density modulation, and a second undulator where bunched electrons radiate. Assuming that the undulator segments and the dispersive section are well compensated, the electrons do not suffer velocity and position shifts during their travel in the device. The dispersive section acts as a magnetic chicane: the electrons are more or less deviated in the strong magnetic field according to their energy and become bunched thanks to a velocity modulation process. The concept of the optical klystron was then explored further around the world [106–108].

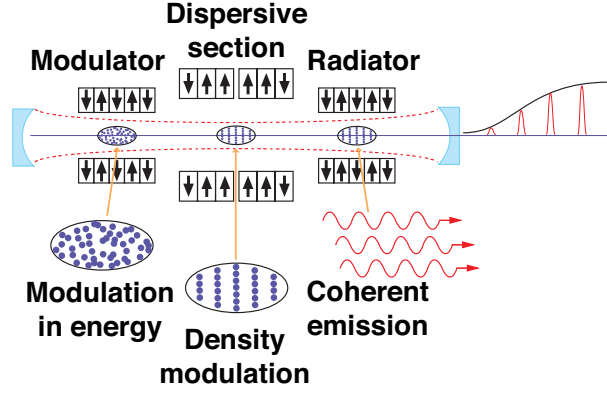


Fig. 28: Scheme of the optical klystron

The radiation emitted in the two undulator segments interfere, as in the Young slit experiment. The spectrum is contained in an envelope which corresponds to the spectral line of one single undulator emission, with an internal fine structure resulting from the interference [107, 109]. It can be expressed as

$$\left(\frac{d^2 I}{d\Omega d\omega}\right)_{\text{optical klystron}} \approx \left(\frac{d^2 I}{d\Omega d\omega}\right)_{\text{one undulator}} (1 + f \cos \alpha_{\text{optical klystron}}) \quad (73)$$

with

$$\alpha_{\text{optical klystron}} = 2\pi(N_u + N_d) \frac{\lambda_r \gamma_r^2}{\lambda \gamma^2}. \quad (74)$$

Here

$$N_d = \frac{\omega L_d}{4\gamma_r^2 c} \left[1 + \frac{e^2}{L_d m^2 c^2} \int_0^u L_d \left[\int_0^u B_d(s) ds \right]^2 du \right] \quad (75)$$

is the equivalent number of periods of the dispersive section, and scales its strength. $(N_u + N_d)$ represents the number of optical wavelengths which pass the electron during its travel in the dispersive section. The fringe contrast, called the modulation rate f , results from different contributions (magnetic field inhomogeneity, width of energy distribution of the electrons, transverse position of the electron beam), the main one coming from the electron beam energy spread, as

$$f_\gamma = \exp(-8\pi^2(N_u + N_d)^2(\sigma_\gamma/\gamma)^2). \quad (76)$$

An example of an optical klystron spectrum is shown in Fig. 29.

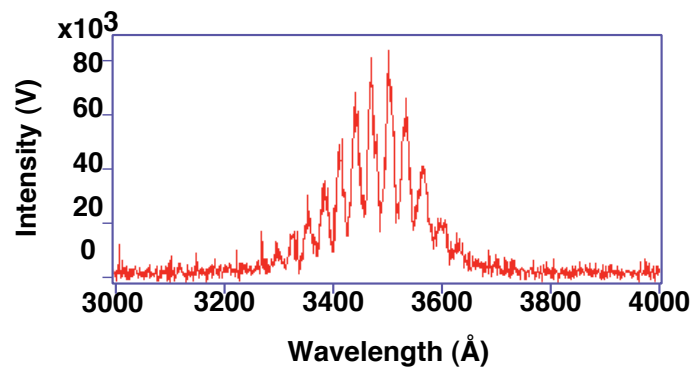


Fig. 29: Measured spectrum in the case of the Super-ACO optical klystron (Orsay, France)

The optical klystron provides a very easy means to measure the energy spread on an electron beam. Besides, the variation of the intensity in the spectra being much faster than in the single undulator case, the derivative of the spontaneous emission (proportional to the gain according to Madey's theorem) reaches much larger values than for a single undulator of total length L_d .

The gain enhancement for an optical klystron of length L_{ok} is

$$G_{\text{optical klystron}} = \frac{f L_{ok}^2 (N_u + N_d)}{N_u^3 \lambda_u} G_{\text{one undulator}}. \quad (77)$$

The gain enhancement takes place to the detriment of the total saturated power [104–106].

The concept of the multiple optical klystron was further developed [110–112].

4.5.2 The FEL evolution

Independently to Colson's approach, V. N. Baier and A. I. Milstein investigated the FEL theory in considering the motion of relativistic particles in the superposition of a transverse magnetic field and a plane electromagnetic wave propagating along the direction of motion. They could find the small signal gain, its maximum, and then considered the case of a strong signal in the optical cavity configuration. They distinguished the case of the initially uniform phase distribution to the bunched one, where phase oscillations can occur and limit the output power [113, 114]. Coherent radiation close to the cyclotron resonance was also discussed [115]. A. N. Kondratenko and A. I. Saldin (19th FEL Prize in 2006) considered very early the possibility of production of coherent radiation from a self-instability, without the use of an optical resonator [116–118]. This pioneering work will be discussed in the high gain section. They also developed a linear theory of free electron lasers with Fabry–Perot cavities [119].

4.6 Saturation and efficiency

4.6.1 Saturation

Different phenomena contribute to the gain reduction leading to the saturation of the output power.

4.6.1.1 Electron energy loss

If too much energy is taken by the light wave, the resonant condition is no longer fulfilled since the electron energy is reduced, the electrons consequently slow down. When the optical wave power grows, an increasing number of electrons are trapped in the ponderomotive potential. When going down in phase space, the electrons lose kinetic energy to the advantage of the light wave. When they reach the bottom of the accessible space and cannot give any more energy, the laser saturates. Indeed, the electrons can even undergo several rotations in phase space before escaping the undulator because of slippage, while alternately providing to or taking energy from the optical wave. These oscillations are called 'synchrotron oscillations' [120–122]. They induce sidebands in the radiation spectrum. Strategies for sideband suppression have been examined [123]. While the laser intensity saturates, the gain is reduced. The electron energy decreases due to the kinetic energy loss enabling FEL amplification [124], the electron beam energy can also be reduced by the accumulated effects of spontaneous emission along the undulator, given by $\frac{\Delta\gamma_{SR}}{\gamma_0} = -\frac{1}{3}r_e\gamma_0 K_u^2 k_u^2 L_u$, with r_e the classical electron radius.

4.6.1.2 Increase of energy spread

The electron bunching and interaction via an energy exchange with the optical wave leads to an increase of the energy spread of the beam, reducing in consequence the gain via the contribution of F_{inh} that becomes more important. Intuitively, the gain bandwidth (related to the spontaneous emission bandwidth proportional to the inverse of the number of undulator periods) gets larger because of the inhomogeneous

contribution and the gain distribution flattens. In consequence, the gain bandwidth and the limits set by the energy spread, provide a maximum undulator length.

4.6.1.3 Slippage

The slippage can stop the interaction: the electrons travel slightly slower than the photons, and once at the exit of the undulator, the time difference becomes typically $\frac{N_u \lambda}{c}$. For the radiation to not escape from an electron bunch of duration σ_1 , one can even consider that the radiation advance should remain in the peak of the distribution: $\frac{N_u \lambda}{c} < \frac{\sigma_1}{10}$ or $N_u < \frac{\sigma_1 c}{10 \lambda}$. This gives 300 periods for 1 nm radiation, 10 fs electron bunch, 300 periods, or for 1 μm , 10 ps electron bunch. Slippage thus sets another limit in terms of undulator length, the electron bunch duration should be larger than $N_u \lambda_u$.

4.6.2 Efficiency

4.6.2.1 Efficiency increase by undulator tapering

Electrons travelling on half the width of the gain curve of $1/2N_u$ can deliver a relative energy of $\frac{\Delta\gamma}{\gamma} = \frac{1}{2} \frac{\Delta\lambda}{\lambda} = \frac{1}{4N_u}$ of their kinetic energy, the efficiency r becomes

$$r = \frac{1}{4N_u}. \quad (78)$$

The maximum efficiency is found by considering the total width of the gain curve, which would lead to $r = \frac{1}{2N_u}$. It is however less realistic because the energy spread effect can limit the process. For example, for 50 undulator periods, the efficiency is of the order of 0.5%.

If too much energy is taken by the light wave, the resonant condition is no longer fulfilled since the electron energy is reduced, the electrons consequently slow down. A way to enhance the efficiency is to control the push further the saturation, i.e. electron trapping in the slow space charge wave. Indeed, “the nonlinearity of the oscillations of the trapped particle in the potential well of the wave leads to phase scrambling and finally the particle phase distribution becomes uniform (no bunching). The space-charge Coulomb forces in the electron bunches and the ripple magnetic field strength can also contribute to beam thermalization. The wave growth vanishes if the electron distribution is uniform at the phase velocity of the wave” [125], so it was proposed to increase the intensity of the magnetic field (an exponential profile was chosen) just before the space charge wave saturates, enabling an increase in the radiation rate [125].

One can delay saturation and let the intensity grow further by adjusting the undulator magnetic field so that the resonance condition remains fulfilled. Such a configuration of undulator is called a ‘tapered undulator’ either by changing the period [126], proposed by P. Sprangle *et al.* (fourth FEL Prize in 1991), or by changing the amplitude of the magnetic field proposed by Kroll [120]. One introduces a magnetic field dependent on the longitudinal position, as $B_{uz}(s)$, as shown in Fig. 30. Technically, the change of magnetic field can be done by setting an angle between the girders of the magnetic arrays on which are located the undulator magnets, or by adopting a variable period [127]. The spontaneous emission properties of a tapered undulator have been calculated [128].

For a tapered undulator provides a varying magnetic field along the longitudinal direction $B_{uz}(s)$, the resonance condition can be maintained according to

$$\lambda = \frac{\lambda_u}{2\gamma_s^2} \left[1 + \frac{1}{2} \left[\frac{eB_z(s)\lambda_u(s)}{2\pi m_0 c^2} \right]^2 \right]. \quad (79)$$

The efficiency then depends on the number of electrons trapped in the potential well (bucket) and on the average energy loss of the resonant electrons.

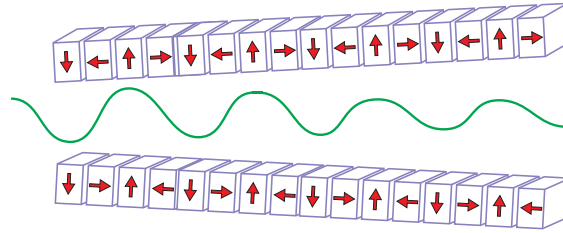


Fig. 30: Tapered undulator: the magnetic field amplitude depends on the longitudinal position. In the example here, an angle is set between the two girders supporting the magnet arrays.

4.6.2.2 Efficiency increase by energy recovery on the accelerator

There was also a strong interest to use recirculating accelerators for driving a FEL to recover the electron from one pass to another, and in particular of storage rings which exhibited good beam quality. The FEL theory was thus developed by the Italian team in particular, in considering both amplifier [129, 130] and oscillator [131] configurations. The electron beam distribution is modelled using the Fokker–Planck distribution. The energy spread enhancement and associated bunch lengthening due to the FEL interaction is kept on several turns. The competition with the anomalous bunch lengthening has also to be considered [132]. In the case of a storage ring FEL, the average power scales as

$$P \propto \left(\frac{\Delta\sigma_\gamma}{\gamma} \right)^2 P_{\text{sync}} \quad \text{with} \quad P_{\text{sync}} \propto IE^4. \quad (80)$$

It provides the limit which can be achieved on a storage ring FEL. It results from the radiative heating of the energy spread in electrons circulating in the storage ring. It is known as the ‘Renieri’s limit’. It has been independently found in Novosibirsk by N. A. Vinokurov [104].

4.7 FEL properties

The laser tuneability, one of the major advantages of FEL sources, is obtained by merely modifying the magnetic field of the undulator in a given spectral range set by the electron beam energy. The polarization depends on the undulator configuration.

The multimode theory was developed [133, 134] and the super-mode, defined “as the configuration of spatial modes, which reproduces itself after one passage throughout the interaction region” is introduced [135]. The evolution of the modes in the optical resonator was also used to evaluate the filling factor [88] and the multimode theory was examined considering the three-dimensional parabolic wave equation coupled to the Lorentz force equation [80, 136], enabling us to obtain different transverse mode patterns and dynamics [137]. FEL spatial and temporal behaviours were also examined as a coherent superposition of the exact Lienard–Wiechert fields produced by each electron in the beam [138]. The evolution of the free electron laser oscillator was further modelled using a Lagrangian formalism to follow the dynamics of the interaction between the electron beam and optical wave in a single pass [139].

After having a description of the gain and the saturation, theoreticians started to investigate coherence properties. R. Bonifacio [140] introduced the description in terms of electron field coherent quasi-classical states, where both the photon number and the electron momentum follow a Poisson distribution centred on the classical trajectories. G. Dattoli [141] examined the case of a given initial classical state, using a quantum description and looking at the coherent states of angular momentum and he found that “both the laser and wiggler fields are in the Glauber [142, 143] coherent state in the many mode case”. The study was then continued in the classical conditions [144] and quantum analysis [94, 145] showing that in fact, strictly speaking, FEL does not exhibit Glauber coherence [145].

4.8 Low gain FEL configurations

So far we have discussed mainly the oscillator configuration where the synchrotron radiation from the undulator (spontaneous emission) is stored in an optical resonator. The electron light interaction leads to bunched electrons which emit in phase with the incident wave which gets amplified.

An external laser tuned on the undulator resonant wavelength λ can be sent in the undulator, synchronized with the electron arrival. The light wave and the electrons can interact in the undulator, leading to the external light amplification. This configuration is called the ‘master amplifier’. Radiation is achieved on the same wavelength as the incident wave.

Using an external light wave tuned on the undulator resonance, the light wave interacts with the electron bunch in the undulator, inducing an energy modulation of the electrons; which is gradually transformed into density modulation at λ and leads to a coherent radiation emission at λ and λ/n , n being an integer (fundamental and harmonics) [81–83, 146–149].

Figure 31 presents the scheme of coherent harmonic generation: an external laser tuned on the fundamental of the undulator is used to modulate in energy, setting the emitters in phase for the radiation on the harmonics to emit coherently.

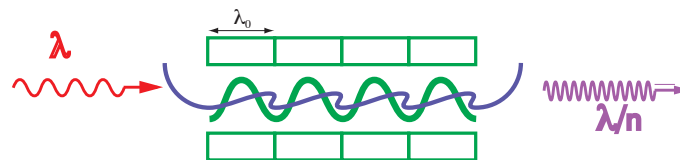


Fig. 31: Coherent harmonic generation scheme: an external laser tuned on the resonant wavelength of the undulator enables us to perform efficiently the energy exchange leading further to the density modulation and coherent emission on the harmonics.

4.9 Classical and quantum approaches: unification and quantum effects

Started with a first FEL theory discussed with quantum mechanics, FEL classical theory appeared to be very useful and applicable to the majority of the cases. While new theoretical approaches were investigated, unified models were searched. The formalism of the quasi-Bloch equations enables us to unify the quantum and classical approaches [144, 150]. Further, a unified theory of magnetic bremsstrahlung, electrostatic bremsstrahlung, Compton–Raman scattering, and Cerenkov–Smith–Purcell free electron lasers, are also proposed by A. Gover (18th FEL Prize in 2005) [151]. Quantum features and in particular coherence were also analysed using a non-linear quantum model [152, 153]. The limits of classical models were found when quantum effects start to influence the FEL process [124]. Quantum FELs have been actively studied in the R. Bonifacio’s group [154–158].

4.9.1 Quantum recoil

When an electron emits a photon $\hbar\omega_{\text{ph}}$, its energy is reduced by such an amount due to the quantum recoil. If the energy change due to the recoil is of the order or larger than the FEL gain bandwidth, i.e. given by the spontaneous emission width $\frac{\Delta\omega}{\omega} \approx \sqrt{(\frac{\Delta\omega}{\omega})_{\text{h}}^2 + (\frac{\Delta\omega}{\omega})_{\text{inh}}^2}$, then the quantum recoil may significantly affect the FEL gain. Consider a typical gain bandwidth of 10^{-3} , for a short wavelength FEL, the fraction of the energy change $\frac{\hbar\omega_{\text{ph}}}{E}$ is more than 10^{-6} , the quantum electron recoil is then negligible. It can then start to play a role with low energy electron beams and high energy emitted photons (for example in the X-ray range), such as in using an optical undulator (created by an optical wave).

4.9.2 Quantum diffusion

The emission of spontaneous emission radiation, if not affecting the electron energy by a significant amount, introduces an energy loss. In addition, the discrete nature of photon emission (over a wide energy spectrum) increases the uncorrelated energy spread, as for quantum excitation in a storage ring. The diffusion rate of the energy spread is given by [124]: $\frac{d((\Delta\gamma))^2}{ds} = -\frac{7}{15}r_e\bar{\lambda}_{\text{Compton}}\gamma_o^4 K_u^2 k_u^3 F(K_u)$ with $F(K_u) = 1.2K_u + \frac{1}{1+1.33K_u+0.40K_u^2}$ and $\bar{\lambda}_{\text{Compton}} = \hbar/m_o c \approx 3.86 \times 10^{-13}$ the reduced Compton wavelength [159].

5 The first FEL experimental results

5.1 The first FEL in Stanford (USA) in the infrared in 1977

5.1.1 The first FEL amplification in the infrared in 1976

After the theoretical prediction of the FEL concept in 1971, J. M. M. Madey searched how to set-up an experiment to test his idea of a FEL a [55]. Indeed, the High Energy Physics Laboratory on the Stanford campus concentrated a high knowledge on accelerator physics, both for normal conducting and superconducting devices. S-band accelerators had been developed by William W. Hansen (1909–1949) and Edward Ginzton (1915–1998) after the second World War, which led to the construction of the Stanford Linear Accelerator Laboratory (SLAC), a three kilometre S-band linac with upgraded klystrons under the direction of Wolfgang K. H. Panofsky (1919–2007). First superconducting linear accelerators were developed by William Fairbank (1917–1989) and Alan Schwettman (15th FEL Prize in 2002) [160], in order to exploit higher gradients and reduced power consumption of superconducting niobium cavities. High stability and sufficiently low energy spread beams for the low gain free electron laser exploration could be achieved on the superconducting linear accelerator.

J. M. J. Madey obtained financial support from the Air Force Office of Scientific Research (AFOSR) in 1972 in two steps: a first one to demonstrate gain, and a second one to achieve the FEL oscillation provided the first was a success. A team was gathered with J.M. J. Madey for laser physics, electronic instrumentation, cryogenic systems, superconducting undulator, Luis Elias (third FEL prior in 1990) for the optics, optical instrumentation, and conventional laser sources, superconducting undulator, and Todd Smith (third FEL Prize in 1990) for the accelerator. The composition of this new research team logically balanced the expertise between accelerators and electron tubes, and optics and lasers.

The first experimental demonstration of the FEL amplification was performed in Stanford in 1976 [161]. The electron beam has been produced by a 24 MeV electron beam generated by a superconducting undulator at 1.3 GHz. A 5.2 m long 3.2 cm period NbTi superconducting helical undulator was built (see Fig. 32) with a very high mechanical precision for the coil winding. It provided an undulator field of 0.24 T. A CO₂ laser at 10.6 μm with variable intensity and polarization was focused inside the undulator to a waist of 3.3 mm. The wavelength of the CO₂ laser being fixed, tuning was performed by changing the energy of the electrons around 24 MeV. The signal was detected with a high speed helium-cooled CuGe detector, synchronized with 1.3 GHz from the accelerator.

The CO₂ has been amplified, demonstrating a single pass gain of 7%, as shown in Fig. 33. Good agreement was found on the theoretical expectations regarding the gain. One notices that the gain is the derivative of the spontaneous emission, as understood by Madey [60, 87].

This FEL amplifier first experiment was a major step for the validation of the FEL concept with its gain medium using relativistic electrons in periodic magnetic fields.

5.1.2 The first FEL oscillator in the infrared in 1977

Because of the low value of the gain (7%), a high finesse optical resonator was necessary for attempting the oscillator experiment in order to insure cavity losses smaller than gain. An intermediate wavelength of (3.4 μm) was selected despite the small gain reduction, enabling the propagation of the desired funda-

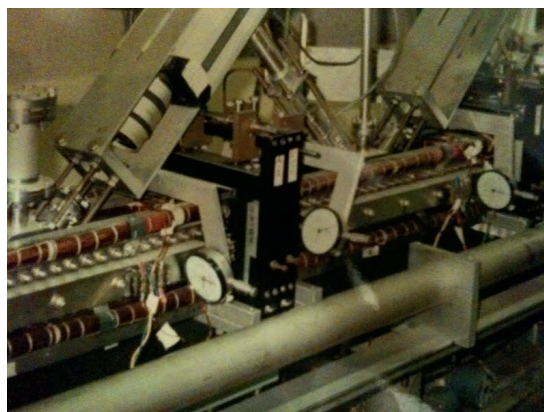


Fig. 32: Picture of the superconducting undulator used for the Madey's experiment

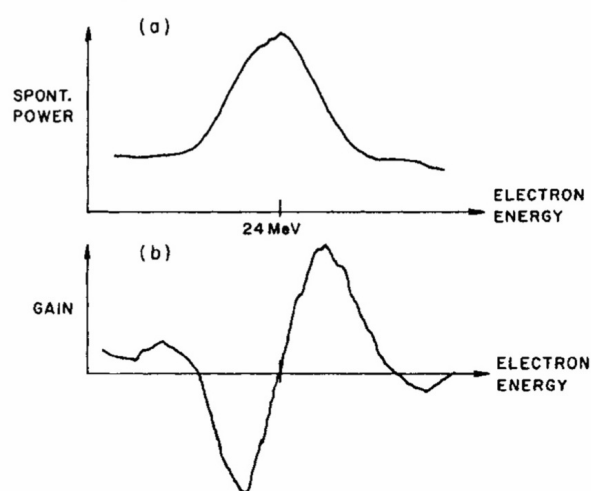


Fig. 33: (a) Spontaneous undulator emission and (b) measured gain which corresponds to the derivative of the spontaneous emission, from the first FEL amplification measurement by the Madey's group [161]. Undulator field of 0.24 T, peak current of 70 mA.

mental Gaussian resonator mode through the undulator vacuum chamber with minimal diffraction losses and to pre-align the optical resonator mirrors with an intracavity He–Ne plasma tube. Two new members joined the team: David Deacon as a PhD student, and G. Ramian for the accelerator injector since a higher peak current electron gun was required. Thanks to a gridded dispenser cathode (Eimac) driven by microwave triode amplifiers, 4 ps long electron macro-pulses with 2.6 A peak current at 11.8 MHz were achieved. Under such conditions, the expected gain reaching typically 100% appeared sufficient to overcome the cavity losses of 3% at $3.4 \mu\text{m}$. The undulator having being damaged by an unanticipated surge in the voltage provided by its high current power supply, a second superconducting undulator had been also built but it happened that a failure of the insulation of the wire drastically limited the rate at which the magnet could be ramped up or down during operation.

The experiment was finally ready for operation in December 1976, and the FEL oscillation was rapidly observed, in January 1977 after optimizing the electron beam steering and focusing and optical cavity tuning. Figure 34 shows the FEL line, as compared to the spontaneous emission: the FEL line is sharper (relative bandwidth of 0.23% Full Width Half Maximum FWHM), and much more intense. The FEL provided a 360 mW average power, corresponding to an estimated 7 kW peak power and 500 kW

intracavity peak power [162]. The output power reached nearly twice the power extracted from the electron beam in the amplifier experiment.

It can be pointed out that this first FEL result owes thanks to the quality of the electron beam delivered by the linear accelerator, together with its ability to provide rather long trains of electrons, enabling sufficient passes in the optical resonator to achieve the FEL saturation, (thanks to the high number of micro-pulses). Saturation was reached typically after $100 \mu\text{s}$. Cryogenic operation being rather heavy, the next experiments took place in 1981 [163, 164], enabling further analysis of the FEL properties, to be compared with theoretical expectations.

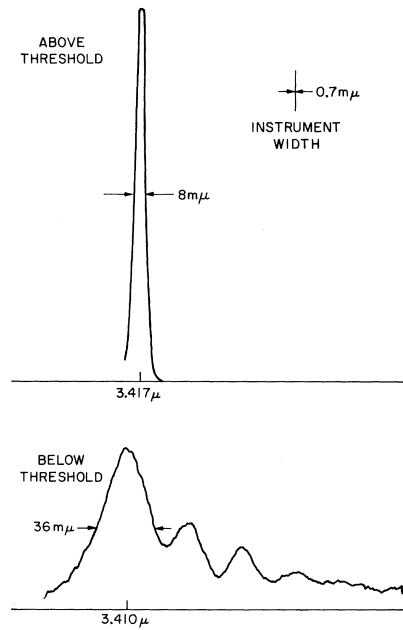


Fig. 34: First FEL: (a) FEL line at $3.4 \mu\text{m}$. (b) Spontaneous undulator emission [162]. Electron beam from the MARK-III superconducting accelerator at Stanford, superconducting helical undulator.

This infrared FEL oscillator achieved in 1977 on the superconducting linear accelerator (Stanford, USA) established the first experimental demonstration of the FEL concept as a new laser type. It had thus evidenced that this new type of laser based on stimulated Compton backscattering could effectively work and opened bright perspectives in terms of average and peak power outputs. It indeed paved the way towards the further advent of X-ray tuneable FELs as unique sources of radiation for matter investigation. It was also the first laboratory experiment of stimulated Compton backscattering.

5.1.3 New directions after the first results

The first FEL paper terminates with the following “Because the gain falls at short wavelengths, a higher electron current will be required to support laser operation in the visible and the ultra-violet. Based on the small-signal gain equations sufficient current has been stored in existing electron storage rings to sustain laser operation at wavelengths as short as 1200 \AA ” [162]. It thus gave directions of evolution. The first one dealt with the required improvement of electron beam parameters. The second concerned the attractiveness of the storage rings as an accelerator to drive the FEL, even in the isochronous operation [165]. Besides improvements on the electron characteristics, ways of increasing the undulator gain were investigated, such as the optical klystron [102] proposed by N. Vinokurov and Skrinsky, or the transverse gradient undulator enabling to handle a rather high level of energy spread [166]. “The transport system is designed to resolve the energy spread of the incident electrons into a transverse position and/or momentum spread at the entrance to the laser magnet. The magnet is designed to take advantage

of the different trajectories followed by electrons of different energies, with the result that the optical wavelength at which gain is a maximum is far less sensitive to the electron energy than it would be in a conventional system” [166, 167].

5.1.3.1 Towards a better efficiency using storage rings or electrostatic accelerators

From the very beginning, great hope was put in recirculating accelerators, since “the RF accelerating field for the ring would have to supply only the energy actually transformed to radiation in the periodic field. The overall efficiency of such a system thus would not be limited to the fraction of the electrons’ energy convertible to radiation in a single pass through the interaction region” [161]. In particular, free electron lasers on storage rings, as illustrated in Fig. 35, are considered in detail.

Specificities regarding the energy spread evolution due to the recirculation of the electrons in the storage ring after their heating by the FEL interaction have been investigated from a theoretical point of view. The energy spread can be enhanced via the FEL process but it can then be relaxed via the natural damping which takes place in the storage ring [129, 131].

One constraint comes nevertheless from the fact that the length of the straight section is limited.

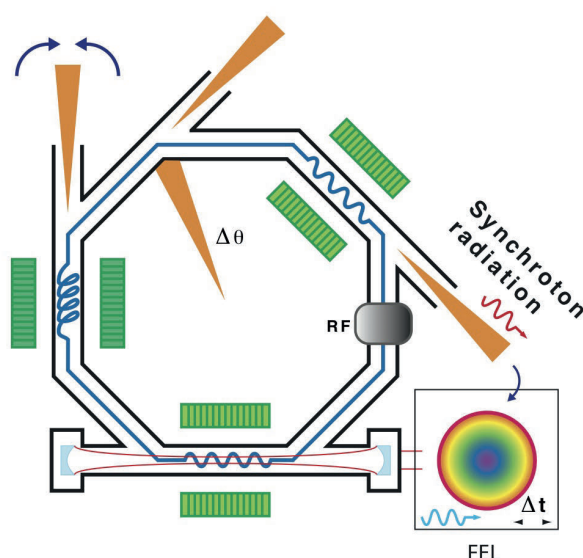


Fig. 35: Scheme of the storage ring free electron laser

J. M. J. Madey then searched for a storage ring to implement a storage ring FEL test experiment. Yves Petroff and Yves Farge, the director of LURE (Laboratoire d’Utilisation du Rayonnement Electromagnétique) in France were quite positive on the idea of using the ACO (Anneau de Collisions d’Orsay) storage ring for FEL investigations. ACO was initially build for high energy physics, and it turned to a parasitic use of synchrotron radiation in the beginning of the eighties. J. M. J. Madey came with some collaborators (D. Deacon, K. Robinson) while Y. Farge and Y. Petroff settled some team on the French side, with Michel Billardon (14th FEL Prize in 2001), Jean-Michel Ortéga (14th FEL Prize in 2001). M. E. Couprie (14th FEL Prize in 2001) and R. Prazeres joined the team later. An experiment was also set up on VEPP-3, in Novosibirsk [168], on Adone (Frascati, Italy) [169], and Brookhaven National Laboratory [170].

Besides the storage ring type of accelerator, L. Elias (Third FEL Prize in 1991) did consider the use of a DC electrostatic accelerator such as Van der Graff for the operation of high power efficient tuneable FEL [171] with low energy electron beams. Indeed, “Wall power to laser power efficiencies greater than 10% are possible” and should be compared to the 0.2% value in the case of the first Stanford experiment.

Analysis are carried out for a 9.38 MeV for 400 nm, and 3.55 MeV for 16 μm . Further analysis confirmed the possibility of highly efficient energy recovery [172] with DC electrostatic accelerators enabling to reach the required high average currents in the long pulse and CW operation modes for a FEL application [173].

5.1.3.2 *Towards lower emittances and higher electron beam current*

Besides the storage rings and electrostatic accelerators, realizable FELs on linear accelerators were considered [174], especially in terms of emittance, current density, electron bunch length, and stability. J. M. J. Madey nevertheless states that “As satisfying as it was to have completed two key proof of principal experiments, it was also clear that the development of useful devices based on this new gain mechanism would require both further theoretical and technical efforts. Although the experiments had established the capability of the new mechanism to operate at respectable signal levels, some significant questions remained as to the physical basis of these results. Higher electron currents and lower e-beam emittances would also clearly be required for operation of shorter wavelength and more compact systems” [55].

5.1.3.3 *Following years of expectations*

The great enthusiasm due to the success of the first FEL demonstration led to several experimental initiatives around the world, to extend the FEL achievements. It was followed by six years of expectations, as reported by C. A. Brau [1] as follows “Unfortunately, none of the electron-beam sources available at that time had enough electron-beam current and satisfactory electron-beam quality to make lasing easy. Although gain was measured in several experiments, it was not until six years later, in 1983, that the second free-electron laser was operated in the optical part of the spectrum. In that year, three devices began to lase”.

The first was at Laboratoire pour l’ Utilisation du Rayonnement Electromagnétique (LURE), in Orsay, France, where the electron beam in the storage ring ACO was used to achieve lasing in the visible [175, 176].

The second was at Stanford, a team from TRW (Thompson Ramo Wooldridge (Northrop Grumman since 2002)) used the superconducting accelerator previously used by Madey to achieve lasing in the near infrared [177].

The third was Los Alamos, where a newly constructed electron accelerator was used to achieve lasing in the mid-infrared [178].

During the same period, development of ubitron-type devices began at several laboratories. Because the threshold electron beam current at which the space charge wave can be excited increases as the third power of the electron energy, these devices were limited to low electron energy (no more than a few megaelectronvolts), and long wavelength. Nevertheless, Marshall and his co-workers at Columbia and Naval Research Laboratory achieved lasing at 400 μm with an electron beam having an energy of 1.2 MeV and a peak current of 25 kA [179]. “These devices are limited to wavelengths in the submillimetre region and beyond, where the optical radiation is transmitted through a waveguide’, and “the physics in this regime involves collective oscillations (space charge waves) in the electron beam”, the development of ubitron-type devices is not developed in this FEL history [69].

At the end of 1982 (September 26–October 1) the ‘Bendor Free Electron Laser’ conference was held in France, whose subject matter was limited to the FEL in the Compton regime. It gathered 62 participants. The atmosphere was particular, since a lot of efforts devoted towards the operation of new free electron lasers started to provide preliminary results. In the foreword of the proceeding by D. A. D. Deacon and M. Billardon, it is said: “The most striking aspect of the collection of papers contributed to this volume is the amount of experimental progresses which have been made in the 12 months since the last summary of progress of the field. Four new undulators have been brought into operation, and measurements have been made on the spontaneous emission spectra, gain, electron trapping in the linac

and bunch lengthening in the storage ring, sub-threshold effects and mirror degradation, time dependent short pulse phenomena; and laser-induced harmonic generation. This sudden (and exhausting) blooming of experimental results has in fact been in the making for two or three years. The perseverance of the authors of these works during this long preparation time deserves recognition and applause.

In the short wavelength $\lambda < 1 \mu\text{m}$ range, where the storage ring is the universally favoured device because of its current density and duty factor, four projects are underway at Brookhaven, Frascati, Orsay, and Novosibirsk. The Frascati and Orsay groups have contributed to the proceedings two valuable papers which summarized a wide variety of measurements and FEL diagnostics. These two groups (along with the Novosibirsk physicists who were unable to attend the conference) have been able to probe and verify the theory of the FEL to a level of precision and complexity which is unthinkable in the linear accelerator machines.

In the long wavelength $\lambda > 1 \mu\text{m}$ range, a lower current density is required to drive the interaction, and a wide variety of electron beam sources are now being put into use at 11 experimental centres. There are two induction linac sources, two microtrons, six RF linacs, one storage ring, and one van de Graaf sources being set up or used for FEL work at the following respective centre, Lawrence Livermore Laboratory, Naval Research Labs., Bell Labs., Frascati (ENEA), Los Alamos national Laboratory, Math. Sciences Northwest, NRL, Stanford (H. E. L. P.), TRW, the UK Collaboration, Berlin, and Santa-Barbara. At present, all the experimental work in this wavelength region has been done with the RF linacs. As is the case for short wavelength work, in the previous 12 months an unprecedented flow of new research results have been produced in the infrared devices. During the conference, these results were described by the Stanford group, who had succeeded in measuring the time structure of their picosecond laser pulses, and by the Los Alamos, the MSNW (Mathematical Sciences NorthWest), and the TRW groups, who have been able to measure the electron trapping in tapered wigglers.”

Next we discuss the three new FEL operations achieved in 1983.

5.2 The second FEL in Orsay (France) in 1983

5.2.1 The second FEL oscillator in Orsay (France) in the visible in 1983

At that time, storage rings appeared as suitable accelerators because of the electron beam performance. A picture of the ACO (Anneau de Collisions d'Orsay) storage ring (LURE, Orsay, France) is shown in Fig. 36.



Fig. 36: ACO storage ring used for the second world wide FEL in Orsay (France), dipoles in blue

First measurements started with a superconducting undulator (23×40 mm periods, maximum field of 0.45 T, $K = 1.68$ T) with an inverse T-shape vacuum chamber [180, 181], enabling to observe visible radiation between 140 and 240 MeV. The gain has been measured [182] and found to be very small, it thus required mirrors of extremely low losses. It appeared that significant imperfections in the magnetic field led to a broadening of the line and a gain reduction of 50%.

It was followed by the construction of a SmCo_5 permanent magnet-based undulator [183, 184] ($17 \text{ mm} \times 78 \text{ mm}$), using the configuration proposed by Halbach [32] with magnets rotated by $\pi/2$ from one position to another. The radiation produced by such an undulator was observed in the Vacuum Ultra Violet (VUV) for the first time using the ACO electron beam at 536 MeV. However, the straight section length being limited to 1.3 m, the gain was limited to a few 10^{-4} [185] and made the laser oscillation impossible despite the efforts concerning high reflectivity mirrors [186]. The gain could be enhanced by a factor of 2 up to 7 by turning the undulator to the optical klystron configuration by replacing the three central periods by a three pole wiggler [187]. The radiation has been measured and analysed, as shown in Fig. 37 [184].

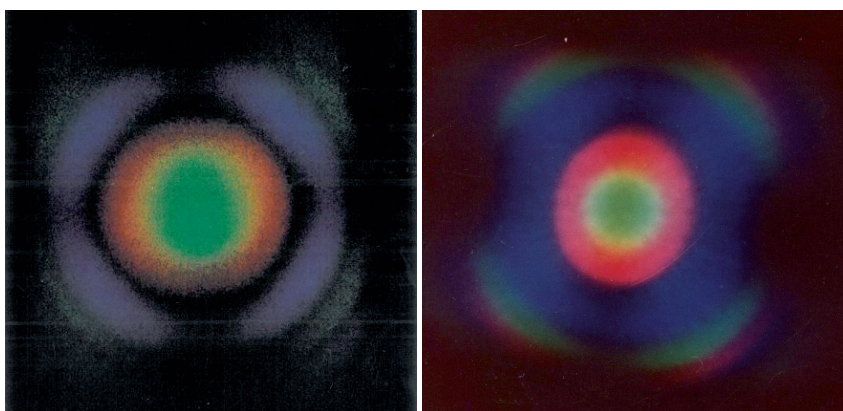


Fig. 37: ACO optical klystron spontaneous emission for different undulator gaps

Because of the mirror reflectivity degradation induced by the harmonic content of the undulator, the electron beam energy has been set between 160 and 166 MeV to minimize the undulator harmonic content. The optical cavity has a length of 5.5 m with round trip cavity losses of 7×10^{-4} . ACO (Orsay, France) [175] provided the second worldwide FEL (first visible radiation) in 1983. Figure 38 shows the laser tuneability achieved on ACO by changing the optical klystron gap. Getting the level of the cavity losses smaller than the gain was at time very challenging, and issues with mirror degradation induced by synchrotron radiation and mirror measurements were investigated [186].

Lasing was occurring on different lines of the optical klystron spectrum, as shown in Fig. 39. When the electron bunches circulating in the ring are not synchronized with the optical pulses bouncing between the mirrors, i.e. in the optical cavity detuned configuration, the energy exchange could not take place, and the measured spectrum corresponds to that of the spontaneous emission. When the cavity is properly tuned and the gain is larger than the cavity losses, then the optical klystron lines are growing and lead to the laser effect. Because of the fringe structure of the optical klystron, three lines are simultaneously lasing with the most intense one at $647.6 \mu\text{m}$, each wavelength being located at a maximum of the gain versus wavelength curve, fulfilling properly the Madey theorem. This ACO FEL can be considered as the first multi-colour FEL.

Various studies were carried out after the first laser oscillation on ACO [185, 188, 189]. The FEL dynamics involves an interplay between the electron energy heating induced by the FEL interaction and the synchrotron damping. The FEL was exhibiting a naturally pulsed macro-temporal structure for perfect synchronism (synchronization between the electron circulating in the storage ring and the optical pulses bouncing around the mirrors of the optical resonator) [190], as shown in Fig. 40. Due

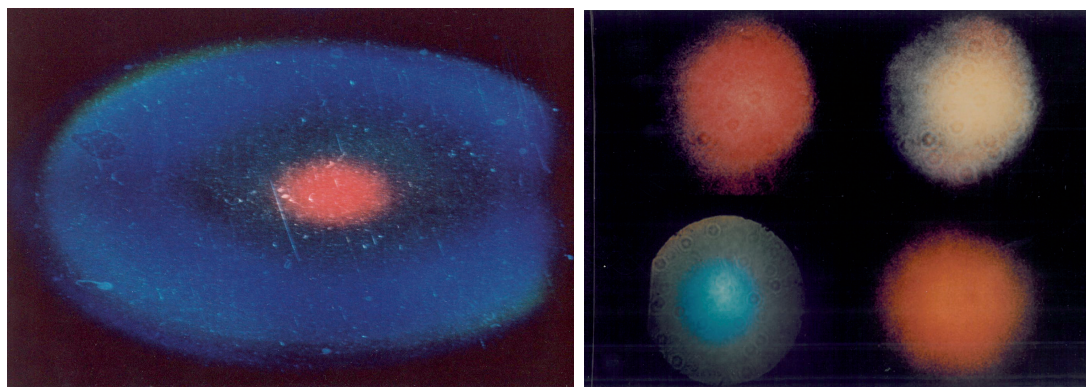


Fig. 38: First visible FEL on ACO storage ring in France in 1983. Left : Laser oscillation with red central wavelength, right : free electron laser tuneability in the visible

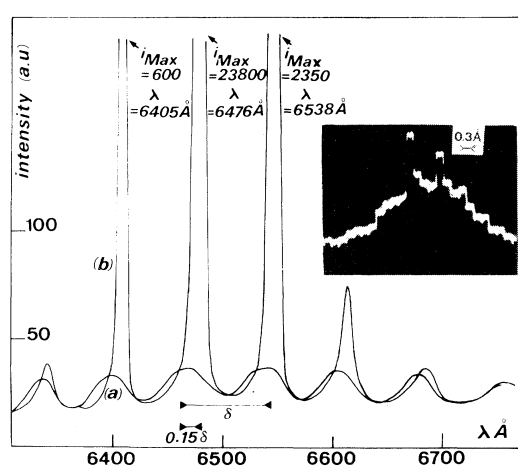


Fig. 39: First visible FEL on ACO storage ring in France in 1983 Spectra of the cavity output radiation under two conditions: a) cavity detuned without amplification and b) cavity tuned (laser on), from [175]. Insert: zoom on one laser line.

to the electron beam recirculation, the electron bunch heating induced by the FEL interaction leads to an electron bunch lengthening [191] and even to a modification of the shape of the electron bunch longitudinal distribution [192]. The FEL was operated in the Q-switching mode, in cancelling the optical gain by a small variation of the RF frequency, triggered by an external pulsed low frequency generator or by applying a modulation of the transverse position of the electron beam with the electric field of a pick up electrode. During a few milliseconds, the optical resonator being tuned, the FEL pulse can develop. Then, the pulse naturally decays, and afterwards, the cavity is detuned enabling the electron beam to be cooled down, and the FEL pulse to restart with the maximum power starting from non-heated electron beam.

5.2.2 Coherent harmonic generation in the VUV on the ACO storage ring Orsay (France) in the UV and VUV

Coherent harmonic generation [193] was achieved in the UV and VUV on the ACO storage ring. a Nd-Yag laser (1.06 μm wavelength, 20 Hz repetition rate, 15 MW peak power, 12 ns pulse duration) was tuned on the optical klystron first harmonic. The coherent third and the fifth harmonic of Nd-Yag laser were observed, with a spectral ration of 6000 for the third one, and 100 for the fifth one. It was then followed by further measurements in the VUV [194, 195].

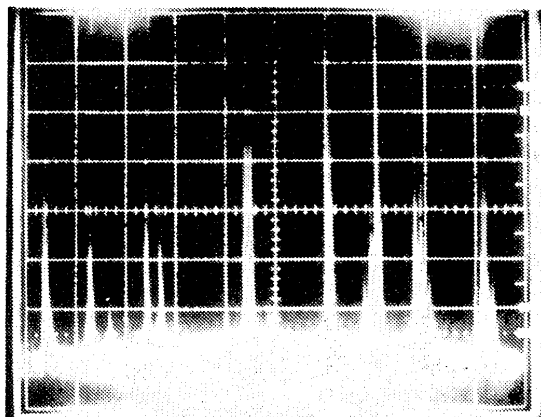


Fig. 40: Temporal structure at perfect synchronism on the ACO storage ring FEL, from [175]

5.3 The next two FEL oscillators in 1983

5.3.1 *The new developments on the Stanford HEPL FEL*

Led by a team of TRW, Space and Technology Group, the Stanford FEL has been operated with a tapered undulator in order to enhance the efficiency [177]. The FEL has been operated above threshold at the wavelength of 1.57 μm . The employed undulator is a permanent magnet one in the Halbach configuration [196] using SmCo_5 magnets with a period of 36 mm reaching up to 0.29 T. The peak field is varied longitudinally by controlling the spacing between the magnet planes. Inspired from the optical klystron, the undulator consisted of different segments: a prebuncher with a constant undulator field providing energy modulator of the electron beam, a dispersive section, a tapered section to improve trapping and higher extraction efficiency, and a radiator with constant undulator field. The laser was operated with 0%, 1%, and 2% tapers in energy, achieving laser efficiency of 0.4%, 1.1%, and 1.2%, respectively. The efficiency of the 2% taper was three times the untapered case. T. Smith converted the FEL to a user facility.

5.3.2 *The Los Alamos FEL*

Los Alamos National Laboratory had set up a FEL programme, aiming at demonstrating high power at 10.6 μm .

A first objective was to demonstrate the advantages offered by permanent magnet-based undulators, by developing a permanent magnet undulator in the Halbach configuration [196]. An undulator of 1 m long, 27.3 mm period, 8.8 mm gap, 0.31 T peak field, thanks to a funding from the Department of Energy, was built by R. Warren (sixth FEL Prize in 1993). It was decided to set the magnets directly in a vacuum in order to reach a higher magnetic field. Three fluorescent targets were installed on the electron path, for a proper alignment of the vacuum chamber and overlap of the electron / photon beams [197].

A linear accelerator of 20 MeV energy at 1.3 GHz was built on purpose for the experiment. It provided a peak current of 20 A, with an emittance of 2 mm mrad, an energy spread of $\pm 1\%$, and a total length of 10 m. It is the first FEL experiment with a dedicated accelerator, whereas the competing experiments are sharing the use of the electron beam.

The FEL operation by itself required the use of highly reflecting dielectric mirrors placed directly in vacuum and with a good resistance to high laser power. Besides, the electron beam macro-pulse should be sufficiently long to enable the growth of the FEL power. The optical resonator had a length of 9.92 m, matching the electron micro-pulse separation of 46.15 ns and cavity losses of 3%. Mirrors were compatible with an alignment with a He-Ne laser.

The FEL gain using a CO₂ laser was measured. FEL oscillation was obtained in 1983 in the 9–11 μm spectral range, with an intra-cavity peak power of 20 MW and an average output power of 1 kW in 70 μs macro-pulses [178, 198]. Nine orders of magnitude of power growth were observed with a net growth of 17%. A Germanium detector was used for the analysis of the optical signal. Harmonic lasing was observed on the second and third harmonics and characterized by different decays in the optical cavity. The FEL was then studied in details [199, 200]. The dependence of gain and saturation on cavity length, alignment, beam parameters, and other critical variables were compared with theory.

The Los Alamos team was eager to improve the FEL efficiency and first demonstrated an extraction efficiency larger than 3% [201] in the amplifier configuration with a tapered undulator. An efficiency larger than 4% [202] in an oscillator configuration was then obtained, as shown in Fig. 41.

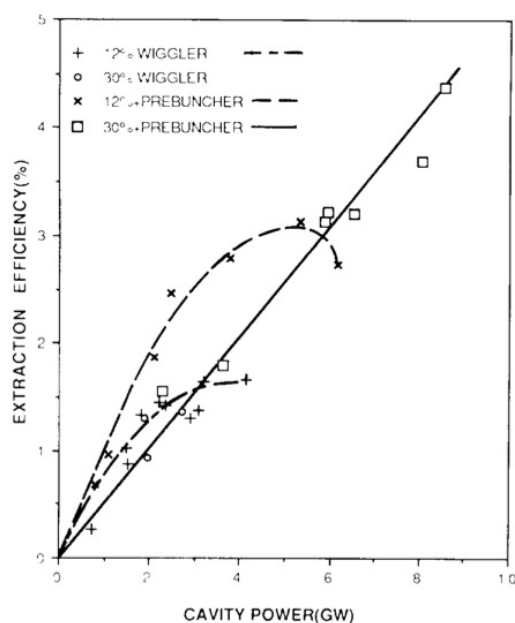


Fig. 41: Efficiency in the case of a tapered undulator in the Los Alamos oscillator experiment from [200]

5.3.3 The Santa Barbara FEL

Besides the interest of storage rings for electron beam recirculation, the use of energy recovery on an electrostatic accelerator was studied [171]. An experiment was thus set at the University of California, Santa Barbara, using an electrostatic accelerator [173], as shown in Fig. 42.

The electron beam is produced in an electron gun, then goes through a pelletron charging chain so that it is charged to a negative high voltage with respect to the ground, and it is accelerated in the accelerator column. It is transported and matched to the FEL line with the undulator and the optical cavity thanks to a set of achromatic bends and quadrupoles, and then sent back to the electrostatic tube entrance where it is captured by the low voltage multistage collector and restored the lost energy by FEL interaction. Energy recovery is of interest for FEL since only typically one percent of electron beam energy is converted to the FEL. It can also lead to a more stable electron beam. The FEL was operated with a permanent magnet Halbach type undulator (36 mm period, 38 mm gap, 0.46 T peak field) with a waveguide resonator [203] using electrons of 2.98 MeV providing a peak current of 1.25 A, with macro-pulses of 50 μs long and a 90% recovery efficiency. The optical beam was produced in the far infrared at 750 GHz with 30% gain per cycle for 11% losses per cycle, with 10 kW estimated peak power. The saturation was reached in 4 μs [204]. Single-mode operation in a free electron laser was then observed [205].

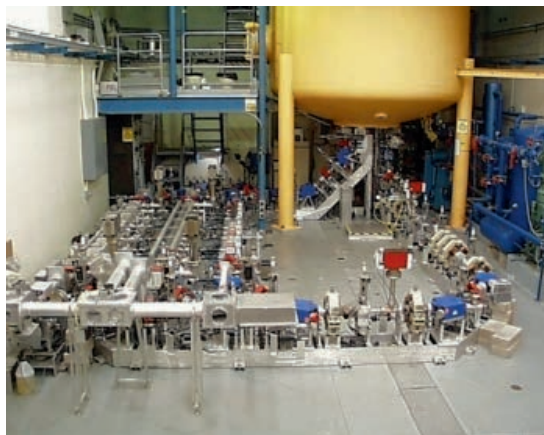


Fig. 42: Picture of the Santa Barbara (USA) FEL

5.4 Following developments on low gain FELs

Following these new FEL operations, the field was in rapid expansion, and FEL experiments were installed on various types of accelerators. There was a quest for wavelengths of operation, which depended on the electron beam, the mirror performance for the oscillator configuration and the ways to increase the gain. In addition, coherent harmonic generation using an external laser was continued. However, not all the projects have been successful as states C. Brau in his book in 1990: “It should be pointed out that of the free electron lasers which have been constructed thus far, considering only those built to operate in the optical regime, only a few have worked. The reason for failure, in most cases, has been that the available electron accelerator was not satisfactory for free-electron laser experiments and could not, within time and budget restrictions, be suitably modified. One or two of the lasers which have not yet worked may yet be brought into operation, but free-electron lasers remain subtle, expensive devices” [1]. Ten years after the first Stanford demonstration, there were still less than 10 Compton FEL under operations [2] but there was already a great interest for user application. Are given below examples of FEL launched in the continuity of the first FELs and which contributed significantly to the FEL field growth. These examples are not intended to be exhaustive. W. B. Colson was, during FEL conference, collecting the information on the different FELs under operation and progress [206, 206–208]. In the report of the FEL conference held in 1994 a national research Council FEL Committee report [209] is mentioned, chaired by D. Levy, recommending building infrared FELs as user facilities, developing the technology for UV FELs, and research and development for X-ray FEL.

5.4.1 FEL oscillators

In the early years of FELs, the type of accelerator, especially because of electron beam performance, defined somehow the reachable spectral range, as illustrated in Fig. 43. The main progress on the FELs built after the results of 1983 are described below, classified per accelerator type.

5.4.1.1 Storage ring based FELs

The activity continued on storage rings [210, 211] especially for the quest towards short wavelength of operation, since high quality electron beams were still produced. In addition, the interplay between the beam dynamics in the ring and the FEL interaction was of great interest.

VEPP-3 FEL IN RUSSIA

The second storage ring FEL following the one on ACO was achieved on VEPP3 (Novosibirsk, USSR) [212–215] in 1988. The team led by N. Vinokurov (fourth FEL Prize in 1991) included in particular

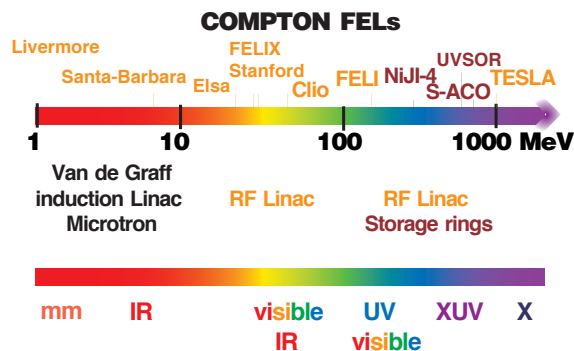


Fig. 43: Accelerator type used for FEL and corresponding spectral range. Examples of FELs

V. Litvinenko (17th FEL Prize, in 2004), I. Pinaiev, V. Popik, N. G. Garvilov, A. S. Sokolov, as younger scientists at that time, and senior ones with A. N. Skrinski and G. N. Kulipanov. Mutual coherence of spontaneous radiation from two undulators separated by an achromatic bend was observed [216, 217]. The experiment was renewed, with an electromagnetic optical klystron implemented [218] on a bypass [219], as shown in Fig. 44.



Fig. 44: Picture of the VEPP3 FEL optical klystron (the FEL was installed on the ceiling)

Because of the very low gain, despite the enhancement close to the optical klystron, the cavity losses were very critical. A method of mirror measurement with a reflectivity close to unit was proposed [220]. The confocal configuration for the optical cavity was studied [221]. The laser covered from the visible to the UV down to 240 nm with three sets of mirrors. Linewidth narrowing was achieved with a Fabry–Perot etalon [222–224], reaching a relative band width of 10^{-5} , as shown in Fig. 44.

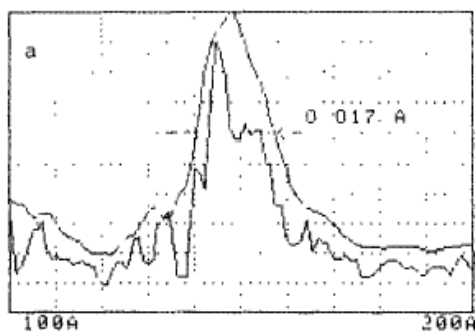


Fig. 45: Linewidth narrowing on the VEPP3 FEL with an etalon installed inside the optical resonator, from [223]

VEPP3 FEL kept for a while the record of the shortest FEL wavelength at 200 nm. Measurements of FEL spectra and temporal structures were compared to the theory [225].

SUPER-ACO FEL IN FRANCE

Then, the third storage ring FEL was obtained on the Super-ACO (Orsay, France) [226–228] following the successful results achieved on ACO. Super-ACO was a storage ring built on purpose for synchrotron radiation use. Super-ACO FEL was operated at 600 MeV, and then 800 MeV, which was the highest electron beam energy for a storage ring FEL. The Super-ACO optical klystron spectrum and associated gain are shown in Fig. 46. The gain is the derivative of the spontaneous emission, as given by the Madey’s theorem.

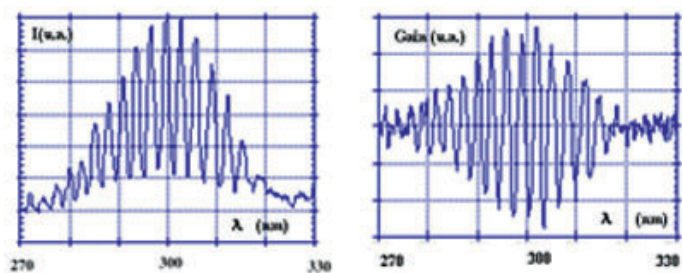


Fig. 46: Super-ACO optical klystron spontaneous emission for different undulator gaps

The undulator synchrotron radiation led to even more drastic conditions of degradation of the multilayer mirrors in the optical cavity [229] requiring specific mirror characterizations [230]. The FEL was then obtained in the UV [231, 232]. The FEL was fully characterized. Transverse modes can be controlled via the optical resonator [233] as shown in Fig. 47.

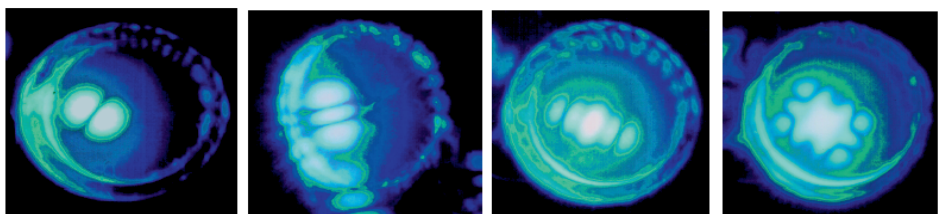


Fig. 47: Super-ACO transverse mode resulting from a misalignment of the optical cavity axis with respect to the magnetic axis of the undulator.

The temporal profile was studied [234, 235]. The zero detuning regime with CW operation of the FEL was stabilized using longitudinal feedback [236]. Extensive studies on longitudinal dynamics were carried out [237]: the coupled dynamics of the electrons in the storage ring [238], mutual influence of the coherent synchrotron oscillations [239], local energy exchange between the FEL and the electron beam [240], FEL-induced suppression of the sawtooth instability [241], control of the pulsed zones versus detuning [242], and advection-induced spectro-temporal defects [243]. The super-ACO ring was shut down in 2003.

TERAS (TSUKUBA ELECTRON RING FOR ACCELERATING AND STORAGE) AND NIJI-IV FEL IN JAPAN

Storage ring FEL oscillation was then obtained on TERAS (Tsukuba, Japan) [244], NIJI-IV (Tsukuba, Japan) (Niji is the Japanese word for "rainbow") [245].

UVSOR (ULTRAVIOLET SYNCHROTRON ORBITAL RADIATION) FEL IN JAPAN

A storage ring FEL was developed on UVSOR (Okazaki, Japan) [246]. The first developments of the UVSOR FEL were led by H. Hama (17th FEL Prize in 2004). One of its specificities is the use of an helical optical klystron [247]. Temporal dynamics was studied [248, 249], longitudinal feedback was developed to stabilize the temporal position of the FEL micropulse [250].

DUKE FEL IN THE USA

The DUKE (Duke, North Carolina, USA) FEL, shown in Fig. 48, was first operated in the visible [251], and then in the UV–deep UV [252] below 200 nm [253] with a distributed optical klystron implanted on a long straight section, enabling a reasonable gain. The DUKE FEL conducted also various dynamical studies [254], such as the observation of giant pulses [255], self-induced harmonic generation [256], time structure [257], and output power limitations [258]. Micropulses are Fourier limited [259]. The DUKE FEL was first developed by V. Litvnenko (17th FEL Prize in 2004).

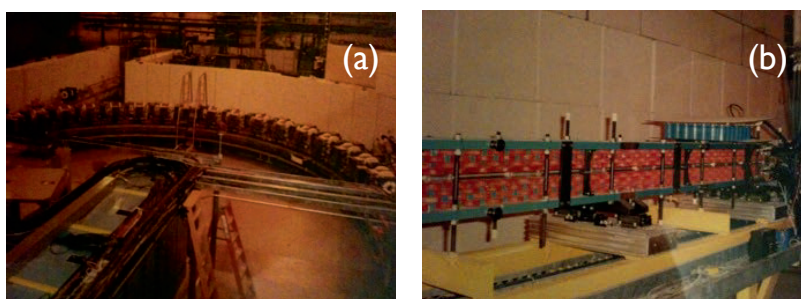


Fig. 48: DUKE FEL pictures: (a) the ring, (b) the multiple optical klystron

The DUKE storage ring is a dedicated accelerator for FEL operation and it is still under operation.

DELTA (DORTMUND ELECTRON ACCELERATOR) FEL IN GERMANY

The FEL was also achieved on the DELTA (Dortmund, Germany) storage ring in the visible and UV [260].

ELETTRA FEL IN ITALY

The FEL on the ELETTRA (Trieste, Italy), using a helical optical klystron, could provide sufficient gain as well [261]. After its first operation [262], it enabled operation at shorter wavelengths [263, 264] in the VUV at 190 nm, setting the record of the shortest wavelength achieved on a FEL oscillator. For short wavelengths, mirror degradation due to undulator synchrotron radiation appeared to be critical [265–268].

Even though the ELETTRA FEL was quite successful, it had to be operated in dedicated shifts [269]. A storage ring FEL is usually operated at a lower beam energy than the one employed for conventional synchrotron radiation users, setting a limit in the development of the storage rings FELs. This was also the main reason for the withdrawal of the SOLEIL FEL [270].

5.4.1.2 Linac based FELs

MARK III FEL STANFORD AND THEN DUKE UNIVERSITY, USA

The MARK III FEL (started in 1986 at Stanford University and then moved to Duke University, USA)

used a normal conducting linear accelerator (26–45 MeV, 10π mm mrad emittance, 0.7% energy spread, 20–40 A peak current) operated in the infrared (1.4–8 μm) and enabled different FEL studies such as harmonic lasing [271], coherent harmonic emission [272], pulse compression using energy chirp [273, 274], and master oscillator power amplifier (MOPA) configuration [275]. User applications were then developed.

Dedicated linac-based FELs were then built for user applications.

VANDERBILT UNIVERSITY FEL, USA

The Vanderbilt University FEL (Nashville, USA), led by C. Brau (ninth FEL Prize in 1996) used a MARK III-type linear accelerator and a 1.08 m length, 23 mm period, 0.4 T field undulator [276] and was established to serve the medicine and material science fields [276, 277]. It operated in the infrared (2–10 μm).

FELIX, THE NETHERLAND

FELIX (The Netherland), led by A. Van der Meer (12th FEL Prize, 2002), uses a normal conducting linear accelerator (15–45 MeV, 50π mm mrad emittance, 0.25% energy spread) 38×65 mm period, 0.22 T field undulator first operated in the 6–100 μm spectral range [278]. Various studies have been carried out, such as phase locking [279], limit-cycle operation [280], and single mode selection [281]. FELIX has been operating for 25 years.

CLIO (CENTRE LASER INFRAROUGE D'ORSAY), FRANCE.

CLIO (Orsay, France), led by Jean-Michel Ortéga (11th FEL Prize, 2001), uses a normal conducting linear accelerator (30–70 MeV, 50π mm mrad emittance, 0.2% energy spread, 100 A peak current) 1.08 m length, 48 mm \times 23 mm period, 0.4 T field undulator [282] first operated in the 2–17 μm [283] and then 3–120 μm [284] spectral range for users. Various operating modes were investigated, such as two colour operation [285], efficiency improvement [286], sub-picosecond pulse regimes [287]. CLIO has been in operation for 25 years.

ELSA (ETUDE D'UN LASER ACCORDABLE, STUDY OF A TUNEABLE LASER), FRANCE

Another infrared FEL was built and operated in France, on the linear accelerator ELSA, enabling lasing [288] and studies on high efficiency [289].

FELBE, GERMANY

FELBE (FEL at the Electron Linear Accelerator with High Brilliance and Low Emittance) (Forschungszentrum Dresden-Rossendorf, Germany) [290], uses a superconducting linear accelerator consisting of two 20 MV superconducting units operating in CW mode with a pulse repetition rate of 13 MHz, with 1 mA average current. It serves two free electron lasers (U27-FEL (until end of 2016) and U100-FEL), produces coherent electromagnetic radiation in the mid and far infrared (4–250 μm). Pulse energies are in the few 100 nJ range with pulse durations of a few picoseconds. The typical operation mode offers a 13 MHz micropulse repetition rate in macropulses of a few 100 μs at up to 25 Hz or, alternatively, FEL operation in a continuous 13 MHz mode.

FELI (FREE ELECTRON LASER RESEARCH INSTITUTE), JAPAN

FELI (Japan) was built in Japan and serves different user beamlines [291–293].

5.4.1.3 Induction linac based FELs

High power FELs were developed both at Livermore (USA) [294] and at CESTA (France) [295]. These results will be described further in the high gain section.

5.4.1.4 Microtron based FELs

A Cherenkov FEL was built in ENEA (Frascati, Italy). The electron beam at 5.3 MeV with a 200 mA current, with emittances of 6π mm mrad in the vertical, 18π mm mrad in the horizontal, and a 0.5% energy spread is focused to travel close and parallel to the dielectric (polyethylene). A quasi-optical resonator using a mirror and an output coupler provides feedback to the radiation. The FEL was emitted at $1660 \mu\text{mrad}$ [296, 297].

A FEL in the mm wavelength range was achieved on the Pahra microtron in the Lebedev Physical Institute (Moscow, Russia) with an electron beam of at 7 MeV, 50 mA current, 40π mm mrad (6π mm mrad) radial (vertical) emittances, a 0.1% energy spread, an undulator (6×168 mm periods, 0.26 T) and a waveguide, mylar mirrors [298, 299].

KAERI (Korea) has developed a compact far infrared (FIR) FEL driven by a 7 MeV microtron [300].

5.4.1.5 Energy recovery accelerator based FELs

Besides electrostatic accelerators, energy recovery can also be performed using linear accelerators. In energy recovery linacs (ERL), the electron beam is recirculated in a loop so that it enters again the accelerating sections, but dephased by π , so that the beam energy is given back to the accelerating sections [301]. It thus provides a high electron beam efficiency and reduces the radiation hazard by setting the beam dump at low energy. ERL-based FELs are suitable for high average power output [302].

JEFFERSON LABORATORY FEL, USA

An ERL-based FEL was first operated in the infrared at Jefferson Laboratory (Virginia, USA) by the team of G. Neil (13th FEL Prize in 2000) and S. Benson (13th FEL Prize in 2000). The superconducting energy recovery linac provides an electron beam at 18.7 MeV with a 5 mA current, 80 pC charge, 60 A peak current, 7.5π mm mrad emittance, and transforms 75% of the beam power back to RF power. The FEL has been operated at $3.1 \mu\text{m}$ [303] with an undulator of 40×27 mm period, 1.4 deflection parameter and an 8 m long optical cavity with infrared mirrors of reflectivity of 99.85%. Laser damage could be an issue [304]. The average power reached 1 kW [305]. The FEL was operated in the tapered configuration [306] In July 2004, 10 kW of CW operation was achieved at a wavelength of $6 \mu\text{m}$ [307], and then extended in 2006 to 14.2 kW at $1.6 \mu\text{m}$ in a CW mode of operation [308]. After a machine modification, the spectral range has been extended to the UV in 2010 down to 363 nm with 100 W average power level [308].

JAERI FEL, JAPAN

E.J. Minehara (13th FEL Prize in 2000) led the team of the JAERI FEL installed on the superconducting energy recovery linac in JAEA in Japan [309, 310]. Superradiance [311] sustained saturation [312] was studied. A 1.7 kW operation was achieved [313].

NOVOSIBIRSK ENERGY RECOVERY FEL, RUSSIA

The only FEL room temperature energy recovery linac is located in the Budker Institute (Novosibirsk, Russia) [314, 315].

KAERI ENERGY RECOVERY FELS, KOREA

KAERI has developed three types of FELs since 1992: a millimetre wave driven by a 0.4 MeV electrostatic accelerator [316], a compact FIR FEL driven by a 7 MeV microtron, and an infrared FEL with average power of 1 kW driven by a 40 MeV superconducting accelerator [317]. The research is led by Y. U. Jeong (24th FEL Prize in 2013).

5.4.1.6 FEL oscillator performance and limits

Figure 49 reports on the spectral range covered by several FEL oscillators in the visible and UV-VUV. Reaching shorter and shorter wavelengths was getting difficult since the gain, that had to overcome the mirror losses, was typically decreasing for equivalent beam parameters. Some new developments were carried out for the UV dielectric multilayer mirrors [266–268] whereas the conditions of mirror degradation became even worse [265]. The shortest wavelength was obtained on the ELETTRA FEL at 190 nm. The figure shows as well the output power, which is of course, larger for larger electron beam energies, but which makes the obtention of a sufficient gain more difficult.

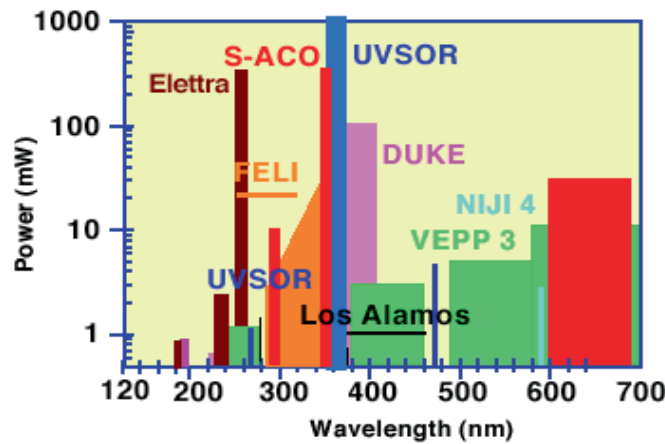


Fig. 49: Short wavelength FEL oscillators

Because of the oscillator configuration, the multi-pass in the optical resonator enables us to increase the coherence of the FEL. Figure 50 displays the pulse duration versus wavelength for different FEL oscillators. They are all operating close to the Fourier limit.

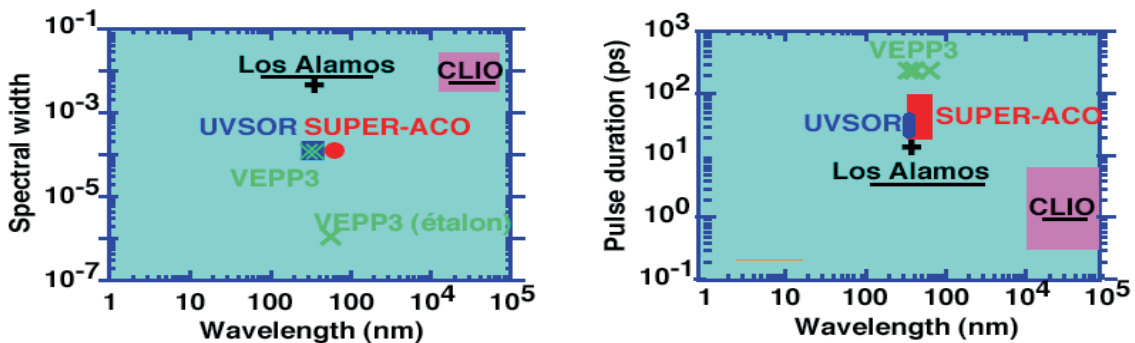


Fig. 50: Pulse duration versus wavelength for several FEL oscillators

Presently, thanks to the performance of Bragg reflectors such as diamond crystals in the X-ray, X-ray FEL Oscillators (XFEL) driven by a CW superconducting linac or an Energy Recovery Linac

(ERL) are under study [318–320]. Such an XFEL will be fully coherent, providing spectrally pure X-ray pulses.

5.4.2 Coherent harmonic generation

Following the VUV radiation obtained on the ACO storage ring, coherent harmonic generation was successfully continued on the Super-ACO storage ring FEL [321, 322]. At DUKE, the storage ring FEL in OK-4 with its sufficiently powerful super-pulses enabled us to generate second, third, fourth, fifth, and seventh coherent harmonics in the range from 37 to 135 nm [323]. The tuneability of the FEL wavelength provided for natural wavelength tuneability of the harmonic radiation. Coherent harmonics were also generated in ELETTRA [324]. At the UVSOR storage ring FEL, various features of the coherent harmonics [325] were studied, such as the influence of the synchrotron sidebands [326], the undulator, and injected laser helicity [327]. A test experiment was set-up in Sweden [328]. It used a photoinjector, with two accelerating sections, in which the beam is recirculated to reach 375 MeV and compressed in a dog-leg. The generation of circularly polarized coherent light pulses at 66 nm by seeding at 263 nm in a first modulator (planar undulator of 30×48 mm, 13.2 mm gap, deflection parameter of 3.52) and an APPLE-II type elliptical radiator (30×56 mm, 15.2 mm gap, deflection parameters for horizontal, circular, and vertical polarizations of 4.20, 3.44, and 2.98). Coherent pulses at higher harmonics in linear polarization have been produced up to the sixth order (44 nm), with 200 fs pulse duration [329].

Self-induced coherent harmonic generation was also produced in MARK-III [272], and enabled us to achieve radiation down to 36.5 nm [256]. The FEL was obtained simultaneously on the fundamental and third harmonic at Los Alamos [330]. Harmonic lasing was also performed at the Jefferson Laboratory FEL [331].

5.5 Exotic FELS

Variants of the FEL concept can be proposed by modifying the gain medium.

In the case of a gas-loaded FEL [332–334] with a gas of refractive index n_g , the resonance condition is modified according to

$$\pm\lambda_r = \frac{\lambda_u}{2n\gamma^2} \left(1 + \frac{K_u^2}{2} \right) - \lambda_u(n_g - 1). \quad (81)$$

In such a case, tuneability can then be also adjusted with the gas pressure. For a given wavelength, the required electron beam energy is smaller than in the case of a conventional FEL. Experiments were carried out [335–338].

Radiation observed from electrons skimming over a diffraction grating was observed [339].

Cherenkov radiation can also be produced in dielectric loaded waveguides: a relativistic electron beam passes at grazing incidence above the surface of a dielectric loaded waveguide and excites TM-like surface waves. The longitudinal component of the evanescent electric field induced electron bunching, leading to coherent emission [340, 341]. The synchronism condition for a single-slab geometry is given by

$$\lambda_r = \frac{2\pi d\gamma(\epsilon - 1)}{\epsilon} \quad (82)$$

with d the film thickness and ϵ the dielectric constant.

Cherenkov-based FEL radiation has been observed using a 2.5 MeV electron beam [297].

In a Smith–Purcell FEL [342–345] proposed by J. E. Walsh (1939–2000, 11th FEL Prize in 1998), the radiation is emitted when an electron passes close to the surface of a grating of period λ_u . The

wavelength of the emitted radiation depends on the radiation observed at the angle θ from the normal is:

$$\lambda_r = \lambda_u \left(\frac{1}{\beta} - \sin \theta \right). \quad (83)$$

With a sufficiently high current, the electrons interact with the fields above the grating and get bunched, so the Smith–Purcell radiation is enhanced [345]. This has been experimentally demonstrated [346–348].

5.5.1 First user applications

First user applications were started [2, 349, 350] slightly more than 10 years after the first FEL oscillation, so in fact rather rapidly. First FEL applications were conducted in the infrared on the Stanford Superconducting Linear Accelerator [337, 351–354] with a strong impulse given by A. Schwettmann, on MARK III FEL [355]. Human surgery had even started, thanks to the possibility to get the required wavelength [356]. Different user activities were developed on CLIO [357–359], on FELIX [360], on FELI [361], and on FELBE [362, 363]. The Jefferson Lab. infrared FEL carried out various types of user applications, such as vibrational modes in myoglobin [364], clusters [365] and industrial applications of kW UV [366]. Imaging is carried out with mm range FEL in Russia [367] and Korea [368].

In the UV, user applications started on the Super-ACO FEL in France [369], first in biology [356, 370] in 1993 for the study of the time-resolved fluorescence of the coenzyme NADH (nicotinamide adenine dinucleotide). Then, the FEL was coupled to the VUV synchrotron radiation produced in a beam line to perform a pump-probe two-colour experiments [371], enabling us to excite the system with the UV FEL and to probe the excited state with synchrotron radiation. It was first applied to surface photo-voltage effects studies [372, 373]. User experiments were also carried out on various storage ring FELs, such as DUKE [374], UVSOR [375, 376], ELETTRA [377].

Generation of short wavelength radiation on small accelerators coupled to a laser by Compton backscattering is becoming attracting again nowadays in order to deliver X-rays in a compact installation. Indeed, radiation generated by Compton backscattering was easily produced with the electron beam at the origin of the FEL and the FEL itself. The two beams are already transversally overlapped and synchronized, for the FEL generation (indeed, the FEL being itself a stimulated Compton backscattering process). X-rays were generated on CLIO [378], then gamma-rays on UVSOR FEL [379], on the Super-ACO FEL [232, 380, 381], and on the DUKE FEL [382, 383] which developed a unique gamma-ray facility [384, 385].

These encouraging results in the early days of FELs let the community envision prospects for XUV (Xray Ultra Violet range) FELs [386]. The high gain regime, for which theory was actively developed, appeared to be quite suitable. First results were achieved in Livermore.

6 The high gain FEL

The study of the high gain FEL started rather early. After the small-signal low gain studies, considerations for the strong-signal case were explored in order to understand saturation. Modelling moved then towards a self-consistent theory, taking into account the evolution of both the electromagnetic field and electronic distribution during the interaction [62]. The self-consistent theories were then naturally applied to the high gain case.

6.1 Plasma type studies

The work by P. Sprangle *et al.* [64] was continued using a plasma approach in deriving the general FEL dispersion relation and in applying it to both low and high gain limits [387]. Saturation was analysed in terms of electron trapping in the space charge and ponderomotive potential and efficiencies were

deduced. Scaling laws were found. A practical two stage case has been considered: a first radiation generated in a first undulator (called a ‘magnetic pump’ in the paper) is reflected to act as a seed (called ‘pump’ in the paper) of wavelength 2 cm for the second pass of the electron beam in the undulator leading to radiation at 190 μm in the second stage, for a 3 MeV energy. Further theoretical developments along such lines were carried out [151, 388–390] including the role of collective effects of the space charge [391]. “The equations of the free-electron laser amplifier are generalized to include higher order modes. The density and velocity fluctuations in the entering electron beam cause noise excitation in the amplifier. The electron beam fluctuations have been studied extensively, both theoretically and experimentally, in travelling wave tubes, and hence the well-tested formalism developed for this purpose is conveniently applied to the present problem. It is found that the fluctuations put a severe constraint on the achievable exponential gain in a proposed Raman-type free-electron laser operating at optical frequencies” [65]. The gain degradation has been investigated [392].

6.2 Instability type studies: emission of coherent radiation from a self-modulated electron beam in an undulator

In Novosibirsk, at the Institute of Nuclear Physics of the former USSR Academy of Sciences, A. I. Saldin (19th FEL Prize in 2006) and A. N. Kondratenko considered very early the possibility of producing coherent radiation from a self-instability, without the use of an optical resonator [116–118]. The work was first presented at the Russian Academy of Sciences [116], then in 1979 as a preprint of the Institute of Nuclear Physics [117], and then in an international particle accelerator conference [118].

They considered a situation without an optical cavity and investigated the question of “radiative instability of the beam in an undulator”. The required initial level of density oscillation for the instability to occur could result from statistic density fluctuations. They said “For sufficient length of the undulator, the resonant harmonics of density fluctuations become large enough during a pass that the modulated beam radiates from a definite section of the undulator. Such a scheme may be used as an independent source of coherent radiation or as an amplifier”. A first analysis of the self-modulation in the single pass regime was first discussed by Kroll *et al.* [62] in a plasma physics context or by using high frequency device models. The instability growth was analysed using methods applied for those of storage rings, using canonical conjugate variables of the Hamiltonian describing the relative motion of electrons with radiation, and particle density. It was found that in the case of a wide beam, the amplitude of the modulation can grow exponentially and coherent power is calculated with L_g the characteristic length in which the amplitude becomes e times larger. Conditions of applications of the results were examined. Besides, “To reveal the effect of self-modulation, a knowledge of the initial level of the harmonics of beam density is necessary. In a realistic situation, if the initial conditions are not prepared in a special manner, there exists a continuous spectrum of fluctuations of density harmonics that arise from the fact that there is a finite number of particles in the beam. Hence all the harmonics in a given band width ($\Delta K/K \sim \lambda_u/(2\pi L_g)$) will become unstable and grow by a few times in the length L_g ”. The evolution of the width of the harmonics after the pass of a given length is analysed, and its corresponding correlation length is estimated (of the order of $L_g/(2\gamma_{\parallel})$).

The reduction down to shorter wavelengths has also been analysed [393] using the Russian approach. The possibility of using a high gain FEL amplifier to start from noise was first considered on a storage ring to produce X-ray radiation. Examples were given for a 2.8 MeV energy, 100 A current, 50 μm rad emittance electron beam, helical undulator ($\lambda_u = 20$ mm, $B_u = 0.3$ T) leading to radiation at 450 μm with a growth length of 14 cm, or for a 10.2 MeV energy, 30 kA current, 50 μm rad emittance electron beam, helical undulator ($\lambda_u = 60$ mm, $B_u = 0.1$ T) leading to radiation at 100 μm with a growth length of 22 cm. Also considered was the case of a 20.4 MeV energy, 14 kA current, 5 nm.rad emittance electron beam in a storage ring, helical undulator ($\lambda_u = 70$ mm, $B_u = 0.2$ T, length of 15 m) leading to radiation at 5 nm with a growth length of 2 m and an output peak power of the order of 1 TW. Conditions are given for the energy spread (that should be less than 10^{-3}) and angular spread (that should be less

than 3×10^{-5}). These parameters are in fact not so different from the ones of the present LCLS (Linac Coherent Light Source) X-ray FEL, as discussed later. Instead of a storage ring, a linear accelerator is presently used on LCLS. It took also several decades to achieve, technologically speaking, the required electron beam parameters.

This pioneering work indeed was considered for the first time to start from the spontaneous emission to amplify it in the high gain regime until saturation, in the case of an infrared FEL with a 10 MeV electron beam [117, 118]. It is now usually called self-amplified spontaneous emission, in reference to the amplified spontaneous emission in conventional lasers. Its sketch is shown in Fig. 51.

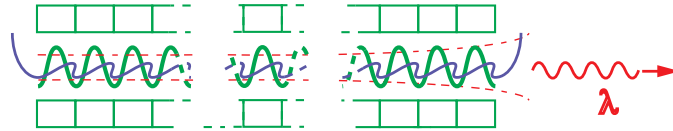


Fig. 51: FEL self-amplified spontaneous emission (SASE) configuration: the spontaneous emission emitted in the beginning of the undulator is amplified in one single pass. Operation at short wavelengths requires high beam energies for reaching the resonant wavelength, and thus long undulators (0.1–1 km for 0.1 nm) and high electron beam density (small emittance and short bunches) for ensuring a sufficient gain.

6.3 Hamiltonian-type studies

The Hamiltonian description was also applied to the high gain case [93]. Using the Hamiltonian description in the moving frame [394], R. Bonifacio (1940–2016) *et al.* investigated cooperative and chaotic transition (a kind of phase transition from a regime of small gain amplifier to that of a large gain amplifier): “below this threshold value the electrons radiate weakly and almost independently whereas above threshold the electrons strongly interact via the emitted radiation field. In the latter case the particles exhibit strong self-bunching and give rise to cooperative emission of radiation” [395]. “The exact threshold value w_T of the coupling parameter is analytically obtained by investigating, for any number of electrons N , the stability property of an initial condition with zero field excitation and totally unbunched electrons (i.e. electrons uniformly spread over an optical wavelength)”. Results are compared to simulations. It is pointed out that the transition can be stimulated by noise within the interaction volume.

The analysis was continued by the introduction of the notion of collective instability [396]. The electrons communicate with each other through the radiation and the space charge field. Thus, they ‘self-bunch’ on the scale of the radiation wavelength periods. The electrons have nearly the same phase and emit collectively coherent synchrotron radiation. R. Bonifacio, C. Pellegrini (12th FEL Prize, in 1999) and L. M. Narducci introduced the plasma frequency and the Pierce parameter. The exponential growth is found as a solution for the cubic equation which has one real and two complex conjugate roots. The instability condition could then be derived in terms of Pierce parameter and spectral detuning. The notion of lethargy, the “time required for the initial pulse to build up” was also discussed. It is also found that in the high gain case, the maximum growth is found for zero detuning. This regime is called the self-amplified spontaneous emission (SASE) regime. SASE has been studied in detail [397, 398], in particular with issues regarding the transient behaviour of the system, using the Maxwell–Vlasov equations [399]. Effects of harmonics, space charge, and electron energy spread on the collective instability are discussed [400]. The model covers both Compton and Raman regimes [401]. The regime of superradiance for a high gain FEL was analysed [402]. Prospective SASE sources were designed [398]. The diagram block in the SASE case is shown in Fig. 52. Semi-analytical models were developed [403, 404]. High gain single-pass free electron laser dynamics and pulse propagation effects were also considered [405].

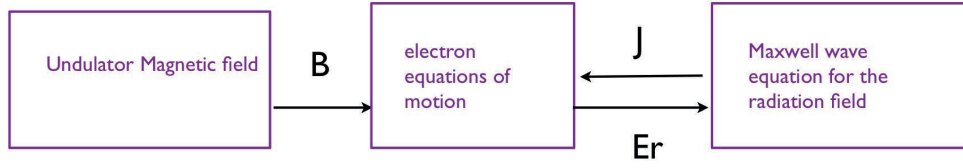


Fig. 52: SASE diagram block with the process of collective instability arising from communication from the neighbouring electrons.

6.4 One-dimensional high gain FEL modelling

6.4.1 The coupled system of equations

With high density electron beams and long undulators, a strong bunching takes place (space charge) and the change in electric field can no longer be neglected. Thus, the FEL is treated via a set of coupled equations [396, 398, 401]:

- the coupled pendulum equation, describing the phase space evolution of the particles under the combined undulator magnetic field and electric field of the optical wave;
- the evolution of the optical field in the presence of an electronic density and current;
- the evolution of the bunching coupled to the longitudinal space charge forces, enabling us to evaluate the electronic density and current.

The electronic density and the current resulting from the electrons in the undulator are first evaluated to treat the light wave evolution.

6.4.1.1 Radiation field evolution

The radiated field now depends on the longitudinal coordinate as

$$E_x(s, t) = E_x(s) \exp[-i(ks - ct)]. \quad (84)$$

Its evolution is ruled by the Maxwell equation

$$\left[\frac{\partial^2}{\partial s^2} - \frac{1}{c^2} \frac{\partial^2}{\partial t^2} \right] E_x(s, t) = \mu_0 \frac{\partial j_x}{\partial t} + \frac{1}{\epsilon_0} \frac{\partial \rho}{\partial x}$$

with j_x the average over the electron beam cross-section of the transverse electron peak current. In one-dimensional FEL theory, the electronic density is assumed to be independent of x , so $\frac{\partial \rho}{\partial x} = 0$. The transverse current is mainly due to the electrons in the wiggler, and to a small extent to the radiation field.

The phase of E_x may vary with s , i.e. the FEL phase velocity, may differ slightly from that of a plane electromagnetic wave at the speed of light c . Inserting the electric field expression in the Maxwell equation, it becomes

$$\left[2ikE'_x(s) + E''_x(s) \right] \exp[-i(ks - ct)] = \mu_0 \frac{\partial j_x}{\partial t} + \frac{1}{\epsilon_0} \frac{\partial \rho}{\partial x}. \quad (85)$$

Under the slowly varying envelope approximation (SVEA) the electric field does not change much over a few undulator periods even though its increase over the whole undulator length is large. The change in one wavelength is even smaller, so is its first-order derivative. It can be written as $|E'_x(s)|\lambda \ll |E_x(s)|$ and $|E'_x(s)| \ll k|E_x|$. However, one should keep the first-order derivative in order to describe the FEL growth as a function of the distance in the undulator. One can neglect the change of slope over one undulator period λ_u , as $|E''_x(s)|\lambda \ll |E_x(s)|$ and $|E''_x(s)| \ll k|E_x|$. The second-order derivative can

be neglected. So, in the paraxial approximation, one has $\frac{d}{dt} = c\left(\frac{\partial}{\partial s} + \frac{1}{v_s}\frac{\partial}{\partial t}\right)$. The field evolution then becomes

$$\frac{dE_x(s)}{dt} = -i\frac{\mu_o}{2k}\frac{\partial j_x}{\partial t}\exp[-i(k_s - ct)]. \quad (86)$$

6.4.1.2 Current sources

The current comes first from the displacement of the electron because of the undulator field. Then, a bunching takes place and, if important, an electron can be affected by the neighbouring electrons due to space charge forces.

The transverse current source due to the electron movement in the undulator is expressed using the electron transverse velocity as

$$\vec{j} = \rho_e \vec{v} \quad \text{so} \quad j_x = j_s \frac{v_x}{v_s} \simeq j_s \frac{K_u}{\gamma} \sin(k_u s) \quad (87)$$

The field evolution becomes $\frac{dE_x(s)}{dt} = -i\frac{\mu_o K_u}{2k\gamma}\frac{\partial j_s}{\partial t}\exp[-i(k_s - ct)]\sin(k_u s)$. While the electrons and the light wave interact, periodic density modulation (micro-bunching) is taking place, and the current can be developed as a function of the ponderomotive phase ψ :

$$\tilde{j} = \tilde{j}_0 + \tilde{j}_1 \exp(i\psi) \quad (88)$$

where the term $\exp(i\psi)$ represents the bunching,

$$\frac{\partial j_s}{\partial t} = \frac{\partial j_s}{\partial \psi} \frac{\partial \psi}{\partial t} = -i\omega \tilde{j}_1 e^{i\psi} = -i\omega \tilde{j}_1 \exp(ik(s - ct) + ik_u s).$$

Combining the expression of the current and the electric field derivative terms, the field evolution becomes

$$\frac{dE_x(s)}{dt} = -\frac{\mu_o c K_u}{2\gamma} \tilde{j}_1 \exp[ik(s - ct) + ik_u s] \exp[-i(k_s - ct)] \frac{e^{(ik_u s)} - c.c.}{2} = -\frac{\mu_o c K_u}{4\gamma} \tilde{j}_1 [1 + \exp[i2k_u s]]$$

with *c.c.* meaning complex conjugate. As the complex field amplitude is slowly varying on the scale of the wavelength λ , it can be driven by a current averaged longitudinally over several wavelengths. One can thus average the transverse current longitudinally. The phase factor carries out two oscillations per period and averages to zero. Thus, one gets

$$\frac{dE_x(s)}{dt} = -\frac{\mu_o c K_u}{4\gamma} \tilde{j}_1 [1 + \exp[i2k_u s]]. \quad (89)$$

Then, let's consider the space charge term due to the longitudinal field. The electric field is created by the modulation ρ_e of the charge density in the electron bunch, as illustrated in Fig. 53.

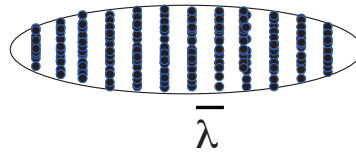


Fig. 53: Schematic representation of the slices of length λ_r along a bunched electron beam

According to Maxwell's equation, $\nabla \cdot \vec{E} = \frac{\rho_e(\psi, s)}{\epsilon_0}$. Similarly to the current, one can develop the electronic density as

$$\rho_e(\psi, s) = \rho_{e0} + \tilde{\rho}_1 \exp(i\psi). \quad (90)$$

It then becomes $\frac{dE_s}{dt} = \frac{\tilde{\rho}_1}{\epsilon_0} \exp(i[(k + k_u)s - \omega t])$, so, the amplitude of the induced space charge longitudinal field is

$$E_s = -i \frac{1}{\epsilon_0(k + k_u)} \tilde{\rho}_1 \approx -i \frac{\mu_0 c^2}{\epsilon_0 \omega} \tilde{j}_1. \quad (91)$$

6.4.1.3 Energy change due to the field

In the low gain low field case (in neglecting the field variation over one undulator pass), one has

$$\frac{d\eta}{ds} = -\frac{eE_1 K_u}{2\gamma^2 m_0 c^2} \left[J_{\frac{n-1}{2}}(\xi) - J_{\frac{n+1}{2}}(\xi) \right] \sin(\xi + \phi).$$

In the high field case with a bunched beam, one gets

$$\frac{d\eta}{ds} = -\frac{eK_u}{2\gamma^2 m_0 c^2} \left[J_{\frac{n-1}{2}}(\xi) - J_{\frac{n+1}{2}}(\xi) \right] \text{Re}(E_x e^{i\psi}) - \frac{e}{\gamma_r m_0 c^2} \text{Re}(E_s e^{i\psi}).$$

The first term corresponds to the electron motion and the second one to the space charge contribution. One has

$$\frac{d\eta}{ds} = -\frac{e}{m_0 c^2 \gamma_r} \text{Re} \left[\left(\frac{K_u \left[J_{\frac{n-1}{2}}(\xi) - J_{\frac{n+1}{2}}(\xi) \right] E_x}{2\gamma_r} + E_s \right) e^{i\psi} \right]. \quad (92)$$

Due to the bunching process, the electrons are grouped periodically in the electron bunch with a spatial modulation equal to the wavelength λ_r and its harmonics of order n λ_{rn} , and the electron bunch is described as a series of slices of length λ_r and number of electrons N_{slice} , which correspond to slices of length 2π in the phase ψ representation. The shape function $S(\psi)$ is given by

$$S(\psi) = \sum_{j=1} N_{\text{slice}} \delta(\psi - \psi_j(t)), \quad (93)$$

j being the current electron number. By developing in Fourier series, one gets

$$S(\psi) = \frac{c_0}{2} + \text{Re} \left(\sum_{k=1}^{\infty} c_k \exp(ik\psi) \right), \quad c_k = \int_0^{2\pi} S(\psi) \exp(ik\psi) d\psi. \quad (94)$$

In the case of the first harmonic, the current becomes

$$j_1 = -ecn_e \frac{2}{N_{\text{slice}}} \sum_{j=1} N_{\text{slice}} \exp(i\psi_j). \quad (95)$$

6.4.1.4 High signal set of equations

The FEL dynamics is now ruled by a set of coupled equations. The source current, depending on the electron bunching, evolves as $j_1 = -ecn_e \frac{2}{N_{\text{slice}}} \sum_{j=1} N_{\text{slice}} \exp(i\psi_j)$. The transverse electric field evolution is ruled by the current source term, depending on the electrons in the undulator, as $\frac{dE_x(s)}{dt} = -\frac{\mu_0 c K_u}{4\gamma} \tilde{j}_1$. The phase evolution is related to the energy exchange as

$$\frac{d\psi_j}{ds} = 2k_u\eta_n, \quad j = 1, \dots, N_{\text{slice}}. \quad (96)$$

The energy exchange is governed by the current term due to the electron movement and to the space charge induced electric field:

$$\frac{d\eta}{ds} = -\frac{e}{m_0c^2\gamma_r} \text{Re} \left[\left(\frac{K_u \left[J_{\frac{n-1}{2}}(\xi) - J_{\frac{n+1}{2}}(\xi) \right] E_x}{2\gamma_r} + E_s \right) e^{(i\psi)} \right]. \quad (97)$$

These equations are usually solved numerically. One can obtain however an analytic solution under certain approximations.

6.4.2 Evolution of the light wave in the high gain regime of FEL

6.4.2.1 The FEL cubic equation

In the case of a rather ‘small’ periodic density modulation, a normalized particle distribution function, obeying the Vlasov equation, is defined. After mathematical manipulation [396, 402], one can show that the radiation amplitude E_x satisfies

$$\frac{\dot{E}_x}{\Gamma^3} + 2i\frac{\eta}{\rho_{\text{FEL}}}\frac{\ddot{E}_x}{\Gamma^2} + \left[\frac{k_p^2}{\Gamma^2} - \frac{\eta^2}{\rho_{\text{FEL}}^2} \right] \frac{\dot{E}_x}{\Gamma} - iE_x = 0 \quad (98)$$

ρ_{FEL} is the so-called Pierce parameter, or FEL parameter. It depends on the electron beam density and energy and on the undulator characteristics (deflection parameter, Bessel function term, undulator wavenumber):

$$\rho_{\text{FEL}} = \left[\frac{K_u [JJ] \omega_p}{4\omega_u} \right]^{2/3} = \frac{1}{2\gamma k_u} \left(\frac{\mu_0 e^2 K_u^2 [JJ]^2 k_u n_e}{4m_0} \right)^{1/3}, \quad (99)$$

where Γ , the gain parameter, is proportional to the Pierce parameter,

$$\Gamma = 2k_u \rho_{\text{FEL}}, \quad (100)$$

and k_p , the space charge parameter, is given by $k_p = \frac{\omega_p}{c\gamma} \sqrt{\frac{2\lambda}{\lambda_u}}$ with ω_p the plasma pulsation $\omega_p = \sqrt{\frac{4\pi e^2 n_e}{m_0}}$. In the specific case of $\eta = 0$ (on resonance) and for $k_p = 0$, i.e. for negligible space charge, the cubic equation takes its simplest form, as

$$\frac{\dot{E}_x}{\Gamma^3} - \Gamma^3 i E_x = 0. \quad (101)$$

Considering the electric field expressed as $\approx e^{(i\kappa s)}$, it becomes $\kappa^3 = i\Gamma^3$ with three solutions:

$$\kappa_1 = -i\Gamma, \quad \kappa_2 = (i + \sqrt{3})\Gamma/2, \quad \kappa_3 = (i - \sqrt{3})\Gamma/2.$$

κ_2 leads to an exponential growth of the electric field.

6.4.2.2 The FEL power growth and evolution of the light wave in the high gain regime

The power grows as

$$E_x(s) = E_{x0} \exp(s/L_{\text{go}}), \quad L_{\text{go}} = \frac{1}{\sqrt{3}\Gamma} = \frac{1}{\sqrt{3}} \left(\frac{4m_0\gamma^3}{\mu_0 e^2 K_u^2 [JJ]^2 k_u n_e} \right)^{1/3}. \quad (102)$$

The bunching factor B evolves similarly. It is noticeable that there is amplification at resonance, this feature differs from the small signal gain case. At the beginning of the undulator, the three terms of the cubic equation do contribute to the change in the field intensity and the exponential growth is not dominant, the bunching takes place. This regime is called the ‘lethargy’. Solving the cubic equation for a non-zero detuning (slightly off resonance) provides the dependence of the imaginary solution with detuning, i.e. the gain bandwidth. It has a maximum for zero detuning and decreases for both positive and negative detunings. From the analysis of the behaviour, one can deduce that the FEL bandwidth is given by the Pierce parameter:

$$\frac{\Delta\lambda}{\lambda} = \rho_{\text{FEL}}. \quad (103)$$

Adopting the same type of evaluation as in the small signal gain case, one estimates that the saturation power of the radiated field is the electron beam power multiplied by the gain bandwidth:

$$P_{\text{sat}} = \rho_{\text{FEL}} E I_{\text{p}}, \quad (104)$$

with E the electron beam energy and I_{p} the peak current. Since the radiation pulse duration is close to that of the electron bunch, the Pierce parameter gives the efficiency of the FEL, i.e. the fraction of the beam energy given to the radiation field. Typically, the saturation power is reached after roughly 20 gain lengths, at the saturation length L_{s} .

$$L_{\text{s}} \approx 20L_{\text{go}} \approx \frac{1}{\sqrt{3}\Gamma} = \frac{20\lambda_{\text{u}}}{4\pi\sqrt{3}\rho_{\text{FEL}}} = \frac{5\lambda_{\text{u}}}{\pi\sqrt{3}\rho_{\text{FEL}}}. \quad (105)$$

So the saturation can be achieved with N_{s} , given by

$$N_{\text{s}} = \frac{L_{\text{s}}}{\lambda_{\text{u}}} = \frac{5}{\pi\sqrt{3}\rho_{\text{FEL}}}. \quad (106)$$

The FEL parameter defines the growth rate, measured in undulator periods.

The start-up comes from the spontaneous emission noise. It is followed by an exponential growth due to a collective instability (self-organization of the electrons from a random initial state). When the power saturates, there is a cyclic energy exchange between the electrons and the radiated field and a consequent change of power which corresponds to rotations in phase space. Growth and bunching also occur on the harmonics of the fundamental wavelength. The number of radiated coherent photons per electron at saturation $N_{\text{coh.ph}}$ is given by $N_{\text{coh.ph}} \sim \frac{\rho_{\text{FEL}} E}{E_{\text{ph}}}$, with E_{ph} the photon energy. For photons of 10 keV with a beam of 15 GeV, a Pierce parameter of 0.001, at 10 keV, $N_{\text{coh.ph}} \sim 1500!$

6.4.2.3 The SASE spectral and temporal properties

The uncorrelated trains of radiation, which result from the interaction of electrons progressing jointly with the previously emitted spontaneous radiation, lead to spiky longitudinal and temporal distributions, apart from single spike operation for low charge short bunch regime [406, 407]. The emission usually presents poor longitudinal coherence properties. There is some particularity of the temporal structure of the SASE pulse. Because the photons move faster than the electrons, the radiation emitted by one electron moves ahead and slips by one wavelength per undulator period, so for the total undulator length by $N_{\text{u}}\lambda$. The analysis [402] of the effect of slippage for an electron bunch of finite length, when the slippage effect cannot be neglected, shows that the interaction between the electrons is only effective over a cooperation length, the slippage in one gain length. In a one-dimensional model the cooperation length can be written as

$$L_{\text{coop}} = \frac{\lambda}{2\sqrt{3}\rho_{\text{FEL}}}. \quad (107)$$

Since the initial noise varies along the bunch length, the output radiation pulse consists of a series of spikes of random intensity separated by a distance proportional to the cooperation length [408]. In the case of spontaneous radiation, the intensity along the pulse varies randomly in each wavelength. For SASE at saturation, the interaction between electrons and their emitted radiation generates a number of spikes of random intensity and duration proportional to the cooperation length. The number of spikes in a pulse is given by the ratio of the bunch length to the cooperation length. The intensity in each spike fluctuates from pulse to pulse. There is no correlation between the phases of different spikes. The statistical distribution of the total intensity, summed over all spikes, is given by a gamma distribution function [407]. The line width, in a SASE FEL, is inversely proportional to the spike length, and not to the bunch length. The width is of the order of the FEL parameter. In consequence, a SASE radiation pulse is not Fourier transform limited, except for the case of an electron bunch length shorter than the cooperation length, when a single spike is produced. Examples of spikes are shown in Fig. 54.

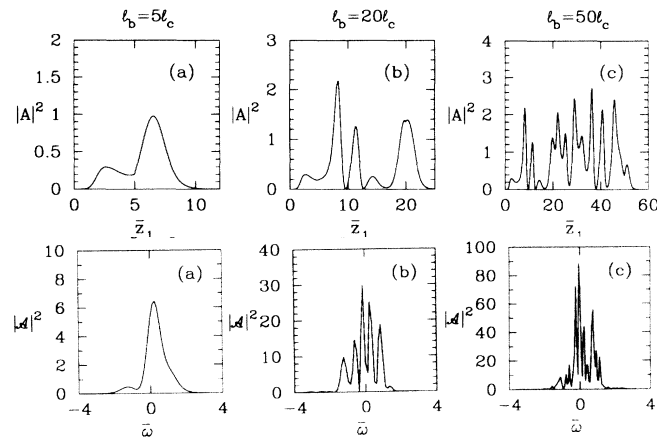


Fig. 54: SASE spikes for different bunch lengths. Temporal (up) and spectral (down) distributions, from [408]

On a single pass FEL, transverse coherence results from the electron beam emittance (which should be of the order of the emitted wavelength) and from possible optical guiding. The optical guide can arise from gain guiding (quadratic gain medium [45]) or from the contribution of a refractive index [409]. As a consequence, the undulator can even be longer than a few Rayleigh lengths!

6.5 Three-dimensional analysis

The role played by diffraction is analysed: exponentially growing modes, which have a profile independent of the longitudinal coordinate, exist and a dimensionless parameter, which is proportional to the radius of the electron beam and independent of the interaction length, determines whether diffraction is important [410]. Then, the small-signal gain of the fundamental exponentially growing mode of the high gain free electron laser is calculated, taking both diffraction and electron energy spread into account. As the electron beam radius is reduced, the gain bandwidth increases by a large amount [411]. A two-dimensional analysis using the properties of optical fibres shows that optical guiding can take place in a free electron laser [409, 412, 413].

Three-dimensional analysis of coherent amplification and self-amplified spontaneous emission in free electron lasers was carried out [414, 415] using the three-dimensional Maxwell–Klimontovich equation. The Klimontovich distribution function takes into account the discreteness of the electrons.

The radiation field, represented by a complex amplitude, which is the slowly varying part of the full amplitude, satisfies Maxwell equation. Slowly varying and high- frequency components of the electronic distribution are treated separately. It is found that transversally, optical guiding takes place for high gain FEL [410, 411]. Electron correlation, transverse radiation profiles, spectral features, transverse coherence, and intensity characteristics are analysed, as shown in Fig. 55. The results, which agree with recent microwave experiments, are applied to proposed schemes for generation of short-wavelength coherent radiation. Corrections terms (from the three-dimensional theory) can be introduced [416, 417].

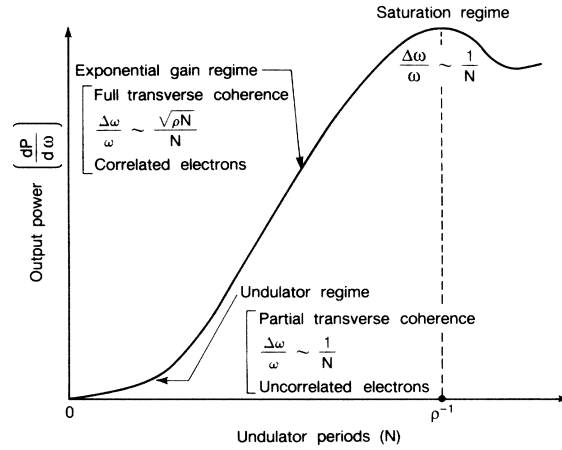


Fig. 55: Schematic representation of SASE properties from the three-dimensional analysis by K. J. Kim in [414]

Semi-analytical models of SASE FEL based on the logistic FEL equation [404] are developed. They include diffraction, beam quality and pulse propagation.

6.6 Conditions for SASE amplification

Conditions for SASE amplification are detailed below.

6.6.1 Emittance requirement

There should be a proper transverse matching (size, divergence) between the electron beam and the photon beam along the undulator for insuring a proper interaction. It means that the emittance should not be too large at short wavelength. The FEL gain increases with the beam current provided that

$$\frac{\epsilon_n}{\gamma} < \frac{\lambda}{4\pi}. \tag{108}$$

High power short wavelength FELs require thus low emittance electron beams (much smaller than 100π mm mrad and peak currents of the order of 100 A).

6.6.2 Energy spread requirement

The electron beam should be rather ‘cold’, its energy spread should be smaller than the bandwidth, i.e.

$$\frac{\sigma_\gamma}{\gamma} < \rho_{\text{FEL}}. \tag{109}$$

6.6.3 Rayleigh length requirement

The radiation diffraction losses should be smaller than the FEL gain, i.e. the Rayleigh length should be larger than the gain length:

$$Z_r > L_{go}. \quad (110)$$

For long undulators, intermediate focusing is then put between undulator segments.

Reviews of the free electron laser theory are presented in [124,418]. Different numerical codes can be used for FEL calculations, such as GINGER [419] by W. Fawley (25th FEL Prize in 2014), GENESIS [420] written by S. Reiche (21st FEL Prize in 2010), PERSEO [421] by L. Giannessi (24th FEL Prize in 2013), MEDUSA [422] by H. Freund, PUFFIN [423] by B. Mac Neil and L. T. Campbell, TDA [424] by J. S. Wurtele etc.

6.7 High gain up-frequency conversion

6.7.1 High gain harmonic generation theory

As for the case of the low gain FEL, harmonic generation can take place, as schematized in Fig. 56.

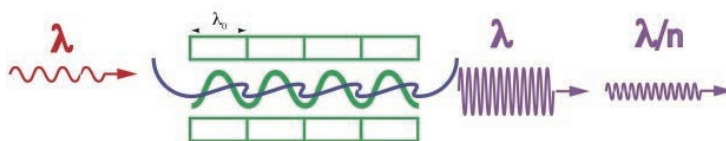


Fig. 56: High gain harmonic generation

Three-dimensional analysis of harmonic generation in high gain free electron lasers has been carried out [425] in the case of a planar undulator using the coupled Maxwell–Klimontovich equations that take into account non-linear harmonic interactions. “Strong bunching at the fundamental wavelength can drive substantial bunching and power levels at the harmonic frequencies”. “Each harmonic field is a sum of a linear amplification term and a term driven by nonlinear harmonic interactions. After a certain stage of exponential growth, the dominant nonlinear term is determined by interactions of the lower nonlinear harmonics and the fundamental radiation. As a result, the gain length, transverse profile, and temporal structure of the first few harmonics are eventually governed by those of the fundamental. Transversely coherent third-harmonic radiation power is found to approach 1% of the fundamental power level for current high-gain FEL projects” [425].

Non-linear harmonic generation in high gain free electron lasers [426] can also be treated semi-analytically using a theoretical ansatz and fitting methods, providing “the most significant aspects of the high-gain free-electron laser dynamics” [426]. Expressions are found for the growth of the laser power, of the e-beam-induced energy spread, and of the higher-order non-linearly generated harmonics. They are applied to treat pulse propagation and non-linear harmonic generation in free electron laser oscillators [148], two harmonic undulators, and harmonic generation in high gain free electron lasers [427].

Different variants have been considered.

In the high gain harmonic-generation (HG) configuration [428–432], a small energy modulation is imposed on the electron beam by its interaction with a seed laser in a first undulator (the modulator) tuned to the seed frequency, it is then converted into a longitudinal density modulation thanks to a dispersive section (chicane) and in a second undulator (the radiator), which is tuned to the n th harmonic of the seed frequency, the microbunched electron beam emits coherent radiation at the harmonic frequency of the first one, which is then amplified in the radiator until saturation is reached. By some means, it recalls the optical klystron scheme. The HG configuration is shown in Fig. 57, The seed signal should then overshoot the shot noise from the start-up SASE radiation.

In such a way, the higher-order harmonic components of the density modulation induced by the FEL process are exploited in a ‘harmonic converter’ configuration, to multiply the frequency, and extend the original spectral range of operation of the FEL. To be more efficient, it is combined to the ‘fresh

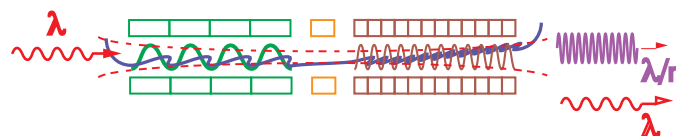


Fig. 57: High gain harmonic generation: seeding is performed in two stages, the first stage is seeded with an external laser, where a density modulation of the electron bunch takes place, whereas the second stage is seeded by the FEL from the first stage while the undulator is set on a harmonic of the radiation from the first stage; and the electron bunch radiates coherently after passing through a dispersive magnetic chicane.

bunch technique’ [433] where a proper delay is applied on the electron bunch with respect to the optical path so that a ‘non-heated’ part of the electron bunch is used for the second stage.

The HGHG can be put in cascade with a series of modulator/radiator undulators, enabling potentially effective frequency conversion. L. H. Yu considered that “the cascading of several HGHG stages (35) can provide a route for x-ray generation using current near-ultraviolet seed laser performance. In this approach, the output of one HGHG stage provides the input seed to the next undulator. Each stage is composed of a modulator, dispersion section, and radiator. Within a single stage, the frequency is multiplied by a factor of 3 to 5. For each stage, the coherent radiation produced by the prebunched beam in the radiator at the harmonic of the seed is many orders of magnitude higher in intensity than the SASE generated. In a specific example (35), after cascading five HGHG stages, the frequency of the output is a factor $5 \times 5 \times 5 \times 4 \times 3$, i.e. 1500 times the frequency of the input seed to the first stage. Dispersion sections are placed between stages to shift the radiation to fresh portions (36) of the electron bunch to avoid the loss of gain due to the energy spread induced in the previous stage” [429]. Shot noise at the different stages can then become an issue [434]. Schemes for reducing this shot noise are proposed [435].

In the harmonic cascade configuration (see Fig. 58), the wavelength ratio of the two stages is a ratio of integers [436, 437].

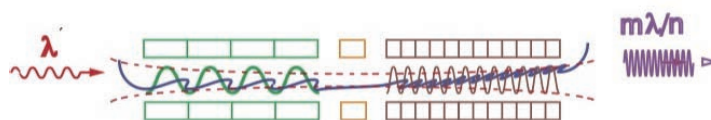


Fig. 58: Harmonic cascade configuration: seeding is performed in two stages, the first stage is seeded with an external laser, whereas the second stage is seeded by the FEL from the first stage while the undulator is set so that the wavelength ratio of the two stages is a ratio of integers.

In particular seeding cases, the seeded FEL can become super-radiant [436], leading to further pulse shortening and intensity increase. Depending on the respective electron bunch and slippage length, complex spatio-temporal deformation of the amplified pulse can lead ultimately to a FEL pulse splitting effect [438].

6.7.2 Echo enabled harmonic generation

In the echo enabled harmonic generation (EEHG) [439] scheme (see Fig. 59), two successive laser–electron interactions are performed, using two undulators, in order to imprint a sheet-like structure in phase space. As a result, higher-order harmonics can be obtained in an extraordinary efficient way.

Figure 60 shows the imprinted modulation applied in the echo scheme.

Schemes derived from EEHG, such as the triple mode chicane, open perspectives for very high up-frequency conversion for short wavelength (nm) light of short duration at moderate cost [441]. The echo concept can also be applied to storage ring based light sources [442]. EEHG opens the way to

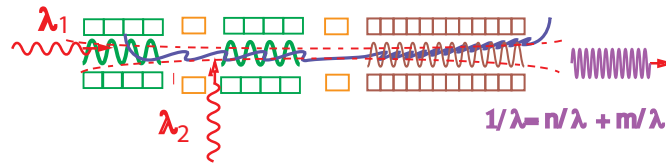


Fig. 59: FEL EEHG: a coherent source tuned on the resonant wavelength of the undulator applies a first energy modulation, electrons move according to their energy in the chicane where a second energy modulation is applied, imprinting a fine structure in phase space.

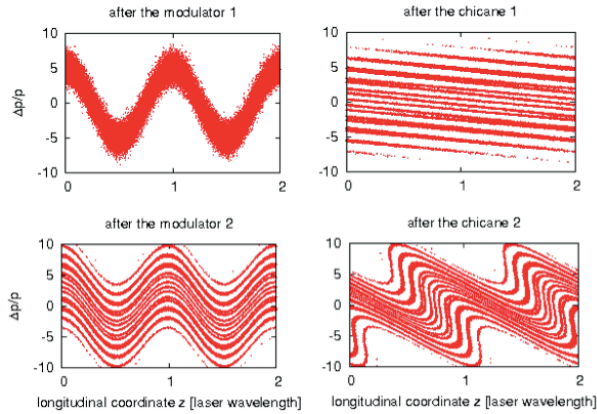


Fig. 60: Evolution of the particle phase space along the EEHG stages. Phase space of the beam after the first modulator (top left), the first chicane (top right), the second modulator (bottom left), and the second chicane (bottom right). Horizontal axis: phase, vertical axis: relative energy, from [440].

shorter wavelengths when operating on a high-order harmonics of the seed wavelength. Echo has no equivalent in classical optics.

7 Single-pass short wavelength FEL experimental results

These encouraging results in the early FEL research let the community envision prospects for XUV FELs [386] and soft X-ray FELs [443–445] to be installed on storage rings, the accelerators providing the best performance at that time (energy spread of $\sim 0.1\%$, peak current of a few hundreds of ampere).

The high gain regime, for which theory was actively developed, appeared to be quite suitable. First, high gain FEL experiments took place on oscillators, then experiments aiming at demonstration of SASE at intermediate wavelengths were undertaken. However, the decrease in wavelength was accompanied by an improvement of accelerator technology, enabling us to fulfil the requirements for SASE. The advent of the photoinjector became really crucial for ensuring the development of FELs at shorter wavelengths. In addition, the requirements in terms of linear accelerator performance for future colliders met the needs of X-ray FELs, and the technological developments were fruitfully applied within the FEL community. In particular, the high electron beam density also suited for getting a short gain length.

7.1 Towards VUV X-ray FELs?

7.1.1 Limits of storage ring driven FEL for short wavelength FELs

The electron beam quality is an essential contribution to the success of a given FEL. Indeed, the energy spread should be sufficiently small to enable a proper bunching. At the end of the twentieth century, the shortest FEL wavelength on an oscillator has been achieved on a storage ring FEL [263, 264]. How-

ever, the electron beam recirculation is limiting the output power according to the Renieri limit, and compatibility of the use of the storage ring with normal synchrotron radiation use became an issue.

7.1.2 Early development of photoinjectors

With respect to conventional thermoionic guns, photoinjectors [446, 447] in which a laser illuminated photocathode is located directly in the high gradient accelerating cavity, can enable us to provide a high quality electron beam. Compared to a thermionic gun, the current density can be very high so that bunching is not necessary. The time structure can also be controlled by the laser beam, and matched into the RF accelerators without degrading the emittance. The electrons produced on the photocathode surface are quickly accelerated in a RF cavity in order to limit the emittance blow-up due to the space charge force. Several laboratories have initiated the development of photoinjectors.

The first photocathode-driven electron beam enabling FEL was achieved at Stanford on the MARK III linear accelerator [448]. The gun used a LaB_6 cathode, illuminated by a tripled Nd:Yag laser, leading to an energy spread of 0.8% and an horizontal (vertical) emittance of $8(4)\pi$ mm mrad.

At Los Alamos, the facility has been modified to target FEL oscillation in the visible. For this purpose, the thermoionic gun was replaced by a photoinjector [449–452]. The pioneering work of the Los Alamos team on photo-injectors was recognised by the FEL prize 2017 awarded to Bruce Carlsten and Richard Sheffield (27th FEL prize 2017). The photoinjector (26 MeV/m at the CsK_2Sb cathode at 1.3 GHz in the $\pi/2$ mode) produced 6 MeV, 300 A, 15 ps electron pulses at 22 MHz repetition rate. The drive laser was a Nd-YLF laser at 527 nm with very low phase (< 1 ps) and amplitude ($< 1\%$) jitters. Changing from the thermoionic gun to the photoinjector enabled to reduce the emittance by a factor of 4 and the energy spread by nearly a factor of two. Typically, the electron phase space density could be larger by one order of magnitude. B. Carlsten proposed the idea of emittance compensation [453], leading to a significant reduction of the normalized emittance with respect to usual thermoionic guns.

Another photoinjector was developed at Brookhaven National Laboratory (Center for Accelerator Physics) [454]. In the frame of a SLAC/BNL, UCLA collaboration, a research and development (R&D) effort was launched on the development of a photoinjector. A 4.5 MeV 1.5 cell standing wave RF (2.856 GHz) photoinjector gun based on the Brookhaven design, using a copper cathode, was completed at UCLA [455]. Driven by sub 2 ps pulses of UV (266 nm) light (up to 200 μ J/pulse) and powered by a SLAC XK5 type klystron (24 MW, 4 μ s), it could generate up to 3 nC charge. Accelerating gradients of up to 100 MV/m were achieved. A 0.25 kA peak current (with 9 ps duration pulses) could be produced with emittance in the $1 - 10\pi$ mm mrad range.

A gun test facility at SLAC was then implemented with a 3 m S-band linac section [456] and the design was improved. Four copies of the gun were fabricated.

The CANDELA photoinjector was also developed at Orsay [457].

The development of photoinjectors continued, and became crucial for single-pass FELs, because it permitted to provide electron beams with higher performance.

7.1.3 Considerations for short wavelength single-pass FEL in the SASE regime

Because of the limited performance of mirrors in terms of reflectivity, short wavelength FEL are usually operated in the so-called SASE set-up, where the spontaneous emission at the input of the FEL amplifier is amplified, typically up to saturation in a single pass after a regime of exponential growth. In the beginning of the twentieth century, several authors started to design X-ray FELs in the SASE regime [458]. A workshop on prospects for a 1 Å FEL in Sag Harbor in 1990 [459] aiming at answering the questions: “*What are the prospects for a 1 Å Free-Electron Laser? Can we obtain electron sources bright enough to get down to the 1 Å region ?*” “To focus the workshop, the initial discussion by R. Palmer defined three canonical 1 Å FEL cases as possible alternatives, i.e. with 1.6, 5, and 28 GeV electron beam sources. Each is a loose optimization of conflicting requirements needed to achieve $\lambda = 1$ Å on

the electron beam quality, brightness, peak current focusing properties and its incidence on the wiggler period and total length.”

L. H. Yu [460] introduced the problematics as such: “The Free Electron Laser (FEL) holds great promise as a tuneable source of coherent radiation. At the present, the shortest wavelength achieved by a FEL is 2500 Å. However, as recent progress in the development of laser driven photocathode electron guns has provided electron beams with lower and lower emittance and higher and higher current, it has become clear that FEL’s with much shorter wavelength can be achieved. A FEL operating below 1000 Å will yield important advances in fields such as photochemistry, atomic and molecular physics. A FEL with wavelength of 30 Å will bring new era to the development of holography of living cells. And, if a FEL with 1 Å wavelength can be developed, its impact on solid physics, molecular biology, and many other fields can hardly be exaggerated. Is it possible for a FEL to achieve 1 Å? What are the difficulties and the challenges to the present technology to build a 1 Å FEL? What are the requirements on electron beam quality and the wiggler magnets required to build a 1 Å FEL? To lase at 1 Å, the FEL must operate in the high gain regime. For oscillator configuration, aside from the difficulties associated with the requirements on the mirrors which must stand high intensity 1 Å radiation, we need high gain to overcome the loss in the cavity mirrors. The difficulties with the mirrors make the single pass FEL a more likely solution. For single pass configuration we also need high gain to minimize the total length of the wiggler. To achieve high gain for 1 Å FEL, the electron beam must have high peak current, low normalized emittance, and small energy spread. Strong focusing of the electron beam becomes necessary for such a short wavelength. In order to achieve short gain length, the wiggler should have high magnetic field on axis and short wiggler period. The requirements for a 1 Å FEL should be determined by the gain calculation for these various system parameters. It is usually carried out by numerical simulations. However, to explore the large parameter space for a possible FEL configuration, an analytical tool to calculate the gain would be much more convenient than the simulation”. C. Pellegrini [461] concluded with the following words “The FEL in the SASE regime offers an attractive route to an X-ray laser. To make this laser a reality it is necessary to solve many problems; produce electron beams with very high quality and refine the understanding of the physics of FELs. We also need to produce long, short-period undulators with good field quality. To reach these goals we need an extensive experimental and theoretical effort on electron guns, accelerators and FEL with a number of intermediate steps that will take us from the present region of 240 nm and 1 W to 0.1–1 nm and 1 GW”. J. C. Golstein [462] examined more particularly the undulator errors and concluded more generally as “All of the separate, requirements on the electron beam and the wiggler for this sort of one- Angstrom SASE FEL amplifier seem to substantially exceed achievements in existing devices. To achieve all of these requirements simultaneously, as is required for this device, would appear to require many years of development”. K. J. Kim examined emittance and current density achievable in RF photo-cathode guns, and investigated the effect of space charge and RF curvature induced emittance growth.

The work in such a direction was continued during discussions held during fourth generation light source workshops [463,464].

7.2 Historical observations of high gain single-pass SASE FEL

7.2.1 SASE observations at long wavelength

The activity continued on storage rings [210,211] especially for the quest towards a short wavelength of operation, since high quality electron beams were still being produced. In addition, the interplay between the beam dynamics in the ring and the FEL interaction was of great interest.

Following theoretical development on high gain FEL, various experiments were carried out.

LIVERMORE NATIONAL LABORATORY, USA

Saturated high gain amplification has first been observed in the mm waves (34.6 GHz) in the mid eighties

in a collaboration between Lawrence Livermore National Laboratory and Lawrence Berkeley Laboratory (USA) [294]. The electron beam from the Electron Laser Facility (ELF) (Lawrence Livermore National Laboratory) provided 6 kA, -3.3–3.8 MeV beam with a normalized emittance of 1500π mm mrad, which goes through a slit, bringing to beam to a current of approximately 500 A with 15 ns pulses with a normalized edge emittance of 470π mm mrad. The 3 m long wiggler of 98 mm period was composed of specifically shaped solenoids with independent power supplies providing a peak field of 0.5 T surrounded by a stainless-steel waveguide. The experiments were first carried out in the amplifier configuration where saturation was observed, before moving to the SASE one, for which saturation was also achieved after 2 or 3 m of undulator, depending on the experimental conditions. The power growth is shown in Fig. 61.

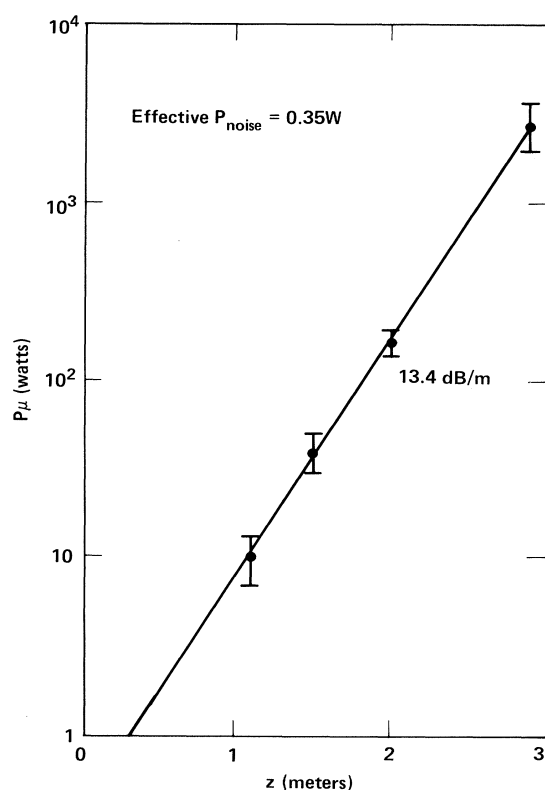


Fig. 61: Power growth in the Livermore–Berkeley experiment, figure taken from [294]

The extraction efficiency first reached 5% and then 34% by undulator tapering, leading to an output signal of 1 GW [465]. This was also an experimental demonstration of the undulator tapering for improving efficiency and it provided a very important result for the community. However, the radiation being propagated in a waveguide, it did not provide a full test of the diffraction effects that can affect the FEL, especially at shorter wavelengths, when the radiation is propagating in vacuum.

MASSACHUSETTS INSTITUTE OF TECHNOLOGY (MIT), USA

A superradiant emission (18 MW) at $640 \mu\text{m}$ with a 4% relative bandwidth has been observed with a 2 MeV 1 kA electron beam on the PULSERAD accelerator with a helical undulator (31.4 mm period) [466]. It would correspond to an efficiency of 7%.

CENTRE D'ETUDES SCIENTIFIQUES ET TECHNIQUES D'AQUITAINE (CESTA), BORDEAUX, FRANCE
Bunching has been demonstrated at CESTA (France) at 8 mm (35 GHz) with the LELIA induction

linac [295] delivering a 1 kA electron beam at 2.2 MeV, leading after transport to 800 A [467], as illustrated in Fig. 62. The 12 cm period 3.12 m long helical undulator was fed by a capacitor discharge providing a peak field of 1.1 T [468]. Cherenkov radiation was produced and measured with a picosecond streak camera. A 40 MW SASE has also been observed [469].

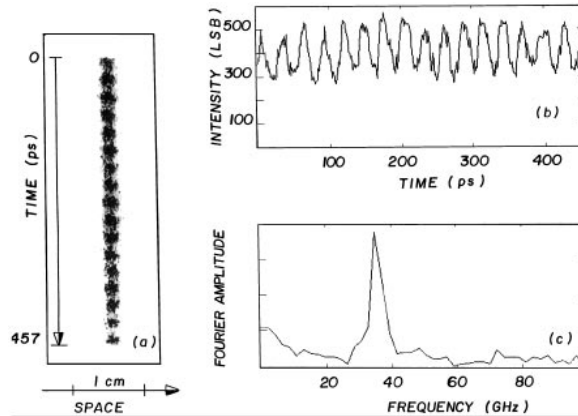


Fig. 62: Bunching observed on Cherenkov radiation observed with a streak camera (ARP) from the CESTA SASE FEL experiment from [467]. Radiation observed on a narrow rectangular slit 10 mm wide and 0.3 mm high. The slit was then displaced in time to provide a photographic record of the light intensity. Sweep speed of 25 ps/mm at a position 27.5 cm after the wiggler exit: (a) streak camera recording; (b) digitized intensity of (a) plotted vs time, and (c) frequency spectrum of (b).

7.2.2 SASE observation in the near infrared, visible and UV

The progress of the SASE observations is discussed.

INSTITUTE OF SCIENTIFIC AND INDUSTRIAL RESEARCH (ISIR), OSAKA UNIVERSITY, OSAKA, JAPAN

An increase of undulator radiation intensity by 5–100 times has been observed using the 38 MeV electron beam from a L-band linac (28 nC charge, 30 ps pulse length, 0.7 – –2.5% energy spread), a 2 m long undulator (60 mm period) in the 20–40 μm spectral range, as shown in in Fig. 63 [470].

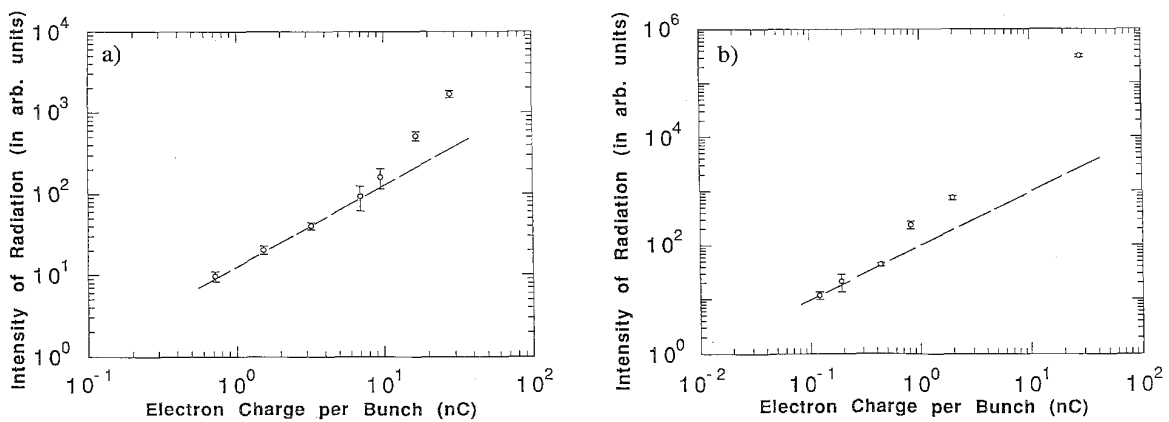


Fig. 63: Undulator radiation signal versus charge, solid line: spontaneous emission, from [470]

SUNSHINE, STANFORD UNIVERSITY, STANFORD, JAPAN

Coherent, far-infrared undulator radiation from sub-picosecond electron pulses consistent with SASE predictions with a gain length of 45.4 cm have been observed using electrons from the 16 MeV SUNSHINE S-band linac (350 ps) travelling in a 26×77 mm period permanent magnet undulator ($K = 0.3-0.2$) [471].

CLIO, ORSAY, FRANCE

SASE at start-up in the mid infrared (5–10 μm) has been observed on CLIO (France) [472] at the Laboratoire d'Utilisation du Rayonnement Electromagnétique as shown in Fig. 64.

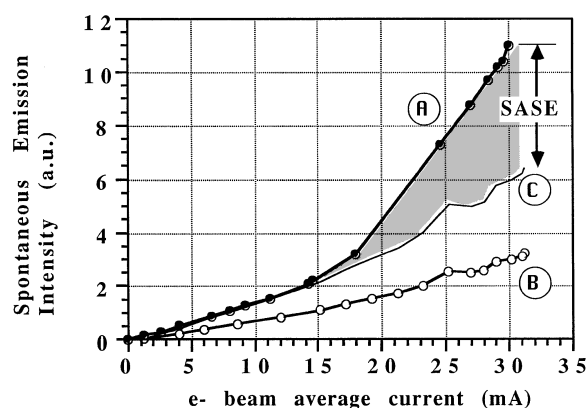


Fig. 64: Undulator radiation signal for (A) two undulator segments, i.e. 38 periods, (B) one undulator segment, i.e. 19 periods, (C) twice the intensity for one undulator segment, from [472].

A 50 MeV 3 GHz linear accelerator was providing a peak current of 100 A with an emittance of 150π mm mrad to two planar undulators of 19×50.4 mm period. Up to 500% gain has been measured, with a Pierce parameter of 1.9×10^{-3} . The growth in (A) is clearly non-linear, as an evidence of the SASE regime, and it differs from (B) corresponding to coherent synchrotron radiation for an equivalent number of undulator periods. SASE spectra were compared to spontaneous emission ones and present “a noisy intensity from bunch to bunch, with about 100% fluctuations”, corresponding to the “spiky regime of the SASE which is, intrinsically, not a stable process” [472].

BNL, LONG ISLAND, USA

SASE was then achieved at 1064 and 633 nm, using a 61 8.8 mm period pulsed electromagnet Massachusetts Institute of Technology (MIT) micro-undulator with a peak field of 0.45 T [473]. The electron beam is produced at the Accelerator Test Facility at BNL using a photocathode RF gun: a single micropulse at 34 MeV with a variable charge of 01 nC and less than 5 ps full width at half maximum bunch length is used. Undulator radiation at 1064 nm is amplified from 2 to 6 times with respect to the spontaneous emission. SASE gain at a wavelength of 633 nm at a beam energy of 48 MeV was also observed, as illustrated in Fig. 65.

Then, SASE high gain and intensity fluctuations have been measured at 16 μm using a photocathode RF gun, a half-cell linear SATURNUS accelerator at Brookhaven National Laboratory with an emittance of $8-10\pi$ mm mrad, an energy spread of 0.08–0.14%, a transport line and an undulator from the Kurchatov Institute (40×15 mm period, 0.75 T field) leading to a Pierce parameter of 1×10^{-2} . One should note at this point the significant reduction of the electron beam emittance thanks to the RF photoinjector. First statistical analysis of SASE radiation was performed [474].

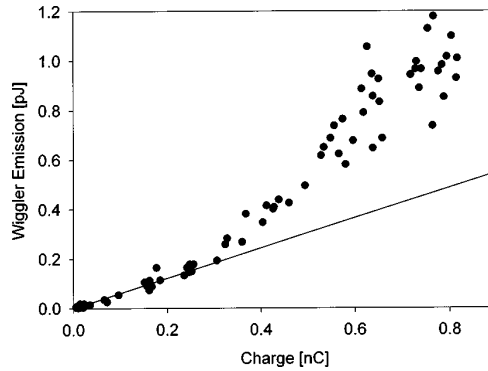


Fig. 65: Undulator radiation signal versus charge, solid line: spontaneous emission, from [473]

LOS ALAMOS NATIONAL LABORATORY, LOS ALAMOS, USA

The Los Alamos high brightness photoinjector integrated into a L-band linac 1.3 GHz at 17 MeV coupled to a 20 mm period 2 m long undulator generating a 0.7 T magnetic field and tapering [475] enabled high gain SASE 15 μm [476]. The pioneering work was recognised by the FEL prize award to Bruce Carlsten, Dinh Nguyen and Richard Sheffield for application of RF photo-injector to first high gain SASE FEL in 2017, as one of the keys for the success of present X-ray FELs. Then five orders of magnitude of amplification and saturation in the mid-infrared have been achieved in the frame of a UCLA, L. Alamos, Stanford, Kurchatov collaboration [474]. The experiment has been performed on the Advanced Free Electron Laser (AFEL) linac at the Los Alamos National Laboratory with a CsTe₂ photocathode at the Los Alamos National Laboratory (18 MeV, 0.25%) with the Kurchatov undulator. It led to more than five orders of magnitude amplification at 12 μm [477], as shown in Fig. 66.

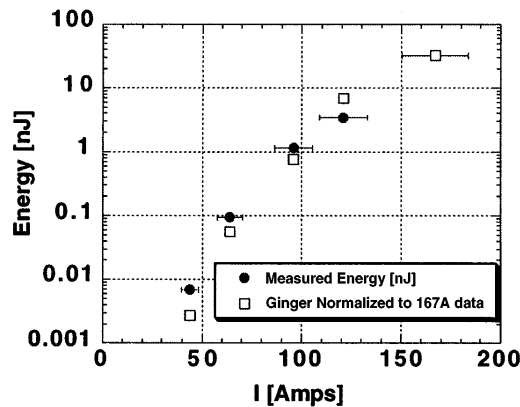


Fig. 66: Undulator radiation signal versus current and comparison with theory, from [477]

This result showed that the high gain single-pass FEL potentialities at intermediate wavelengths opened new perspectives. The electron beam micro-bunching at the exit of the SASE FEL was measured by observing coherent transition radiation, presenting a narrowband frequency spectrum [478].

LEULT, ARGONNE, USA

SASE saturation was then achieved in 2000 at Argonne National Laboratory in the visible at 530 nm, 385 nm [479, 480]. The electron bunch from the Low-Energy Undulator Test Line (LEUTL) is initially accelerated to 5 MeV (8π mm mrad emittance), then injected into the linear accelerator, and further accelerated to the desired energy (up to a maximum of 650 MeV), and compressed to increase the peak

current. Nine undulators 2.4 m long undulator segments (72×33 mm period, 1 T field, deflection parameter of 3.1) are used. They are separated by 38 cm in order to insure a proper phase matching and accommodate diagnostics, a quadrupole magnet, and steerers. An effective gain length of about 1.5 m was first measured [479] while saturation was then observed [480] as shown in Fig. 67.

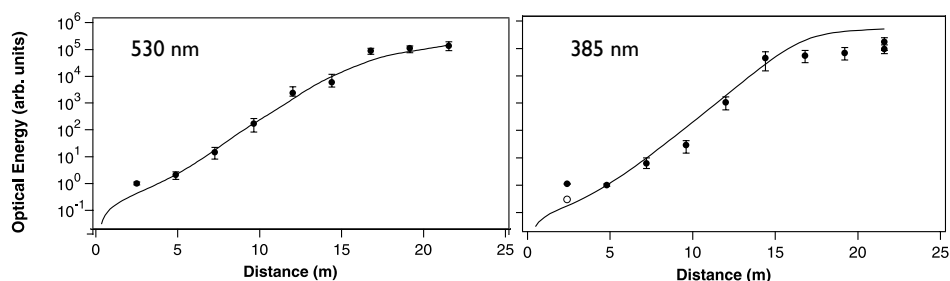


Fig. 67: SASE versus undulator length at 530 and 385 nm, from [480]

VISA, BNL-SLAC-LLNL-UCLA, USA

Saturation has been observed on the VISA (Visible to Infrared SASE Amplifier) experiment on the Accelerator Test Facility (ATF) at Brookhaven National Laboratory [481, 482]. The electron beam from an S-band, 1.6 cell photocathode RF gun is accelerated to 72 MeV (200 A peak current, 2π mm mrad emittance, 0.17% energy spread) and sent into the 4 m long VISA planar undulator (18 mm period, 6 mm gap) [481]. Non-linear harmonic radiation of 845 nm at 423 nm and 281 nm was observed using the VISA SASE FEL at saturation [481], as shown in Fig. 68. The measured non-linear harmonic gain lengths decreased with harmonic number, as expected. Both the second and third non-linear harmonics energies are about 1% of the fundamental energy. This result was the first observation of non-linear harmonic SASE FEL radiation which demonstrated its potentialities to produce coherent, femtosecond X-rays.

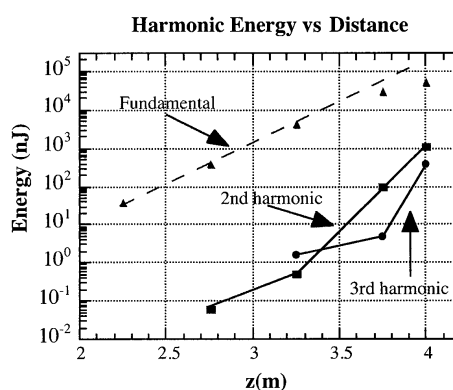


Fig. 68: Energy growth on the first, second, and third harmonics on the VISA experiment, from [481]

7.2.3 SASE observation in the VUV-soft X-ray

In the same years, a major step was achieved with the observation of SASE radiation in the VUV spectral range. The test facilities were then used as a source for scientific applications. Indeed, the pioneering users had also to learn about these new sources with their high peak power, spiky structure, pulse to pulse jitter, and short pulses.

FLASH, HAMBURG, GERMANY

B. Wiik, director of DESY (Deutsches Elektronen-Synchrotron), after a sabbatical at SLAC in 1992, considered, with G. Materlik, the possibility to build a short wavelength FEL using the TESLA accelerator, developed for the future collider. Indeed, the electron beam requirements were similar. A first Review Committee was set in 1995 and gave a positive feedback on the FEL proposal. TTF (TESLA Test Facility) was built in 1997 to test the superconducting technology for the planned linear collider TESLA, which has been replaced by the International Linear Collider. J. Schnieder reported about this time as: “Based on the good experience with superconducting technology at the large hadron lepton collider HERA at DESY and the need for high luminosity at the linear collider, the challenge was accepted to realize the accelerator in superconducting RF technology in a large international effort. The so-called TESLA collaboration was founded, which by the end of 2002 included 50 institutions from 12 countries. The ambitious goal was to increase the gradient of the accelerator by a factor of 5 and to reduce the cost of the cryomodules by a factor of 5, which has now been achieved” [483]. The FEL on TESTA-TTF [484, 485] was seen as a test-bench for the technology and physics for a future European XFEL project. The first design considered a 1 GeV electron beam with an emittance of 2π mm mrad, a peak current of 2 kA, a relative energy spread of 0.1%, a 25 m effective undulator length (27.3 mm period, 12 mm gap, 0.5 T field) for generating a FEL at 6.4 nm with a 3 GW saturation power, up to 7200 pulses can be present in the 800 μ m long macropulse, at 10 Hz repetition rate thanks to the choice of a superconducting linear accelerator. Later, the TTF-FEL was renamed FLASH (free electron laser in Hamburg).

A UV (7 ps pulses) laser-driven 1.5 cell RF gun at 1.3 GHz with a Cs₂Te cathode delivers electrons which are sent in superconducting TESLA-type accelerator modules for reaching a 1 GeV electron beam, with a compression chicane in between before reaching fixed gap undulator segments (0.46 T magnetic field). First experiments were carried out with 233 MeV electron beam (emittance of 6π mm mrad, a peak current of 0.4 kA, a relative energy spread of 0.13%), enabling a gain of 3000 at 109 nm and studies of statistical properties, as shown in Fig. 69 [486], in 2000 and then saturation [487] in 2001, i.e. 25 years after the FEL invention. Tuneability in 80–120 nm range was demonstrated, and a very high degree of photon beam transverse coherence was observed. This result competed the shortest wavelength achieved on a FEL oscillator (on a storage ring).

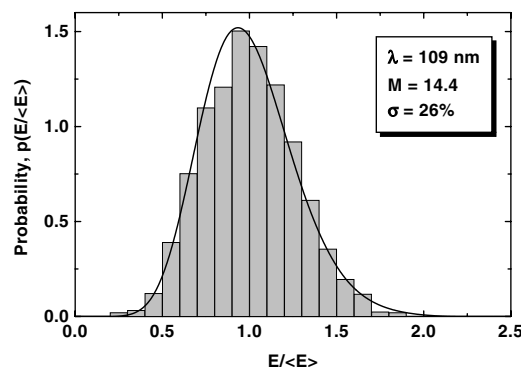


Fig. 69: SASE probability distribution, from [486]

With higher peak current, the GW level (close to 1 μ J energy) had been reached in the 95–105 nm spectral range [488] with a gain length of 67 cm, leading to a cooperation length of 5 μ m.

These results constitute a major step in the SASE history. First user experiments were started quickly afterwards [489] and it became a user facility since summer 2005. Then, with some improvements on the accelerator, the 32 nm wavelength was reached with GW level power, ultra-short pulses (25 fs FWHM, and a high degree of transverse and longitudinal coherence [490] in 2006, at 13.7 nm

with up to 170 mJ/pulse, 10 fs pulse duration, leading to peak powers of 10 GW [491]. With 700 pulses per second, the average power reached 20 mW. Harmonics were also quite intense with one or two orders of magnitude of power reduction (0.6% for the third (4.6 nm) and 0.03% and the fifth (2.75 nm) harmonics) in the water window of interest for biological samples. With an upgrade of the linac enabling us to reach 1 GeV, the spectral range was extended down to 6.5 nm [492]. Then a third harmonic RF cavity for phase space linearization coupled to an energy increase up to 1.25 GeV led to FEL operation down to 4.1 nm [493], i.e. in the water window on the fundamental wavelength.

Thanks to the high repetition rate of the superconducting linac, two FEL branches can be operated simultaneously, as shown in Fig. 70, with the development of FLASH-II branch with variable gap undulators [494].

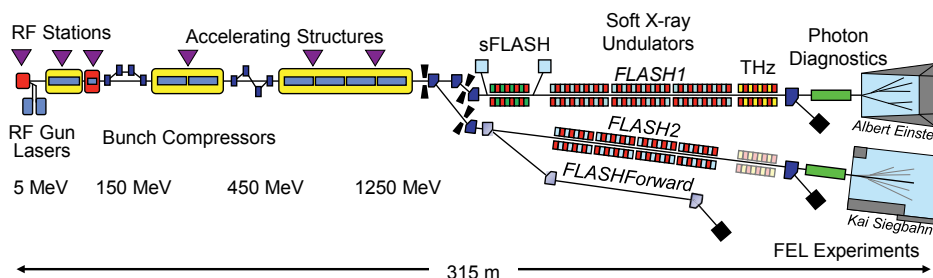


Fig. 70: Present FLASH layout from <https://flash.desy.de/>

While electron beam requirements from colliders and FEL met and considering the growing demand of synchrotron radiation, DESY had developed further light sources with respect to high energy physics after the shutdown of the accelerator HERA in 2007, with third generation light sources (PETRA III a very low emittance ring, the synchrotron research lab HASYLAB), and FEL-based fourth generation ones (FLASH, European XFEL). The light sources became the most important facilities of DESY. E. Saldin (19th FEL Prize in 2006), M. Yurkov (26th FEL Prize in 2015), E. Schneidmiller (26th FEL Prize in 2015) for the theoretical solid basis of the project and J. Rossbach (19th FEL Prize in 2006) for project lead brought a significant contribution to the success of FLASH. FLASH results made also confident the scientific community about the development of even shorter wavelength FELs.

SCSS TEST ACCELERATOR, HARIMA, JAPAN

The idea to combine the high level expertise on high density electron beams generated by linear accelerators in C band technology associated with a specific thermoionic gun developed following the work of T. Shintake (22nd FEL Prize in 2011), on in-vacuum undulators [495, 496] by the H. Kitamura group and on use of X-ray synchrotron radiation at SPring-8 by T. Ishikawa *et al.* led to a draft of a compact and low cost XFEL development concept in April 2000 [497]. R & D was launched on specific hardware and led to the completion of an in-vacuum undulator with a shorter period and higher magnetic field in 2002, an electron gun and the achievement of a very low emittance in 2003 [498]. After a first RIKEN symposium held in July 2003, a R&D group for XFEL was established in 2004. The SPring-8 SASE Source XFEL project was included in January 2005 as an important research objective for future R & D in the Ministry of Education, Culture, Sports, Science and Technology (MEXT) policy report on promoting science and technology of light and photons. An international Review Committee (M. E. Couprie, J. Galayda, J. Hastings, S. I. Kurokawa, W. Namkung, J. Schneider, chaired by K. J. Kim) underlined the specificities of the project: “The SPring-8 Compact SASE Source (SCSS) is an innovative project for generation and use of intense, coherent, short-pulse X-ray beams. Although its goals are similar to other X-ray free-electron laser (FEL) projects in the USA and Europe, the SCSS is unique in its compactness of design and in its co-location with the SPring-8, the world’s leading third-generation X-ray synchrotron radiation facility” and underlined the more critical components or aspects of the project. Some choices

were quite original, such as the use of thermo-ionic gun operating at 1450°C with a graphite heater instead of a photoinjector (see Fig. 71), the C-band (5.7 GHz) accelerator technology enabling a 35 MeV/m with high precision high purity oxygen-free copper structures, short period in-vacuum undulators.



Fig. 71: Thermoionic gun of SCSS Test Accelerator, with T. Shintake

In 2005, the construction of SCSS test accelerator at 250 MeV was launched, recognized by MEXT as “critical technology of national importance” and a XFEL user group was established and an electron beam was successfully transported at the end of the year. The key components such as the CeB_6 electron gun [499] with an ultra-low emittance 0.6π mm mrad, the C-band structures and power sources, leading to an electron beam of 0.3 nC charge (0.3 kA), the in-vacuum undulators (600×15 mm period, maximum deflection parameter of 1.5 with a 3 mm minimum gap), were successfully developed. In 2006, 49 nm FEL radiation was obtained and then extended in the 60–40 nm spectral range with an energy of 30 mJ [500, 501].

7.2.4 SASE observation in the X-ray

Reaching the SASE regime experimentally took one decade after the achievement of the VUV storage ring FEL oscillator and typically 25 years after the SASE in the far infrared measured on the Livermore experiment. The FEL in the X-ray in the 0.1 nm spectral region was indeed obtained at Stanford in 2009, i.e. at the same place where the first FEL was successfully demonstrated in 1977, i.e. 32 years later. Several X-ray FEL facilities followed.

7.2.4.1 The first observation of SASE radiation in the X-ray domain at Stanford

LCLS, STANFORD, USA

The first considerations to use the SLAC linac combined to a low emittance photoinjector goes back to the fourth generation workshop held in 1992 [463], the consecutive FEL studies [502], and progress on high peak current low emittance linear accelerators [503]. A study group was formed in 1992 by H. Winick at SLAC to study FEL design, performance, and optimization, accelerator (gun, acceleration up to 70 GeV) and associated beam transport, undulators, lay-out, and scientific applications. The targeted spectral range was the water window. It led to the study [502] for a 2–4 nm wavelength FEL using a 10 MeV, S-band photoinjector; part of the SLAC linac to accelerate the beam up to 10 GeV (at 7 GeV with an emittance of 3π mm mrad, peak current of 2.5 kA, an energy spread of 0.04% (uncorrelated), 0.1% (correlated); two longitudinal bunch compressors to increase the peak current and reduce the bunch length to 0.16 ps; and an undulator (83 mm period, 0.78 T field) enabling a 4 nm FEL with 11 mJ energy per pulse and a 60 m saturation length. The considered photoinjector was consisting of a 3.5 cell π -mode standing wave 100 MV/m accelerating structure, with a metal photocathode illuminated by a 2 ps laser pulse, providing a 3π mm mrad emittance, 250AA peak current, 1.6 ps RMS pulse duration, 0.15% relative energy spread. “In April 1992, it was considered to submit a proposal for a 2 to 4 nm

FEL to the US Department of Energy for construction starting in 1995, and development work to be done between 1992 and 1995. The name LCLS, introduced by Winick, appears for the first time in a memorandum dated June 13, 1992” [3]. Applications were discussed in the “Scientific applications of short wavelengths coherent light sources” workshop (chairs: W. Spicer, J. Arthur, H. Winick, Oct. 1992) and concerns were expressed about the sample damage induced by the high intensity of such a FEL. The working group studies were presented to a review committee (J. Bisognano, L. Elias, J. Goldstein, B. Newnam, K. Robinson, A. Sessler, R. Sheffield, chair: I. Ben Zvi) that concluded that “there is no physical principle saying that the device would not work” and R&D was recommended (electron density via electron source emittance and longitudinal pulse compression, beam alignment in the undulators at 20 μm). In 1994, the Department of Energy, upon the request for funding, asked for a review by the National Research Council, which ended up with the recommendation from the ‘FEL and other Advanced Coherent Light’ Committee [209] to continue the research and development towards an X-ray FEL in order to improve the technology and thus to reduce the cost. A second workshop on ‘Scientific Applications of Coherent X-rays’ in 1994 (J. Arthur, G. Materlik, H. Winick) [504] pointed out the advantage to use the SLAC linac and the existing building to limit the cost of X-ray FEL, and the required R&D to reduce the wavelength from 4 nm to 0.15 nm. It envisioned the new paths that could be opened by a X-ray FEL: “Such an x-ray laser should in fact lead to the same sort of revolutionary developments in x-ray studies of matter that was produced in optical studies by the introduction of the visible/UV laser”. The feasibility of accelerating and compressing electron beams for reaching high peak currents (several 100 A) while keeping emittance constant was assessed [503]. A Conceptual Design Report for a XFEL in the 0.15–1.5 nm range was completed [505], it was reviewed in 1997. The Basic Energy Science of US Department of Energy [506] recognized as top priorities funding for LCLS R&D in the frame of a national effort and the importance of the first SASE experimental results.

The LCLS design [398] considered the use of the existing SLAC accelerating sections, combined to a photoinjector and undulators. The photoinjector was developed [507, 508] relying on preliminary results obtained in the frame of the BNL/UCLA/SLAC collaboration. Funds were given following the recommendations from a panel chaired by S. Leone, and the work has been distributed between different laboratories: SLAC, UCLA, Livermore Nat. Lab., Argonne, Brookhaven, Los Alamos. A formal project management structure has been established, with a Scientific Advisory Committee (co-chaired by J. Stohr and G. Shenoy). A new Conceptual design report was issued in 2002 [509], and additional funds were provided. A view of LCLS is shown in Fig. 72.

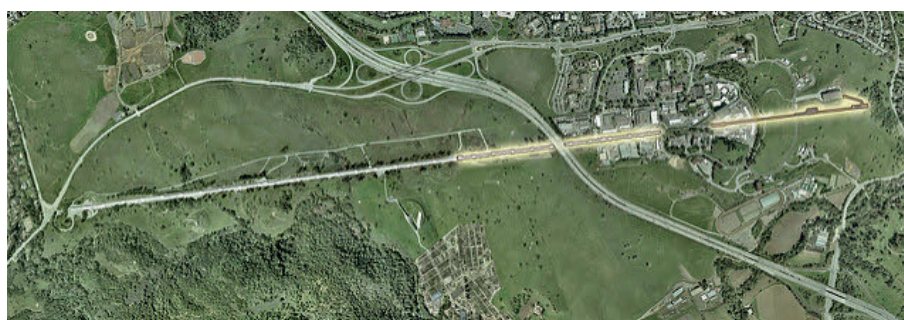


Fig. 72: View of LCLS, from portal.slac.stanford.edu/sites/lcls_public/Pages/Default.aspx

LCLS consists in a photoinjector, derived from the one of the BNL/SLAC/UCLA collaboration (0.4 π mm mrad emittance for 0.4 nC charge, or 0.15 π mm mrad emittance for 0.02 nC, the SLAC accelerating sections leading to an electron beam of 13.6 GeV, 250 pC (respectively 20 pC) for 0.5 π mm mrad (respectively 0.14 π mm mrad) normalized emittance, a relative energy spread of 0.01% and a 3 kA peak current, thanks to two bunch compressors. A view is shown in Fig. 73. A laser heater is also implemented to cure from microbunching instability [510].



Fig. 73: View of LCLS, from portal.slac.stanford.edu/sites/lcls_public/Pages/Default.aspx

The fixed gap undulator 3.4 m long segments (30 mm period, 130 m total length) were built by Argonne National Lab [511]. Some canting of the magnetic poles (5.5 mrad) was introduced so that the resonant wavelength can be adjusted by a horizontal translation of the undulator segment. Beam position monitor and focusing was installed between the undulator modules.

After the commissioning of the injector led by David Dowell (twentieth FEL Prize in 2009), SASE radiation was achieved in April 2009 at 0.15 nm, very rapidly after sending the electron beam in the undulators. Saturation was obtained without using the total number of undulator segments [512]. LCLS was also adjusted with a low charge and shorter electron bunches [513]. The commissioning of LCLS was led by Paul Emma (twentieth FEL Prize in 2009), under the project management of John Galayda (23rd FEL Prize in 2012). Beam based alignment was required [514]. Microbunching instability and effect of the laser heater were also studied [515]. LCLS now operates in the 0.25–9.5 keV spectral range, with a 120 Hz repetition rate, with several mJ and pulses as short as 5 fs.

The success of LCLS, the first tuneable X-ray FEL, was a major advance in FEL history. It opened the way to explore new areas of matter investigation with such a high energy per pulse. There are now six experimental stations.

7.2.4.2 *The second observation of SASE radiation in the X-ray domain in Japan*

SACLA, HARIMA, JAPAN

Following the success of the test facility SCSS Test Accelerator in 2006, a review working group concluded that “the XFEL plan should be actively carried forward and the project should be started at an early date”, and 2.3 billion yen was allocated for construction and research on use of the XFEL facility by the government at the end of the year. XFEL Project Head Office was established in 2006, and the project was jointly promoted by RIKEN and Japan Synchrotron Radiation Research Institute (JASRI). The construction of the XFEL facility in Japan began in July 2009. In 2009, the accelerator and undulator buildings were completed, the thermoionic gun operating at 1450°C with a graphite heater, the acceleration tubes (see Fig. 74) were installed, undulators started, the experimental building was built in 2011. A fifth XFEL symposium was held in 2009.

The FEL was achieved on June 7, 2011. SASE is operated at SACLA down to 0.08 nm [516]. For the final adjustments, the undulator segments have been aligned using the photon beam itself [517].

SACLA has also some specificities: it gathers XFEL and SPring-8 in such a way that radiation from both light sources can be combined on a sample, or the electron beam from the linear accelerator



Fig. 74: SACLA C-band linac

of SACLA can serve to inject the storage ring for short pulse operation as shown in Fig. 75.



Fig. 75: SACLA FEL top view from <http://xfel.riken.jp/eng/>. In the long building is installed SACLA with the different FEL branches, whereas in the rear of the picture, one of the third generation storage ring beamlines, a very intense laser, and SACLA photon beam can be coupled. The configuration also enables to use the linac electron beam to inject in the storage ring for very short pulse synchrotron radiation production.

It is the only X-FEL not having a photoinjector, but a thermoionic gun. It is the first X-ray FEL to have adopted the C-band accelerator technology and in-vacuum undulators (18 mm period).

SACLA now operates with two hard X-ray beamlines. In addition, SCSS Test Accelerator has been moved, the electron beam energy has been raised and undulators have been added, providing an additional soft X-ray beamline, presently open to users [518].

7.2.4.3 *The next X-ray SASE FELs in the X-ray domain*

PAL FEL, POHANG, KOREA

Pohang Accelerator Laboratory launched the study of a XFEL [519] in the beginning of the twentieth century. Studies were carried out and reviewed. PAL-XFEL uses a 10 GeV S-band linac (0.4π mm mrad emittance, 60 Hz), two series of undulators (for the hard X-ray line at 10 GeV: 20 segments of 26 mm period, 0.81 T peak field, 8.3 mm minimum gap; and for the soft-ray beamline at 3.15 GeV: 20 segments of 35 mm period, 1 T peak field, 9 mm minimum gap) [520] to cover the 0.1–4.5 nm spectral range. The site of the facility is shown in Fig. 76.



Fig. 76: PAL FEL site, from <http://pal.postech.ac.kr/paleng/Menu.pal?method=menuView-&pageMode=paleng&top=7&sub=5&sub2=0&sub3=0>

The installation of the linac and undulator was completed in January 2016. After approval from the Radiation Safety Control Agency, commissioning of the accelerator was started from a 135 MeV injector on April 14, 2016: the first beam from the RF-gun [521] was achieved, and in 11 days, the beam was accelerated up to 10 GeV and was transported 715 m away from the gun.

The electron beam was then sent at the entrance of the undulator lines, 794 m away from the gun. The beam was compressed to 3 kA peak current. The first FEL was obtained at 0.5 nm on June 14. Korea Bizwire made the following announcement on June 30, 2016: “Following the United States and Japan, Korea became the third country to successfully produce an ‘x-ray free-electron laser’ (XFEL), often referred to as the ‘dream light’. According to the Ministry of Science, ICT and Future Planning, the POSTECH (Pohang University of Science and Technology) Pohang Accelerator Laboratory has succeeded in producing an XFEL with a wavelength of 0.5 nm. The lab started a trial run of the PAL-XFEL on April 14. The laser was first observed in the early morning of June 14, and the facility was visited on June 29 by an external verification committee to confirm the laser’s successful production” [522].

Saturation was achieved at 0.144 nm on 27 November 2016, with an energy per pulse of 132 μ J for a 8 GeV electron beam and an undulator deflection parameter of 1.87, as shown in Fig. 77. The gain length is 3.43 m. Undulator tapering applied for the last eight undulators led to a further increase of the FEL intensity [523]. PAL-FEL has two hard X-ray beamlines and one soft X-ray one.

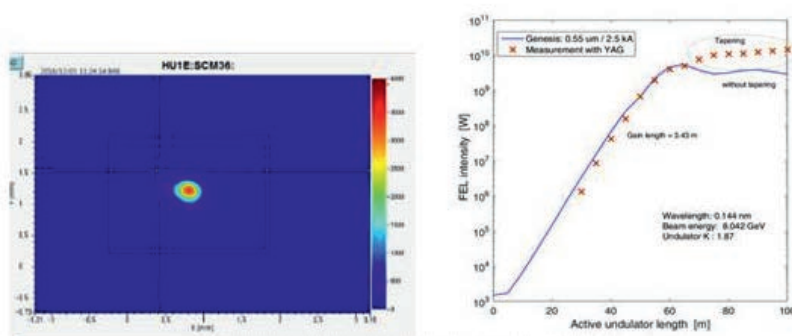


Fig. 77: X-ray FEL at PAL: X-ray spot and power saturation curve, from [523]

SWISSFEL, VILLIGEN, SWITZERLAND

SwissFEL is developed at Paul Scherrer Institute. Following the conceptual design report [525], the construction started. A special care was dedicated to the preservation of nature, of the site of the Swiss FEL facility (see lay-out displayed in Fig. 78).

SwissFEL [526] consists of a very low emittance injector, C-band accelerating sections leading to 5.8 GeV for a 100 Hz repetition rate, and 15 mm period in-vacuum undulators [527], for two different FEL beamlines: ARAMIS (0.1–0.7 nm) and ATHOS (0.7–7 nm). First, the injector was commissioned [528]. Then, the full installation was completed. A first lasing was achieved in December 2, 2016 with a 377 MeV electron beam at 24 nm, in May 2017 at 4.1 nm [524] and in October 2017 at 1.2 nm [529].



Fig. 78: SwissFEL layout, from <https://www.psi.ch/swissfel/>

EUROPEAN FEL, HAMBURG, GERMANY

The European XFEL has a long history. It was already discussed here with the introduction of the TESLA-TTF FEL. The German Federal Ministry of Education and Research granted permission to build the XFEL in 2007 at a cost of 850 M euros, under the provision that it should be financed as a European project. The FEL on TESTA-TTF [484, 485] was seen as a test-bench for the technology and physics of the future European XFEL project. In 2004–2007 a ‘Science and Technology Issues’ group chaired by F. Sette was created. In 2007, the European XFEL project was officially launched. The European XFEL GmbH company, has been founded in 2009 for building and operating the facility has been founded in 2009. It gathers a consortium of different countries: Denmark, France, Germany, Greece, Hungary, Italy, Poland, Russia, Slovakia, Spain, Sweden, Switzerland, bringing financial and/or in-kind contributions. The 3.4 km long X-ray free electron laser facility extends from Hamburg to the neighbouring town of Schenefeld in the German federal state of Schleswig-Holstein. Technically, European XFEL [530] uses a superconducting linac of extremely good electron beam parameters, enabling operation at high repetition rate. The electrons will be accelerated up to 17.5 GeV over 2.1 km. There are 101 accelerator modules. EFEL will provide three different SASE sources for six experimental stations, as shown in Fig. 79.

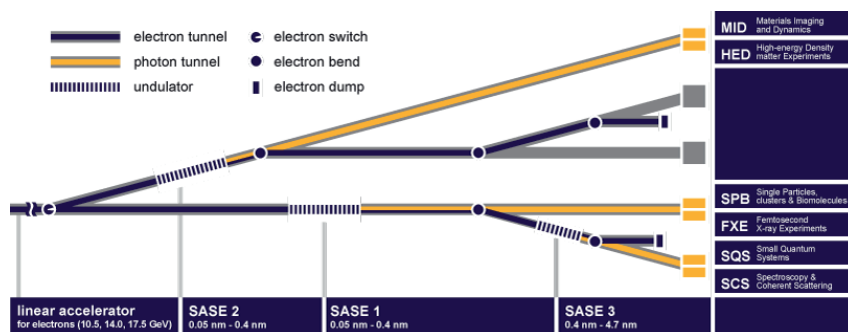


Fig. 79: Sketch of the European X FEL facility, from [531]

SASE 1 and SASE 2 cover 0.4–0.05 nm spectral range, with a 175 m undulator length, whereas SASE 3 covers 4.7–0.4 nm spectral range, with a 105 m undulator length. Pulse duration will be shorter than 100 fs. The flux reaches 10^{12} ph/s. The specificity of the EXFEL is its repetition rate of 27 000 pulses per second, leading to a peak brilliance a billion times higher than that of the best synchrotron X-ray radiation sources (5×10^{33} ph/s/mm²/mrad²/0.1% BW).

Civil construction of the facility started in 2009, and continued with the completion of the 3.4 km tunnel in 2012, and underground in 2013. The overall cost for the construction and commissioning of the facility is as of 2015 estimated at 1.22 B euros. First electrons have been guided from the injector into the first four 2 K superconducting accelerator modules at -271°C and compression chicane in January 2017 [531] in the cooled main accelerator, as presented in Fig. 80. First lasing was achieved on May 2nd 2017 at a moderate energy of 6.4 GeV at 0.9 nm [532], and after beam based alignment and systematic tuning of the electron beam properties, at 0.2 nm on May 24nd 2017 with a energy of 1 mJ achieved three days later. The SASE 1 beam was transported to the experimental hutch in June [533].



Fig. 80: View into the accelerator tunnel: electrons guided into the first four superconducting accelerator modules (yellow) and in a chicane (in front, blue and red), from [531].

European XFEL is the next world's brightest source of ultrashort X-ray pulses and will open up new research opportunities for scientists and industrial users. Thanks to its ultrashort X-ray flashes, the facility will enable scientists to map the atomic details of viruses, decipher the molecular composition of cells, take three-dimensional images of the nanoworld, film chemical reactions, and study processes such as those occurring deep inside planets.

LCLS-II, STANFORD, USA

LCLS-II [534] will move to the use of a 4 GeV superconducting accelerator technology, in the CW mode of operation. It will provide a major jump in capability, moving from 120 pulses per second to 1 million pulses per second. The electron beam properties will be of high quality: normalized slice emittance of 0.45π mm mrad, slice energy spread of 0.12×10^{-4} . The project will also incorporate variable gap hybrid undulators to cover soft (0.2–1.3 keV, i.e. 0.95–6.2 nm) and hard (1–5 keV, i.e. 0.25–1.2 nm) X-ray photons at up to MHz rates; hard X-ray above 25 keV (i.e. below 0.05 nm at 120 Hz), with performance comparable to or exceeding that of the existing LCLS. The project is conducted in the frame of a collaboration between SLAC, Fermilab, Jefferson Lab., Argonne, Cornell University.

SHANGHAI XFEL, SHANGHAI, CHINA

The construction on the Shanghai Coherent Light Facility (SCLF) for a high repetition rate X-ray Free Electron Laser at Shanghai relying on a 8 GeV superconducting accelerator technology has been approved. The super-conducting electron accelerator, undulators and photon beamlines and endstations

are all installed in 3.1 km under-ground tunnels. Using 3 phase-I undulator lines, the SCLF aims at generating X-rays between 0.4 and 25 keV at rates up to 1MHz [535].

7.3 SASE properties

7.3.1 SASE longitudinal properties

The SASE emission starts from of the amplification on spontaneous emission and presents generally spikes in the temporal and spectral distributions, because of non-correlated trains of pulses, resulting in a partial longitudinal coherence. The SASE spectra observed on FLASH are shown in Fig. 81. They illustrate the SASE fluctuations: the number of spikes (wave packets) M is typically 2.5, leading, in using the value of the cooperation length, to FEL pulses of about 50 fs. It can be understood in terms of statistical properties [536].

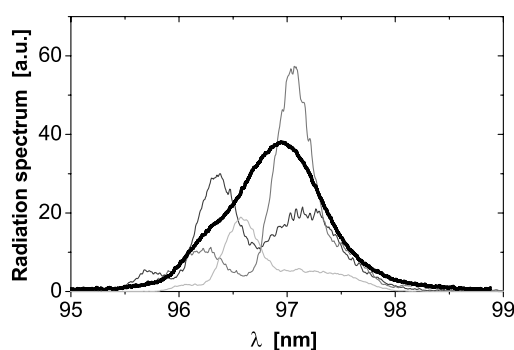


Fig. 81: SASE spectra, from [488]

There are particular cases where this spiky spectral and temporal structure of the SASE can be handled, such as seeding, as developed in the next solution. Alternatively, the FEL can be operated in a low-charge short electron bunches [537] as demonstrated in LCLS [513], or in combining an electron beam energy chirp combined with an undulator taper [538], as shown in SPARC (Test facility in Italy) [539]. Proper combinations of chicanes and undulator segments can enable to phase lock the radiation [540].

Different schemes have been proposed and/or tested for achieving extremely short pulses [541–551] with a selective amplification, modulation, phase locking of the radiation from different segments, superradiance [552]. The partial FEL coherence can be taken into account in the pulse duration measurement [553].

7.3.2 SASE transverse properties

Thanks to the rather low emittance of the electron beam and eventually to gain guiding, SASE FEL presents generally a good transverse coherence [554] and a proper wavefront [555].

7.3.3 SASE polarization

The polarization of the FEL mainly results in the choice of the undulator. Whereas the majority of the SASE FEL started with planar undulators leading to linear polarization, there is a recent trend to provide more polarization flexibility for users. For example, LCLS recently operated with a DELTA undulator [556] leading to hundreds of microjoules of circular polarization in the 1–2.5 nm spectral range [557].

7.4 Seeding

7.4.1 External laser seeding

Following coherent harmonic generation carried out on low gain FEL, the idea of sending an external laser tuned on the undulator fundamental wavelength was developed, in the so-called ‘seeding configuration’ as shown in Fig. 82. The seed provides a sufficiently intense input field that generates an efficient bunching even in a short undulator, leading to coherent emission of undulator radiation and of its higher-order harmonics. The FEL may then operate as an amplifier of the initial seed, capable of increasing the peak power of a light source to approximately the same saturation power level as for the SASE case. The seed should overcome the initial shot noise.

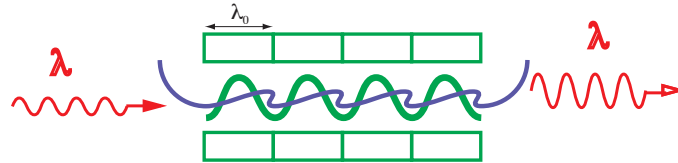


Fig. 82: FEL seeding: a coherent source tuned on the resonant wavelength of the undulator enables to perform efficiently the energy exchange leading further to the density modulation

Concerning the temporal properties, seeding could somehow enable to manipulate the FEL properties. The temporal and spectral distributions of the pulse result from the seed and the FEL intrinsic dynamics and could be modified by the interaction with an external laser. Seeding offers a good strategy for suppressing the spikes inherent to the SASE process and thus for improving the longitudinal coherence, and for reducing the intensity fluctuations, and jitter. In addition, since the electron bunch modulation is controlled by the external laser source, the saturation length can become shorter, the cost can be reduced [558]. Seeding can be used also to efficiently generate harmonics.

Experimentally, the electron beam and the seed should be synchronized, the radiation should overlap transversally and spectrally.

The progress of seeding on high gain single pass FELs is described below, starting with the use of conventional lasers first in the mid infrared, then with that of high-order harmonics generated in gas for a seed at shorter wavelength.

7.4.2 External conventional laser seeding

BNL FEL EXPERIMENT/NSLS DUV FEL, BNL, USA

The first experimental demonstration was carried out by L. H. Yu (16th FEL Prize in 2003) at Brookhaven national Laboratory [429]. The set-up was composed of a 10.6 μm with a 0.5 MW seed CO_2 laser, a 40 MeV electron beam with 120 A peak current (6 ps FWHM, with 5π mm mrad and 0.6% energy spread); a 0.76 m long first modulator (80 mm period, 0.16 T magnetic field), a 0.3 m long dispersive section, and a 2 m long radiator (33 mm period, 0.47 T magnetic field). It led to the saturated, amplified free electron laser second harmonic at 5.3 μm , as shown in Fig. 83.

The experimental results showed that the SASE output was multiplied by six orders of magnitude in the HGHG spectrum. The measured FWHM HGHG bandwidth was of 20 nm, i.e. six times smaller than the SASE one. The spectral bandwidth was significantly reduced by seeding, and longitudinal coherence improved. A single shot HGHG shown in B shows a nice spectral profile, quite different from the spiky SASE pulse.

Such a result has been a major contribution in 2000 for the FEL community, since the use of a laser-seeded free electron laser enabled to produce amplified, longitudinally coherent, Fourier transform

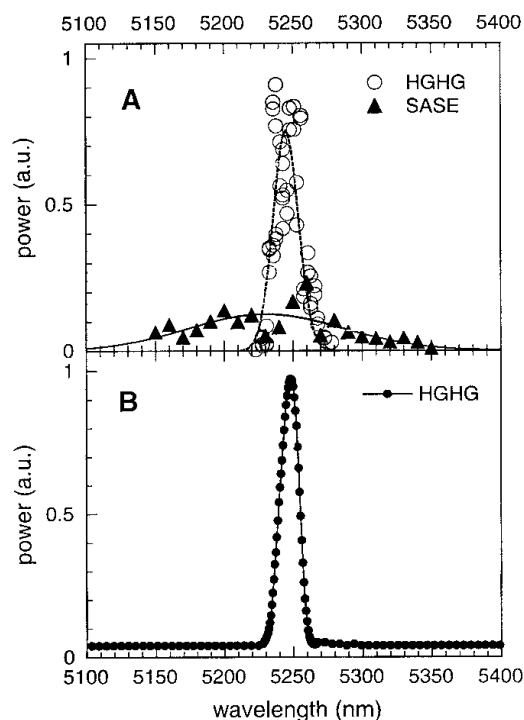


Fig. 83: High gain harmonic generation demonstration using a 800 nm laser, from [429]. A SASE point: an average of 10 shots, HGHG points: single shots normalized to the total HGHG pulse energy. B: Single shot HGHG pulse recorded with a thermal imaging camera at the exit plane of the spectrometer

limited output at the harmonic of the seed laser. “The experiment verifies the theoretical foundation for the technique and prepares the way for the application of this technique in the vacuum ultraviolet region of the spectrum, with the ultimate goal of extending the approach to provide an intense, highly coherent source of hard x-rays” [429]. “The HGHG approach offers an alternative and attractive FEL scheme that combines the benefits of the coherence properties of a laser with the short-wavelength capabilities of an accelerator based light source. A future X-ray HGHG FEL could use the best advances in short-wavelength tabletop lasers as seeds for amplifying and pushing toward shorter wavelengths” [429]. The measurements were in good agreement with the theoretical expectations.

The next step in shorting the wavelength [559]. The beam (4 ps FWHM, with 4.7π mm mrad) from the DUV FEL is produced with the BNL photoinjector where the cathode is illuminated at 266 nm, accelerated with four SLAC accelerating section bringing the energy to 177 MeV, with a chicane between the second and third accelerator module. The modulator was the same as for the previous experiment, whereas the radiation was the 10 m long NISIUS undulator with 38.9 mm period, 0.31 T peak field ($K = 1.13$) with focusing in both planes thanks to canted poles. The seed was taken from the Ti–Sa laser at 800 nm with 30 MW used for the photoinjector. The seeded FEL spectrum is shown in Fig. 84 at 266 nm, the third harmonic of the laser seed. It exhibits a nice line, of 0.1% bandwidth, as compared to the broad spiky SASE spectra. The HGHG width is close to one single SASE spike. An estimate of the pulse length of 0.9 ps was found, close to the 1 ps electron beam duration after compression. These results provided evidence of the high temporal coherence in the HGHG output and significant improvement due to the seeding, with respect to the SASE.

Figure 85 shows the output energy measured for different seed levels versus the wiggler length, by kicking the electron beam at different locations in the undulator. A 0.8 m long gain length was found. The total length of the NISIUS undulator was not sufficient for getting a saturated SASE whereas saturation can be reached in the seeded configuration. Saturation was also more rapidly reached than in the SASE

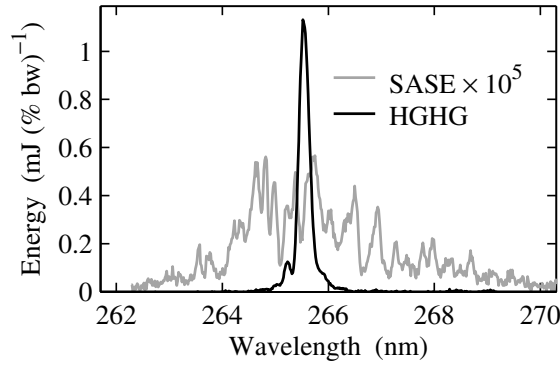


Fig. 84: High gain harmonic generation demonstration using a 800 nm laser, from [559]

case, which makes the system more compact.

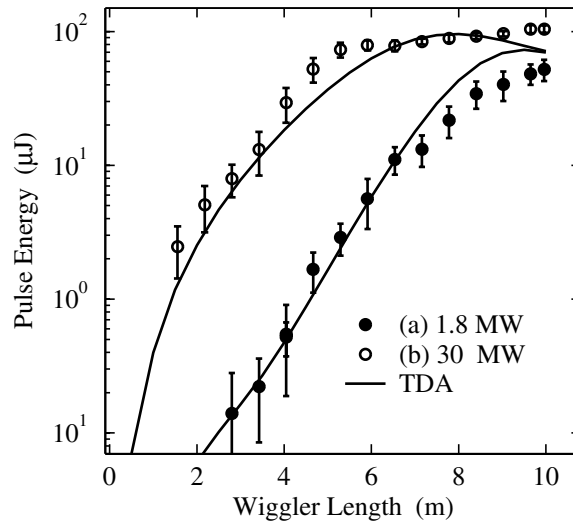


Fig. 85: High gain harmonic generation demonstration using a 800 nm laser, from [559]

Together with the fundamental radiation at 266 nm (100 μJ), significant signal was found on the second (0.1 μJ) and third (0.3 μJ) harmonics [560]. The harmonic radiation at 89 nm of the seeded FEL was successfully used for a first scientific applications in molecular physics [561]. Tuneability is achieved by applying a chirp on the electron beam [562].

A super-radiant seeded FEL was experimentally demonstrated at BNL [563].

SPARC TEST FACILITY, FRASCATI, ITALY

In Italy, a budget dedicated to FEL research has been implemented. Two proposals have been funded, the SPARC FEL test facility, and the FERMI@ELETTRA seeded FEL facility. The SPARC FEL amplifier [539, 564] is driven by a high brightness accelerator providing energies between 80 and 180 MeV and an undulator composed by six modules of variable gap. A super-radiant seeded FEL was experimentally demonstrated on SPARC up to the 11th order [565] and in the cascade configuration [566].

7.4.3 External seeding with high-order harmonics generated in gas

Conventional lasers are limited in terms of the short wavelength they can provide, even though frequency mixing schemes can be used. However, in the landscape of available light sources in the VUV and soft X-ray [567, 568], Harmonic generation in gas (HHG) is one of the most promising methods to generate radiation at short wavelengths in the vacuum and extreme ultraviolet region of the spectrum [569, 570], and is currently in operation for user applications. The high-order harmonics result from the strong non-linear polarization induced on rare-gas atoms, such as Ar, Xe, Ne, and He, by the focused intense electromagnetic field of a pump laser. As the strength of the external electromagnetic field is comparable to that of the internal static field of the atom in the interaction region close to laser focus, atoms ionize by tunnelling of the outer electrons. The ejected free electrons, far from the core, are then accelerated in the external laser field and gain kinetic energy, they can be driven back close to the core and be scattered or recombine to the ground state emitting a burst of XUV photons every half-optical cycle. Correspondingly in the spectral domain, the harmonic spectrum includes the odd harmonics of the fundamental laser frequency. The characteristic distribution of intensities is almost constant for harmonic order in the ‘plateau’ region, where, depending on the generating gas, the conversion efficiency varies in the range 10^{-4} – 10^{-7} . For higher orders, the conversion efficiency decreases rapidly, in the ‘cut-off’ region, which is determined by the gas ionization and the ponderomotive energies. The lighter is the gas (i.e. the higher is the ionization energy the higher is the cut-off energy). High-order harmonics are linearly polarized sources from hundreds of nm to nm, of good temporal and spatial coherence, emitting very short pulses (fs to as), at rather high repetition rate (up to a few kilohertz). The radiation spectrum is completely tuneable in the VUV–XUV region. The harmonic radiation is emitted on the axis of the laser propagation with a small divergence (1 to 10 mrad). Fraction of a microjoule of energy can be obtained at wavelengths down to tens of nm [571]. It was then thought that HHG could suit for being considered as a seed for a high gain FEL [111] for the ARC-EN-CIEL project in France, and on the SCSS Test Accelerator [572] in the frame of a French–Japanese collaboration.

SCSS TEST ACCELERATOR, HARIMA, JAPAN

The HHG chamber has been prepared in France and sent to Japan, whereas an existing laser has been upgraded with a delay line added for such an experiment. The HHG seeding chamber, with a Xe gas cell was located inside the accelerator tunnel. A second chamber handled the transverse focus of the seed in the first undulator. An injection chamber, containing a set of steering mirrors, was located in a magnetic chicane. HHG seeding has been first performed on SCSS Test Accelerator at 160 nm [573]. The HHG seed was strongly amplified in the first undulator segment and the unseeded signal was amplified by three orders of magnitude. The saturation length was reduced by a factor of 2, making the system more compact. The fundamental wavelength was accompanied by the non-linear harmonics (NLH) at 54 nm and 32 nm [574]. Figure 86 shows that light up to the seventh harmonic of the FEL resonance can be measured while in presence of the seed. The seventh harmonic could not be detected when the FEL amplifier was operated with no seed, in SASE mode. A significant increase of the non linear harmonics signal, as compared to the unseeded case, was also observed at the third and fifth harmonics, which were amplified by factors 312 and 47 for the third (0.3 nJ at 53.55 nm) and for the fifth (12 pJ at 32.1 nm) respectively. Spectral narrowing was also observed at the harmonics (from 2.66% to 0.84% for the third harmonic and 2.54% to 1.1% for the fifth harmonic). The seed level required to overcome the shot-noise [571, 575] was studied.

The HHG layout was modified to use a SiC harmonic separator mirror, set at the Brewster angle (69°), for the Ti–Sa pump laser. By introducing a pair of Pt-coated, nearly normal incidence mirrors, both the collimation and the focusing of the HHG radiation were achieved. HHG seed FEL was then obtained at 60 nm [576] with a seed energy of 2 nJ/pulse (i.e. 40 kW, with 50 fs pulse duration). The pulse energy of the seeded FEL (1.3 μ J), was twice larger than in SASE mode (0.7 μ J) and 650 times larger than the HHG seed level (2 nJ).

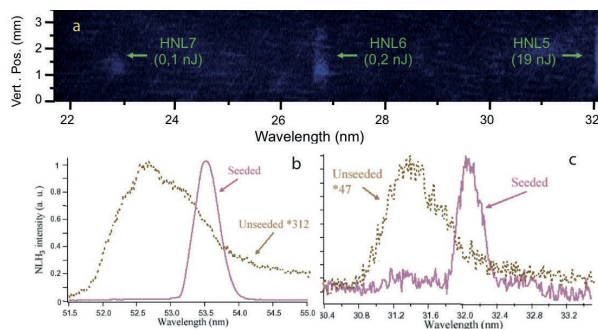


Fig. 86: Nonlinear harmonics of SCSS Test Accelerator FEL seed with HHG at 60 nm (a) fifth to seventh harmonic image of the spectrometer. Comparison of SASE and seeded FEL harmonics of third order (b) and fifth one (c), from [571].

The synchronization was then improved with electro-optical sampling [577, 578], leading to a better hit rate. A few tens of microjoule could then be obtained [579] EUV-FEL.

SCSS test accelerator components have now been moved to SACLA for providing a HHG seeded FEL in the soft X-ray region down to 3 nm, with additional accelerating sections and undulator modules. It could then be combined with HGHG.

SPARC TEST FACILITY, FRASCATI, ITALY

With the flexibility of SPARC for the HGHG configuration, it appeared also to be a good candidate for testing HHG seeding. It was performed in the frame of an Italian (ENEA, INFN)–French (CEA /synchrotron SOLEIL) collaboration. The Ti–Sa laser delivering up to 2.5 mJ at 800 nm with a pulse duration of about 120 fs was focused by a 2 m focal length lens to an in-vacuum cell, where a synchronized valve injected Argon gas at 15 bar. Seeding at 160 nm was performed. Then, for a 50 nJ 266 nm seed, the resonance can be set both on the fundamental and second harmonics. The six 2.1 m long undulator segments could be independently tuned at the seed wavelength, operating as modulators, or at its second harmonic, 133 nm, as radiators of a frequency-doubling cascade. A beam of 176 MeV with a 50–70 A peak current with 0.9π mm mrad emittance was employed. Figure 87 shows the comparison between the experimental data and the results of a statistical study made with 100 random shots, simulated by GENESIS 1.3. An output energy of 1 mJ at 133 nm was obtained with four modulators and two radiators at 133 nm. The estimated gain length in the modulator of 1.1 m was sufficient to increase the input seed to a level close to saturation, and up to 4×10^{12} photons were produced at 133 nm [580].

SFLASH, HAMBURG, GERMANY

The sFLASH seed laser system producing 800 nm, 50 mJ adjustable pulse length (down to 30 fs), connected to the accelerator tunnel by a 7 m long tube, was sent to a gas filled capillary for the production of the seed at 38 nm of 2 nJ, the 21st harmonic of the 800 nm Ti–Sa laser. The seed was sent in the accelerator. The first undulator was located 5 meters after the point of injection into the tunnel. A proof of the interaction and amplification of the seed, coupled to the electron bunch, was obtained on the first and second harmonics at 38 nm and 19 nm [581]. This is the shortest wavelength where harmonics generated in gas have been amplified in a single-pass FEL.

7.4.4 Seeded FEL facilities

FERMI, TRIESTE, ITALY

FERMI is the first seeded FEL user facility VUV/soft X-ray located at Trieste in Italy. It was launched

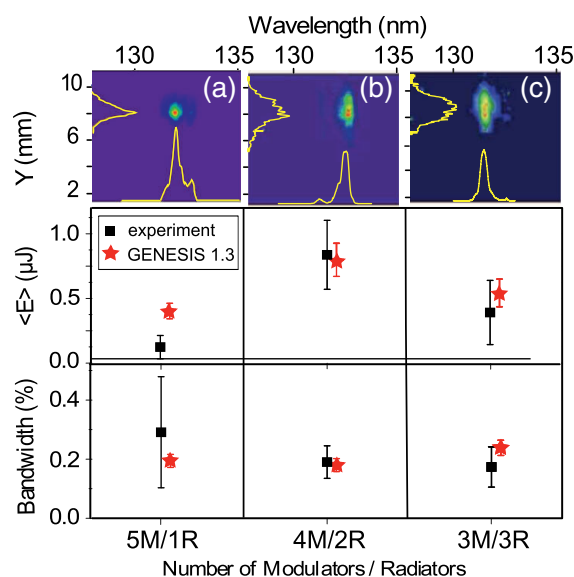


Fig. 87: HHG seeding at SPARC with 266 nm with (a) five modulators, one radiator, (b) four modulators, two radiators, (c) three modulators, three radiators. Data averaged over 100 shots with one standard deviation error bar and compared with GENESIS simulations. [580].

after the Italian initiative for FEL [582–585]. The electron bunches generated in a high-gradient photocathode gun is accelerated by a normal conducting linear accelerator up to a beam energy of 1.2 GeV (1π mm mrad emittance, 0.016% energy spread, 0.8 kA peak current) before reaching the two FEL branches in the HHG cascade configuration, in order to provide a good longitudinal coherence. It relies on the two FEL branches, FEL 1 in the 100–20 nm via a single cascade harmonic generation, and FEL 2 in the 20–4 nm via a double cascade harmonic generation [586], as shown in Fig. 88. The seed laser is based on an optical parametric amplifier continuously tuneable in the range 230–260 nm, delivering pulses of few tens of microjoules [587, 588]. The modulators are planar undulators, and radiators are APPLE-II [589] type undulators for providing adjustable polarization. For FEL 1, the modulator is a 3.03 m long undulator of 160 mm period, providing a deflection parameter ranging between 3.9 to 4.9. The APPLE-II type radiators are 2.34 m long with 65 mm period, from a deflection parameter ranging between 2.4 and 4. For FEL 2, the modulator of the first stage has 30×100 mm periods, the three first stage radiators and second stage modulator have 44×55 mm periods in variable polarization, and the six second stage radiators have 69×35 mm periods in variable polarization.

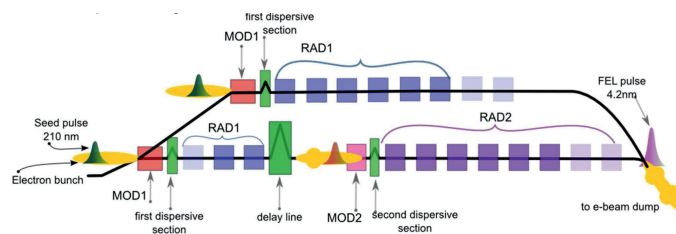


Fig. 88: FERMI HHG FEL lines

FERMI lasing was achieved in December 2010 on FEL1 and in May 2012 on FEL2 [587, 588, 590]. Tuneability can be achieved on the injection source coupled to a gap change or by applying a chirp (frequency drift) both on the seed and on the electron bunch [591]. The combination of HHG, fresh bunch technique, and harmonic cascade has recently enabled an up-frequency conversion by a factor of 192 [592]. Two-colour operation was achieved both with the pulse splitting technique [593, 594] or with

a twin-pulse electron beam [595]. The polarization can be efficiently controlled thanks to the APPLE-II type undulators [596]. FERMI results constitute a major step in the community with the control of the temporal FEL distribution at short wavelength, and the flexibility in polarization.

There are different experimental stations for coherent diffraction imaging (DIPROI), absorption and elastic scattering from materials under extreme conditions (EIS-TIMEX), gas phase and cluster spectroscopy (LDM) with additional facilities for inelastic and transient grating spectroscopy (EIS-TIMER), and terahertz applications (TERAFERMI). Optical laser pulses are also available for pump-probe experiments (SLU).

DALIAN FEL, DALIAN, CHINA

The project was started in early 2012 within a collaboration between Dalian Institute of Chemical Physics (X. Yang), Shanghai Institute of Applied Source (Z. Zhao, D. Wang), from China Academy of Science. The Dalian facility covers 50–150 nm (8–24 eV) in both HGHG and SASE modes [597]. The Dalian FEL is sketched in Fig. 89.



Fig. 89: Dalian FEL sketch, from <https://www.asianscientist.com/2017/01/topnews/brightest-vuv-free-electron-laser/>

The FEL has been commissioned in January 2017. A flux of 1.4×10^{14} ph/pulse was achieved with undulator tapering [597]. Then, the performance of the Dalian FEL were achieved with pulses ranging between 100 fs and 1 ps and an energy reaching 1 mJ [598]. It be used to probe fuel combustion, biomolecules behaviour in gases, and reactions process at solid–gas interfaces.

7.4.5 Echo demonstration

NLCTA TEST EXPERIMENT, STANFORD, USA

Experimentally demonstrated so far in the UV experiment on the Next Linear Collider Test Accelerator at SLAC [599–601] with an up-frequency conversion up to the 75th harmonic and later on the 75th harmonic [602]. It constitutes a breakthrough in up-frequency conversion from a conceptual point of view, and in terms of compactness and pulse properties. Echo enables us to provide vortices [603, 604].

SHANGHAI FEL, SHANGHAI, CHINA

A first multipurpose test experiment SDUV-FEL was set in the Shanghai Jiading campus for FEL principle studies, with an emphasis on seeding schemes. It uses an 148 MeV electron beam (0.2% energy spread, $4-6\pi$ mm mrad emittance, 100–300 pC charge, 2–8 ps duration), a 10 μ J seed at 1.16–1.58 μ m, a modulator of 10 \times 50 mm period ($K = 2-3$), a radiator of 80 \times 40 mm period ($K = 0.9-2.5$). Different features of harmonic generation have been studied: local energy spread measurements thanks to coherent harmonic generation [605], wide tuneability in the HGHG and cascaded HGHG configurations [606],

phase-merging enhanced harmonic generation [607], phase space manipulation for seeding [608]. Polarization switching was tested [609]. Phase space linearization using corrugated chambers was demonstrated [610]. Echo was also achieved on the SDUV-FEL [611].

The SDUV FEL was a test facility in view of the development of the Shanghai X-ray FEL (SXFEL) in the main campus, a user facility in the soft X-ray (8.8 nm with 0.84 GeV with C-band accelerating structures, 0.5 nC charge, below 0.15% energy spread, 2π mm mrad) with cascaded HGHG or echo configurations to be extended to the hard X-ray (2 nm with 1.6 GeV with cascaded HGHG). The installation is completed and the SXFEL is presently under commissioning [612].

7.4.6 FEL self-seeding

Seeding with the FEL itself is also an alternative [613]. Indeed, self-seeding suits better the hard X-ray domain: a monochromator installed after the first undulator spectrally cleans the radiation before the last amplification in the final undulator. Recently, self-seeding with the spectral cleaning of the SASE radiation in a single crystal monochromator [614] appears to be very promising, as experimentally demonstrated at LCLS [615,616] and at SACLA [617].

7.5 Applications of X-ray FELs

The recent advent of tuneable coherent X-ray FELs (XFELs) [418,618] opened a new era for the investigation of matter [619]. “It is worthwhile to recount that the first five years of LCLS operation generated many unanticipated methods and discoveries. With many new next-generation x-ray FEL sources coming online in the next five years, the advancement of science will only continue to accelerate” [619]. They enable us to decrypt the structure of biomolecules and cells [620–622], to provide novel insight in the electronic structure of atoms and molecules [623–626], to observe non-equilibrium nuclear motion, disordered media, and distorted crystal lattices, thanks to recent progress of fs spectroscopy [627], and pump-probe techniques [628]. Detailed structural dynamics can be inferred from spectroscopic signatures [629]. XFELs can also reveal chemical reactions movies. With new imaging techniques [630,631], they are exceptional tools for the investigation of ultrafast evolution of the electronic structure and provide a deeper insight in the extreme states of matter [632].

8 Conclusion and prospects

Among the various light sources such as synchrotron radiation [633], high-order harmonics generated in gas [567,568], X-ray FELs are unique tuneable coherent light sources from far infrared to the X-ray domain.

Figure 90 shows the evolution of the FEL wavelength versus years. After the first lasing in the infrared in 1977, the second lasing in the visible in 1983, 2000 appeared to bring a transition where VUV is reached both in the oscillator and SASE configurations [634]. Then, thanks to the development of photoinjectors and more generally, to accelerator technology, the X-ray range was reached less than 10 years later, in 2009, 2011 with presently new facilities commissioned in 2016 and 2017, including the European XFEL being a high repetition rate one.

The FEL spatial coherence is usually quite good: in the resonator configuration, it results from the optical cavity for resonators and from the electron beam emittance on single pass systems, and possibly from the seed with optical guiding in the high gain regime. Temporal Coherence is usually good, the Fourier limit is reached in some cases (oscillators, seeding). Femtosecond pulses are possible (and there are various schemes proposed schemes for reaching 100 attosecond pulses). Polarization results from the undulator choice.

Major steps of FEL progress are recalled in Fig. 91.

Present developments are oriented in providing further advanced properties. The two-colour FEL

HISTORICAL SURVEY OF FREE ELECTRON LASERS

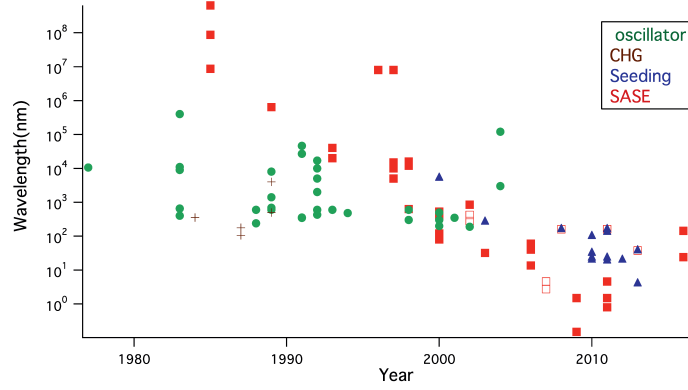


Fig. 90: Achieved FEL wavelengths versus year for various configurations (oscillators, coherent harmonic generation, SASE, seeding).

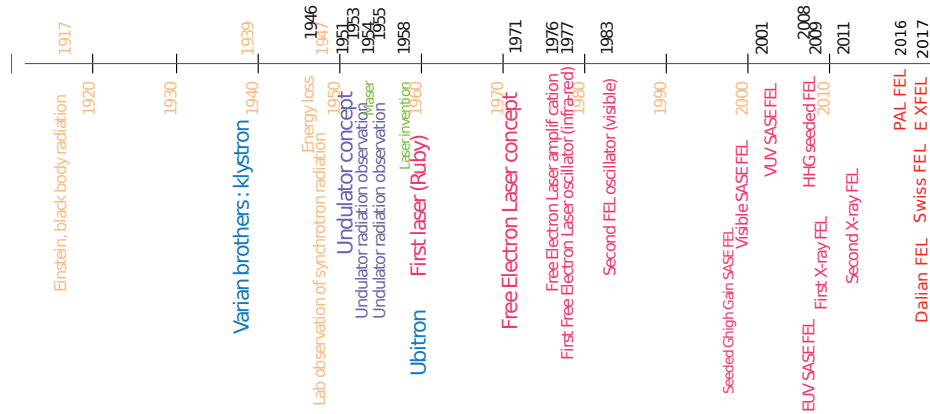


Fig. 91: Major FEL historical steps

concept can be applied to the X-ray domain in the SASE regime, either tuning the two series of undulators at different wavelengths [635–637], the delay being adjusted by a chicane, or by using twin bunches at different energies [638], enabling also operation in the self-seeded case. In the external seeding case, one can take advantage of the pulse splitting effect [438] combined with chirp [593, 594], or apply a double seeding [595, 639]. Several strategies are investigated in the quest towards attosecond pulses and high peak power.

Another evolution trend is the search for compactness. Besides seeding and up-frequency conversion, one considers implementing the FEL using a compact accelerator or undulator. In a Laser Wakefield Accelerator (LWFA) [640], an intense laser pulse drives plasma density wakes to produce, by charge separation, strong longitudinal electric fields, with accelerating gradient that can reach a 100 GV/m [641, 642]. Electrons have to be set at a proper phase with respect to the wake, to be efficiently accelerated. LWFA can nowadays produce electron beams in the few hundreds of MeV to 1 GeV range

with a typical current of a few kiloamperes with reasonable beam characteristics (relative energy spread of the order of 1%, and a normalized emittance of the order of 1π mm mrad). This new accelerating concept could thus be qualified by a FEL application [643, 644]. LWFA based undulator radiation has been observed, even at short wavelengths [645–648]. The present LWFA electron beam properties are not directly suited for enabling FEL amplification, and electron beam manipulation is required: the handling of the divergence with strong permanent magnet quadrupoles, the reduction of the slice energy spread by a demixing chicane [649, 650] where advantage can be taken from the introduced correlation between the energy and the position to focus the slices can be focused in synchronization with the optical wave advance, in the so-called supermatching scheme [651], or in using a transverse gradient undulator [652] coming back to the old FEL times where large energy spread had to be managed [166]. Several experiments are under way.

Fifty years after the laser discovery [653] and more than 30 years after the first FEL, the emergence of several mJ X-ray lasers for users in the Angstrom range constitutes a major breakthrough. Higher availability of X-ray pulses with stable energy, synchronized to an external pump laser, for jitter-free optical pump/resonant X-ray probe experiments will enable us to step further. Besides, exploration of future compact FELs has started. Present X-ray FELs enable us to pave the way towards unrevealed properties of matter and dynamical processes.

Acknowledgements

I would like to dedicate this work to John Madey (1943–2016), the inventor of the FEL, who passed away during summer 2016 and to P. Elleaume (1956–2011), Y. Petroff, M. Billardon, J. M. Ortéga, M. Velghe, who welcomed me in this field. Acknowledgments go also to my former and present students and post-docs, and to Sabine and Amin for careful checks of this report.

References

- [1] C.A. Brau, *Free-Electron Lasers* (Academic Press, Boston, 1990).
- [2] C.A. Brau, *Science* **239** (1988) 1115–1122, <https://doi.org/10.1126/science.239.4844.1115>.
- [3] C. Pellegrini, *Eur. Phys. J. H.* **37** (2012) 659–708, <https://doi.org/10.1140/epjh/e2012-20064-5>.
- [4] A.L. Schawlow, C.H. Townes, *Phys. Rev.* **112** (1958) 1940, <https://doi.org/10.1103/physrev.112.1940>.
- [5] T.H. Maiman, *Nature* **187** (1960) 493–494, <https://doi.org/10.1038/187493a0>.
- [6] J.M.J. Madey, *J. Appl. Phys.* **42** (1971) 1906–1913, <https://doi.org/10.1063/1.1660466>.
- [7] A. Einstein, *Phys. Z.* **18** (1917) 121.
- [8] J.H. van Vleck, *Phys. Rev.* **24** (1924) 330–346, <https://doi.org/10.1103/physrev.24.330>.
- [9] J.H. van Vleck and D.L. Huber, *Rev. Mod. Phys.* **49** (1977) 939–959, <https://doi.org/10.1103/revmodphys.49.939>.
- [10] Y. Petroff, *Les rayons X: de l’astrophysique à la nanophysique* (1998).
- [11] U.E. Kruse, L. Marshall and J.R. Platt, *Astrophys. J.* **124** (1956) 601.
- [12] J.D. Jackson, *Classical Electrodynamics* (Wiley, New York Ld, 1962), Vol. 3.
- [13] J. Larmor, *London, Edinburgh, Dublin Philos. Mag. J. Sci.* **44** (1897) 503–512, <https://doi.org/10.1080/14786444108520780>.
- [14] A. Liénard, *Éclairage Électrique.* **16** (1898) 320–334.
- [15] G.A. Schott, *Ann. Phys.* **24** (1907) 635–660.
- [16] G.A. Schott, *Electromagnetic Radiation* (Cambridge University Press, Cambridge, 1912).
- [17] D. Iwanenko and I. Pomeranchuk, *Phys. Rev.* **65** (1944) 343, <https://doi.org/10.1103/physrev.65.343>.

- [18] M.O. Oliphant, The acceleration of particles to very high energies. *Classified memo submitted to DSIR University of Birmingham Archive* (1943).
- [19] E.M. McMillan, *Phys. Rev.* **68** (1945) 143, <https://doi.org/10.1103/physrev.68.143>.
- [20] V. Veksler, *J. Phys. USSR.* **9** (1945) 153–158.
- [21] F.K. Goward and D.E. Barnes, *Nature* **158** (1946) 413, <https://doi.org/10.1038/158413a0>.
- [22] J. Schwinger, *Phys. Rev.* **70** (1946) 798–799, <https://doi.org/10.1103/physrev.70.41>.
- [23] J. Schwinger, *Phys. Rev.* **75** (1949) 1912, <https://doi.org/10.1103/physrev.75.1912>.
- [24] J.P. Blewett, *Phys. Rev.* **69** (1946) 87, <https://doi.org/10.1103/physrev.69.87>.
- [25] J.P. Blewett, *J. Synchrotron Radiat.* **5** (1998) 135–139, <https://doi.org/10.1107/s0909049597043306>.
- [26] F.R. Elder, A.M. Gurewitsch, R.V. Langmuir and H.C. Pollock, *Phys. Rev.* **71** (1947) 829, <https://doi.org/10.1103/physrev.71.829.5>.
- [27] V.L. Ginzburg, *Bull. Acad. Sci. USSR.* **11** (1947) 165–182.
- [28] H. Motz, *J. Appl. Phys.* **22** (1951) 527–535, <https://doi.org/10.1063/1.1700002>.
- [29] H. Motz and M. Nakamura, *Ann. Phys.* **7** (1959) 84–131, [https://doi.org/10.1016/0003-4916\(59\)90049-1](https://doi.org/10.1016/0003-4916(59)90049-1).
- [30] H. Motz, W. Thon and R.N. Whitehurst, *J. Appl. Phys.* **24** (1953) 826–833, <https://doi.org/10.1063/1.1721389>.
- [31] R. Combes and T. Frelot, *C R Hebd. Scéance Acad. Sci. Paris.* **241** (1955) 1559–1560.
- [32] K. Halbach, *Le J. Phys. Colloq.* **44(C1)** (1983) 211–216, <https://doi.org/10.1051/jphyscol:1983120>.
- [33] P.L. Csonka, *Part Accel.* **8** (1978) 225–234.
- [34] T. Nakazato, M. Oyamada, N. Niimura, S. Urasawa, O. Konno, *et al.*, *Phys. Rev. Lett.* **63** (1989) 1245, <https://doi.org/10.1103/physrevlett.63.1245>.
- [35] R.H. Varian and S.F. Varian, *J. Appl. Phys.* **10** (1939) 321–327, <https://doi.org/10.1063/1.1707311>.
- [36] J.M. Ortéga, Généralités sur le LEL, Notes de cours.
- [37] K. Landecker, *Phys. Rev.* **86** (1952) 852, <https://doi.org/10.1103/physrev.86.852>.
- [38] R.M. Phillips, *Nucl. Instrum. Methods Phys. Res. A.* **272** (1988) 1–9, <https://doi.org/10.1016/j.nima.2016.03.040>.
- [39] R.M. Phillips, *IRE Trans. Electron Devices, ED-7.* **7** (1960) 231–241.
- [40] C.E. Enderby and R.M. Phillips, *Proc. IEEE.* **53** (1965) 1648–1648.
- [41] R.B. Palmer, *J. Appl. Phys.* **43** (1972) 3014–3023, <https://doi.org/10.1063/1.1661650>.
- [42] R.H. Pantell, G. Soncini and H.E. Puthoff, *IEEE J. Quantum Electron.* **4** (1968) 905–907, <https://doi.org/10.1109/jqe.1968.1074989>.
- [43] J.P. Gordon, H.J. Zeiger and C.H. Townes, *NH₃ Phys. Rev.* **95** (1954) 282, <https://doi.org/10.1103/physrev.95.282>.
- [44] R.G. Gould, The laser, light amplification by stimulated emission of radiation. *The Ann Arbor Conference on Optical Pumping* (The University of Michigan, 1959), vol. 15, p. 128.
- [45] H. Kogelnik, T. Li, *Appl. Opt.* **5** (1966) 1550–1567, <https://doi.org/10.1364/ao.5.001550>.
- [46] A. Yariv. *Quantum Electronics* (John Wiley & Sons, New York, 1975), p. 123.
- [47] T.H. Maiman, R.H. Hoskins, I.J. D’Haenens, C.K. Asawa and V. Evtuhov, *Phys. Rev.* **123** (1961) 1151, <https://doi.org/10.1103/physrev.123.1151>.
- [48] C. Fabre, *Images Phys* **30** (2010) 3–9.
- [49] A. Javan, W.R. Bennett and D.R. Herriott, *Phys. Rev. Lett.* **6** (1961) 106, <https://doi.org/10.1103/physrevlett.6.106>.

- [50] R.N. Hall, G.E. Fenner, J.D. Kingsley, T.J. Soltys and R.O. Carlson, *Phys. Rev. Lett.* **9** (1962) 366, <https://doi.org/10.1103/physrevlett.9.366>.
- [51] R.J. Keyes and T.M. Quist, *Proc. IRE.* **1822** (1962) 16 IEEE.
- [52] E. Schrödinger, *Ann. Phys.* **387** (1927) 257–264, <https://doi.org/10.1002/andp.19273870210>.
- [53] P.L. Kapitza and P.A.M. Dirac, *Math. Proc. Cambridge Philos. Soc.* **29** (1933) 297–300, <https://doi.org/10.1017/s0305004100011105>.
- [54] M.V. Fedorov, *Sov. J. Exp. Theor. Phys.* **24** (1967) 529.
- [55] J.M.J. Madey, *Phys. Rev. Special Topics-Accelerators Beams.* **17** (2015) 074901, <https://doi.org/10.1103/physrevstab.17.074901>.
- [56] J.M.J. Madey, Free Electron Lasers and the path to understanding. *Nobel Symposium on Free Electron Laser Research* (2015), pp. 14–18.
- [57] H. Dreicer, *Phys. Fluids.* **7** (1964) 735–753, <https://doi.org/10.1063/1.1711276>.
- [58] D. Marcuse, *Bell Syst Tech. J.* **41** (1962) 1557–1571, <https://doi.org/10.1002/j.1538-7305.1962.tb03994.x>.
- [59] R.Q. Twiss, *Aust. J. Phys.* **11** (1958) 564–579, <https://doi.org/10.1071/ph580564>.
- [60] J.M.J. Madey, E.T. Scharlemann and W.M. Fairbank, *IEEE Trans. Nucl. Sci.* **20** (1973) 980–980, <https://doi.org/10.1109/tns.1973.4327304>.
- [61] V.P. Sukhatme and P.A. Wolff, *J. Appl. Phys.* **44** (1973) 2331–2334, <https://doi.org/10.1063/1.1662560>.
- [62] N.M. Kroll and W.A. McMullin, *Phys. Rev. A.* **17** (1978) 300, <https://doi.org/10.1103/physreva.17.300>.
- [63] P. Sprangle and V.L. Granatstein, *Appl. Phys. Lett.* **25** (1974) 377–379.
- [64] P. Sprangle, V.L. Granatstein and L. Baker, *Phys. Rev. A.* **12** (1975) 1697.
- [65] H. Haus, *IEEE J. Quantum Electron.* **17** (1981) 1427–1435, <https://doi.org/10.1109/jqe.1981.1071289>.
- [66] A. Fruchtman, *Phys. Rev. A.* **37** (1988) 4252, <https://doi.org/10.1103/physreva.37.4252>.
- [67] J. Fajans, J.S. Wurtele, G. Bekefi, D.S. Knowles and K. Xu, *Phys. Rev. Lett.* **57** (1986) 579, <https://doi.org/10.1103/physrevlett.57.579>.
- [68] M.E. Conde and G. Bekefi, *Phys. Rev. Lett.* **67** (1991) 3082, <https://doi.org/10.1103/physrevlett.67.3082>.
- [69] T.C. Marshall, *Free Electron Lasers* (Macmillan, New York, 1985).
- [70] F.A. Hopf, P. Meystre, M.O. Scully and W.H. Louisell, *Phys. Rev. Lett.* **37** (1976) 1215, <https://doi.org/10.1103/physrevlett.37.1215>.
- [71] F.A. Hopf, P. Meystre, M.O. Scully and W.H. Louisell, *Phys. Rev. Lett.* **37** (1976) 1342, <https://doi.org/10.1103/physrevlett.37.1342>.
- [72] H. Al Abawi, F.A. Hopf, P. Meystre, *Phys. Rev. A.* **16** (1977) 666, <https://doi.org/10.1103/physreva.16.666>.
- [73] P. Sarangle, *J. Plasma Phys.* **11** (1974) 299–309, <https://doi.org/10.1017/s002237780002465x>.
- [74] T. Kwan, J.M. Dawson and A.T. Lin, *Plasma Phys* **20** (1977) 486–506,
- [75] W.B. Colson, *Phys. Lett. A.* **59** (1976) 187–190, [https://doi.org/10.1016/0375-9601\(76\)90561-2](https://doi.org/10.1016/0375-9601(76)90561-2).
- [76] W.B. Colson, *Phys. Lett. A.* **64** (1977) 190–192, [https://doi.org/10.1016/0375-9601\(77\)90712-5](https://doi.org/10.1016/0375-9601(77)90712-5).
- [77] W.B. Colson, Ph.D. thesis, Stanford University, 1977.
- [78] W.B. Colson, Free electron laser theory, a dissertation submitted to the department of physics and the committee on graduate studies of stanford university. Technical report (Stanford University, 1977).
- [79] W.H. Louisell, J.F. Lam, D.A. Copeland and W.B. Colson, *Phys. Rev. A.* **19** (1979) 288,

- <https://doi.org/10.1103/physreva.19.288>.
- [80] W.B. Colson and S.K. Ride, *Phys. Lett. A*. **76** (1980) 379–382, [https://doi.org/10.1016/0375-9601\(80\)90737-9](https://doi.org/10.1016/0375-9601(80)90737-9).
- [81] W.B. Colson, *IEEE J. Quantum Electron.* **17** (1981) 1417–1427, <https://doi.org/10.1109/jqe.1981.1071273>.
- [82] W.B. Colson, *Phys. Rev. A*. **24** (1981) 639, <https://doi.org/10.1103/physreva.24.639>.
- [83] R. Coisson and F. De Martini, *Free-Electron Generators of Coherent Radiat.* **9** (1982) 939–1003.
- [84] W.B. Colson, C. Pellegrini and A. Renieri, *Laser Handbook, Volume 6: Free Electron Lasers* (North Holland, 1990).
- [85] W.B. Colson, *Nucl. Instrum. Methods Phys. Res. A*. **237** (1985) 1–9, [https://doi.org/10.1016/0168-9002\(85\)90323-7](https://doi.org/10.1016/0168-9002(85)90323-7).
- [86] Z. Abramowitz and I.A. Stegun, *Handbook of Mathematical Functions*, National Bureau of Standards, now National Institute of Standards and Technology (NIST) Applied Mathematics Series - 55, Issued June 1964, Seventh printing, (1968).
- [87] J.M.J. Madey, *Il Nuovo Cim. B Series 11*. **50** (1979) 64–88, <https://doi.org/10.1007/bf02737619>.
- [88] W.B. Colson and P. Elleaume, *Appl. Phys. B*. **29** (1982) 101–109, <https://doi.org/10.1007/bf00692771>.
- [89] D. Nutarelli, D. Garzella, M.E. Couprie, M. Billardon, *Nucl. Instrum. Methods Phys. Res. A*. **393** (1997) 64–69.
- [90] A. Bambini and A. Renieri, *Coherence Spectrosc. Mod. Phys* **37** (1978) 361–379, https://doi.org/10.1007/978-1-4613-2871-1_18.
- [91] A. Bambini, A. Renieri and S. Stenholm, *Phys. Rev. A*. **19** (1979) 2013, <https://doi.org/10.1103/physreva.19.2013>.
- [92] A. Bambini, R. Bonifacio and S. Stenholm, *Opt. Commun.* **32** (1980) 306–308, [https://doi.org/10.1016/0030-4018\(80\)90130-3](https://doi.org/10.1016/0030-4018(80)90130-3).
- [93] G. Dattoli, A. Marino, A. Renieri and F. Romanelli, *IEEE J. Quantum Electron.* **17** (1981) 1371–1387, <https://doi.org/10.1109/jqe.1981.1071268>.
- [94] G. Dattoli and R. Mignani, *J. Math. Phys.* **26** (1985) 3200–3203, <https://doi.org/10.1063/1.526649>.
- [95] R. Bonifacio and M.O. Scully, *Opt. Commun.* **32** (1980) 291–294, [https://doi.org/10.1016/0030-4018\(80\)90127-3](https://doi.org/10.1016/0030-4018(80)90127-3).
- [96] G. Dattoli, T. Hermsen, A. Renieri, A. Torre and J.C. Gallardo, *Phys. Rev. A*. **37** (1988) 4326, <https://doi.org/10.1103/physreva.37.4326>.
- [97] G. Dattoli, T. Hermsen, L. Mezi, A. Renieri and A. Torre, *Phys. Rev. A*. **37** (1988) 4334, <https://doi.org/10.1103/physreva.37.4334>.
- [98] G. Dattoli, *J. Appl. Phys.* **84** (1998) 2393–2398, <https://doi.org/10.1063/1.368365>.
- [99] G. Dattoli, A. Renieri and A. Torre, *Lectures on the Free Electron Laser Theory and Related Topics* (World Scientific, Singapore, 1993), Vol. 637.
- [100] F. Ciocci, G. Dattoli, A. Torre and A. Renieri, in *Series on Synchrotron Radiation Techniques and Applications*, Eds. D.H. Bilderback, K.O. Hodgson, M.P. Kiskinov and R. Rossi (World Scientific, Singapore, 2000), Vol. 6.
- [101] F.V. Bunkin and V.D. Novikov, *Vestn. Akad. Nauk SSSR*. **8** (1981) 111–113.
- [102] N.A. Vinokurov and A.N. Skrinky, Power limit for an optical klystron installed on storage ring. *Preprint INP*, (1977) pp. 77–59.
- [103] N.A. Vinokurov and A.N. Skrinky, Generatornii klystron opticheskovogo diapazona na ultrarelativistiskii elektropnax. klystron generating in the optical range with relativistic electrons, preprint

- INP 77–59. Technical report, Institute of Nuclear Physics of the Siberian Division of the USSR Academy of Sciences, Novosibirsk (1977).
- [104] N.A. Vinokurov and A.N. Skrinsky, O predelnoi mochnosti opticheskovo klystrona, ustanovlenno na elektronii nakonitel. maximum power out of an optical klystron installed on the electron storage ring, preprint INP 77-67. Technical report, Institute of Nuclear Physics of the Siberian Division of the USSR Academy of Sciences, Novosibirsk (1977).
- [105] N.A. Vinokurov and A.N. Skrinsky, O predelnoi mochnosti opticheskovo klystrona, ustanovlenno na lineinii uskoritel elektronob. maximum power of an optical klystron installed on a linear accelerator, preprint INP 78-88. Technical report, Institute of Nuclear Physics of the Siberian Division of the USSR Academy of Sciences, Novosibirsk (1977).
- [106] R. Coisson, *Part. Accel.* **11** (1981) 245–253.
- [107] P. Elleaume, *Le J. Phys. Colloques.* **44(C1)** (1983) C1–333, <https://doi.org/10.1051/jphyscol:1983127>.
- [108] R.R. Freeman and B.M. Kincaid, in *Laser Techniques in the Extreme Ultraviolet*, (AIP Publishing, 1984), Vol. 119, pp. 278–292.
- [109] P. Elleaume, *Nucl. Instrum. Methods Phys. Res. A.* **250** (1986) 220–227, [https://doi.org/10.1016/0168-9002\(86\)90884-3](https://doi.org/10.1016/0168-9002(86)90884-3).
- [110] V.N. Litvinenko, J.M.J. Madey and N.A. Vinokurov, UV-VUV FEL Program at Duke Storage Ring with OK-4 optical klystron. In *Particle Accelerator Conference* (IEEE, 1993), pp. 1442–1444.
- [111] M.E. Couprie, M. Belakhovsky, B. Gilquin, D. Garzella, M. Jablonka, F. Méot, P. Monot, A. Mosnier, L. Nahon and A. Rousse, *Nucl. Instrum. Methods Phys. Res. A.* **528** (2004) 557–561, <https://doi.org/10.1016/j.nima.2004.04.101>.
- [112] Y.K. Wu, N.A. Vinokurov, S. Mikhailov, J. Li and V. Popov, *Phys. Rev. Lett.* **96** (2006) 224801, <https://doi.org/10.1103/physrevlett.96.224801>.
- [113] V.N. Baier and A.I. Milstein. To the theory of a free-electron laser, preprint INP 77-67. Technical report (Institute of Nuclear Physics of the Siberian Division of the USSR Academy of Sciences, Novosibirsk, 1977).
- [114] V.N. Baier and A.I. Milstein, *Phys. Lett. A.* **65** (1978) 319–322, [https://doi.org/10.1016/0375-9601\(78\)90716-8](https://doi.org/10.1016/0375-9601(78)90716-8).
- [115] V.N. Baier and A.I. Milstein, O generatsii kogerentnovo izlucheniya blizko tsiklotronnovo rezonansa, generation of coherent radiation close to the cyclotron resonance, preprint INP 78-61. Technical report, Institute of Nuclear Physics of the Siberian Division of the USSR Academy of Sciences, Novosibirsk (1978).
- [116] A.M. Kondratenko, *Sou Phys. Dokl. Part. Accelerators.* **24** (1979) 989.
- [117] A.M. Kondratenko and E.L. Saldin, Generation of coherent radiation by a relativistic-electron beam in an undulator, preprint INP 79-48. Technical report (Institute of Nuclear Physics of the Siberian Division of the USSR Academy of Sciences, Novosibirsk, 1978).
- [118] A.M. Kondratenko and E.L. Saldin, Generation of coherent radiation by a relativistic-electron beam in an undulator. In *Particle Accelerator Conference*, vol. 10 (1986), pp. 207–216, Gordon and Breach, Science Publishers, Inc..
- [119] A.M. Kondratenko and E.L. Saldin, On the linear theory of free electron lasers with Fabry-Perot cavities, Preprint INP 80-172. Technical report (Institute of Nuclear Physics of the Siberian Division of the USSR Academy of Sciences, Novosibirsk, 1980).
- [120] N.M. Kroll, Ph.L. Morton and M.N. Rosenbluth, in *Free-Electron Generators of Coherent Radiation*, Eds. SF Jacobs, HS Pilloff, M. Sargent, MO Scully and R. Spitzer, Vol. 1 (1980), pp. 89–112, Physics of Quantum Electronics, (Addison-Wesley, Reading, MA).
- [121] W.B. Colson and R.A. Freedman, *Opt. Commun.* **46** (1983) 37–42, [296](https://doi.org/10.1016/0030-</p>
</div>
<div data-bbox=)

- 4018(83)90026-3.
- [122] W.B. Colson, *Nucl. Instrum. Methods Phys. Res. A.* **250** (1986) 168–175, [https://doi.org/10.1016/0168-9002\(86\)90878-8](https://doi.org/10.1016/0168-9002(86)90878-8).
- [123] J.E. Sollid, D.W. Feldman and R.W. Warren, *Nucl. Instrum. Methods Phys. Res. A.* **285** (1989) 153–157, [https://doi.org/10.1016/0168-9002\(89\)90443-9](https://doi.org/10.1016/0168-9002(89)90443-9).
- [124] Z. Huang and K.-J. Kim, *Phys. Rev. Special Topics-Accelerators and Beams.* **10** (2007) 034801.
- [125] A.T. Lin and J.M. Dawson, *Phys. Rev. Lett.* **42** (1979) 1670, <https://doi.org/10.1103/physrevlett.42.1670>.
- [126] P. Sprangle, C.-M. Tang and W.M. Manheimer, *Phys. Rev. Lett.* **43** (1979) 1932, <https://doi.org/10.1103/physrevlett.43.1932>.
- [127] N.A. Vinokurov, O.A. Shevchenko and V.G. Tcheskidov, *Phys. Rev. Special Topics-Accelerators and Beams.* **14** (2011) 040701.
- [128] P. Bosco and W.B. Colson, *Phys. Rev. A.* **28** (1983) 319, <https://doi.org/10.1103/physreva.28.319>.
- [129] A. Renieri, *Il Nuovo Cim. B (1971–1996).* **53** (1979) 160–178, <https://doi.org/10.1007/bf02739308>.
- [130] A. Renieri, *IEEE Trans. Nucl. Sci.* **26** (1979) 3827–3829, <https://doi.org/10.1109/tns.1979.4330622>.
- [131] G. Dattoli and A. Renieri, *Il Nuovo Cim. B Series 11.* **59** (1980) 1–39, <https://doi.org/10.1007/bf02739044>.
- [132] A. Renieri, Turbulence and bunch lengthening in electron-positron storage rings. *Frascati, Report. No. LNF-76* (1976), p. 11.
- [133] G. Dattoli and A. Renieri, *Lett. Nuovo Cim.* **24** (1979) 121–128, <https://doi.org/10.1007/bf02725605>.
- [134] G. Dattoli and A. Renieri, *Il Nuovo Cim. B.* **61** (1981) 153–180, <https://doi.org/10.1007/bf02721321>.
- [135] G. Dattoli, A. Marino and A. Renieri. *Opt. Commun.* **35** (1980) 407–412, [https://doi.org/10.1016/0030-4018\(80\)90062-0](https://doi.org/10.1016/0030-4018(80)90062-0).
- [136] W.B. Colson and J.L. Richardson, *Phys. Rev. Lett.* **50** (1983) 1050, <https://doi.org/10.1103/physrevlett.50.1050>.
- [137] P. Elleaume and D.A.G. Deacon, *Appl. Phys. B.* **33** (1984) 9–16, <https://doi.org/10.1007/bf00690020>.
- [138] L.R. Elias and J.C. Gallardo, *Phys. Rev. A.* **24** (1981) 3276, <https://doi.org/10.1103/physreva.24.3276>. [138] W.B. Colson and R.A. Freedman, *Phys. Rev. A.* **27** (1983) 1399, <https://doi.org/10.1103/physreva.27.1399>.
- [139] W.B. Colson and R.A. Freedman, *Phys. Rev. A.* **27** (1983) 1399, <https://doi.org/10.1103/physreva.27.1399>.
- [140] R. Bonifacio, *Opt. Commun.* **32** (1980) 440–442, [https://doi.org/10.1016/0030-4018\(80\)90279-5](https://doi.org/10.1016/0030-4018(80)90279-5).
- [141] G. Dattoli, A. Renieri, F. Romanelli and R. Bonifacio, *Opt. Commun.* **34** (1980) 240–244, [https://doi.org/10.1016/0030-4018\(80\)90024-3](https://doi.org/10.1016/0030-4018(80)90024-3).
- [142] R.J. Glauber, *Phys. Rev.* **130** (1963) 2529, <https://doi.org/10.1103/physrev.130.2529>.
- [143] R.J. Glauber, *Phys. Rev.* **131** (1963) 2766, <https://doi.org/10.1103/physrev.131.2766>.
- [144] G. Dattoli and A. Renieri, *Opt. Commun.* **39** (1981) 328–330, [https://doi.org/10.1016/0030-4018\(81\)90102-4](https://doi.org/10.1016/0030-4018(81)90102-4).
- [145] G. Dattoli and A. Renieri, *Nucl. Instrum. Methods Phys. Res.* **208** (1983) 193–197, [https://doi.org/10.1016/0167-5087\(83\)91124-9](https://doi.org/10.1016/0167-5087(83)91124-9).
- [146] I. Boscolo and V. Stagno, *Il Nuovo Cim. B.* **58** (1980) 267–285,

- <https://doi.org/10.1007/bf02874012>.
- [147] G. Penn, M. Reinsch and J.S. Wurtele, *Phys. Rev. Spec. Top. Accel. Beams*. **9** (2006) 060702, <https://doi.org/10.1103/physrevstab.9.060702>.
- [148] G. Dattoli, P.L. Ottaviani and S. Pagnutti, *J. Appl. Phys.* **101** (2007) 024914, <https://doi.org/10.1063/1.2424398>.
- [149] J.M. Ortéga, *Synchrotron Radiat. News*. **2** (1989) 18–23, <https://doi.org/10.1080/08940888908261211>.
- [150] G. Dattoli, *Lett. Nuovo Cim.* **27** (1980) 247–251, <https://doi.org/10.1007/bf02750352>.
- [151] A. Gover and P. Sprangle, *IEEE J. Quantum Electron.* **17** (1981) 1196–1215, <https://doi.org/10.1109/jqe.1981.1071257>.
- [152] M. Orszag and R. Ramirez, *J. Opt. Soc. Am. B*. **3** (1986) 895–900, <https://doi.org/10.1364/josab.3.000895>.
- [153] M. Orszag, *Phys. Rev. A*. **36** (1987) 189, <https://doi.org/10.1103/physreva.36.189>.
- [154] R. Bonifacio, N. Piovela and G.R.M. Robb, *Nucl. Instrum. Methods Phys. Res. A*. **543** (2005) 645–652, <https://doi.org/10.1016/j.nima.2005.01.324>.
- [155] R. Bonifacio, N. Piovela, G.R.M. Robb and A. Schiavi, *Phys. Rev. Spec. Top. Accel. Beams*. **9** (2006) 090701, <https://doi.org/10.1103/physrevstab.9.090701>.
- [156] N. Piovela, M.M. Cola, L. Volpe, A. Schiavi and R. Bonifacio, *Phys. Rev. Lett.* **100** (2008) 044801, <https://doi.org/10.1103/physrevlett.100.044801>.
- [157] R. Bonifacio and F. Casagrande, *Opt. Commun.* **50** (1984) 251–255, [https://doi.org/10.1016/0030-4018\(84\)90327-4](https://doi.org/10.1016/0030-4018(84)90327-4).
- [158] R. Bonifacio, N. Piovela, G.R.M. Robb and M.M. Cola, *Opt. Commun.* **252** (2005) 381–396, <https://doi.org/10.1016/j.optcom.2005.04.037>.
- [159] J. Rossbach, E.L. Saldin, E.A. Schneidmiller and M.V. Yurkov, *Nucl. Instrum. Methods Phys. Res. A*. **374** (1996) 401–407, [https://doi.org/10.1016/0168-9002\(96\)00189-1](https://doi.org/10.1016/0168-9002(96)00189-1).
- [160] M.S. McAshan, K. Mittag, H.A. Schwettman, L.R. Suelzle and J.P. Turneaure, *Appl. Phys. Lett.* **22** (1973) 605–607, <https://doi.org/10.1063/1.1654525>.
- [161] L.R. Elias, W.M. Fairbank, J.M.J. Madey, H.A. Schwettman and T.I. Smith, *Phys. Rev. Lett.* **36** (1976) 717, <https://doi.org/10.1103/physrevlett.36.717>.
- [162] D.A.G. Deacon, L.R. Elias, J.M.J. Madey, G.J. Ramian, H.A. Schwettman and T.I. Smith, *Phys. Rev. Lett.* **38** (1977) 892–894, <https://doi.org/10.1103/physrevlett.38.892>.
- [163] J.N. Eckstein, J.M.J. Madey, K. Robinson and T.I. Smith. Internal report HEPL-894. Technical Report, Stanford University (1981).
- [164] S. Benson, D.A.G. Deacon, J.N. Eckstein, J.M.J. Madey, K. Robinson, T.I. Smith and R. Taber, *Phys. Rev. Lett.* **48** (1982) 235, <https://doi.org/10.1103/physrevlett.48.235>.
- [165] D.A.G. Deacon and J.M.J. Madey, *Phys. Rev. Lett.* **44** (1980) 449, <https://doi.org/10.1103/physrevlett.44.449>.
- [166] T.I. Smith, J.M.J. Madey, L.R. Elias and D.A.G. Deacon, *J. Appl. Phys.* **50** (1979) 4580–4583, <https://doi.org/10.1063/1.326564>.
- [167] J.M.J. Madey, *J. Phys. Colloq.* **44(C1)** (1983) C1–169, <https://doi.org/10.1051/jphyscol:1983116>.
- [168] A.S. Artamonov, N.A. Vinokurov, P.D. Voblyi, E.S. Gluskin, G.A. Korniyukhin, V.A. Kochubei, G.N. Kulipanov, V.N. Litvinenko, N.A. Mezentsev and A.N. Skrinisky, *Nucl. Instrum. Methods*. **177** (1980) 247–252, [https://doi.org/10.1016/0029-554x\(80\)90557-1](https://doi.org/10.1016/0029-554x(80)90557-1).
- [169] R. Barbini, G. Vignola, S. Trillo, R. Boni, S. De Simone, S. Faini, S. Guiducci, M. Preger, M. Serio, B. Spataro, *et al.*, *J. Phys. Colloq.* **44(C1)** (1983) C1–1, <https://doi.org/10.1051/jphyscol:1983101>.

- [170] S. Krinsky, A. Luccio, C. Pellegrini, A. Van Steenbergen and L.H. Yu, *J. Phys. Colloq.* **44(C1)** (1983) C1–113, <https://doi.org/10.1051/jphyscol:1983107>.
- [171] L.R. Elias, *Phys. Rev. Lett.* **42** (1979) 977, <https://doi.org/10.1103/physrevlett.42.977>.
- [172] L.R. Elias and G. Ramian, *IEEE Trans. Nucl. Sci.* **32** (1985) 1732–1735.
- [173] L.R. Elias and G. Ramian. Design of the UCSB FEL electron beam system. Technical Report, DTIC Document (1981).
- [174] T.I. Smith and J.M.J. Madey, *Appl. Phys. B.* **27** (1982) 195–199, <https://doi.org/10.1007/bf00697441>.
- [175] M. Billardon, P. Elleaume, J.M. Ortéga, C. Bazin, M. Bergher, M. Velghe, Y. Petroff, D.A.G. Deacon, K.E. Robinson and J.M.J. Madey, *Phys. Rev. Lett.* **51** (1983) 1652–1655, <https://doi.org/10.1103/physrevlett.51.1652>.
- [176] M. Billardon, P. Elleaume, J.M. Ortéga, C. Bazin, M. Bergher, Y. Petroff, M. Velghe, D.A.G. Deacon and J.M.J. Madey. First operation of a storage ring free-electron laser. In *Free-electron generators of coherent radiation* (International Society for Optics and Photonics, 1984), pp. 269–274.
- [177] J.A. Edighoffer, G.R. Neil, C.E. Hess, T.I. Smith, S.W. Fornaca and H.A. Schwettman, *Phys. Rev. Lett.* **52** (1984) 344, <https://doi.org/10.1103/physrevlett.52.344>.
- [178] R.W. Warren, B.E. Newnam, W.E. Stein, J.G. Winston, R.L. Sheffield, M.T. Lynch, J.C. Goldstein, M.C. Whitehead, O.R. Norris and G. Luedemann. First operation of the Los Alamos free-electron laser oscillator. Technical Report, Los Alamos National Lab (1983).
- [179] D.B. McDermott, T.C. Marshall, S.P. Schlesinger, R.K. Parker and V.L. Granatstein, *Phys. Rev. Lett.* **41** (1978) 1368, <https://doi.org/10.1103/physrevlett.41.1368>.
- [180] M. Bazin, Y. Farge, M. Lemonnier, J. Perot and Y. Petroff, *Nucl. Instrum. Methods.* **172** (1980) 61–65, [https://doi.org/10.1016/0029-554x\(80\)90608-4](https://doi.org/10.1016/0029-554x(80)90608-4).
- [181] C. Bazin, M. Billardon, D. Deacon, Y. Farge, J.M. Ortéga, J. Pérot, Y. Petroff and M. Velghe, *J. Phys. Lett.* **41** (1980) 547–550, <https://doi.org/10.1051/jphyslet:019800041023054700>.
- [182] D.A.G. Deacon, K.E. Robinson, J.M.J. Madey, C. Bazin, M. Billardon, P. Elleaume, Y. Farge, J.M. Ortéga, Y. Petroff and M.F. Velghe, *Opt. Commun.* **40** (1982) 373–378, [https://doi.org/10.1016/0030-4018\(82\)90366-2](https://doi.org/10.1016/0030-4018(82)90366-2).
- [183] J.M. Ortéga, C. Bazin, D.A.G. Deacon, C. Depautex and P. Elleaume, *Nucl. Instrum. Methods Phys. Res.* **206** (1983) 281–288, [https://doi.org/10.1016/0167-5087\(83\)91269-3](https://doi.org/10.1016/0167-5087(83)91269-3).
- [184] J.M. Ortéga, M. Billardon, G. Jezequel, P. Thiry and Y. Petroff, *J. Phys.* **45** (1984) 1883–1888, <https://doi.org/10.1051/jphys:0198400450120188300>.
- [185] M. Billardon, D.A.G. Deacon, P. Elleaume, J.M. Ortéga, K.E. Robinson, C. Bazin, M. Bergher, J.M.J. Madey, Y. Petroff and M. Velghe, *J. Phys. Colloq.* **44(C1)** (1983) C1–29, <https://doi.org/10.1051/jphyscol:1983103>.
- [186] P. Elleaume, M. Velghe, M. Billardon and J.M. Ortéga, *Appl. Opt.* **24** (1985) 2762–2770, <https://doi.org/10.1364/ao.24.002762>.
- [187] D.A.G. Deacon, M. Billardon, P. Elleaume, J.M. Ortéga, K.E. Robinson, C. Bazin, M. Bergher, M. Velghe, J.M.J. Madey and Y. Petroff, *Appl. Phys. B.* **34** (1984) 207–219, <https://doi.org/10.1007/bf00697637>.
- [188] P. Elleaume, J.M. Ortéga, M. Billardon, C. Bazin, M. Bergher, M. Velghe, Y. Petroff, D.A.G. Deacon, K.E. Robinson and J.M.J. Madey, *J. Phys.* **45** (1984) 989–996, <https://doi.org/10.1051/jphys:01984004506098900>.
- [189] M. Billardon, J.M. Ortéga, P. Elleaume, C. Bazin, M. Bergher, M. Velghe, D. Deacon and Y. Petroff, *IEEE J. Quantum Electron.* **21** (1985) 805–823, <https://doi.org/10.1109/jqe.1985.1072733>.

- [190] P. Elleaume, *J. Phys.* **45** (1984) 997–1001, <https://doi.org/10.1051/jphys:01984004506099700>.
- [191] K.E. Robinson, J.M.J. Madey, M.F. Velghe and D.A.G. Deacon, *IEEE Trans. Nucl. Sci.* **30** (1983) 3088–3090, <https://doi.org/10.1109/tns.1983.4336578>.
- [192] M.E. Couprie and P. Elleaume, *Nucl. Instrum. Methods Phys. Res. A.* **259** (1987) 77–82, [https://doi.org/10.1016/0168-9002\(87\)90432-3](https://doi.org/10.1016/0168-9002(87)90432-3).
- [193] B. Girard, Y. Lapiere, J.M. Ortéga, C. Bazin, M. Billardon, P. Elleaume, M. Bergher, M. Velghe and Y. Petroff, *Phys. Rev. Lett.* **53** (1984) 2405–2408, <https://doi.org/10.1103/physrevlett.53.2405>.
- [194] R. Prazeres, J.M. Ortéga, C. Bazin, M. Bergher, M. Billardon, M.E. Couprie, H. Fang, M. Velghe and Y. Petroff, *Europhys. Lett.* **4** (1987) 817, <https://doi.org/10.1209/0295-5075/4/7/010>.
- [195] R. Prazeres, J.M. Ortéga, C. Bazin, M. Bergher, M. Billardon, M.E. Couprie, M. Velghe and Y. Petroff, *Nucl. Instrum. Methods Phys. Res. A.* **272** (1988) 68–72, [https://doi.org/10.1016/0168-9002\(88\)90197-0](https://doi.org/10.1016/0168-9002(88)90197-0).
- [196] K. Halbach, *Nucl. Instrum. Methods.* **169** (1980) 1–10, [https://doi.org/10.1016/0029-554x\(80\)90094-4](https://doi.org/10.1016/0029-554x(80)90094-4).
- [197] R. Warren, B. Newnam, J. Winston, W. Stein, L. Young and C. Brau, *IEEE J. Quantum Electron.* **19** (1983) 391–401, <https://doi.org/10.1109/jqe.1983.1071854>.
- [198] R.W. Warren, B.E. Newnam, W.E. Stein, J.G. Winston, R.L. Sheffield, M.T. Lynch, J.C. Goldstein, M.C. Whitehead, O.R. Norris, G. Luedemann, T.O. Gibson and C.M. Humphry. First operation of the Los Alamos free-electron laser oscillator. In *Sixth International Conference on Lasers and Applications, Lasers, San Francisco, 12–16 December 1983*, vol. 425 (Society for Optical and Quantum Electronics, 1983), p. 042016.
- [199] B.E. Newnam, R.W. Warren, K. Boyer, J.C. Goldstein, M.C. Whitehead and C.A. Brau. Optical gain results of the Los Alamos free-electron laser amplifier experiment. In *Free-electron generators of coherent radiation* (International Society for Optics and Photonics, 1984), pp. 118–129.
- [200] B.E. Newnam, R.W. Warren, R.L. Sheffield, J.C. Goldstein and C.A. Brau, *Nucl. Instrum. Methods Phys. Res. A.* **237** (1985) 187–198, [https://doi.org/10.1016/0168-9002\(85\)90347-x](https://doi.org/10.1016/0168-9002(85)90347-x).
- [201] K. Boyer, C.A. Brau, B.E. Newnam, W.E. Stein, R.W. Warren, J.G. Winston and L.M. Young, *J. Phys.* **C1** (1983) 109–111, <https://doi.org/10.2172/6346334>.
- [202] D.W. Feldman, H. Takeda, R.W. Warren, J.E. Sollid, W.E. Stein, W.J. Johnson, A.H. Lumpkin and R.B. Feldman, *Nucl. Instrum. Methods Phys. Res. A.* **285** (1989) 11–16, [https://doi.org/10.1016/0168-9002\(89\)90418-x](https://doi.org/10.1016/0168-9002(89)90418-x).
- [203] L.R. Elias and J.C. Gallardo, *Appl. Phys. B.* **31** (1983) 229–233, <https://doi.org/10.1007/bf00690793>.
- [204] L.R. Elias, J. Hu and G. Ramian, *Nucl. Instrum. Methods Phys. Res. A.* **237** (1985) 203–206, [https://doi.org/10.1016/0168-9002\(85\)90349-3](https://doi.org/10.1016/0168-9002(85)90349-3).
- [205] L.R. Elias, G. Ramian, J. Hu and A. Amir, *Phys. Rev. Lett.* **57** (1986) 424, <https://doi.org/10.1103/physrevlett.57.424>.
- [206] W.B. Colson, *Nucl. Instrum. Methods Phys. Res. A.* **358** (1995) 532–535, [https://doi.org/10.1016/0168-9002\(94\)01547-3](https://doi.org/10.1016/0168-9002(94)01547-3).
- [207] W.B. Colson, *Nucl. Instrum. Methods Phys. Res. A.* **393** (1997) 6–8, [https://doi.org/10.1016/s0168-9002\(97\)00418-x](https://doi.org/10.1016/s0168-9002(97)00418-x).
- [208] W.B. Colson, *Nucl. Instrum. Methods Phys. Res. A.* **475** (2001) 397–400, [https://doi.org/10.1016/s0168-9002\(01\)01687-4](https://doi.org/10.1016/s0168-9002(01)01687-4).
- [209] D.H.C.C. Levy *et al.*, *Free Electron Lasers and Other Advanced Sources of Light: Scientific Research Opportunities* (National Academy Press, Washington, 1994).
- [210] M.E. Couprie, *Ann. Phys.* **19(C1)** (1994) C1–127, <https://doi.org/10.1051/anphys/1994028>.
- [211] M.E. Couprie, *Nucl. Instrum. Methods Phys. Res. A.* **393** (1997) 13–17,

- [https://doi.org/10.1016/s0168-9002\(97\)00420-8](https://doi.org/10.1016/s0168-9002(97)00420-8).
- [212] I.B. Drobyazko, G.N. Kulipanov, V.N. Litvinenko, I.V. Pinayev, V.M. Popik, I.G. Silvestrov, A.N. Skrinsky, A.S. Sokolov and N.A. Vinokurov. Lasing in visible and ultraviolet regions in an optical klystron installed on the VEPP-3 storage ring. *Preprint INP* (1989) 89–118.
- [213] I.B. Drobyazko, G.N. Kulipanov, V.N. Litvinenko, I.V. Pinayev, V.M. Popik, I.G. Silvestrov, A.N. Skrinsky, A.S. Sokolov and N.A. Vinokurov. Lasing in visible and ultraviolet regions in optical klystron installed on the VEPP-3 storage ring. In *1989 Intl Congress on Optical Science and Engineering* (International Society for Optics and Photonics, 1989), pp. 2–10.
- [214] N.A. Vinokurov, I.B. Drobyazko, G.N. Kulipanov, V.N. Litvinenko and I.V. Pinayev, *Rev. Sci. Instrum.* **60** (1989) 1435–1438, <https://doi.org/10.1063/1.1141084>.
- [215] G.N. Kulipanov, V.N. Litvinenko, I.V. Pinaev, V.M. Popik, A.N. Skrinsky, A.S. Sokolov and N.A. Vinokurov, *Nucl. Instrum. Methods Phys. Res. A.* **296** (1990) 1–3, [https://doi.org/10.1016/0168-9002\(90\)91179-f](https://doi.org/10.1016/0168-9002(90)91179-f).
- [216] G.N. Kulipanov, V.N. Litvinenko, A.S. Sokolov and N.A. Vinokurov, On mutual coherency of spontaneous radiation from two undulators separated by achromatic bend. *Preprint INP* (1989) 89–84.
- [217] N.G. Gavrilov, G.N. Kulipanov, V.N. Litvinenko, I.V. Pinayev, V.M. Popik, I.G. Silvestrov, A.N. Skrinsky, A.S. Sokolov, N.A. Vinokurov and P.D. Vobly, *Nucl. Instrum. Methods Phys. Res. A.* **304** (1991) 63–65, [https://doi.org/10.1016/0168-9002\(91\)90821-7](https://doi.org/10.1016/0168-9002(91)90821-7).
- [218] N.G. Gavrilov, L.G. Isayeva, G.N. Kulipanov, V.N. Litvinenko, S.F. Mikhailov, V.M. Popik, I.G. Silvestrov, A.S. Sokolov, E.M. Trakhtenberg, N.A. Vinokurov, *et al.*, *Nucl. Instrum. Methods Phys. Res. A.* **282** (1989) 422–423, [https://doi.org/10.1016/0168-9002\(89\)90016-8](https://doi.org/10.1016/0168-9002(89)90016-8).
- [219] V.V. Anashin, M.M. Brovin, N.A. Vinokurov, P.D. Vobly, A.A. Didenko, I.B. Drobyazko, A.S. Kalinin, G.N. Kulipanov, V.N. Litvinenko, L.A. Mironenko, S.F. Mikhailov, S.I. Mishnev, V.M. Popik, Y.A. Pupkov, I.G. Silvestrov, A.N. Skrinsky, A.S. Sokolov and E.M. Trakhtenberg, VEPP-3 dedicated straight section for OK operation. *Preprint INP* (1989) 89–126.
- [220] G.N. Kulipanov, V.N. Litvinenko, A.S. Sokolov and N.A. Vinokurov, Metod izmerenie koeffitsentov otrajeniia blizkix k edinitse, method of measurement of coefficient of reflectivity close to unity. *Preprint INP* (1979) 79–24.
- [221] G.N. Kulipanov, I.V. Pinayev, V.M. Popik, T.V. Shaftan, A.S. Sokolov and N.A. Vinokurov, *Nucl. Instrum. Methods Phys. Res. A.* **331** (1993) 98–102, [https://doi.org/10.1016/0168-9002\(93\)90022-a](https://doi.org/10.1016/0168-9002(93)90022-a).
- [222] V.N. Litvinenko, M.E. Couprie, N.G. Gavrilov, G.N. Kulipanov, I.V. Pinaev, V.M. Popik, A.N. Skrinsky and N.A. Vinokurov, *IEEE J. Quantum Electron.* **27** (1991) 2560–2565, <https://doi.org/10.1109/3.104133>.
- [223] M.-E. Couprie, N.G. Gavrilov, G.N. Kulipanov, V.N. Litvinenko, I.V. Pinaev, V.M. Popik, A.N. Skrinsky and N.A. Vinokurov, *Nucl. Instrum. Methods Phys. Res. A.* **308** (1991) 39–44, [https://doi.org/10.1016/0168-9002\(91\)90583-c](https://doi.org/10.1016/0168-9002(91)90583-c).
- [224] V.M. Popik and N.A. Vinokurov, The simple model of the supermodes in FEL with an intracavity etalon. *Preprint INP* (1993) 93–72.
- [225] V.N. Litvinenko and N.A. Vinokurov, *Nucl. Instrum. Methods Phys. Res. A.* **304** (1991) 66–71, [https://doi.org/10.1016/0168-9002\(91\)90822-8](https://doi.org/10.1016/0168-9002(91)90822-8).
- [226] M.E. Couprie, C. Bazin, M. Billardon and M. Velghe, *Nucl. Instrum. Methods Phys. Res. A.* **285** (1989) 31–42, [https://doi.org/10.1016/0168-9002\(89\)90421-x](https://doi.org/10.1016/0168-9002(89)90421-x).
- [227] M.E. Couprie, M. Billardon, M. Velghe, C. Bazin, J.M. Ortéga, R. Prazeres and Y. Petroff, *Nucl. Instrum. Methods Phys. Res. A.* **296** (1990) 13–19, [https://doi.org/10.1016/0168-9002\(90\)91182-b](https://doi.org/10.1016/0168-9002(90)91182-b).

- [228] M.E. Couprie, M. Velghe, R. Prazeres, D. Jaroszynski and M. Billardon, *Phys. Rev. A* **44** (1991) 1301, <https://doi.org/10.1103/physreva.44.1301>.
- [229] M.E. Couprie, M. Billardon, M. Velghe, C. Bazin, M. Bergher, H. Fang, J.M. Ortéga, Y. Petroff and R. Prazeres, *Nucl. Instrum. Methods Phys. Res. A* **272** (1988) 166–173, [https://doi.org/10.1016/0168-9002\(88\)90217-3](https://doi.org/10.1016/0168-9002(88)90217-3).
- [230] M. Billardon, M.E. Couprie, J.M. Ortéga and M. Velghe, *Appl. Opt.* **30** (1991) 344–351, <https://doi.org/10.1364/ao.30.000344>.
- [231] M.E. Couprie, D. Garzella and M. Billardon, *Europhys. Lett.* **21** (1993) 909, <https://doi.org/10.1209/0295-5075/21/9/006>.
- [232] D. Nutarelli, D. Garzella, E. Renault, L. Nahon and M.E. Couprie, *Nucl. Instrum. Methods Phys. Res. A* **445** (2000) 143–148, [https://doi.org/10.1016/s0168-9002\(00\)00051-6](https://doi.org/10.1016/s0168-9002(00)00051-6).
- [233] M.E. Couprie, M. Velghe, R. Prazeres and M. Billardon, *Nucl. Instrum. Methods Phys. Res. A* **304** (1991) 53–57, [https://doi.org/10.1016/0168-9002\(91\)90819-c](https://doi.org/10.1016/0168-9002(91)90819-c).
- [234] M.E. Couprie, T. Hara, D. Gontier, P. Troussel, D. Garzella, A. Delboulbé and M. Billardon, *Phys. Rev. E* **53** (1996) 1871–1889, <https://doi.org/10.1103/physreve.53.1871>.
- [235] T. Hara, M.E. Couprie and M. Billardon, *Nucl. Instrum. Methods Phys. Res. A* **375** (1996) 67–70, [https://doi.org/10.1016/0168-9002\(95\)01425-x](https://doi.org/10.1016/0168-9002(95)01425-x).
- [236] M.E. Couprie, D. Garzella, T. Hara, J.H. Codar and M. Billardon, *Nucl. Instrum. Methods Phys. Res. A* **358** (1995) 374–377, [https://doi.org/10.1016/0168-9002\(94\)01576-7](https://doi.org/10.1016/0168-9002(94)01576-7).
- [237] M.E. Couprie, V. Litvinienko, D. Garzella, A. Delboulbé, M. Velghe and M. Billardon, *Nucl. Instrum. Methods Phys. Res. A* **331** (1993) 37–41, [https://doi.org/10.1016/0168-9002\(93\)90009-7](https://doi.org/10.1016/0168-9002(93)90009-7).
- [238] M. Billardon, D. Garzella and M.E. Couprie, *Phys. Rev. Lett.* **69** (1992) 2368, <https://doi.org/10.1103/physrevlett.69.2368>.
- [239] M.E. Couprie, M. Velghe, D. Jaroszynski and M. Billardon, *Nucl. Instrum. Methods Phys. Res. A* **304** (1991) 58–62, [https://doi.org/10.1016/0168-9002\(91\)90820-g](https://doi.org/10.1016/0168-9002(91)90820-g).
- [240] G. De Ninno, M.E. Couprie, D. Nutarelli, D. Garzella, E. Renault and M. Billardon, *Phys. Rev. E* **64** (2001) 026502, <https://doi.org/10.1103/physreve.64.026502>.
- [241] R. Bartolini, G. Dattoli, L. Mezi, A. Renieri, M. Migliorati, M.E. Couprie, G. De Ninno and R. Roux, *Phys. Rev. Lett.* **87** (2001) 134801, <https://doi.org/10.1103/physrevlett.87.134801>.
- [242] S. Bielawski, C. Bruni, G.L. Orlandi, D. Garzella and M.E. Couprie, *Phys. Rev. E* **69** (2004) 045502, <https://doi.org/10.1103/physreve.69.045502>.
- [243] S. Bielawski, C. Szwaj, C. Bruni, D. Garzella, G.L. Orlandi and M.E. Couprie, *Phys. Rev. Lett.* **95** (2005) 034801, <https://doi.org/10.1103/physrevlett.95.034801>.
- [244] K. Yamada, T. Yamazaki, S. Sugiyama, T. Tomimasu, H. Ohgaki, T. Noguchi, T. Mikado, M. Chiwaki and R. Suzuki, *Nucl. Instrum. Methods Phys. Res. A* **318** (1992) IN1–37, [https://doi.org/10.1016/0168-9002\(92\)91019-6](https://doi.org/10.1016/0168-9002(92)91019-6).
- [245] T. Yamazaki, K. Yamada, S. Sugiyama, H. Ohgaki, N. Sei, T. Mikado, T. Noguchi, M. Chiwaki, R. Suzuki, M. Kawai, *et al.*, *Nucl. Instrum. Methods Phys. Res. A* **331** (1993) 27–33, [https://doi.org/10.1016/0168-9002\(93\)90008-6](https://doi.org/10.1016/0168-9002(93)90008-6).
- [246] H. Hama, J. Yamazaki and G. Isoyama, *Nucl. Instrum. Methods Phys. Res. A* **341** (1994) 12–16, [https://doi.org/10.1016/0168-9002\(94\)90307-7](https://doi.org/10.1016/0168-9002(94)90307-7).
- [247] H. Hama, *Nucl. Instrum. Methods Phys. Res. A* **375** (1996) 57–61, [https://doi.org/10.1016/0168-9002\(95\)01428-4](https://doi.org/10.1016/0168-9002(95)01428-4).
- [248] H. Hama, K. Kimura, J. Yamazaki, S. Takano, T. Kinoshita and M.-E. Couprie, *Nucl. Instrum. Methods Phys. Res. A* **375** (1996) 32–38, [https://doi.org/10.1016/0168-9002\(96\)00103-9](https://doi.org/10.1016/0168-9002(96)00103-9).
- [249] H. Hama, J. Yamazaki, T. Kinoshita, K. Kimura and G. Isoyama, *Nucl. Instrum. Methods Phys.*

- Res. A.* **358** (1995) 365–368, [https://doi.org/10.1016/0168-9002\(94\)01513-9](https://doi.org/10.1016/0168-9002(94)01513-9).
- [250] S. Koda, M. Hosaka, J. Yamazaki, M. Katoh and H. Hama, *Nucl. Instrum. Methods Phys. Res. A.* **475** (2001) 211–216, [https://doi.org/10.1016/s0168-9002\(01\)01574-1](https://doi.org/10.1016/s0168-9002(01)01574-1).
- [251] V.N. Litvinenko, B. Burnham, S.H. Park, Y. Wu, R. Cataldo, M. Emamian, J. Faircloth, S. Goetz, N. Hower, J.M.J. Madey, *et al.*, *Nucl. Instrum. Methods Phys. Res. A.* **407** (1998) 8–15, <https://doi.org/10.1016/b978-0-444-82978-8.50008-7>.
- [252] V.N. Litvinenko, S.H. Park, I.V. Pinayev, Y. Wu, M. Emamian, N. Hower, P. Morcombe, O. Oakeley, G. Swift and P. Wang, *Nucl. Instrum. Methods Phys. Res. A.* **429** (1999) 151–158, [https://doi.org/10.1016/s0168-9002\(99\)00096-0](https://doi.org/10.1016/s0168-9002(99)00096-0).
- [253] V.N. Litvinenko, S.H. Park, I.V. Pinayev and Y. Wu, *Nucl. Instrum. Methods Phys. Res. A.* **475** (2001) 195–204, [https://doi.org/10.1016/s0168-9002\(01\)01559-5](https://doi.org/10.1016/s0168-9002(01)01559-5).
- [254] V.N. Litvinenko, B. Burnham, J.M.J. Madey and Y. Wu, *Nucl. Instrum. Methods Phys. Res. A.* **358** (1995) 369–373, [https://doi.org/10.1016/0168-9002\(94\)01575-9](https://doi.org/10.1016/0168-9002(94)01575-9).
- [255] V.N. Litvinenko, B. Burnham, J.M.J. Madey and Y. Wu, *Nucl. Instrum. Methods Phys. Res. A.* **358** (1995) 334–337, [https://doi.org/10.1016/0168-9002\(94\)01290-3](https://doi.org/10.1016/0168-9002(94)01290-3).
- [256] G. De Ninno, E. Allaria, M. Coreno, S. Chowdhury, F. Curbis, M.B. Danailov, B. Divi-acco, M. Ferianis, E. Karantzoulis, E.C. Longhi, *et al.*, *Phys. Rev. Lett.* **100** (2008) 104801, <https://doi.org/10.1103/physrevlett.100.104801>.
- [257] V.N. Litvinenko, S.H. Park, I.V. Pinayev and Y. Wu, *Nucl. Instrum. Methods Phys. Res. A.* **475** (2001) 240–246, [https://doi.org/10.1016/s0168-9002\(01\)01569-8](https://doi.org/10.1016/s0168-9002(01)01569-8).
- [258] V.N. Litvinenko, S.H. Park, I.V. Pinayev and Y. Wu, *Nucl. Instrum. Methods Phys. Res. A.* **475** (2001) 65–73, [https://doi.org/10.1016/s0168-9002\(01\)01536-4](https://doi.org/10.1016/s0168-9002(01)01536-4).
- [259] V.N. Litvinenko, S.H. Park, I.V. Pinayev, Y. Wu, A. Lumpkin and B. Yang, *Nucl. Instrum. Methods Phys. Res. A.* **475** (2001) 234–239, [https://doi.org/10.1016/s0168-9002\(01\)01570-4](https://doi.org/10.1016/s0168-9002(01)01570-4).
- [260] The DELTA Group Berges, D. Nölle, D. Garzella, A. Geisler, L. Giannessi, M. Hirsch, H. Quick, M. Ridder, T. Schmidt and K. Wille, *Nucl. Instrum. Methods Phys. Res. A.* **445** (2000) 128–133, [https://doi.org/10.1016/s0168-9002\(00\)00044-9](https://doi.org/10.1016/s0168-9002(00)00044-9).
- [261] R.P. Walker, B. Diviacco, C. Fava, A. Gambitta, M. Marsi, F. Mazzolini, M.E. Couprie, L. Nahon, D. Nutarelli, E. Renault, *et al.*, *Nucl. Instrum. Methods Phys. Res. A.* **429** (1999) 179–184, [https://doi.org/10.1016/s0168-9002\(99\)00100-x](https://doi.org/10.1016/s0168-9002(99)00100-x).
- [262] R.P. Walker, J.A. Clarke, M.E. Couprie, G. Dattoli, M. Eriksson, D. Garzella, L. Giannessi, M. Marsi, L. Nahon, D. Nölle, *et al.*, *Nucl. Instrum. Methods Phys. Res. A.* **475** (2001) 20–27, [https://doi.org/10.1016/s0168-9002\(01\)01529-7](https://doi.org/10.1016/s0168-9002(01)01529-7).
- [263] M. Marsi, M. Trovo, R.P. Walker, L. Giannessi, G. Dattoli, A. Gatto, N. Kaiser, S. Günster, D. Ristau, M.E. Couprie, D. Garzella, J.A. Clarke and M.W. Poole, *190 nm Appl. Phys. Lett.* **80** (2002) 2851–2853, <https://doi.org/10.1063/1.1471934>.
- [264] M. Trovo, J.A. Clarke, M.E. Couprie, G. Dattoli, D. Garzella, A. Gatto, L. Giannessi, S. Günster, N. Kaiser, M. Marsi, *et al.*, *Nucl. Instrum. Methods Phys. Res. A.* **483** (2002) 157–161.
- [265] D. Garzella, M.E. Couprie, T. Hara, L. Nahon, M. Brazuna, A. Delboulbé and M. Billardon, *Nucl. Instrum. Methods Phys. Res. A.* **358** (1995) 387–391, [https://doi.org/10.1016/0168-9002\(94\)01594-5](https://doi.org/10.1016/0168-9002(94)01594-5).
- [266] A. Gatto, J. Heber, N. Kaiser, D. Ristau, S. Günster, J. Kohlhaas, M. Marsi, M. Trovo and R.P. Walker, *Nucl. Instrum. Methods Phys. Res. A.* **483** (2002) 357–362, [https://doi.org/10.1016/s0168-9002\(02\)00343-1](https://doi.org/10.1016/s0168-9002(02)00343-1).
- [267] A. Gatto, T. Feigl, N. Kaiser, D. Garzella, G. De Ninno, M.E. Couprie, M. Marsi, M. Trovo, R. Walker, M. Grewe, *et al.*, *Nucl. Instrum. Methods Phys. Res. A.* **483** (2002) 172–176, [https://doi.org/10.1016/s0168-9002\(02\)00306-6](https://doi.org/10.1016/s0168-9002(02)00306-6).

- [268] A. Gatto, R. Thielsch, N. Kaiser, M. Hirsch, D. Garzella, D. Nutarelli, G. De Ninno, E. Renault, M.-E. Couprie, P. Torchio, *et al.*, Toward resistant UV mirrors at 200 nm for free electron lasers: manufacture, characterizations, and degradation tests. In *International Symposium on Optical Science and Technology* (International Society for Optics and Photonics, 2000), pp. 261–275.
- [269] G. De Ninno, M. Trovó, M. Danailov, M. Marsi, E. Karantzoulis, B. Diviacco, R.P. Walker, R. Bartolini, G. Dattoli, L. Giannessi, *et al.*, *Nucl. Instrum. Methods Phys. Res. A* **507** (2003) 274–280, [https://doi.org/10.1016/s0168-9002\(03\)00928-8](https://doi.org/10.1016/s0168-9002(03)00928-8).
- [270] M.E. Couprie, D. Nutarelli and M. Billardon, *Nucl. Instrum. Methods Phys. Res. B*, **144** (1998) 66–74, [https://doi.org/10.1016/s0168-583x\(98\)00297-3](https://doi.org/10.1016/s0168-583x(98)00297-3).
- [271] S.V. Benson and J.M.J. Madey, *Phys. Rev. A* **39** (1989) 1579, <https://doi.org/10.1103/physreva.39.1579>.
- [272] D.J. Bamford and D.A.G. Deacon, *Phys. Rev. Lett.* **62** (1989) 1106, <https://doi.org/10.1103/physrevlett.62.1106>.
- [273] E.B. Szarmes, S.V. Benson and J.M.J. Madey, *Nucl. Instrum. Methods Phys. Res. A* **296** (1990) 755–761, [https://doi.org/10.1016/0168-9002\(90\)91302-r](https://doi.org/10.1016/0168-9002(90)91302-r).
- [274] E.B. Szarmes, A.D. Madden and J.M.J. Madey, *Nucl. Instrum. Methods Phys. Res. A* **358** (1995) 220–223, [https://doi.org/10.1016/0168-9002\(94\)01514-7](https://doi.org/10.1016/0168-9002(94)01514-7).
- [275] A. Bhowmik, M.S. Curtin, W.A. McMullin, S.V. Benson, J.M.J. Madey, B.A. Richman and L. Vintro, *Nucl. Instrum. Methods Phys. Res. A* **296** (1990) 20–24, [https://doi.org/10.1016/0168-9002\(90\)91183-c](https://doi.org/10.1016/0168-9002(90)91183-c).
- [276] C.A. Brau, *Nucl. Instrum. Methods Phys. Res. A* **318** (1992) 38–41, [https://doi.org/10.1016/0168-9002\(92\)91020-a](https://doi.org/10.1016/0168-9002(92)91020-a).
- [277] C.A. Brau and M.H. Mendenhall, *Nucl. Instrum. Methods Phys. Res. A* **331** (1993) ABS4–ABS6, [https://doi.org/10.1016/0168-9002\(93\)90165-e](https://doi.org/10.1016/0168-9002(93)90165-e).
- [278] P.W. Van Amersfoort, R.J. Bakker, J.B. Bekkers, R.W.B. Best, R. Van Buuren, P.F.M. Delmee, B. Faatz, C.A.J. Van der Geer, D.A. Jaroszynski, P. Manintveld, *et al.* *Nucl. Instrum. Methods Phys. Res. A* **318** (1992) 42–46.
- [279] D. Oepts, R.J. Bakker, D.A. Jaroszynski, A.F.G. van der Meer and P.W. van Amersfoort. *Phys. Rev. Lett.* **68** (1992) 3543, <https://doi.org/10.1103/physrevlett.68.3543>.
- [280] D.A. Jaroszynski, R.J. Bakker, A.F.G. Van der Meer, D. Oepts and P.W. van Amersfoort. Experimental observation of limit-cycle oscillations in a short-pulse free-electron laser. *Phys. Rev. Lett.* **70** (1993) 3412, <https://doi.org/10.1103/physrevlett.70.3412>.
- [281] D. Oepts, A.F.G. Van der Meer, R.J. Bakker and P.W. Van Amersfoort. *Phys. Rev. Lett.* **70** (1993) 3255, <https://doi.org/10.1103/physrevlett.70.3255>.
- [282] M.E. Couprie, P. Bourgeois, P.J. Carlos, J.L. Fallou, P. Garganne, A. Leprêtre, J. Martin and J.M. Ortéga. *Nucl. Instrum. Methods Phys. Res. A* **304** (1991) 710–713, [https://doi.org/10.1016/0168-9002\(91\)90962-p](https://doi.org/10.1016/0168-9002(91)90962-p).
- [283] R. Prazeres, J.M. Berset, F. Glotin, D. Jaroszynski and J.M. Ortéga. *Nucl. Instrum. Methods Phys. Res. A* **331** (1993) 15–19, [https://doi.org/10.1016/0168-9002\(93\)90006-4](https://doi.org/10.1016/0168-9002(93)90006-4).
- [284] R. Prazeres, F. Glotin and J.M. Ortéga. *Nucl. Instrum. Methods Phys. Res. A* **528** (2004) 83–87, <https://doi.org/10.1016/b978-0-444-51727-2.50025-0>.
- [285] R. Prazeres, F. Glotin, C. Insa, D.A. Jaroszynski and J.M. Ortéga. *The European Physical Journal D-Atomic, Molecular, Optical and Plasma Physics*. **3** (1998) 87–93, <https://doi.org/10.1007/s100530050151>.
- [286] D.A. Jaroszynski, R. Prazeres, F. Glotin, J.M. Ortéga, D. Oepts, A.F.G. van der Meer, G.M.H. Knippels and P.W. van Amersfoort. *Phys. Rev. Lett.* **74** (1995) 2224, <https://doi.org/10.1103/physrevlett.74.2224>.

- [287] F. Glotin, R. Chaput, D. Jaroszynski, R. Prazeres and J.-M. Ortéga. *Phys. Rev. Lett.* **71** (1993) 2587, <https://doi.org/10.1103/physrevlett.71.2587>.
- [288] S. Joly, P. Balleyguier, M.A. Beuve, A. Binet, J.P. Bleses, R. Bois, C. Bonetti, J.P. de Brion, C. Couillaud, R. Dei-Cas, *et al.* *Nucl. Instrum. Methods Phys. Res. A.* **331** (1993) 199–203, [https://doi.org/10.1016/0168-9002\(93\)90042-g](https://doi.org/10.1016/0168-9002(93)90042-g).
- [289] D. Iracane, V. Fontenay, P. Guimbal, S. Joly, S. Striby and D. Touati. *Phys. Rev. Lett.* **72** (1994) 3985, <https://doi.org/10.1103/physrevlett.72.3985>.
- [290] P. Michel, F. Gabriel, E. Grosse, P. Evtuschenko, T. Dekorsy, M. Krenz, M. Helm, U. Lehnert, W. Seidel, R. Wunsch, *et al.* First lasing of the ELBE mid-IR FEL. In *Proceedings of the 2004 FEL Conference* (2004), Jacow, pp. 8–13.
- [291] T. Tomimasu, E. Oshita, S. Okuma, K. Wakita, T. Takii, A. Koga, S. Nishihara, A. Nagai, H. Tongu, K. Wakisaka, *et al.* *μ Nucl. Instrum. Methods Phys. Res. A.* **383** (1996) 337–341, [https://doi.org/10.1016/s0168-9002\(96\)00827-3](https://doi.org/10.1016/s0168-9002(96)00827-3).
- [292] T. Tomimasu, K. Saeki, Y. Miyauchi, E. Oshita, S. Okuma, K. Wakita, A. Kobayashi, T. Suzuki, A. Zako, S. Nishihara, *et al.* *Nucl. Instrum. Methods Phys. Res. A.* **375** (1996) 626–631, [https://doi.org/10.1016/0168-9002\(96\)00097-6](https://doi.org/10.1016/0168-9002(96)00097-6).
- [293] A. Zako, Y. Kanazawa, Y. Konishi, S. Yamaguchi, A. Nagai and T. Tomimasu. *Nucl. Instrum. Methods Phys. Res. A.* **429** (1999) 136–140, [https://doi.org/10.1016/s0168-9002\(99\)00093-5](https://doi.org/10.1016/s0168-9002(99)00093-5).
- [294] T.J. Orzechowski, B. Anderson, W.M. Fawley, D. Prosnitz, E.T. Scharlemann, S. Yarema, D. Hopkins, A.C. Paul, A.M. Sessler and J. Wurtele. *Phys. Rev. Lett.* **54** (1985) 889, <https://doi.org/10.1103/physrevlett.54.889>.
- [295] H. Bottollier-Curtet, J. Gardelle, J. Bardy, C. Bonnafond, A. Devin, G. Germain, J. Labrousche, J. Launsbach, P. Le Taillandier and J. de Mascureau. *Nucl. Instrum. Methods Phys. Res. A.* **304** (1991) 197–199, [https://doi.org/10.1016/0168-9002\(91\)90848-k](https://doi.org/10.1016/0168-9002(91)90848-k).
- [296] F. Ciocci, G. Dattoli, A. Doria, G.P. Gallerano, G. Schettini and A. Torre. *Phys. Rev. A.* **36** (1987) 207, <https://doi.org/10.1103/physreva.36.207>.
- [297] F. Ciocci, A. Doria, G.P. Gallerano, I. Giabbai, M.F. Kimmitt, G. Messina, A. Renieri and J.E. Walsh. *Phys. Rev. Lett.* **66** (1991) 699, <https://doi.org/10.1103/physrevlett.66.699>.
- [298] V.I. Alexeev, A.V. Alieva, K.A. Belovintsev, E.G. Bessonov, A.V. Serov and P.A. Cherenkov. Observations on emission generation in the free electron laser based on the microtron, Preprint FIAN 87-339. Technical Report, P. N. Institute Lebedev Physical Institute of the Academy of Science of USSR, Moscow (1987).
- [299] V.I. Alexeev, E.V. Alieva, K.A. Belovintsev, E.G. Bessonov, A.V. Serov and P.A. Cherenkov. *Nucl. Instrum. Methods Phys. Res. A.* **282** (1989) 436–438, [https://doi.org/10.1016/0168-9002\(89\)90019-3](https://doi.org/10.1016/0168-9002(89)90019-3).
- [300] Y.U. Jeong, B.C. Lee, S.K. Kim, S.O. Cho, B.H. Cha, J. Lee, G. M. Kazakevitch, P. D. Vobly, N.G. Gavrilov, V.V. Kubarev, *et al.* *Nucl. Instrum. Methods Phys. Res. A.* **475** (2001) 47–50, [https://doi.org/10.1016/s0168-9002\(01\)01533-9](https://doi.org/10.1016/s0168-9002(01)01533-9).
- [301] M. Tigner. *Il Nuovo Cim.* **37** (1965) 1228–1231, <https://doi.org/10.1007/bf02773204>.
- [302] G. R. Neil and L. Merminga. *Reviews of Modern Physics.* **74** (2002) 685, <https://doi.org/10.1103/revmodphys.74.685>.
- [303] G.R. Neil, S. Benson, G. Biallas, C.L. Bohn, D. Douglas, H.F. Dylla, R. Evans, J. Fugitt, J. Gubeli, R. Hill, *et al.* *Nucl. Instrum. Methods Phys. Res. A.* **445** (2000) 192–196, [https://doi.org/10.1016/s0168-9002\(00\)00064-4](https://doi.org/10.1016/s0168-9002(00)00064-4).
- [304] R.W. Thomson, L.R. Short, R.D. McGinnis, W.B. Colson, M.D. Shinn, J.F. Gubeli, K.C. Jordan, R.A. Hill, G.H. Biallas, R.L. Walker, *et al.* *Nucl. Instrum. Methods Phys. Res. A.* **475** (2001) 625–629, [https://doi.org/10.1016/s0168-9002\(01\)01580-7](https://doi.org/10.1016/s0168-9002(01)01580-7).

- [305] G.R. Neil, C.L. Bohn, S.V. Benson, G. Biallas, D. Douglas, H.F. Dylla, R. Evans, J. Fugitt, A. Grippo, J. Gubeli, *et al. Phys. Rev. Lett.* **84** (2000) 662, <https://doi.org/10.1103/physrevlett.84.662>.
- [306] A. Christodoulou, D. Lampiris, K. Polykandriotis, W.B. Colson, P.P. Crooker, S. Benson, J. Gubeli and G.R. Neil. *Phys. Rev. E.* **66** (2002) 056502, <https://doi.org/10.1103/physreve.66.056502>.
- [307] C. Behre, S. Benson, G. Biallas, J. Boyce, C. Curtis, D. Douglas, H.F. Dylla, L. Dillon-Townes, R. Evans, A. Grippo, *et al. Nucl. Instrum. Methods Phys. Res. A.* **528** (2004) 19–22, <https://doi.org/10.1016/b978-0-444-51727-2.50012-2>.
- [308] G.R. Neil, C. Behre, S.V. Benson, M. Bevins, G. Biallas, J. Boyce, J. Coleman, L.A. Dillon-Townes, D. Douglas, H.F. Dylla, *et al. Nucl. Instrum. Methods Phys. Res. A.* **557** (2006) 9–15, <https://doi.org/10.1016/j.nima.2005.10.047>.
- [309] E.J. Minehara, M. Sugimoto, M. Sawamura, R. Nagai, N. Kikuzawa, T. Yamanouchi and N. Nishimori. *Nucl. Instrum. Methods Phys. Res. A.* **429** (1999) 9–11, [https://doi.org/10.1016/s0168-9002\(99\)00050-9](https://doi.org/10.1016/s0168-9002(99)00050-9).
- [310] R. Hajima, T. Shizuma, M. Sawamura, R. Nagai, N. Nishimori, N. Kikuzawa and E.J. Minehara. *Nucl. Instrum. Methods Phys. Res. A.* **507** (2003) 115–119, [https://doi.org/10.1016/s0168-9002\(03\)00849-0](https://doi.org/10.1016/s0168-9002(03)00849-0).
- [311] R. Hajima, N. Nishimori, R. Nagai and E.J. Minehara. *Nucl. Instrum. Methods Phys. Res. A.* **475** (2001) 270–275, [https://doi.org/10.1016/s0168-9002\(01\)01621-7](https://doi.org/10.1016/s0168-9002(01)01621-7).
- [312] N. Nishimori, R. Hajima, R. Nagai and E.J. Minehara. *Phys. Rev. Lett.* **86** (2001) 5707, <https://doi.org/10.1103/physrevlett.86.5707>.
- [313] N. Nishimori, R. Hajima, R. Nagai and E.J. Minehara. *Nucl. Instrum. Methods Phys. Res. A.* **475** (2001) 266–269, [https://doi.org/10.1016/s0168-9002\(01\)01638-2](https://doi.org/10.1016/s0168-9002(01)01638-2).
- [314] N.G. Gavrilov, E.U. Gorniker, G.N. Kulipanov, I.V. Kupsov, I.V. Pinaev, I.K. Sedlyarov, A.N. Skrinsky, A.S. Sokolov, V.G. Veshcherevich, N.A. Vinokurov and P.D. Vobly. Project of a race-track microtron-recuperator for free electron laser, preprint INP 90-82. *Preprint INP* (1990) pp. 90–82.
- [315] E.A. Antokhin, R.R. Akberdin, V.S. Arbutov, M.A. Bokov, V.P. Bolotin, D.B. Burenkov, A.A. Bushuev, V.F. Veremeenko, N.A. Vinokurov, P.D. Vobly, *et al. Nucl. Instrum. Methods Phys. Res. A.* **528** (2004) 15–18.
- [316] B.C. Lee, S.K. Kim, Y.U. Jeong, S.O. Cho, B.H. Cha and J. Lee. *Nucl. Instrum. Methods Phys. Res. A.* **375** (1996) 28–31, [https://doi.org/10.1016/0168-9002\(95\)01502-7](https://doi.org/10.1016/0168-9002(95)01502-7).
- [317] B.C. Lee, Y.U. Jeong, S.H. Park, Y.G. Lim and S. Miginsky. *Nucl. Instrum. Methods Phys. Res. A.* **528** (2004) 106–109, <https://doi.org/10.1016/j.nima.2004.04.028>.
- [318] K.-J. Kim, Y. Shvyd'ko and S. Reiche. *Phys. Rev. Lett.* **100** (2008) 244802, <https://doi.org/10.1103/physrevlett.100.244802>.
- [319] K.-J. Kim and Y.V. Shvyd'ko. *Phys. Rev. Special Topics-Accelerators and Beams.* **12** (2009) 030703, <https://doi.org/10.1103/physrevstab.12.030703>.
- [320] R.R. Lindberg, K.-J Kim, Y. Shvyd'ko and W.M. Fawley. *Phys. Rev. Special Topics-Accelerators and Beams.* **14** (2011) 010701, <https://doi.org/10.1103/physrevstab.14.010701>.
- [321] R. Prazeres, P. Guyot-Sionnest, J.M. Ortéga, D. Jaroszynski, M. Billardon, M.E. Couprie, M. Velghe and Y. Petroff. *Nucl. Instrum. Methods Phys. Res. A.* **304** (1991) 72–76.
- [322] R. Prazeres, P. Guyot-Sionnest, J.M. Ortéga, D. Jaroszynski, M. Billardon, M.E. Couprie, M. Velghe and Y. Petroff. *IEEE journal of Quantum Electronics.* **27** (1991) 1061–1068, <https://doi.org/10.1109/3.83341>.
- [323] V.N. Litvinenko. *Nucl. Instrum. Methods Phys. Res. A.* **507** (2003) 265–273, [https://doi.org/10.1016/s0168-9002\(03\)00927-6](https://doi.org/10.1016/s0168-9002(03)00927-6).
- [324] G. D. Ninno, E. Allaria, M. Coreno, F. Curbis, M.B. Danailov, E. Karantzoulis, A. Lo-

- catelli, T.O. Montes, M.A. Nino, C. Spezzani, *et al.* *Phys. Rev. Lett.* **101** (2008) 053902, <https://doi.org/10.1103/physrevlett.101.053902>.
- [325] M. Labat, M. Hosaka, A. Mochihashi, M. Shimada, M. Katoh, G. Lambert, T. Hara, Y. Takashima and M.E. Couprie. *Eur. Phys. J. D.* **44** (2007) 187, <https://doi.org/10.1140/epjd/e2007-00177-6>.
- [326] M. Labat, M. Hosaka, M. Shimada, N. Yamamoto, M. Katoh and M.E. Couprie. *Phys. Rev. Lett.* **102** (2009) 014801, <https://doi.org/10.1103/physrevlett.102.014801>.
- [327] M Labat, M Hosaka, M Shimada, M Katoh, and ME Couprie. Optimization of a seeded free-electron laser with helical undulators. *Phys. Rev. Lett.* **101** (2008) 164803.
- [328] S. Thorin, M. Brandin, S. Werin, K. Goldammer and J. Bahrtdt. *Phys. Rev. Special Topics-Accelerators and Beams.* **10** (2007) 110701, <https://doi.org/10.1103/physrevstab.10.110701>.
- [329] N. Čutić, F. Lindau, S. Thorin, S. Werin, J. Bahrtdt, W. Eberhardt, K. Holldack, C. Erny, A.L'Huillier and E. Mansten. *Phys. Rev. Special Topics-Accelerators and Beams.* **14** (2011) 030706, <https://doi.org/10.1103/physrevstab.14.030706>.
- [330] R.W. Warren, L.C. Haynes, D.W. Feldman, W.E. Stein and S.J. Gitomer. *Nucl. Instrum. Methods Phys. Res. A.* **296** (1990) 84–88.
- [331] S. Benson and M. Shinn. In *Proceedings of FEL 2006, BESSY, Berlin, Germany*, Jacow, (2006) pp. 323–326.
- [332] A.-M. Fauchet, J. Feinstein, A. Gover and R. Pantell. *IEEE Journal of Quantum Electronics.* **20** (1984) 1332–1341, <https://doi.org/10.1109/jqe.1984.1072332>.
- [333] R.H. Pantell, J. Feinstein, A.S. Fisher, T.L. Deloney, M.B. Reid and W.M. Grossman. *Nucl. Instrum. Methods Phys. Res. A.* **250** (1986) 312–315, [https://doi.org/10.1016/0168-9002\(86\)90901-0](https://doi.org/10.1016/0168-9002(86)90901-0).
- [334] R.H. Pantell and M. Özcan. *Phys. Fluids B.* **2** (1990) 1311–1312, <https://doi.org/10.1063/1.859547>.
- [335] J.A. Edighoffer, W.D. Kimura, R.H. Pantell, M.A. Piestrup and D.Y. Wang. *Phys. Rev. A.* **23** (1981) 1848, <https://doi.org/10.1103/physreva.23.1848>.
- [336] J. Feinstein, A.S. Fisher, M.B. Reid, A. Ho, M. Özcan, H.D. Dulman and R.H. Pantell. *Phys. Rev. Lett.* **60** (1988) 18, <https://doi.org/10.1103/physrevlett.60.18>.
- [337] R.H. Pantell, A.S. Fisher, J. Feinstein, A.H. Ho, M. Özcan, H.D. Dulman and M.B. Reid. *JOSA B.* **6** (1989) 1008–1014, <https://doi.org/10.1364/josab.6.001008>.
- [338] M.B. Reid, A.S. Fisher, J. Feinstein, A.H. Ho, M. Özcan, H.D. Dulman, Y.J. Lee and R.H. Pantell. *Phys. Rev. Lett.* **62** (1989) 249, <https://doi.org/10.1103/physrevlett.62.249>.
- [339] S.J. Smith and E.M. Purcell. *Phys. Rev.* **92** (1953) 1069, <https://doi.org/10.1103/physrev.92.1069>.
- [340] M. Piestrup. *IEEE Journal of Quantum Electronics.* **24** (1988) 591–597, <https://doi.org/10.1109/3.167>.
- [341] G. Dattoli, A. Doria, G.P. Gallerano, A. Renieri, G. Schettini and A. Torre. *Il Nuovo Cim B.* **101** (1988) 79–84, <https://doi.org/10.1007/bf02828071>.
- [342] J.E. Walsh. Free electron laser utilizing grating coupling, November 16 1993. US Patent 5,263,043.
- [343] J. Walsh, K. Woods and S. Yeager. *Nucl. Instrum. Methods Phys. Res. A.* **341** (1994) 277–279, [https://doi.org/10.1016/0168-9002\(94\)90364-6](https://doi.org/10.1016/0168-9002(94)90364-6).
- [344] J.E. Walsh. *Nucl. Instrum. Methods Phys. Res. A.* **445** (2000) 214–221, [https://doi.org/10.1016/s0168-9002\(00\)00069-3](https://doi.org/10.1016/s0168-9002(00)00069-3).
- [345] H.L. Andrews and C.A. Brau. *Phys. Rev. Special Topics-Accelerators and Beams.* **7** (2004) 070701, <https://doi.org/10.1103/physrevstab.7.070701>.
- [346] G. Doucas, J.H. Mulvey, M. Omori, J. Walsh and M.F. Kimmitt. *Phys. Rev. Lett.* **69** (1992) 1761, <https://doi.org/10.1103/physrevlett.69.1761>.

- [347] A. Bakhtyari, J.E. Walsh and J.H. Brownell. *Phys. Rev. E.* **65** (2002) 066503, <https://doi.org/10.1103/physreve.65.066503>.
- [348] J. Urata, M. Goldstein, M.F. Kimmitt, A. Naumov, C. Platt and J.E. Walsh. *Phys. Rev. Lett.* **80** (1998) 516, <https://doi.org/10.1103/physrevlett.80.516>.
- [349] T.I. Smith and H.A. Schwettman. *Nucl. Instrum. Methods Phys. Res. A.* **304** (1991) 812–821, [https://doi.org/10.1016/0168-9002\(91\)90982-v](https://doi.org/10.1016/0168-9002(91)90982-v).
- [350] M.-E. Couprie and J.-M. Ortéga. *Analisis.* **28** (2000) 725–736.
- [351] T.I. Smith, J.C. Frisch, R. Rohatgi, H.A. Schwettman and R.L. Swent. *Nucl. Instrum. Methods Phys. Res. A.* **296** (1990) 33–36, [https://doi.org/10.1016/0168-9002\(90\)91185-e](https://doi.org/10.1016/0168-9002(90)91185-e).
- [352] D. Zimdars, A. Tokmakoff, S. Chen, S.R. Greenfield, M.D. Fayer, T.I. Smith and H.A. Schwettman. *Phys. Rev. Lett.* **70** (1993) 2718, <https://doi.org/10.1103/physrevlett.70.2718>.
- [353] S.R. Greenfield, Y.S. Bai and M.D. Fayer. *Chemical Physics Letters.* **170** (1990) 133–138, [https://doi.org/10.1016/0009-2614\(90\)87104-y](https://doi.org/10.1016/0009-2614(90)87104-y).
- [354] T.I. Smith, Y.S. Bai, S.R. Greenfield, J.C. Frisch, R.L. Swent, M.D. Fayer and H.A. Schwettman. *JOSA B.* **8** (1991) 1652–1656, <https://doi.org/10.1364/josab.8.001652>.
- [355] W.S. Fann, S.V. Benson, J.M.J. Madey, S. Etemad, G.L. Baker, L. Rothberg, M. Roberson and R.H. Austin. *Nucl. Instrum. Methods Phys. Res. A.* **296** (1990) 804–808, <https://doi.org/10.1109/fel.1989.716112>.
- [356] G.S. Edwards, R.H. Austin, F.E. Carroll, M.L. Copeland, M.E. Couprie, W.E. Gabella, R.F. Haglund, B.A. Hooper, M.S. Hutson, E.D. Jansen, *et al.* *Rev. Sci. Instrum.* **74** (2003) 3207–3245.
- [357] C. Crépin, M. Broquier, H. Dubost, D. L’hermite, A. Tramer, J.P. Galaup, J.M. Berset and J.M. Ortéga. *Laser Chemistry.* **19** (1999) 65–69, <https://doi.org/10.1155/1999/95804>.
- [358] J. Lemaire, P. Boissel, M. Heninger, G. Mauclaire, G. Bellec, H. Mestdagh, A. Simon, S. Le Caer, J.M. Ortega, F. Glotin, *et al.* *Phys. Rev. Lett.* **89** (2002) 273002, <https://doi.org/10.1103/physrevlett.89.273002>.
- [359] A. Dazzi, R. Prazeres, F. Glotin and J.M. Ortéga. *Optics Letters.* **30** (2005) 2388–2390, <https://doi.org/10.1364/ol.30.002388>.
- [360] D. Oepts, A.F.G. Van der Meer and P.W. Van Amersfoort. *Infrared Physics & Technology.* **36** (1995) 297–308, [https://doi.org/10.1016/1350-4495\(94\)00074-u](https://doi.org/10.1016/1350-4495(94)00074-u).
- [361] T. Tomimasu, T. Takii, T. Suzuki, E. Nishimura, S. Ogino, A. Nagai and M. Yasumoto. *Nucl. Instrum. Methods Phys. Res. A.* **407** (1998) 494–499, [https://doi.org/10.1016/s0168-9002\(98\)00075-8](https://doi.org/10.1016/s0168-9002(98)00075-8).
- [362] U. Lehnert, P. Michel, W. Seidel, G. Staats, J. Teichert and R. Wunsch. First experiences with the FIR-FEL at ELBE. *Proceeding of FEL, Novosibirsk, Jacow, 2007*.
- [363] W. Seidel, E. Cizmar, O. Drachenko, M. Helm, M. Justus, U. Lehnert, P. Michel, M. Ozerov, H. Schneider, R. Schurig, *et al.* Three years of cw-operation at FELBE—experiences and applications. In *Proceedings 30th International Free Electron Laser Conference FEL 2008*, Jacow, Citeseer, 2008.
- [364] A. Xie, L. van der Meer, W. Hoff and R.H. Austin. *Phys. Rev. Lett.* **84** (2000) 5435, <https://doi.org/10.1103/physrevlett.84.5435>.
- [365] Z. Zhu and M.J. Kelley. *Applied Surface Science.* **252** (2006) 6619–6623, <https://doi.org/10.1016/j.apsusc.2006.02.088>.
- [366] G.R. Neil and Jefferson Lab FEL Team. *Nucl. Instrum. Methods Phys. Res. B.* **144** (1998) 40–49, [https://doi.org/10.1016/s0168-583x\(98\)00295-x](https://doi.org/10.1016/s0168-583x(98)00295-x).
- [367] B.A. Knyazev, G.N. Kulipanov and N.A. Vinokurov. *Measurement Science and Technology.* **21** (2010) 054017, <https://doi.org/10.1088/0957-0233/21/5/054017>.
- [368] Y.U. Jeong, G.M. Kazakevitch, H.J. Cha, S.H. Park and B.C. Lee. *Nucl. Instrum. Methods Phys.*

- Res. A.* **575** (2007) 58–62, <https://doi.org/10.1016/j.nima.2007.01.024>.
- [369] L. Nahon, E. Renault, M.E. Couprie, F. Mérola, P. Dumas, M. Marsi, A. Taleb-Ibrahimi, D. Nutarelli, R. Roux and M. Billardon. *Nucl. Instrum. Methods Phys. Res. A.* **429** (1999) 489–496, [https://doi.org/10.1016/s0168-9002\(99\)00153-9](https://doi.org/10.1016/s0168-9002(99)00153-9).
- [370] M.E. Couprie, F. Merola, P. Tauc, D. Garzella, A. Delboulbé, T. Hara and M. Billardon. *Rev. Sci. Instrum.* **65** (1994) 1485–1495, <https://doi.org/10.1063/1.1144880>.
- [371] L. Nahon, E. Renault, M.-E. Couprie, D. Nutarelli, D. Garzella, M. Billardon, G.L. Carr, G.P. Williams and P. Dumas. Two-color experiments combining the UV storage ring free-electron laser and the SA5 IR beamline at Super-ACO. In *SPIE's International Symposium on Optical Science, Engineering, and Instrumentation* (International Society for Optics and Photonics, 1999), pp. 145–154.
- [372] M. Marsi, M.E. Couprie, L. Nahon, D. Garzella, T. Hara, R. Bakker, M. Billardon, A. Delboulbe, G. Indlekofer and A. Taleb-Ibrahimi. *Appl. Phys. Lett.* **70** (1997) 895–897, <https://doi.org/10.1063/1.118307>.
- [373] M. Marsi, R. Belkhou, C. Grupp, G. Panaccione, A. Taleb-Ibrahimi, L. Nahon, D. Garzella, D. Nutarelli, E. Renault, R. Roux, *et al.* *SiO₂/SiPhys. Rev. B.* **61** (2000) R5070, <https://doi.org/10.1103/physrevb.61.r5070>.
- [374] H. Ade, W. Yang, S.L. English, J. Hartman, R.F. Davis, R.J. Nemanich, V.N. Litvinenko, I.V. Pinayev, Y. Wu and J.M.J. Madey. *Surface Review and Letters.* **5** (1998) 1257–1268, <https://doi.org/10.1142/s0218625x98001596>.
- [375] M. Hosaka, S. Koda, M. Katoh, J. Yamazaki, K. Hayashi, K. Takashima, T. Gejo and H. Hama. *Nucl. Instrum. Methods Phys. Res. A.* **483** (2002):146–151, [https://doi.org/10.1016/s0168-9002\(02\)00301-7](https://doi.org/10.1016/s0168-9002(02)00301-7).
- [376] T. Gejo, E. Shigemasa, E. Nakamura, M. Hosaka, S. Koda, A. Mochihashi, M. Katoh, J.-I. Yamazaki, K. Hayashi, Y. Takashima, *et al.* *Nucl. Instrum. Methods Phys. Res. A.* **528** (2004) 627–631, <https://doi.org/10.1016/j.nima.2004.04.116>.
- [377] M. Marsi, A. Locatelli, M. Trovo, R.P. Walker, M.E. Couprie, D. Garzella, L. Nahon, D. Nutarelli, E. Renault, A. Gatto, *et al.* *Surf. Rev. Lett.* **9** (2002) 599–607, <https://doi.org/10.1142/s0218625x02001768>.
- [378] F. Glotin, J.-M. Ortéga, R. Prazeres, G. Devanz and O. Marcouillé. *Phys. Rev. Lett.* **77** (1996) 3130, <https://doi.org/10.1103/physrevlett.77.3130>.
- [379] M. Hosaka, H. Hama, K. Kimura, J. Yamazaki and T. Kinoshita. *Nucl. Instrum. Methods Phys. Res. A.* **393** (1997) 525–529.
- [380] M.E. Couprie, D. Nutarelli, R. Roux, B. Visentin, L. Nahon, R. Bakker, A. Delboulbé and M. Billardon. *Journal of Physics B.* **32** (1999) 5657, <https://doi.org/10.1088/0953-4075/32/24/303>.
- [381] D. Nutarelli, M.E. Couprie, L. Nahon, R. Bakker, A. Delboulbé, R. Roux, B. Visentin and M. Billardon. *Nucl. Instrum. Methods Phys. Res. A.* **407** (1998) 459–463, [https://doi.org/10.1016/s0168-9002\(98\)00068-0](https://doi.org/10.1016/s0168-9002(98)00068-0).
- [382] V.N. Litvinenko, B. Burnham, M. Emamian, N. Hower, J.M.J. Madey, P. Morcombe, P.G. O'Shea, S.H. Park, R. Sachtshale, K.D. Straub, *et al.* *Phys. Rev. Lett.* **78** (1997) 4569.
- [383] S.H. Park, V.N. Litvinenko, W. Tornow and C. Montgomery. *Nucl. Instrum. Methods Phys. Res. A.* **475** (2001) 425–431, [https://doi.org/10.1016/s0168-9002\(01\)01635-7](https://doi.org/10.1016/s0168-9002(01)01635-7).
- [384] V.N. Litvinenko and J.M.J. Madey. High-power inverse Compton γ -ray source at the Duke storage ring. In *SPIE's 1995 International Symposium on Optical Science, Engineering, and Instrumentation* (International Society for Optics and Photonics, 1995), pp. 55–77.
- [385] H.R. Weller and M.W. Ahmed. *Modern Phys. Lett. A.* **18** (2003) 1569–1590, <https://doi.org/10.1142/s0217732303011216>.

- [386] J.M.J. Madey and C. Pellegrini. Free electron generation of extreme ultraviolet coherent radiation-1983. Technical Report, American Institute of Physics, New York (1984).
- [387] P. Sprangle and R.A. Smith. *Phys. Rev. A.* **21** (1980) 293.
- [388] N.M. Kroll, P.L. Morton and M.N. Rosenbluth. *Phys. Quantum Electron.* **7** 147.
- [389] W.A. McMullin and G. Bekefi. *Phys. Rev. A.* **25** (1982) 1826, <https://doi.org/10.1103/physreva.25.1826>.
- [390] E. Jerby and A. Gover. *IEEE J. Quantum Electron.* **21** (1985) 1041–1058, <https://doi.org/10.1109/jqe.1985.1072748>.
- [391] P. Sprangle, C.M. Tang and C.W. Roberson. *Nucl. Instrum. Methods Phys. Res. A.* **239** (1985) 1–18.
- [392] W.B. Colson, J.C. Gallardo and P.M. Bosco. *Phys. Rev. A.* **34** (1986) 4875, <https://doi.org/10.1103/physreva.34.4875>.
- [393] Y.S. Derbenev, A.M. Kondratenko and E.L. Saldin. *Nucl. Instrum. Methods Phys. Res.* **193** (1982) 415–421, [https://doi.org/10.1016/0029-554x\(82\)90233-6](https://doi.org/10.1016/0029-554x(82)90233-6).
- [394] R. Bonifacio, F. Casagrande and L.A. Lugiato. *Opt. Commun.* **36** (1981) 159–163, [https://doi.org/10.1016/0030-4018\(81\)90160-7](https://doi.org/10.1016/0030-4018(81)90160-7).
- [395] R. Bonifacio, F. Casagrande and G. Casati. *Opt. Commun.* **40** (1982) 219–223, [https://doi.org/10.1016/0030-4018\(82\)90265-6](https://doi.org/10.1016/0030-4018(82)90265-6).
- [396] R. Bonifacio, C. Pellegrini and L.M. Narducci. *Opt. Commun.* **50** (1984) 373–378, [https://doi.org/10.1016/0030-4018\(84\)90105-6](https://doi.org/10.1016/0030-4018(84)90105-6).
- [397] W.B. Colson. *Nucl. Instrum. Methods Phys. Res. A.* **393** (1997) 82–85.
- [398] C. Pellegrini. *Nucl. Instrum. Methods Phys. Res. A.* **475** (2001) 1–12, [https://doi.org/10.1016/s0168-9002\(01\)01527-3](https://doi.org/10.1016/s0168-9002(01)01527-3).
- [399] J.-M. Wang and L.-H. Yu. *Nucl. Instrum. Methods Phys. Res. A.* **250** (1986) 484–489, [https://doi.org/10.1016/0168-9002\(86\)90928-9](https://doi.org/10.1016/0168-9002(86)90928-9).
- [400] J.B. Murphy, C. Pellegrini and R. Bonifacio. *Opt. Commun.* **53** (1985) 197–202, [https://doi.org/10.1016/0030-4018\(85\)90331-1](https://doi.org/10.1016/0030-4018(85)90331-1).
- [401] R. Bonifacio, F. Casagrande and C. Pellegrini. *Opt. Commun.* **61** (1987) 55–60, [https://doi.org/10.1016/0030-4018\(87\)90124-6](https://doi.org/10.1016/0030-4018(87)90124-6).
- [402] R. Bonifacio, F. Casagrande, G. Cerchioni, L. de S. Souza, P. Pierini and N. Piovella. *J. Quantum Electron.* **17** (1990) 1417–1427.
- [403] G. Dattoli and P.L. Ottaviani. *Opt. Commun.* **204** (2002) 283–297, [https://doi.org/10.1016/s0030-4018\(02\)01201-4](https://doi.org/10.1016/s0030-4018(02)01201-4).
- [404] G. Dattoli, L. Giannessi, P.L. Ottaviani and C. Ronsivalle. *J. Appl. Phys.* **95** (2004) 3206–3210, <https://doi.org/10.1063/1.1645979>.
- [405] G. Dattoli and P.L. Ottaviani. *Opt. Commun.* **254** (2005) 330–339, <https://doi.org/10.1016/j.optcom.2005.05.056>.
- [406] Y. Ding, A. Brachmann, F.-J. Decker, D. Dowell, P. Emma, J. Frisch, S. Gilevich, G. Hays, P. Hering, Z. Huang, R. Iverson, H. Loos, A. Miahnahri, H.-D. Nuhn, D. Ratner, J. Turner, J. Welch, W. White and J. Wu. *Phys. Rev. Lett.* **102** (2009) 254801–254805, <https://doi.org/10.1103/physrevlett.102.254801>.
- [407] E.L. Saldin, E.A. Schneidmiller and M.V. Yurkov. *Opt. Commun.* **148** (1998) 383–403, [https://doi.org/10.1016/s0030-4018\(97\)00670-6](https://doi.org/10.1016/s0030-4018(97)00670-6).
- [408] R. Bonifacio, L. De Salvo, P. Pierini, N. Piovella and C. Pellegrini. *Phys. Rev. Lett.* **73** (1994) 70, <https://doi.org/10.1103/physrevlett.73.70>.
- [409] E.T. Scharlemann, A.M. Sessler and J.S. Wurtele. *Phys. Rev. Lett.* **54** (1985) 1925.

- [410] G.T. Moore. *Opt. Commun.* **52** (1984) 46–51, [https://doi.org/10.1016/0030-4018\(84\)90071-3](https://doi.org/10.1016/0030-4018(84)90071-3).
- [411] G.T. Moore. *Opt. Commun.* **54** (1985) 121–125, [https://doi.org/10.1016/0030-4018\(85\)90014-8](https://doi.org/10.1016/0030-4018(85)90014-8).
- [412] E.T. Scharlemann, A.M. Sessler and J.S. Wurtele, *Nucl. Instrum. Methods Phys. Res. A.* **239** (1985) 29–35, [https://doi.org/10.1016/0168-9002\(85\)90694-1](https://doi.org/10.1016/0168-9002(85)90694-1)
- [413] A. Fruchtman, *Phys. Rev. A.* **37** (1988) 2989, <https://doi.org/10.1103/physreva.37.2989>
- [414] K.-J. Kim. *Phys. Rev. Lett.* **57** (1986) 1871–1874, <https://doi.org/10.1103/physrevlett.57.1871>
- [415] Kwang-Je Kim, *Nucl. Instrum. Methods Phys. Res. A.* **250** (1986) 396–403, [https://doi.org/10.1016/0168-9002\(86\)90916-2](https://doi.org/10.1016/0168-9002(86)90916-2)
- [416] M. Xie, *Nucl. Instrum. Methods Phys. Res. A.* **445** (2000) 59–66, [https://doi.org/10.1016/s0168-9002\(00\)00114-5](https://doi.org/10.1016/s0168-9002(00)00114-5)
- [417] Ming Xie, Design optimization for an X-ray free electron laser driven by SLAC linac. In *Particle Accelerator Conference, 1995., Proc. of the 1995*, vol. 1 (IEEE, 1995), pp. 183–185.
- [418] C. Pellegrini, A. Marinelli and S. Reiche. *Rev. Mod. Phys.* **88** (2016) 015006, <https://doi.org/10.1103/revmodphys.88.015006>
- [419] W.M. Fawley, A user manual for GINGER and its post-processor XPLOTGIN. *Lawrence Berkeley National Laboratory* (2002).
- [420] S. Reiche, *Nucl. Instrum. Methods Phys. Res. A.* **429** (1999) 243–248, [https://doi.org/10.1016/s0168-9002\(99\)00114-x](https://doi.org/10.1016/s0168-9002(99)00114-x)
- [421] L. Giannessi, Overview of Perseo, a system for simulating FEL dynamics in Mathcad. In *Proc. of the Free-Electron Laser Conference Jacow* (2006).
- [422] S.G. Biedron, Y.C. Chae, R.J. Dejus, B. Faatz, H.P. Freund, S.V. Milton, H.-D. Nuhn and S. Reiche, *Nucl. Instrum. Methods Phys. Res. A.* **445** (2000) 110–115, [https://doi.org/10.1016/s0168-9002\(00\)00124-8](https://doi.org/10.1016/s0168-9002(00)00124-8)
- [423] L.T. Campbell and B.W.J. McNeil, *Phys of Plasmas.* **19** (2012) 093119, <https://doi.org/10.1063/1.4752743>
- [424] T.M. Tran and J.S. Wurtele, *Comput. Phys. Commun.* **54** (1989) 263–272, [https://doi.org/10.1016/0010-4655\(89\)90090-8](https://doi.org/10.1016/0010-4655(89)90090-8)
- [425] Z. Huang and K.-J. Kim, *Phys. Rev. E.* **62** (2000) 7295, <https://doi.org/10.1103/physreve.62.7295>
- [426] G. Dattoli, P.L. Ottaviani and S. Pagnutti, *J. Appl. Phys.* **97** (2005) 113102, <https://doi.org/10.1063/1.1886890>
- [427] G. Dattoli, L. Giannessi, P.L. Ottaviani, H.P. Freund, S.G. Biedron and S. Milton, *Nucl. Instrum. Methods Phys. Res. A.* **495** (2002) 48–57, [https://doi.org/10.1016/s0168-9002\(02\)01281-0](https://doi.org/10.1016/s0168-9002(02)01281-0)
- [428] I. Ben-Zvi, L.F. Di Mauro, S. Krinsky, M.G. White and L.H. Yu, *Nucl. Instrum. Methods Phys. Res. A.* **304** (1991) 181–186, [https://doi.org/10.1016/0168-9002\(91\)90845-h](https://doi.org/10.1016/0168-9002(91)90845-h)
- [429] L.-H. Yu, M. Babzien, I. Ben-Zvi, L.F. DiMauro, A. Doyuran, W. Graves, E. Johnson, S. Krinsky, R. Malone, I. Pogorelsky, J. Skaritka, G. Rakowsky, L. Solomon, X.J. Wang, M. Woodle, V. Yakimenko, S.G. Biedron, J.N. Galayda, E. Gluskin, J. Jagger, V. Sajaev and I. Vasserman, *Science* **289** (2000) 932–934.
- [430] L.H. Yu, *Phys. Rev. A.* **44** (1991) 5178, <https://doi.org/10.1103/physreva.44.5178>
- [431] L.H. Yu and J. Wu, *Nucl. Instrum. Methods Phys. Res. A.* **483** (2002) 493–498, [https://doi.org/10.1016/s0168-9002\(02\)00368-6](https://doi.org/10.1016/s0168-9002(02)00368-6)
- [432] E. Allaria and G. De Ninno, *Phys. Rev. Lett.* **99** (2007) 014801, <https://doi.org/10.1103/physrevlett.99.014801>
- [433] I. Ben-Zvi, K.M. Yang and L.H. Yu, *Nucl. Instrum. Methods Phys. Res. A.* **318** (1992) 726–729, [https://doi.org/10.1016/0168-9002\(92\)91147-2](https://doi.org/10.1016/0168-9002(92)91147-2)
- [434] E.L. Saldin, E.A. Schneidmiller and M.V. Yurkov, *Opt. Commun.* **202** (2002) 169–187,

- [https://doi.org/10.1016/s0030-4018\(02\)01091-x](https://doi.org/10.1016/s0030-4018(02)01091-x)
- [435] A. Gover and E. Dyunin, *Phys. Rev. Lett.* **102** (2009) 154801, <https://doi.org/10.1103/physrevlett.102.154801>
- [436] L. Giannessi, P. Musumeci and S. Spampinati, *J. Appl. Phys.* **98** (2005) 043110, <https://doi.org/10.1063/1.2010624>
- [437] L. Giannessi and P. Musumeci, *New J. Phys.* **8** (2006) 294, <https://doi.org/10.1088/1367-2630/8/11/294>
- [438] M. Labat, N. Joly, S. Bielawski, C. Sz waj, C. Bruni and M.E. Couprie *Phys. Rev. Lett.* **103** (2009) 264801, <https://doi.org/10.1103/physrevlett.103.264801>
- [439] G. Stupakov, *Phys. Rev. Lett.* **102** (2009) 074801–074804, <https://doi.org/10.1103/physrevlett.102.074801>
- [440] M.E. Couprie, M. Labat, C. Evain, C. Sz waj, S. Bielawski, N. Hubert, C. Benabderahmane, F. Briquez, L. Chapuis, F. Marteau *et al.*, *J. Mod. Opt.* **63** (2016) 309–323, <https://doi.org/10.1080/09500340.2015.1075617>
- [441] D. Xiang and G. Stupakov, *New J. Phys.* **13** (2011) 093028–093036, <https://doi.org/10.1088/1367-2630/13/9/093028>
- [442] C. Evain, A. Loulergue, A. Nadji, J.M. Filhol, M.E. Couprie and A.A. Zholents, *New J. Phys.* **14** (2012) 023003, <https://doi.org/10.1088/1367-2630/14/2/023003>
- [443] J.B. Murphy and C. Pellegrini, *JOSA B.* **2** (1985) 259–264, <https://doi.org/10.1364/josab.2.000259>
- [444] J.B. Murphy and C. Pellegrini, *Nucl. Instrum. Methods Phys. Res. A.* **237** (1985) 159–167, [https://doi.org/10.1016/0168-9002\(85\)90344-4](https://doi.org/10.1016/0168-9002(85)90344-4)
- [445] M. Cornacchia, J. Bisognano, S. Chattopadhyay, A. Garren, K. Halbach, A. Jackson, K.J. Kim, H. Lancaster, J. Peterson, M.S. Zisman *et al.*, *Nucl. Instrum. Methods Phys. Res. A.* **250** (1986) 57–63, [https://doi.org/10.1016/0168-9002\(86\)90860-0](https://doi.org/10.1016/0168-9002(86)90860-0)
- [446] C. Travier, *Nucl. Instrum. Methods Phys. Res. A.* **304** (1991) 285–296, [https://doi.org/10.1016/0168-9002\(91\)90870-v](https://doi.org/10.1016/0168-9002(91)90870-v)
- [447] C. Travier, *Nucl. Instrum. Methods Phys. Res. A.* **340** (1994) 26–39, [https://doi.org/10.1016/0168-9002\(94\)91278-5](https://doi.org/10.1016/0168-9002(94)91278-5)
- [448] M.Curtin, G. Bennett, R. Burke, A. Bhowmik, P. Metty, S. Benson and J.M.J. Madey, *Nucl. Instrum. Methods Phys. Res. A.* **296** (1990) 127–133, [https://doi.org/10.1016/0168-9002\(90\)91199-1](https://doi.org/10.1016/0168-9002(90)91199-1)
- [449] J.S. Fraser, R.L. Sheffield and E.R. Gray, *Nucl. Instrum. Methods Phys. Res. A.* **250** (1986) 71–76, [https://doi.org/10.1016/0168-9002\(86\)90862-4](https://doi.org/10.1016/0168-9002(86)90862-4)
- [450] R.L. Sheffield, E.R. Gray and J.S. Fraser, *Nucl. Instrum. Methods Phys. Res. A.* **272** (1988) 222–226, [https://doi.org/10.1016/0168-9002\(88\)90227-6](https://doi.org/10.1016/0168-9002(88)90227-6)
- [451] P.G. O’Shea, S.C. Bender, B.E. Carlsten, J.W. Early, D.W. Feldman, R.B. Feldman, W.J.D. Johnson, A.H. Lumpkin, R.L. Sheffield, R.W. Springer *et al.* Performance of the photoinjector accelerator for the Los Alamos free-electron laser. In *Proc. IEEE Part. Accel. Conf., San Francisco, CA* (1991).
- [452] D.W. Feldman, S.C. Bender, B.E. Carlsten, J. Early, R.B. Feldman, W.J.D. Johnson, A.H. Lumpkin, P.G. O’Shea, W.E. Stein, R.L. Sheffield *et al.*, *IEEE J. Quantum Electron.* **27** (1991) 2636–2643, <https://doi.org/10.1109/3.104143>
- [453] B.E. Carlsten, *Nucl. Instrum. Methods Phys. Res. A.* **285** (1989) 313–319, [https://doi.org/10.1016/0168-9002\(89\)90472-5](https://doi.org/10.1016/0168-9002(89)90472-5)
- [454] K.T. McDonald, *IEEE Trans. Electron Devices.* **35** (1988) 2052–2059, <https://doi.org/10.1109/16.7427>
- [455] S.C. Hartman, N. Barov, C. Pellegrini, S. Park, J. Rosenzweig, G. Travish, R. Zhang, C. Clayton, P. Davis, M. Everett *et al.*, *Nucl. Instrum. Methods Phys. Res. A.* **340** (1994) 219–230,

- [https://doi.org/10.1016/0168-9002\(94\)91305-6](https://doi.org/10.1016/0168-9002(94)91305-6)
- [456] D.T. Palmer, X.J. Wang, R.H. Miller, M. Babzien, I. Ben-Zvi, C. Pellegrini, J. Sheehan, J. Skaritka, H. Winick, M. Woodle *et al.*, Emission studies of the BNL/SLAC/UCLA 1.6 cell photocathode RF gun. In *Particle Accelerator Conference, 1997. Proc. of the 1997*, vol. 3 (IEEE, 1997), 2687–2689.
- [457] C. Travier, M. Bernard, P. Dufresne, G. Michaud, M. Omeich, M. Roch and J. Kodier, *Nucl. Instrum. Methods Phys. Res. B.* **89** (1994) 27–32, [https://doi.org/10.1016/0168-583x\(94\)95139-x](https://doi.org/10.1016/0168-583x(94)95139-x)
- [458] C. Pellegrini, *Nucl. Instrum. Methods Phys. Res. A.* **272** (1988) 364–367, [https://doi.org/10.1016/0168-9002\(88\)90252-5](https://doi.org/10.1016/0168-9002(88)90252-5)
- [459] J. C. Gallardo. 1 Å In Proc. of the Workshop: Prospects for a 1 Å Free Electron Laser, Sag Harbor, New York, Center for Accelerator Physics, April 22-27, Ed, J. C. Gallardo (1990), pp. iii. Center for Accelerator Physics, Brookhaven National Laboratory, BNL-52273, DE91 007631.
- [460] L.H. Yu. 1 Å In Proc. of the Workshop: Prospects for a 1 Å Free Electron Laser, Sag Harbor, New York, April 22-27, Ed, J. C. Gallardo (1990), pp. 13–30. Center for Accelerator Physics, Brookhaven National Laboratory, BNL-52273, DE91 007631.
- [461] C. Pellegrini, SASE and Development of an X-Ray FEL. In Proc. of the Workshop: Prospects for a 1 Å Free Electron Laser, Sag Harbor, New York, April 22–27, Ed. J. C. Gallardo (1990), pp. 3–12. Center for Accelerator Physics, Brookhaven National Laboratory, BNL-52273, DE91 007631.
- [462] J.C. Goldstein, C.J. Elliot and M.J. Schmitt, Three-Dimensional Simulations of the Generation of One-Angstrom Radiation by a Self-Amplified Spontaneous Emission Free-Electron Laser. In *Proc. of the Workshop: Prospects for a 1 Å Free Electron Laser, Sag Harbor, New York, April 22-27*, Ed. J. C. Gallardo (1990), pp. 13–30. Center for Accelerator Physics, Brookhaven National Laboratory, BNL-52273, DE91 007631.
- [463] M. Cornacchia and H. Winick, Proc. of a Workshop on IV Generation Light Sources. Technical report, SSRL/SLAC Rep. 92/02 (1992).
- [464] J.L. Laclare. Proc. of the 10th ICFA Beam Dynamics Workshop on 4th Generation Light Source. In *Contribution booklet*, Ed., J. L. Laclare (ESRF, 1996).
- [465] T.J. Orzechowski, B.R. Anderson, J.C. Clark, W.M. Fawley, A.C. Paul, D. Prosnitz, E.T. Scharlemann, S.M. Yarema, D.B. Hopkins, A.M. Sessler and J.S. Wurtele, *Phys. Rev. Lett.* **57** (1986) 2172, <https://doi.org/10.1103/physrevlett.57.2172>
- [466] D.A. Kirkpatrick, G. Bekefi, A.C. Dirienzo, H.P. Freund, and A.K. Ganguly, *Nucl. Instrum. Methods Phys. Res. A.* **285** (1989) 43–46, [https://doi.org/10.1016/0168-9002\(89\)90422-1](https://doi.org/10.1016/0168-9002(89)90422-1)
- [467] J. Gardelle, J. Labrousse and J.L. Rullier, *Phys. Rev. Lett.* **76** (1996) 4532, <https://doi.org/10.1103/physrevlett.76.4532>
- [468] J. Gardelle, T. Lefevre, G. Marchese, J.L. Rullier and J.T. Donohue, *Phys. Rev. Lett.* **79** (1997) 3905, <https://doi.org/10.1103/physrevlett.79.3905>
- [469] T. Lefevre, J. Gardelle, G. Marchese, J.L. Rullier and J.T. Donohue, *Phys. Rev. Lett.* **82** (1999) 323, <https://doi.org/10.1103/physrevlett.82.323>
- [470] S. Okuda, J. Ohkuma, N. Kimura, Y. Honda, T. Okada, S. Takamuku, T. Yamamoto and K. Tsumori, *Nucl. Instrum. Methods Phys. Res. A.* **331** (1993) 76–78, [https://doi.org/10.1016/0168-9002\(93\)90017-c](https://doi.org/10.1016/0168-9002(93)90017-c)
- [471] D. Bocek, P. Kung, H.-C. Lihn, C. Settakorn and H. Wiedemann, *Nucl. Instrum. Methods Phys. Res. A.* **375** (1996) 13–16, [https://doi.org/10.1016/0168-9002\(95\)01361-x](https://doi.org/10.1016/0168-9002(95)01361-x)
- [472] R. Prazeres, J.M. Ortéga, F. Glotin, D.A. Jaroszynski and O. Marcouillé, *Phys. Rev. Lett.* **78** (1997) 2124, <https://doi.org/10.1103/physrevlett.78.2124>
- [473] M. Babzien, I. Ben-Zvi, P. Catravas, J.-M. Fang, T.C. Marshall, X.J. Wang, J.S. Wurtele, V. Yaki-

- menko and L.H. Yu, *Phys. Rev. E* **57** (1998) 6093–6100, <https://doi.org/10.1103/physreve.57.6093>
- [474] M. Hogan, C. Pellegrini, J. Rosenzweig, G. Travish, A. Varfolomeev, S. Anderson, K. Bishofberger, P. Frigola, A. Murokh, N. Osmanov *et al.*, *Phys. Rev. Lett.* **80** (1998) 289, <https://doi.org/10.1103/physrevlett.80.289>
- [475] C.M. Fortgang, *Nucl. Instrum. Methods Phys. Res. A.* **393** (1997) 385–388, [https://doi.org/10.1016/s0168-9002\(97\)00519-6](https://doi.org/10.1016/s0168-9002(97)00519-6)
- [476] D.C. Nguyen, R.L. Sheffield, C.M. Fortgang, J.C. Goldstein, J.M. Kinross-Wright and N.A. Ebrahim, *Phys. Rev. Lett.* **81** (1998) 810, <https://doi.org/10.1103/physrevlett.81.810>
- [477] M.J. Hogan, C. Pellegrini, J. Rosenzweig, S. Anderson, P. Frigola, A. Tremaine, C. Fortgang, D.C. Nguyen, R.L. Sheffield, J. Kinross-Wright *et al.*, *Phys. Rev. Lett.* **81** (1998) 4867, <https://doi.org/10.1103/physrevlett.81.4867>.
- [478] A. Tremaine, J.B. Rosenzweig, S. Anderson, P. Frigola, M. Hogan, A. Murokh, C. Pellegrini, D.C. Nguyen and R.L. Sheffield, *Phys. Rev. Lett.* **81** (1998) 5816, <https://doi.org/10.1103/physrevlett.81.5816>.
- [479] S.V. Milton, E. Gluskin, S.G. Biedron, R.J. Dejus, P.K. Den Hartog, J.N. Galayda, K.-J. Kim, J.W. Lewellen, E.R. Moog, V. Sajaev *et al.*, *Phys. Rev. Lett.* **85** (2000) 988, <https://doi.org/10.1103/physrevlett.85.988>.
- [480] S.V. Milton, E. Gluskin, N.D. Arnold, C. Benson, W. Berg, S.G. Biedron, M. Borland, Y.-C. Chae, R.J. Dejus, P.K. Den Hartog, B. Deriy, M. Erdmann, Y.I. Eidelman, M.W. Hahne, Z. Huang, K.-J. Kim, J.W. Lewellen, Y. Li, A.H. Lumpkin, O. Makarov, E.R. Moog, A. Massiri, V. Sajaev, R. Soliday, B.J. Tieman, E.M. Trakhtenberg, G. Travish, I.B. Vasserman, N.A. Vinokurov, X.J. Wang, G. Wiemerslage and B.X. Yang, *Science*. **292** (2001) 2037–2041, <https://doi.org/10.1126/science.1059955>.
- [481] A. Tremaine, X.J. Wang, M. Babzien, I. Ben-Zvi, M. Cornacchia, H.-D. Nuhn, R. Malone, A. Murokh, C. Pellegrini, S. Reiche *et al.*, *Rev. Lett.* **88** (2002) 204801, <https://doi.org/10.1103/physrevlett.88.204801>.
- [482] A. Murokh, R. Agustsson, M. Babzien, I. Ben-Zvi, L. Bertolini, K. van Bibber, R. Carr, M. Cornacchia, P. Frigola, J. Hill *et al.*, *Phys. Rev. E*. **67** (2003) 066501, <https://doi.org/10.1103/physreve.67.066501>.
- [483] J.R. Schneider, *J. Phys. B* **43** (2010) 194001, <https://doi.org/10.1088/0953-4075/43/19/194001>.
- [484] D.A. Edwards *et al.*, TESLA test facility linac-design report. *DESY Print March* (1995) 95–01.
- [485] J. Rossbach, *Nucl. Instrum. Methods Phys. Res. A.* **375** (1996) 269–273, [https://doi.org/10.1016/0168-9002\(95\)01332-6](https://doi.org/10.1016/0168-9002(95)01332-6)
- [486] J. Andruszkow, B. Aune, V. Ayvazyan, N. Baboi, R. Bakker, V. Balakin, D. Barni, A. Bazhan, M. Bernard, A. Bosotti, J.C. Bourdon, W. Brefeld, R. Brinkmann, S. Buhler, J.-P. Carneiro, M. Castellano, P. Castro, L. Catani, S. Chel, Y. Cho, S. Choroba, E.R. Colby, W. Decking, P. Den Hartog, M. Desmons, M. Dohlus, D. Edwards, H.T. Edwards, B. Faatz, J. Feldhaus, M. Ferrario, M.J. Fitch, K. Flöttmann, M. Fouaidy, A. Gamp, T. Garvey, C. Gerth, M. Geitz, E. Gluskin, V. Gretchko, U. Hahn, W.H. Hartung, D. Hubert, M. Hüning, R. Ischebek, M. Jablonka, J.M. Joly, M. Juillard, T. Junquera, P. Jurkiewicz, A. Kabel, J. Kahl, H. Kaiser, T. Kamps, V.V. Katelev, J.L. Kirchgessner, M. Körfer, L. Kravchuk, G. Kreps, J. Krzywinski, T. Lokajczyk, R. Lange, B. Leblond, M. Leenen, J. Lesrel, M. Liepe, A. Liero, T. Limberg, R. Lorenz, L.H. Hua, L.F. Hai, C. Magne, M. Maslov, G. Materlik, A. Matheisen, J. Menzel, P. Michelato, W.-D. Möller, A. Mosnier, U.-C. Müller, O. Napoly, A. Novokhatski, M. Omeich, H.S. Padamsee, C. Pagani, F. Peters, B. Petersen, P. Pierini, J. Pflüger, P. Piot, B.P. Ngoc, L. Plucinski, D. Proch, K. Rehlich, S. Reiche, D. Reschke, I. Reyzl, J. Rosenzweig, J. Rossbach, S. Roth, E.L. Saldin, W. Sandner, Z. Sanok, H. Schlarb, G. Schmidt, P. Schmüser, J.R. Schneider, E.A. Schneidmiller, H.-J. Schreiber, S. Schreiber, P. Schütt, J. Sekutowicz, L. Serafini, D. Sertore, S. Setzer, S. Simrock,

- B. Sonntag, B. Sparr, F. Stephan, V.A. Sytchev, S. Tazzari, F. Tazzioli, M. Tigner, M. Timm, M. Tonutti, E. Trakhtenberg, R. Treusch, D. Trines, V. Verzilov, T. Vielitz, V. Vogel, G.v. Walter, R. Wanzenberg, T. Weiland, H. Weise, J. Weisend, M. Wendt, M. Werner, M.M. White, I. Will, S. Wolff, M.V. Yurkov, K. Zapfe, P. Zhogolev and F. Zhou, *Phys. Rev. Lett.* **85** (2000) 3825–3829, <https://doi.org/10.1103/physrevlett.85.3825>
- [487] V. Ayvazyan, N. Baboi, I. Bohnet, R. Brinkmann, M. Castellano, P. Castro, L. Catani, S. Choroba, A. Cianchi, M. Dohlus *et al.*, *Eur. Phys. J. D-Atomic, Molecular, Optical and Plasma Physics.* **20** (2002) 149–156, <https://doi.org/10.1140/epjd/e2002-00121-4>
- [488] V. Ayvazyan, N. Baboi, I. Bohnet, R. Brinkmann, M. Castellano, P. Castro, L. Catani, S. Choroba, A. Cianchi, M. Dohlus, H.T. Edwards, B. Faatz, A.A. Fateev, J. Feldhaus, K. Flöttmann, A. Gamp, T. Garvey, H. Genz, Ch. Gerth, V. Gretchko, B. Grigoryan, U. Hahn, C. Hessler, K. Honkavaara, M. Hüning, R. Ischebeck, M. Jablonka, T. Kamps, M. Körfer, M. Krassilnikov, J. Krzywinski, M. Liepe, A. Liero, T. Limberg, H. Loos, M. Luong, C. Magne, J. Menzel, P. Michelato, M. Minty, U.-C. Müller, D. Nölle, A. Novokhatski, C. Pagani, F. Peters, J. Pflüger, P. Piot, L. Plucinski, K. Rehlich, I. Reyzl, A. Richter, J. Rossbach, E.L. Saldin, W. Sandner, H. Schlarb, G. Schmidt, P. Schmüser, J.R. Schneider, E.A. Schneidmiller, H.-J. Schreiber, S. Schreiber, D. Sertore, S. Setzer, S. Simrock, R. Sobierajski, B. Sonntag, B. Steeg, F. Stephan, K.P. Sytchev, K. Tiedtke, M. Tonutti, R. Treusch, D. Trines, D. Türke, V. Verzilov, R. Wanzenberg, T. Weiland, H. Weise, M. Wendt, I. Will, S. Wolff, K. Wittenburg, M.V. Yurkov and K. Zapfe, *Phys. Rev. Lett.* **88** (2002) 104802, <https://doi.org/10.1103/physrevlett.88.104802>
- [489] H. Wabnitz, L. Bittner, A.R.B. De Castro, R. Döhrmann, P. Gürtler, T. Laarmann, W. Laasch, J. Schulz, A. Swiderski, K. von Haeften *et al.*, *Nature* **420** (2002) 482–485, <https://doi.org/10.1038/nature01197>
- [490] V. Ayvazyan, N. Baboi, J. Bähr, V. Balandin, B. Beutner, A. Brandt, I. Bohnet, A. Bolzmann, R. Brinkmann, O.I. Brovko *et al.*, *Eur. Phys. J. D-Atomic, Molecular, Optical and Plasma Physics.* **37** (2005) 297–303, <https://doi.org/10.1140/epjd/e2005-00308-1>
- [491] W. Ackermann, G. Asova, V. Ayvazyan, A. Azima, N. Baboi, J. Bähr, V. Balandin, B. Beutner, A. Brandt, A. Bolzmann, R. Brinkmann, O.I. Brovko, M. Castellano, P. Castro, L. Catani, E. Chiadroni, S. Choroba, A. Cianchi, J.T. Costello, D. Cubaynes, J. Dardis, W. Decking, H. Delsim-Hashemi, A. Delserieys, G. Di Pirro, M. Dohlus, S. Dästerer, A. Eckhardt, H.T. Edwards, B. Faatz, J. Feldhaus, K. Flöttmann, J. Frisch, L. Fröhlich, T. Garvey, U. Gensch, Ch. Gerth, M. Gärler, N. Golubeva, H.-J. Grabosch, M. Grecki, O. Grimm, K. Hacker, U. Hahn, J.H. Han, K. Honkavaara, T. Hott, M. Hähnel, Y. Ivanisenko, E. Jaeschke, W. Jalmuzna, T. Jezynski, R. Kammering, V. Katalev, K. Kavanagh, E.T. Kennedy, S. Khodyachykh, K. Klose, V. Kocharyan, M. Kärfer, M. Kollwe, W. Koprek, S. Korepanov, D. Kostin, M. Krassilnikov, G. Kube, M. Kuhlmann, C.L.S. Lewis, L. Lilje, T. Limberg, D. Lipka, F. Löhler, H. Luna, M. Luong, M. Martins, M. Meyer, P. Michelato, V. Miltchev, W.D. Müller, L. Monaco, W.F.O. Müller, O. Napieralski, O. Napoly, P. Nicolosi, D. Nölle, T. Nuñez, A. Opet, C. Pagani, R. Paparella, N. Pchalek, J. Pedregosa-Gutierrez, B. Petersen, B. Petrosyan, G. Petrosyan, L. Petrosyan, J. Pflüger, E. Plünjes, L. Poletto, K. Pozniak, E. Prat, D. Proch, P. Pucyk, P. Radcliffe, H. Redlin, K. Rehlich, M. Richter, M. Roehrs, J. Roensch, R. Romaniuk, M. Ross, J. Rossbach, V. Rybnikov, M. Sachwitz, E.L. Saldin, W. Sandner, H. Schlarb, B. Schmidt, M. Schmitz, P. Schmüser, J.R. Schneider, E.A. Schneidmiller, S. Schnepf, S. Schreiber, M. Seidel, D. Sertore, A.V. Shabunov, C. Simon, S. Simrock, E. Sombrowski, A.A. Sorokin, P. Spanknebel, R. Spesyvtsev, L. Staykov, B. Steffen, F. Stephan, F. Stulle, H. Thom, K. Tiedtke, M. Tischer, S. Toleikis, R. Treusch, D. Trines, I. Tsakov, E. Vogel, T. Weiland, H. Weise, M. Wellhöfer, M. Wendt, I. Will, A. Winter, K. Wittenburg, W. Wurth, P. Yeates, M.V. Yurkov, I. Zagorodnov and K. Zapfe, *Nat Photonics.* **1** (2007) 336–342, <https://doi.org/10.1038/nphoton.2007.76>
- [492] S. Schreiber, B. Faatz and K. Honkavaara. In *Proc. EPAC* (2008).

- [493] S. Schreiber *et al.* In *Proc. of FEL Jacow* (2011).
- [494] B. Faatz, E. Plönjes, S. Ackermann, A. Agababyan, V. Asgekar, V. Ayvazyan, S. Baark, N. Baboi, V. Balandin, N. von Bargen *et al.*, *New J. Phys.* **18** (2016) 062002, <https://doi.org/10.1088/1367-2630/18/6/062002>
- [495] H. Kitamura, *J. Synchrotron Radiat.* **7** (2000) 121–130, <https://doi.org/10.1107/s0909049500002983>
- [496] H. Kitamura, T. Bizen, T. Hara, X. Marechal, T. Seike and T. Tanaka, *Nucl. Instrum. Methods Phys. Res. A.* **467** (2001) 110–113, [https://doi.org/10.1016/s0168-9002\(01\)00242-x](https://doi.org/10.1016/s0168-9002(01)00242-x)
- [497] T. Shintake, H. Matsumoto, T. Ishikawa and H. Kitamura, SPring-8 compact SASE source (SCSS). In *International Symposium on Optical Science and Technology*, pages 12–23. International Society for Optics and Photonics, 2001.
- [498] K. Togawa, H. Baba, K. Onoe, T. Inagaki, T. Shintake and H. Matsumoto, *CeB₆Nucl. Instrum. Methods Phys. Res. A.* **528** (2004) 312–315, <https://doi.org/10.1016/j.nima.2004.04.077>
- [499] K. Togawa, T. Shintake, T. Inagaki, K. Onoe, T. Tanaka, H. Baba and H. Matsumoto, *CeB₆Phys. Rev. Special Topics-Accelerators and Beams.* **10** (2007) 020703, <https://doi.org/10.1103/physrevstab.10.020703>
- [500] T. Shintake, H. Tanaka, T. Hara, T. Tanaka, K. Togawa, M. Yabashi, Y. Otake, Y. Asano, T. Bizen, T. Fukui, S. Goto, A. Higashiya, T. Hirono, N. Hosoda, T. Inagaki, S. Inoue, M. Ishii, Y. Kim, H. Kimura, M. Kitamura, T. Kobayashi, H. Maesaka, T. Masuda, S. Matsui, T. Matsushita, X. Maréchal, M. Nagasono, H. Ohashi, T. Ohata, T. Ohshima, K. Onoe, K. Shirasawa, T. Takagi, S. Takahashi, M. Takeuchi, K. Tamasaku, R. Tanaka, Y. Tanaka, T. Tanikawa, T. Togashi, S. Wu, A. Yamashita, K. Yanagida, C. Zhang, H. Kitamura and T. Ishikawa, *Nat. Photonics.* **2** (2008) 555–559, <https://doi.org/10.1038/nphoton.2008.134>
- [501] T. Shintake, H. Tanaka, T. Hara, T. Tanaka, K. Togawa, Makina ÄÄ, Y. Otake, Y. Asano, T. Fukui, T. Hasegawa *et al.*, *Phys. Rev. Special Topics-Accelerators and Beams.* **12** (2009) 070701, <https://doi.org/10.1103/physrevstab.12.070701>
- [502] C. Pellegrini, J. Rosenzweig, H.-D. Nuhn, P. Pianetta, R. Tatchyn, H. Winick, K. Bane, P. Morton, T. Raubenheimer, J. Seeman *et al.*, *Nucl. Instrum. Methods Phys. Res. A.* **331** (1993) 223–227, [https://doi.org/10.1016/0168-9002\(93\)90047-1](https://doi.org/10.1016/0168-9002(93)90047-1)
- [503] T.O. Raubenheimer, *Nucl. Instrum. Methods Phys. Res. A.* **358** (1995) 40–43, [https://doi.org/10.1016/0168-9002\(94\)01502-3](https://doi.org/10.1016/0168-9002(94)01502-3)
- [504] J. Arthur, G. Materlik and H. Winick, Workshop on scientific applications of coherent X-rays. SLAC Report, 437 (1994).
- [505] M. Cornacchia, Linac coherent light source (LCLS) design study report. Technical report, Stanford Linear Accelerator Center, Menlo Park, CA (US), 1998.
- [506] B. Birgeneau and Z.X. Shen, Report of the Basic Energy Sciences Advisory Committee Panel on DOE synchrotron radiation sources and science. Technical report (1997).
- [507] P.R. Bolton, J.E. Clendenin, D.H. Dowell, M. Ferrario, A.S. Fisher, S.M. Gierman, R.E. Kirby, P. Krejcik, C.G. Limborg, G.A. Mulhollan *et al.*, *Nucl. Instrum. Methods Phys. Res. A.* **483** (2002) 296–300, [https://doi.org/10.1016/s0168-9002\(02\)00331-5](https://doi.org/10.1016/s0168-9002(02)00331-5)
- [508] C. Limborg, P. Bolton, D.H. Dowell, S. Gierman and J.F. Schmerge, *Nucl. Instrum. Methods Phys. Res. A.* **528** (2004) 350–354, <https://doi.org/10.1016/j.nima.2004.04.066>
- [509] J. Arthur *et al.*, Linac Coherent Light Source (LCLS) Conceptual Design Report. Technical report, SLAC-R-593, 2002.
- [510] M. Borland, *Phys. Rev. Special Topics-Accelerators and Beams.* **11** (2008) 030701, <https://doi.org/10.1103/physrevstab.11.030701>
- [511] E. Trakhtenberg, V. Tcheskidov, I. Vasserman, N. Vinokurov, M. Erdmann and J. Pfluger, *Nucl.*

- Instrum. Methods Phys. Res. A.* **543** (2005) 42–46, <https://doi.org/10.1016/j.nima.2005.01.110>
- [512] P. Emma, R. Akre, J. Arthur, R. Bionta, C. Bostedt, J. Bozek, A. Brachmann, P. Bucksbaum, R. Coffee, F.-J. Decker, Y. Ding, D. Dowell, S. Edstrom, A. Fisher, J. Frisch, S. Gilevich, J. Hastings, G. Hays, P.H. Hering, Z. Huang, R. Iverson, H. Loos, M. Messerschmidt, A. Miahnahri, S. Moeller, H.-D. Nuhn, G. Pile, D. Ratner, J. Rzepiela, D. Schultz, T. Smith, P. Stefan, H. Tompkins, J. Turner, J. Welch, W. White, J. Wu, G. Yocky and J. Galayda, *Nat. Photonics.* **4** (2010) 641–647, <https://doi.org/10.1038/nphoton.2010.176>
- [513] Y. Ding, A. Brachmann, F.-J. Decker, D. Dowell, P. Emma, J. Frisch, S. Gilevich, G. Hays, Ph. Hering, Z. Huang *et al.*, *Phys. Rev. Lett.* **102** (2009) 254801, <https://doi.org/10.1103/physrevlett.102.254801>
- [514] P. Emma, R. Carr and H.-D. Nuhn, *Nucl. Instrum. Methods Phys. Res. A.* **429** (1999) 407–413, [https://doi.org/10.1016/s0168-9002\(99\)00117-5](https://doi.org/10.1016/s0168-9002(99)00117-5)
- [515] Z. Huang, A. Brachmann, F.-J. Decker, Y. Ding, D. Dowell, P. Emma, J. Frisch, S. Gilevich, G. Hays, P. Hering, R. Iverson, H. Loos, A. Miahnahri, H.-D. Nuhn, D. Ratner, G. Stupakov, J. Turner, J. Welch, W. White, J. Wu and D. Xiang, *Phys. Rev. Special Topics-Accelerators and Beams.* **13** (2010) 020703, <https://doi.org/10.1103/physrevstab.13.020703>
- [516] T. Ishikawa, H. Aoyagi, T. Asaka, Y. Asano, N. Azumi, T. Bizen, H. Ego, K. Fukami, T. Fukui, Y. Furukawa, S. Goto, H. Hanaki, T. Hara, T. Hasegawa, T. Hatsui, A. Higashiya, T. Hirono, N. Hosoda, M. Ishii, T. Inagaki, Y. Inubushi, T. Itoga, Y. Joti, M. Kago, T. Kameshima, H. Kimura, Y. Kirihara, A. Kiyomichi, T. Kobayashi, C. Kondo, T. Kudo, H. Maesaka, X.M. Maréchal, T. Masuda, S. Matsubara, T. Matsumoto, T. Matsushita, S. Matsui, M. Nagasono, N. Nariyama, H. Ohashi, T. Ohata, T. Ohshima, S. Ono, Y. Otake, C. Saji, T. Sakurai, T. Sato, K. Sawada, T. Seike, K. Shirasawa, T. Sugimoto, S. Suzuki, S. Takahashi, H. Takebe, K. Takeshita, K. Tamasaku, H. Tanaka, R. Tanaka, T. Tanaka, T. Togashi, K. Togawa, A. Tokuhisa, H. Tomizawa, K. Tono, S. Wu, M. Yabashi, M. Yamaga, A. Yamashita, K. Yanagida, C. Zhang, T. Shintake, H. Kitamura and N. Kumagai, *Nat. Photonics.* **6** (2012) 540–544, <https://doi.org/10.1038/nphoton.2012.141>
- [517] T. Tanaka, S. Goto, T. Hara, T. Hatsui, H. Ohashi, K. Togawa, M. Yabashi and H. Tanaka. *Phys. Rev. Special Topics-Accelerators and Beams.* **15** (2012) 110701, <https://doi.org/10.1103/physrevstab.15.110701>
- [518] H. Tanaka, Present status of SACLA. In *Proc. of FEL2017, Santa Fe, NM, USA*, Jacow, (2017).
- [519] J.S. Oh, C.W. Chung, D.E. Kim, E.S. Kim, H.S. Kang, I.S. Ko, K.B. Lee, S.H. Nam, S.J. Park, T.Y. Koo *et al.*, Compact X-ray free electron laser program at the PAL. In *Proc. of APAC 2004, Gyeongju, Korea*, Jacow, (2004), pp. 261–263.
- [520] D.E. Kim, Y.G. Jung, H.S. Kang, I.S. Ko, H.G. Lee, S.B. Lee, W.W. Lee, D.G. Oh, K.H. Park, H.S. Suh and J. Pflueger, Development of PAL-XFEL undulator system. In *Proc. of IPAC 2016, Busan, Korea*, Jacow, (2016), pp. 4044–4046.
- [521] J. Hong, S.-Ik, Moon, Y.-W. Parc, M. Cho, I.S. Ko, C. Kim, S.-J. Park, Y.-J. Park, S.-H. Kim and W. Namkung. *J. Korean Phys. Soc.* **58** (2011) 198–204.
- [522] SEOUL, June 30 (Korea Bizwire), <http://koreabizwire.com/korea-succeeds-in-producing-x-ray-free-electron-laser/59745>.
- [523] PALFEL, <http://pal.postech.ac.kr/paleng/menu.pal?method=menuview&pagemode=paleng&top=7&sub=5&sub2=0&sub3=0>.
- [524] H. H. Braun for SwissFEL team, , Commissioning of SwissFEL. In *Proc. of IPAC 2017, Copenhagen, Denmark*, Jacow, (2017).
- [525] R. Ganter, SwissFEL-Conceptual design report. Technical report, Paul Scherrer Institute (PSI), 2010.
- [526] S. Reiche, Status of the SwissFEL facility at the Paul Scherrer Institute. In *Proc. FEL 2011, Shanghai, China*, Jacow, pages 223–226, 2011.

- [527] T. Schmidt and S. Reiche, Undulators for the SwissFEL. In *Proc. of FEL2009, Liverpool, UK*, Jacow, pages 706–713, 2009.
- [528] T. Schietinger, M. Pedrozzi, M. Aiba, V. Arsov, S. Bettoni, B. Beutner, M. Calvi, P. Craievich, M. Dehler, F. Frei *et al.*, *Phys. Rev. Accelerators and Beams*. **19** (2016) 100702, <https://doi.org/10.1103/physrevaccelbeams.19.034402>
- [529] The Swiss FEL, <https://www.psi.ch/swissfel>.
- [530] M. Altarelli, R. Brinkmann, M. Chergui, W. Decking, B. Dobson, S. Dusterer, G. Grubel, W. Graeff, H. Graafsma, J. Hajdu *et al.*, The European X-ray free electron laser, Technical Design Report, DESY. Technical report, 2006.
- [531] The European X-Ray Laser Project XFEL, www.xfel.eu/.
- [532] W. Decking, H. Weise on behalf of the European XFEL Accelerator Consortium and Commissioning Team, In *Proc. of IPAC2017, Copenhagen, Denmark*, Jacow, MOC03, 2017.
- [533] H. Weise, W. Decking, on behalf of the European XFEL Accelerator Consortium and Commissioning Team, In *Proc. of FEK2017, Santa Fe, NM, USA*, Jacow, MOXAA1, 2017.
- [534] T. Raubenheimer *et al.*, The LCLS-II, a new FEL facility at SLAC. In *Proc. 36th Int. Free-Electron Laser Conf., Basel*, Jacow, (2014).
- [535] Z. Y. Zhu, Z. T. Zhao, D. Wang, Z. Liu, R. X. Li, L. X. Yin, Z. H. Yang for the the SCLF Team. In *Proc. of FEK2017, Santa Fe, NM, USA*, Jacow, MOP055, 2017.
- [536] E.L. Saldin, E.A. Schneidmiller and M.V. Yurkov, *Opt. Commun.* **148** (1998) 383–403, [https://doi.org/10.1016/s0030-4018\(97\)00670-6](https://doi.org/10.1016/s0030-4018(97)00670-6)
- [537] S. Reiche, P. Musumeci, C. Pellegrini and J.B. Rosenzweig, *Nucl. Instrum. Methods Phys. Res. A* **593** (2008) 45–48, <https://doi.org/10.1016/j.nima.2008.04.061>
- [538] L. Giannessi, A. Bacci, M. Bellaveglia, F. Briquez, M. Castellano, E. Chiadroni, A. Cianchi, F. Ciocci, M.E. Couprie, L. Cultrera, G. Dattoli, D. Filippetto, M.D. Franco, G.D. Pirro, M. Ferrario, L. Ficcadenti, F. Frassetto, A. Gallo, G. Gatti, M. Labat, G. Marcus, M. Moreno, A. Mostacci, E. Pace, A. Petralia, V. Petrillo, L. Poletto, M. Quattromini, J.V. Rau, C. Ronsivalle, J. Rosenzweig, A.R. Rossi, V.R. Albertini, E. Sabia, M. Serluca, S. Spampinati, I. Spassovsky, B. Spataro, V. Surrenti, C. Vaccarezza and C. Vicario, *Phys. Rev. Lett.* **106** (2011) 144801, <https://doi.org/10.1103/physrevlett.106.144801>
- [539] L. Giannessi, D. Alesini, P. Antici, A. Bacci, M. Bellaveglia, R. Boni, M. Boscolo, F. Briquez, M. Castellano, L. Catani *et al.*, *Phys. Rev. Special Topics-Accelerators and Beams*. **14** (2011) 060712, <https://doi.org/10.1103/physrevstab.14.102803>
- [540] N.R. Thompson and B.W.J. McNeil, *Phys. Rev. Lett.* **100** (2008) 203901, <https://doi.org/10.1103/physrevlett.100.203901>
- [541] P. Emma, K. Bane, M. Cornacchia, Z. Huang, H. Schlarb, G. Stupakov and D. Walz, *Phys. Rev. Lett.* **92** (2004) 074801, <https://doi.org/10.1103/physrevlett.92.074801>
- [542] C.B. Schroeder, C. Pellegrini, S. Reiche, J. Arthur and P. Emma, *Nucl. Instrum. Methods Phys. Res. A*. **483** (2002) 89–93, [https://doi.org/10.1016/s0168-9002\(02\)00291-7](https://doi.org/10.1016/s0168-9002(02)00291-7)
- [543] A.A. Zholents and W.M. Fawley, *Phys. Rev. Lett.* **92** (2004) 224801, <https://doi.org/10.1103/physrevlett.92.224801>
- [544] E.L. Saldin, E.A. Schneidmiller and M.V. Yurkov, *Opt. Commun.* **239** (2004) 161–172, <https://doi.org/10.1016/j.optcom.2004.05.024>
- [545] A.A. Zholents, *Phys. Rev. Special Topics-Accelerators and Beams*. **8** (2005) 040701, <https://doi.org/10.1103/physrevstab.8.050704>
- [546] E.L. Saldin, E.A. Schneidmiller and M.V. Yurkov, *Phys. Rev. Special Topics-Accelerators and Beams*. **9** (2006) 050702, <https://doi.org/10.1103/physrevstab.9.030702>
- [547] A.A. Zholents and M.S. Zolotarev, *New J. Phys.* **10** (2008) 025005, <https://doi.org/10.1088/1367->

2630/10/2/025005

- [548] T. Tanaka, *Phys. Rev. Lett.* **110** (2013) 084801.
- [549] D.J. Dunning, B.W.J. McNeil and N.R. Thompson, *Phys. Rev. Lett.* **110** (2013) 104801, <https://doi.org/10.1103/physrevlett.110.104801>
- [550] E. Prat and S. Reiche, *Phys. Rev. Lett.* **114** (2015) 244801, <https://doi.org/10.1103/physrevlett.114.244801>
- [551] S. Huang, Y. Ding, Z. Huang and G. Marcus, *Phys. Rev. Accel. Beams.* **19** (2016) 080702, <https://doi.org/10.1103/physrevaccelbeams.19.080702>
- [552] R. Bonifacio, L. De Salvo Souza, P. Pierini and N. Piovela, *Nucl. Instrum. Methods Phys. Res. A.* **296** (1990) 358–367, [https://doi.org/10.1016/0168-9002\(90\)91234-3](https://doi.org/10.1016/0168-9002(90)91234-3)
- [553] C. Bourassin-Bouchet and M.-E. Couprie, *Nat. Commun.* **6** (2015), <https://doi.org/10.1038/ncomms7465> [547] C. Bourassin-Bouchet and M.-E. Couprie, *Nat. Commun.* **6** (2015) 6465, <https://doi.org/10.1038/ncomms7465>.
- [554] A. Singer, I.A. Vartanyants, M. Kuhlmann, S. Duesterer, R. Treusch and J. Feldhaus, *Phys. Rev. Lett.* **101** (2008) 254801, <https://doi.org/10.1103/physrevlett.101.254801>.
- [555] R. Bachelard, P. Mercère, M. Idir, M.-E. Couprie, M. Labat, O. Chubar, Guillaume Lambert, P. Zeitoun, H. Kimura, H. Ohashi, *et al.*, *Phys. Rev. Lett.* **106** (2011) 234801, <https://doi.org/10.1103/physrevlett.106.234801>.
- [556] A.B. Temnykh, *Phys. Rev. ST Accel. Beams* **11** (2008) 120702–120711, <https://doi.org/10.1103/physrevstab.11.120702>.
- [557] A.A. Lutman, J.P. MacArthur, M. Ilchen, A.O. Lindahl, J. Buck, R.N. Coffee, G.L. Dakovski, L. Dammann, Y. Ding, H.A. Dürr, *et al.*, *Nat. Photonics* **10** (2016) 468–472.
- [558] L.-H. Yu and I. Ben-Zvi, High-gain harmonic generation of soft X-rays with the "fresh bunch" technique. *Nucl. Instrum. Methods Phys. Res. A* **393** (1997) 96–99, [https://doi.org/10.1016/s0168-9002\(97\)00435-x](https://doi.org/10.1016/s0168-9002(97)00435-x).
- [559] L.-H. Yu, L. DiMauro, A. Doyuran, W.S. Graves, E.D. Johnson, R. Heese, S. Krinsky, H. Loos, J.B. Murphy, G. Rakowsky, *et al.*, *Phys. Rev. Lett.* **91** (2003) 074801.
- [560] A. Doyuran, M. Babzien, T. Shafan, L.H. Yu, L.F. DiMauro, I. Ben-Zvi, S.G. Biedron, W. Graves, E. Johnson, S. Krinsky, *et al.*, *Phys. Rev. Lett.* **86** (2001) 5902.
- [561] W. Li, R.R. Lucchese, A. Doyuran, Z. Wu, H. Loos, G.E. Hall and A.G. Suits, *Phys. Rev. Lett.* **92** (2004) 083002–083005, <https://doi.org/10.1103/physrevlett.92.083002>.
- [562] T. Shafan and L.H. Yu, *Phys. Rev. E.* **71** (2005) 046501, <https://doi.org/10.1103/physreve.71.046501>.
- [563] T. Watanabe, X.J. Wang, J.B. Murphy, J. Rose, Y. Shen, T. Tsang, L. Giannessi, P. Musumeci and S. Reiche, *Phys. Rev. Lett.* **98** (2007) 034802, <https://doi.org/10.1103/physrevlett.98.034802>.
- [564] M. Ferrario, D. Alesini, A. Bacci, M. Bellaveglia, R. Boni, M. Boscolo, M. Castellano, L. Catani, E. Chiadroni, S. Cialdi, *et al.*, *Phys. Rev. Lett.* **99** (2007) 234801, <https://doi.org/10.1103/physrevlett.99.234801>.
- [565] L. Giannessi, M. Artioli, M. Bellaveglia, F. Briquez, E. Chiadroni, A. Cianchi, M. E. Couprie, G. Dattoli, E. Di Palma, G. Di Pirro, M. Ferrario, D. Filippetto, F. Frassetto, G. Gatti, M. Labat, G. Marcus, A. Mostacci, A. Petralia, V. Petrillo, L. Poletto, M. Quattromini, J. V. Rau, J. Rosenzweig, E. Sabia, M. Serluca, I. Spassovsky and V. Surrenti, *Phys. Rev. Lett.* **108** (2012) 164801, <https://doi.org/10.1103/physrevlett.108.164801>.
- [566] L. Giannessi, M. Bellaveglia, E. Chiadroni, A. Cianchi, M.E. Couprie, M. Del Franco, G. Di Pirro, M. Ferrario, G. Gatti, M. Labat, *et al.*, *Phys. Rev. Lett.* **110** (2013) 044801, <https://doi.org/10.1103/physrevlett.110.044801>.
- [567] Marie Emmanuelle Couprie, *J. Electron Spectros. Relat. Phenomena* **196** (2014) 3–13,

- <https://doi.org/10.1016/j.elspec.2013.12.007>.
- [568] M.E. Couprie, *Nucl. Instrum. Methods Phys. Res. B* **364** (2015) 4–15, <https://doi.org/10.1016/j.nimb.2015.08.084>.
- [569] M. Ferray, A. l’Huillier, X.F. Li, L.A. Lompré, G. Mainfray and C. Manus, *1064 nm J. Phys. B* **21** (1988) L31–L36, <https://doi.org/10.1088/0953-4075/21/3/001>.
- [570] A. McPherson, G. Gibson, H. Jara, U. Johann, Ting S. Luk, I.A. McIntyre, Keith Boyer and Charles K. Rhodes, *J. Opt. Soc. Am. B* **4** (1987) 595–601, <https://doi.org/10.1364/josab.4.000595>.
- [571] F. Canova and L. Poletto, *Optical Technologies for Extreme-Ultraviolet and Soft X-ray Coherent Sources*, Vol. 197 (Springer, 2015).
- [572] D. Garzella, T. Hara, B. Carre, P. Salieres, T. Shintake, H. Kitamura and M.E. Couprie, *Nucl. Instrum. Methods Phys. Res. A* **528** (2004) 502–505, <https://doi.org/10.1016/j.nima.2004.04.089>.
- [573] G. Lambert, T. Hara, D. Garzella, T. Tanikawa, M. Labat, B. Carre, H. Kitamura, T. Shintake, M. Bougeard, S. Inoue, Y. Tanaka, P. Salieres, H. Merdji, O. Chubar, O. Gobert, K. Tahara and M-E. Couprie, *Nat. Phys.* **4** (2008) 296–300, <https://doi.org/10.1038/nphys889>.
- [574] T. Tanikawa, Guillaume Lambert, T. Hara, M. Labat, Y. Tanaka, M. Yabashi, O. Chubar and M.E. Couprie, *EPL (Europhys. Lett.)* **94** (2011) 34001, <https://doi.org/10.1209/0295-5075/94/34001>.
- [575] G. Lambert, T. Hara, M. Labat, T. Tanikawa, Y. Tanaka, M. Yabashi, D. Garzella, B. Carré and M.E. Couprie, *EPL (Europhys. Lett.)* **88** (2009) 54002, <https://doi.org/10.1209/0295-5075/88/54002>.
- [576] T. Togashi, E.J. Takahashi, K. Midorikawa, M. Aoyama, K. Yamakawa, T. Sato, A. Iwasaki, S. Owada, T. Okino, K. Yamanouchi, F. Kannari, A. Yagishita, H. Nakano, M-E. Couprie, K. Fukami, T. Hatsui, T. Hara, T. Kameshima, H. Kitamura, N. Kumagai, S. Matsubara, M. Nagasono, H. Ohashi, T. Ohshima, Y. Otake, T. Shintake, K. Tamasaku, H. Tanaka, T. Tanaka, K. Togawa, H. Tomizawa, T. Watanabe, M. Yabashi and T. Ishikawa, *Opt. Express* **19** (2011) 317–324.
- [577] S. Matsubara, T. Togashi, E.J. Takahashi, K. Midorikawa, M. Aoyama, K. Yamakawa, T. Sato, A. Iwasaki, S. Owada, K. Yamanouchi, *et al.*, in *Lasers and Electro-Optics Europe (CLEO EU-ROPE/IQEC), 2013 Conference on and International Quantum Electronics Conference (IEEE, 2013)*, pp. 1–1.
- [578] K. Ogawa, T. Sato, S. Owada, S. Matsubara, Y. Okayasu, T. Togashi, T. Watanabe, E.J. Takahashi, K. Midorikawa, M. Aoyama, *et al.*, in *International Conference on Ultrafast Phenomena* (Optical Society of America, 2014), p. 07.
- [579] E.J. Takahashi, T. Togashi, M. Aoyama, K. Yamakawa, T. Sato, A. Iwasaki, S. Owada, K. Yamanouchi, T. Hara, S. Matsubara, *et al.* In *Lasers and Electro-Optics (CLEO), 2013 Conference on* (IEEE, 2013), pp. 1–2.
- [580] M. Labat, M. Bellaveglia, M. Bougeard, B. Carré, F. Ciocci, E. Chiadroni, A. Cianchi, M-E. Couprie, L. Cultrera, M. Del Franco, G. Di Pirro, A. Drago, M. Ferrario, D. Filippetto, F. Frassetto, A. Gallo, D. Garzella, G. Gatti, L. Giannessi, G. Lambert, A. Mostacci, A. Petralia, V. Petrillo, L. Poletto, M. Quattromini, J.V. Rau, C. Ronsivalle, E. Sabia, M. Serluca, I. Spassovsky, V. Surrenti, C. Vaccarezza and C. Vicario, *Phys. Rev. Lett.* **107** (2011) 224801–224805.
- [581] S. Ackermann, A. Azima, S. Bajt, J. Bödewadt, F. Curbis, H. Dachraoui, H. Delsim-Hashemi, M. Drescher, S. Düsterer, B. Faatz, *et al.*, *Phys. Rev. Lett.* **111** (2013) 114801, <https://doi.org/10.1103/physrevlett.111.114801>.
- [582] C.J. Bocchetta, D. Bulfone, F. Cargnello, M. Danailov, G. D’Auria, B. Diviacco, M. Ferianis, A. Gambitta, E. Karantzoulis, G. Loda, *et al.*, *Nucl. Instrum. Methods Phys. Res. A* **507** (2003) 484–488, [https://doi.org/10.1016/s0168-9002\(03\)00901-x](https://doi.org/10.1016/s0168-9002(03)00901-x).
- [583] S. Di Mitri, E. Allaria, L. Badano, C. Bontoiu, M. Cornacchia, P. Craievich, M. Danailov, G. De Ninno, B. Diviacco, O. Ferrando, *et al.*, *Nucl. Instrum. Methods Phys. Res. A* **608** (2009) 19–27.

- [584] S. Di Mitri, M. Cornacchia, S. Spampinati and S. Milton, *Phys. Rev. ST Accel. Beams* **13** (2010) 010702, <https://doi.org/10.1103/physrevstab.13.010702>.
- [585] S. Di Mitri, M. Cornacchia, C. Scafuri and Magnus Sjöström, *Phys. Rev. ST Accel. and Beams* **15** (2012) 012802, <https://doi.org/10.1103/physrevstab.15.012802>.
- [586] Enrico Allaria, Carlo Callegari, Daniele Cocco, William M. Fawley, Maya Kiskinova, Claudio Masciovecchio and Fulvio Parmigiani, *New J. Phys.* **12** (2010) 075002, <https://doi.org/10.1088/1367-2630/12/7/075002>.
- [587] E. Allaria, Roberto Appio, L. Badano, W.A. Barletta, S. Bassanese, S.G. Biedron, A. Borga, E. Busetto, D. Castronovo, P. Cinquegrana, *et al.*, *Nat Photonics* **6** (2012) 699–704.
- [588] E. Allaria, Roberto Appio, L. Badano, W.A. Barletta, S. Bassanese, S.G. Biedron, A. Borga, E. Busetto, D. Castronovo, P. Cinquegrana, S. Cleva, D. Cocco, M. Cornacchia, P. Craievich, I. Cudin, G. D’Auria, M. Dal Forno, M.B. Danailov, R. De Monte, G. De Ninno, P. Delgiusto, A. Demidovich, S. Di Mitri, B. Diviacco, A. Fabris, R. Fabris, W. Fawley, M. Ferianis, E. Ferrari, S. Ferry, L. Froehlich, P. Furlan, G. Gaio, F. Gelmetti, L. Giannessi, M. Giannini, R. Gobessi, R. Ivanov, E. Karantzoulis, M. Lonza, A. Lutman, B. Mahieu, M. Milloch, S.V. Milton, M. Musardo, I. Nikolov, S. Noe, F. Parmigiani, G. Penco, M. Petronio, L. Pivetta, M. Predonzani, F. Rossi, L. Rumiz, A. Salom, C. Scafuri, C. Serpico, P. Sigalotti, S. Spampinati, C. Spezzani, M. Svandrik, C. Svetina, S. Tazzari, M. Trovo, R. Umer, A. Vascotto, M. Veronese, R. Visintini, M. Zaccaria, D. Zangrando and M. Zangrando, *Nat Photonics* **6** (2012) 699–704.
- [589] S. Sasaki, K. Miyata and T. Takada, *Jpn. J. Appl. Phys.* **31** (**12B**) (1992) 1794–1796, <https://doi.org/10.1143/jjap.31.11794>.
- [590] E. Allaria, D. Castronovo, P. Cinquegrana, P. Craievich, M. Dal Forno, M.B. Danailov, G. D’Auria, A. Demidovich, G. De Ninno, S. Di Mitri, *et al.*, *Nat Photonics* **7** (2013) 913–918.
- [591] E. Allaria, A. Battistoni, F. Bencivenga, R. Borghes, C. Callegari, F. Capotondi, D. Castronovo, P. Cinquegrana, D. Cocco, M. Coreno, *et al.*, *New J. Phys.* **14** (2012) 113009–113027.
- [592] L. Giannessi, in *Proc. FEL Conference, Basel, Switzerland*, Jacow, (2014), pp. 9–13.
- [593] G. De Ninno, B. Mahieu, E. Allaria, L. Giannessi and S. Spampinati, *Phys. Rev. Lett.* **110** (2013) 064801, <https://doi.org/10.1103/physrevlett.110.064801>.
- [594] B. Mahieu, E. Allaria, D. Castronovo, M. B. Danailov, A. Demidovich, G. De Ninno, S. Di Mitri, W. M. Fawley, E. Ferrari, L. Fröhlich, *et al.*, *Opt. Express* **21** (2013) 22728–22741, <https://doi.org/10.1364/oe.21.022728>.
- [595] E. Allaria, F. Bencivenga, R. Borghes, F. Capotondi, D. Castronovo, P. Charalambous, P. Cinquegrana, M.B. Danailov, G. De Ninno, A. Demidovich, *et al.*, Two-colour pump–probe experiments with a twin-pulse-seed extreme ultraviolet free-electron laser. *Nat. Commun.* **4** (2013) 2476, <https://doi.org/10.1038/ncomms3476>.
- [596] Enrico Allaria, Bruno Diviacco, Carlo Callegari, Paola Finetti, Benot Mahieu, Jens Viefhaus, Marco Zangrando, Giovanni De Ninno, Guillaume Lambert, Eugenio Ferrari, *et al.*, *Phys. Rev. X* **4** (2014) 041040.
- [597] F.E.L. Dalian, (2017) www.laserfocusworld.com/articles/2017/01/china-develops-world-s-brightest-vuv-free-electron-laser-research-facility.html.
- [598] W. Q. Zhang, D. X. Dai, G. L. Wang, G. R. Wu, X. M. Yang, S. Chen, C. Feng, D. Wang, M. Zhang, Z. T. Zhao, in *Proc. FEL Conference, Santa Fe, NM, USA*, Jacow, (2017), MOC04.
- [599] D. Xiang, E. Colby, M. Dunning, S. Gilevich, C. Hast, K. Jobe, D. McCormick, J. Nelson, T.O. Raubenheimer, K. Soong, G. Stupakov, Z. Szalata, D. Walz, S. Weathersby and M. Woodley, *Phys. Rev. Lett.* **105** (2010) 114801–114804, <https://doi.org/10.1103/physrevlett.105.114801>.
- [600] E. Hemsing, M. Dunning, C. Hast, T.O. Raubenheimer, S. Weathersby and D. Xiang, *Phys. Rev. ST Accel. Beams* **17** (2014) 070702, <https://doi.org/10.1103/physrevstab.17.070702>.

- [601] E. Hemsing, D. Xiang, M. Dunning, S. Weathersby, C. Hast and T. Raubenheimer, *Phys. Rev. ST Accel. Beams* **17** (2014) 010703, <https://doi.org/10.1103/physrevstab.17.010703>.
- [602] E. Hemsing, M. Dunning, B. Garcia, C. Hast, T. Raubenheimer, G. Stupakov and D. Xiang, *Nat. Photonics* **10** (2016) 512–515, <https://doi.org/10.1038/nphoton.2016.101>.
- [603] E. Hemsing and A. Marinelli, *Phys. Rev. Lett.* **109** (2012) 224801, <https://doi.org/10.1103/physrevlett.109.224801>.
- [604] E. Hemsing, A. Knyazik, M. Dunning, D. Xiang, A. Marinelli, C. Hast and J.B. Rosenzweig, *Nat. Phys.* **9** (2013) 549–553, <https://doi.org/10.1038/nphys2712>.
- [605] C. Feng, T. Zhang, J. Chen, H. Deng, M. Zhang, X. Wang, B. Liu, T. Lan, D. Wang and Z. Zhao, *Phys. Rev. ST Accel. Beams* **14** (2011) 090701, <https://doi.org/10.1103/physrevstab.14.090701>.
- [606] B. Liu, W.B. Li, J.H. Chen, Z.H. Chen, H.X. Deng, J.G. Ding, Y. Fan, G.P. Fang, C. Feng, L. Feng, *et al.*, *Phys. Rev. ST Accel. Beams* **16** (2013) 020704.
- [607] C. Feng, H. Deng, D. Wang and Z. Zhao, *New J. Phys.* **16** (2014) 043021, <https://doi.org/10.1088/1367-2630/16/4/043021>.
- [608] C. Feng, T. Zhang, H. Deng and Z. Zhao, *Phys. Rev. ST Accel. Beams* **17** (2014) 070701, <https://doi.org/10.1103/physrevstab.17.070701>.
- [609] H. Deng, T. Zhang, L. Feng, C. Feng, B. Liu, X. Wang, T. Lan, G. Wang, W. Zhang, X. Liu, *et al.*, *Phys. Rev. ST Accel. Beams* **17** (2014) 020704, <https://doi.org/10.1103/physrevstab.17.020704>.
- [610] H. Deng, M. Zhang, C. Feng, T. Zhang, X. Wang, T. Lan, L. Feng, W. Zhang, X. Liu, H. Yao, *et al.*, *Phys. Rev. Lett.* **113** (2014) 254802, <https://doi.org/10.1103/physrevlett.113.254802>.
- [611] Z.T. Zhao, Dong Wang, J.H. Chen, Z.H. Chen, H.X. Deng, J.G. Ding, C. Feng, Q. Gu, M.M. Huang, T.H. Lan, Y.B. Leng, D.G. Li, G.Q. Lin, B. Liu, E. Prat, X.T. Wang, Z.S. Wang, K.R. Ye, L.Y. Yu, H.O. Zhang, J.Q. Zhang, Me Zhang, Mi Zhang, T. Zhang, S.P. Zhong and Q.G. Zhou, *Nat. Photonics* **6** (2012) 360–363.
- [612] Z.T. Zhao, D. Wang, L.X. Yin, Q. Gu, G.P. Fang and B. Liu, *AAPS Bull.* **26** (2016) 12–24.
- [613] J. Feldhaus, E.L. Saldin, J.R. Schneider, E.A. Schneidmiller and M.V. Yurkov, *Opt. Commun.* **140** (1997) 341–352, [https://doi.org/10.1016/s0030-4018\(97\)00163-6](https://doi.org/10.1016/s0030-4018(97)00163-6).
- [614] G. Geloni, V. Kocharyan and E. Saldin, A novel self-seeding scheme for hard X-ray FELs. *J. Mod. Opt.* **58** (2011) 1391–1403, <https://doi.org/10.1080/09500340.2011.586473>.
- [615] J. Amann, W. Berg, V. Blank, F.-J. Decker, Y. Ding, P. Emma, Y. Feng, J. Frisch, D. Fritz, J. Hastings, Z. Huang, J. Krzywinski, R. Lindberg, H. Loos, A. Lutman, H.-D. Nuhn, D. Ratner, J. Rzepiela, D. Shu, Yu Shvyd'ko, S. Spampinati, S. Stoupin, S. Terentyev, E. Trakhtenberg, D. Walz, J. Welch, J. Wu, A. Zholents and D. Zhu, *Nat. Photonics* **6** (2012) 693–698.
- [616] D. Ratner, R. Abela, J. Amann, C. Behrens, D. Bohler, G. Bouchard, C. Bostedt, M. Boyes, K. Chow, D. Cocco, *et al.*, *Phys. Rev. Lett.* **114** (2015) 054801.
- [617] M. Yabashi and T. Tanaka, *Nat. Photonics* **6** (2012) 648–649, <https://doi.org/10.1038/nphoton.2012.237>.
- [618] B. McNeil, *Nat. Photonics* **3** (2009) 375–377, <https://doi.org/10.1038/nphoton.2009.110>.
- [619] C. Bostedt, S. Boutet, D.M. Fritz, Z. Huang, H.J. Lee, H.T. Lemke, A. Robert, W.F. Schlotter, J.J. Turner and G.J. Williams, *Rev. Mod. Phys.* **88** (2016) 015007.
- [620] H.N. Chapman, P. Fromme, A. Barty, T. A. White, R. A. Kirian, A. Aquila, M.S. Hunter, J. Schulz, D.P. DePonte, U. Weierstall, R.B. Do Andak, F.R.N.C. Maia, A.V. Martin, I. Schlichting, L. Lomb, N. Coppola, R.L. Shoeman, S.W. Epp, R. Hartmann, D. Rolles, A. Rudenko, L. Foucar, N. Kimmel, G. Weidenspointner, P. Holl, M. Liang, M. Barthelmeß, C. Caleman, S. Boutet, M.J. Bogan, J. Krzywinski, C. Bostedt, S. Bajt, L. Gumprecht, B. Rudek, B. Erk, C. Schmidt, A. Hamke, C. Reich, D. Pietschner, L. Strader, G. Hauser, H. Gorke, J. Ullrich, S. Herrmann, G. Schaller, F. Schopper, H. Soltau, K.-U. Kahnel, M. Messerschmidt, J.-D. Bozek, S.P. Hau-Riege,

- M. Frank, C.Y. Hampton, R.G. Sierra, D. Starodub, G.J. Williams, J. Hajdu, N. Timneanu, M.M. Seibert, J. Andreasson, A. Rocker, O. Jansson, M. Svenda, S. Stern, K. Nass, R. Andritschke, C.D. Schröter, F. Krasniqi, M. Bott, K.E. Schmidt, X. Wang, I. Grotjohann, J.M. Holton, T.R.M. Barends, R. Neutze, S. Marchesini, R. Fromme, S. Schorb, D. Rupp, M. Adolph, T. Gorkhover, I. Andersson, H. Hirsemann, G. Potdevin, H. Graafsma, B. Nilsson and J.C.H. Spence. *Nature* **470** (2011) 73–77.
- [621] M.M. Seibert, T. Ekeberg, F.R.N.C. Maia, M. Svenda, J. Andreasson, O. Jönsson, D. Odic', B. Iwan, A. Rocker, D. Westphal, M. Handantke, D.P. DePonte, A. Barty, J. Schulz, L. Gumprecht, N. Coppola, A. Aquila, M. Liang, T.A. White, A. Martin, C. Caleman, S. Stern, C. Abergel, V. Seltzer, J-M. Claverie, C. Bostedt, J.D. Bozek, S. Boutet, A.A. Miahnahri, M. Messerschmidt, J. Krzywinski, G. Williams, K.O. Hodgson, M.J. Bogan, C.Y. Hampton, R.G. Sierra, D. Starodub, I. Andersson, S. Bajt, M. Barthelmess, J.C.H. Spence, P. Fromme, U. Weierstall, R. Kirian, M. Hunter, R.B. Doak, S. Marchesini, S.P. Hau-Riege, M. Frank, R.L. Shoeman, L. Lomb, S.W. Epp, R. Hartmann, D. Rolles, A. Rudenko, C. Schmidt, L. Foucar, N. Kimmel, P. Holl, B. Rudek, B. Erk, A. Hamke, C. Reich, D. Pietschner, G. Weidenspointner, L. Strader, G. Hauser, H. Gorke, J. Ullrich, I. Schlichting, S. Herrmann, G. Schaller, F. Schopper, H. Soltau, K.U. Kahnel, R. Andritschke, C-D. Schrater, F. Krasniqi, M. Bott, S. Schorb, D. Rupp, M. Adolph, T. Gorkhover, H. Hirsemann, G. Potdevin, H. Graafsma, B. Nilsson, H.N. Chapman and J. Hajdu. *Nature* **470** (2011) 78–81.
- [622] R.A. Kirian, T.A. White, J.M. Holton, H.N. Chapman, P. Fromme, A. Barty, L. Lomb, A. Aquila, F.R.N.C. Maia, A.V. Martin, R. Fromme, X. Wang, M.S. Hunter, K.E. Schmidt and JCH Spence, *Acta Crystallogr. A* **67** (2011) 131–140, <https://doi.org/10.1107/s0108767310050981>.
- [623] L. Young, E.P. Kanter, B. Krässig, Y. Li, A.M. March, S.T. Pratt, R. Santra, S.H. Southworth, N. Rohringer, L.F. DiMauro, G. Doumy, C.A. Roedig, N. Berrah, L. Fang, M. Hoener, P.H. Bucksbaum, J.P. Cryan, S. Ghimire, J.M. Glowina, D.A. Reis, J.D. Bozek, C. Bostedt and M. Messerschmidt, *Nature* **466** (2010) 56–61, <https://doi.org/10.1038/nature09177>.
- [624] N. Berrah, J. Bozek, J.T. Costello, S. Düsterer, L. Fang, J. Feldhaus, H. Fukuzawa, M. Hoener, Y.H. Jiang, P. Johnsson, E.T. Kennedy, M. Meyer, R. Moshhammer, P. Radcliffe, M. Richter, A. Rouzae, A. Rudenko, A.A. Sorokin, K. Tiedtke, K. Ueda, J. Ullrich and M.J.J. Vrakking, *J. Mod. Opt.* **57** (2010) 1015–1040, <https://doi.org/10.1080/09500340.2010.487946>.
- [625] G. Doumy, C. Roedig, S-K. Son, C.I. Blaga, A.D. DiChiara, R. Santra, N. Berrah, C. Bostedt, J.D. Bozek, P.H. Bucksbaum, J.P. Cryan, L. Fang, S. Ghimire, J.M. Glowina, M. Hoener, E.P. Kanter, B. Krässig, M. Kuebel, M. Messerschmidt, G.G. Paulus, D.A. Reis, N. Rohringer, L. Young, P. Agostini and L.F. DiMauro, *Phys. Rev. Lett.* **106** (2011) 083002–083006.
- [626] M. Richter, S.V. Bobashev, A.A. Sorokin and K. Tiedtke, *J. Phys. B At. Mol. Opt. Phys.* **43** (2010) 194005–194012.
- [627] A.H. Zewail, *J. Phys. Chem. A* **104** (2000) 5660–5694, <https://doi.org/10.1021/jp001460h>.
- [628] M. Meyer, J.T. Costello, S. Düsterer, W.B. Li, and P. Radcliffe, *J. Phys. B At. Mol. Opt. Phys.* **43** (2010) 194006–194015.
- [629] C.M. Günther, B. Pfau, R. Mitzner, B. Siemer, S. Røling, H. Zacharias, O. Kutz, I. Rudolph, D. Schöndelmaier, R. Treusch, *et al.*, *Nat. Photonics* **5** (2011) 99–102.
- [630] S. Roy, D. Parks, K.A. Seu, Run Su, J.J. Turner, Weilun Chao, E.H. Anderson, Stefano Cabrini and S.D. Kevan, *Nat. Photonics.* **5** (2011) 243–245, <https://doi.org/10.1038/nphoton.2011.11>.
- [631] J.M. Glowina, J. Cryan, J. Andreasson, A. Belkacem, N. Berrah, C.I. Blaga, C. Bostedt, J. Bozek, L.F. DiMauro, L. Fang, J. Frisch, O. Gessner, M. Gahr, J. Hajdu, M.P. Hertlein, M. Hoener, G. Huang, O. Kornilov, J.P. Marangos, A.M. March, B.K. McFarland, H. Merdji, V.S. Petrovic, C. Raman, D. Ray, D.A. Reis, M. Trigo, J.L. White, W. White, R. Wilcox, L. Young, R.N. Coffee and P.H. Bucksbaum, *Opt. Express* **18** (2010) 17620–17630.

- [632] E. Galtier, F.B. Rosmej, T. Dzelzainis, D. Riley, F.Y. Khattak, P. Heimann, R.W. Lee, A.J. Nelson, S.M. Vinko, T. Whitcher, J.S. Wark, T. Tschentscher, S. Toleikis, R.R. Faustlin, R. Sobierajski, M. Jurek, L. Juha, J. Chalupsky, V. Hajkova, M. Kozlova, J. Krzywinski and B. Nagler *Phys. Rev. Lett.* **106** (2011) 164801–164806, <https://doi.org/10.1103/physrevlett.106.164801>.
- [633] M.-E. Couprie and J.-M. Filhol, *C. R. Phys.* **9** (2008) 487–506, <https://doi.org/10.1016/j.crhy.2008.04.001>.
- [634] M. E. Couprie, *C. R. Acad. Sci. IV Phys.* **1** (2000) 329–345.
- [635] A.A. Lutman, R. Coffee, Y. Ding, Z. Huang, J. Krzywinski, T. Maxwell, M. Messerschmidt and H-D. Nuhn, *Phys. Rev. Lett.* **110** (2013) 134801, <https://doi.org/10.1103/physrevlett.110.134801>.
- [636] A. Marinelli, A.A. Lutman, J. Wu, Y. Ding, J. Krzywinski, H-D. Nuhn, Y. Feng, R.N. Coffee and C. Pellegrini, *Phys. Rev. Lett.* **111** (2013) 134801, <https://doi.org/10.1103/physrevlett.111.134801>.
- [637] T. Hara, Y. Inubushi, T. Katayama, T. Sato, H. Tanaka, T. Tanaka, T. Togashi, K. Togawa, K. Tono, M. Yabashi, *et al.*, *Nat. Commun.* **4** (2013) 2919, <https://doi.org/10.1038/ncomms3919>.
- [638] A. Marinelli, D. Ratner, A.A. Lutman, J. Turner, J. Welch, F-J. Decker, H. Loos, C. Behrens, S. Gilevich, A.A. Miahnahri, *et al.*, *Nat. Commun.* **6** (2015) 6369, <https://doi.org/10.1038/ncomms7369>.
- [639] A. Petralia, M.P. Anania, M. Artioli, A. Bacci, M. Bellaveglia, M. Carpanese, E. Chiodroni, A. Cianchi, F. Ciocci, G. Dattoli, *et al.*, *Phys. Rev. Lett.* **115** (2015) 014801, <https://doi.org/10.1103/physrevlett.115.014801>.
- [640] T. Tajima and J.M. Dawson, *Phys. Rev. Lett.* **43** (1979) 267–270.
- [641] E. Esarey, C.B. Schroeder and W.P. Leemans, *Rev. Mod. Phys.* **81** (2009) 1229, <https://doi.org/10.1103/revmodphys.81.1229>.
- [642] V. Malka, J. Faure, Y.A. Gauduel, E. Lefebvre, A. Rousse and K.T. Phuoc, *Nat. Phys.* **4** (2008) 447–453, <https://doi.org/10.1038/nphys966>.
- [643] K. Nakajima, *Nat. Phys.* **4** (2008) 92–93, <https://doi.org/10.1038/nphys846>.
- [644] F. Grüner, S. Becker, U. Schramm, T. Eichner, M. Fuchs, R. Weingartner, D. Habs, J.M. Vehn, M. Geissler, M. Ferrario, *et al.*, *Appl. Phys. B* **86** (2007) 431–435, <https://doi.org/10.1007/s00340-006-2565-7>.
- [645] H-P. Schlenvoigt, K. Haupt, A. Debus, F. Budde, O. Jäckel, S. Pfotenhauer, H. Schwoerer, E. Rohwer, J.G. Gallacher, E. Brunetti, R.P. Shanks, S.M. Wiggins and D.A. Jaroszynski, *Nat. Phys.* **4** (2008) 130–133, <https://doi.org/10.1038/nphys811>.
- [646] M. Fuchs, R. Weingartner, A. Popp, Z. Major, S. Becker, J. Osterhoff, I. Cortrie, B. Zeitler, R. Hörlein, G.D. Tsakiris, U. Schramm, T.P. Rowlands-Rees, S.M. Hooker, D. Habs, F. Krausz, S. Karsch and F. Grüner, *Nat. Phys.* **5** (2009) 826–829, <https://doi.org/10.1038/nphys1404>.
- [647] M.P. Anania, D. Clark, S.B. van der Geer, M.J. de Loos, R. Isaac, A.J.W. Reitsma, G.H. Welsh, S.M. Wiggins and D.A. Jaroszynski. In *SPIE Europe Optics+ Optoelectronics* (International Society for Optics and Photonics, 2009), pp. 735916–735916.
- [648] G. Lambert, S. Corde, K. Ta Phuoc, V. Malka, A. Ben Ismail, E. Benveniste, A. Specka, M. Labat, A. Loulergue, R. Bachelard and M-E. Couprie. In *Proc. FEL conf., Nara, Japan, Jacow*, (2012), p. 2.
- [649] A.R. Maier, A. Meseck, S. Reiche, C.B. Schroeder, T. Seggebrock and F. Gruener, *Phys. Rev. X* **2** (2012) 031019, <https://doi.org/10.1103/physrevx.2.031019>.
- [650] M.-E. Couprie, A. Loulergue, M. Labat, R. Lehe and Victor Malka, *J. Phys. B At. Mol. Opt. Phys.* **47** (2014) 234001, <https://doi.org/10.1088/0953-4075/47/23/234001>.
- [651] A. Loulergue, M. Labat, C. Evain, C. Benabderrahmane, Victor Malka and M.E. Couprie, *New J. Phys.* **17** (2015) 023028, <https://doi.org/10.1088/1367-2630/17/2/023028>.
- [652] Z. Huang, Y. Ding and C.B. Schroeder, *Phys. Rev. Lett.* **109** (2012) 204801–204805,

<https://doi.org/10.1103/physrevlett.109.204801>.

[653] C. Townes, *A Century of Nature, 21 Discoveries that Changes Science in the World*, The University of Chicago Press Books (2003).

Appendices

This appendix gives the list of FEL Prize winners.

Table .1: FEL Prize winners

Year	Town	Country	FEL	Prize winners
1988	Jerusalem	Israel	FEL 10	John Madey
1989	Naples	USA	FEL11	William Colson
1990	Paris	France	FEL12	Todd Smith and Luis Elias
1991	Santa Fe	USA	FEL13	Phillip Sprangle and Nikolai Vinokurov
1992	Kobe	Japan	FEL14	Robert Phillips
1993	The Hague	The Netherland	FEL15	Roger Warren
1994	Stanford	USA	FEL16	Alberto Renieri and Giuseppe Dattoli
1995	New York	USA	FEL17	Richard Pantell and George Bekefi
1996	Rome	Italy	FEL18	Charles Brau
1997	Beijing	China	FEL 19	Kwang-Je Kim
1998	Williamsburg	USA	FEL 20	John Walsh
1999	Hamburg	Germany	FEL21	Claudio Pellegrini
2000	Durham	USA	FEL 22	Stephen V. Benson, Eisuke J. Minehara and George F
2001	Darmstadt	Germany	FEL 23	Michel Billardon, Marie-Emmanuelle Couprie and Jean-Michel Ortega
2002	Argonne	USA	FEL24	H. Alan Schwettman and Alexander F.G. van der M
2003	Tsukuba	Japan	FEL25	Li-Hua Yu
2004	Trieste	Italy	FEL26	Hiroyuki Hama and Vladimir Livinenko
2005	Stanford	USA	FEL27	Avraham Gover
2006	Berlin	Germany	FEL28	Evgeni Saldin and Jorg Rosbach
2009	Liverpool	Great Britain	FEL29	Paul Emma and David Dowell
2010	Malmö	Sweden	FEL30	Sven Reiche
2011	Shanghai	China	FEL31	Tsumoru Shintake
2012	Nara	Japan	FEL32	John Galayda
2013	New York	USA	FEL33	Luca Giannessi and Young Uk Jeong
2014	Basel	Switzerland	FEL34	William Fawley and Zhirong Huang
2015	Daejeon	Korea	FEL35	Mikhail Yurkov and Evgeny Schneidmiller
2017	Santa-Fe	USA	FEL36	Bruce Carlsten, Dinh Nguyen and Richard Sheffi